Impact of varying NH + NO ratios in nutrient solution on C-isotope composition of leaf- and root-respired CO and putative respiratory substrates in C plants

Yang Xia

NNT : 2019SACLS222

Impact of varying NH_4^+:NO_3^- ratios in nutrient solution on C-isotope composition of leaf- and root-respired CO_2 and putative respiratory substrates in C_3 plants

Thèse de doctorat de l'Université Paris-Saclay
préparée à l'Université Paris-Sud

École doctorale n°567: Sciences du Végétal:
du gène à l'écosystème (SDV)

Spécialité de doctorat: Biologie

Thèse présentée et soutenue à Orsay, le 23 juillet 2019, par

Yang XIA

Composition du Jury :

Jacqui SHYKOFF Directrice de Recherche, Université Paris-Sud (ESE)	Présidente
Enrico BRUGNOLI Professeur, CNR Research Institute of Terrestrial Ecosystems (Italy)	Rapporteur
Daniel EPRON Professeur des Universités, Université de Lorraine (UMR Silva – INRA, Nancy)	Rapporteur
Lisa WINGATE Chargée de Recherche, INRA de Bordeaux (UMR ISPA)	Examinatrice
Jaleh GHASHGHAIE Professeur des Universités, Université Paris-Sud (ESE)	Directrice de thèse

Thèse de doctorat

Acknowledgements

I would like to take this opportunity to thank to the China Scholarship Council (CSC) for my PhD scholarship funding, the Laboratoire d'Ecologie, Systématique et Evolution (ESE), Université Paris-Sud for hosting me and for the financial support of my PhD work, and all the people who supported me scientifically, technically and personally during my PhD time.

First and foremost, many thanks to my supervisor Prof. Jaleh Ghashghaie from ESE, who offered me the opportunity to conduct my PhD thesis in this prestigious and friendly lab, and gave me necessary and professional orientation and support. Thank you for sharing your knowledge of physiology and isotopes, how to deal with scientific problems/questions, and how to structure and write a scientific paper.

I would like to thank Dr. Franz-W. Badeck from Genomics research centre, Council for Agricultural Research and Economics (CREA- GPG), Dr. Camille Bathellier from Elementar-Lyon, and Prof. Guillaume Tcherkez from Australian National University for being my thesis committee members and for the kind constructive suggestions and helpful discussion, mainly Franz for his help in statistical analyses of my data and for critical reading of the dissertation.

I am seriously grateful for Prof. Enrico Brugnoli form CNR Research Institute of Terrestrial Ecosystems (Italy), Prof. Daniel Epron from Université de Lorraine for agreeing to be reviewers of my dissertation, thank you for your valuable comments on my dissertation. I would like to thank Dr. Lisa Wingate from INRA de Bordeaux and Dr. Jacqui Shykoff from ESE to be part of the jury of my PhD defence.

I am also grateful for the contribution of our partners. In particular, Cyril Girardin from Laboratory of ECOSYS (INRA, Grignon), Dr. Roland A. Werner from ETH Zurich (Switzerland) and Prof. Gerd Gleixner from Max-Planck-Institute Biogeochemistry (Germany) for their significantly contributed to training on and assistance in isotope analyses. Thanks Shiva for sharing the recipe of nitrogen solutions and PEPc activity analysing protocol.

I thank many technical staff who helped me during experiments: Annika Ackermann and the Institute of Agricultural Sciences (ETH Zürich) for isotope analyses of organic material; Steffen Ruehlow and Max Planck Institute (Jena, Germany) for training on and assistance in LC-C-IRMS analyses of sugars and organic acids; Marlène Lamothe-Sibold for training on EA-IRMS; and the gardeners of ESE for helping in plant culture/care.

I would like to thank all my colleagues and friends in ESE and IPS2 for providing me such a friendly and scientific environment. In particular, Chantal for your teaching on biochemical analysis and assistance in enzymatic assays, Peter for training on Licor, and Cathleen, Anne-Claire, Ying-cho Lo, Qian Zhang for their friendship and kind help.

Last but not least, my very special thanks go to my family, especially my parents for their unconditionally love, constant support and encouragement.

感谢我最爱的家人所给予我的，最无私的爱与支持。

CONTENTS

ABSTRACT

Carbon isotopic fractionations associated with plant respiration have received increasing attention because of their possible influences on efforts to elucidate factors associated with ecosystem carbon balances *via* carbon isotope analysis (Ghashghaie *et al.,* 2016). Generally, isotope fractionations occur against heavy carbon (^{13}C) in C_3 plants during photosynthetic CO_2 uptake leading to ^{13}C depletion in plant organic matter compared to air CO_2. Thus leaves were found to be in general ^{13}C depleted compared to all other organs (Badeck *et al.,* 2005). One reasonable explanation of these between organ differences is the opposite respiratory isotope fractionations between leaves and roots: leaves release ^{13}C enriched CO_2 during respiration, leaving behind ^{13}C depleted carbon to be incorporated into leaf biomass, while roots release ^{13}C depleted CO_2, leaving behind ^{13}C enriched carbon (Bathellier *et al.,* 2008).

Anaplerotic carbon fixation *via* PEPc may affect respiratory fractionations. Carbon fixed *via* PEPc being ^{13}C enriched, anaplerotic pathway could introduce ^{13}C enriched organic acids (i.e. oxaloacetate and malate) into TCA, thus may lead to ^{13}C enrichment of the respired CO_2. It is well known that the activity of anaplerotic pathway is strongly linked with nitrogen assimilation. Different nitrogen sources (NH_4^+ or NO_3^-) are taken up into cytosol through different mechanisms and their assimilation takes place in different organs (leaf or root). NH_4^+ assimilation dominantly occurs in roots, thus enhances the activity of anaplerotic pathway in these organs. Different to ammonium, NO_3^- reduction takes place in both leaves and roots. In roots, it is considered that the plants fed with NO_3^- have the same isotopic impact on anaplerotic pathway activity as in the plants fed with NH_4^+. But in the case of illuminated leaves, organic acids (in particular, malate) is responsible for maintenance of the charge balance for neutralizing the excess OH^- produced during NO_3^- uptake. With increasing malate synthesis, higher activity of anaplerotic pathway in illuminated leaves fed with NO_3^- is expected. Taken all together, we presumed more ^{13}C enriched respiratory substrates and respired CO_2 in roots under NH_4^+ nutrition, and more ^{13}C enriched in illuminated leaves fed with NO_3^- than NH_4^+.

In order to better understand (i) in which extent the isotopic composition of putative respiratory substrates and respired CO_2 is affected by N-type nutrition in plants, and (ii) in which extent the anaplerotic pathway (*via* PEPc) could explain C-isotope changes between heterotrophic and autotrophic organs under different N-type nutrition, two species, bean (*Phaseolus vulgaris* L.) and

spinach (*Spinacia oleracea* L.), were selected from a preliminary experiment and grown in sand with varying ratios of NH_4^+:NO_3^- in supplied N. C-isotope composition of leaf- and root-respired CO_2 in the dark and that of putative respiratory substrates including soluble sugars and organic acids (malate and citrate), PEPc activity, as well as leaf gas exchanges were determined.

The plants did not show any visual symptoms of NH_4^+ toxicity or growth suppression, probably due to the low light intensity during culture period, which alleviated toxic effect of NH_4^+. No particular trend across N-type gradient was observed for gas exchange parameters nor for biomass in none of the species studied. However, in agreement with our initial hypothesis, leaf-respired CO_2 was ^{13}C enriched under NO_3^- nutrition and became progressively ^{13}C depleted with increasing amount of NH_4^+ in supplied N, while C-isotope composition of root-respired CO_2 remained unchanged across N-type gradient. The changes in C-isotope composition of individual metabolites and their amounts as well as PEPc activity exhibited different patterns between the two species. We suggested that a higher amount of ^{13}C enriched C-pools fixed by PEPc through anaplerotic pathway contributed to respired CO_2 in leaves under NO_3^- nutrition. However, a similar effect in roots expected under NH_4^+ nutrition was masked because of a rather ^{13}C depleted C source (i.e. respired CO_2) refixation by PEPc. The isotopic gap between malate and citrate, different between the 2 species and changing differently through N-type gradient, confirmed a great plasticity of the TCA cycle in plants. According to our results, we suggested that in the case of bean malate and citrate having almost similar C-isotope signatures, malate but even citrate originated mainly from anaplerotically-fixed C pools, but that in the case of spinach malate being more ^{13}C enriched than citrate, malate and citrate branches of TCA are less connected than in bean.

Our results and discussion highlight the potential of the malate/citrate (or other relevant abundant organic acids) ^{13}C-isotopic gap as a valuable proxy to screen for peculiar metabolic TCA organisations across species. Double labelling experiments (^{13}C and ^{15}N) are needed for better understanding the metabolic plasticity of TCA and its impact on isotopic gap between malate and citrate and on C-isotope composition of respired CO_2 in different species.

RESUME

La discrimination isotopique du carbone associée à la respiration des plantes a fait l'objet d'une attention croissante en raison de son influence possible sur les efforts visant à élucider les facteurs associés aux bilans carbonés des écosystèmes *via* l'analyse isotopique du carbone (Ghashghaie *et al.*, 2016). En générale, une discrimination isotopique se produit contre le carbone lourd (^{13}C) chez les plantes C_3 lors de l'assimilation photosynthétique du CO_2, ce qui entraîne un appauvrissement en ^{13}C dans la matière organique des plantes par rapport au CO_2 atmosphérique. Ainsi, on a constaté que les feuilles sont en général appauvries en ^{13}C par rapport à tous les autres organes (Badeck *et al.*, 2005). Les discriminations isotopiques respiratoires opposées entre feuilles et racines peuvent raisonnablement expliquer les différences isotopiques entre ces organes : les feuilles libèrent du CO_2 enrichi en ^{13}C pendant la respiration, ce qui laisse le carbone appauvri en ^{13}C intégrer la biomasse foliaire, tandis que les racines libèrent du CO_2 appauvri en ^{13}C, laissant le carbone enrichi en ^{13}C dans la matière organique (Bathellier *et al.*, 2008).

La fixation anaplérotique du carbone *via* la PEPc peut affecter les fractionnements isotopiques respiratoires. Le carbone fixé *via* la PEPc étant enrichi en ^{13}C, la voie anaplérotique pourrait introduire des acides organiques enrichis en ^{13}C (oxaloacétate et malate) dans le TCA, conduire ainsi à un enrichissement en ^{13}C du CO_2 respiré. Il est bien connu que l'activité de la voie anaplérotique est fortement liée à l'assimilation de l'azote. Différentes sources d'azote (NH_4^+ ou NO_3^-) sont absorbées dans le cytosol par différents mécanismes et leur assimilation a lieu dans différents organes (feuille ou racine). L'assimilation de NH_4^+ se produit principalement dans les racines, ce qui améliore l'activité de la voie anaplérotique dans ces organes. Contrairement à l'ammonium, la réduction de NO_3^- a lieu dans les feuilles et les racines. Au niveau des racines, on considère que les plantes nourries avec NO_3^- ont le même impact isotopique sur l'activité de la voie anaplerotique que chez les plantes nourries avec NH_4^+. Toutefois, dans le cas des feuilles illuminées, les acides organiques (en particulier le malate) sont responsables du maintien de l'équilibre des charges pour la neutralisation de l'excès d'OH^- produit lors de l'absorption de NO_3^-. Avec l'augmentation de la synthèse de malate, une activité plus intense de la voie anaplérotique est attendue dans les feuilles illuminées de plantes nourries avec NO_3^-. Dans l'ensemble, nous avons présumé plus de substrats respiratoires et de CO_2 respiré enrichis en ^{13}C dans les racines de plantes nourries avec NH_4^+, et dans les feuilles illuminées de plantes nourries avec NO_3^-.

Afin de mieux comprendre (i) dans quelle mesure la composition isotopique du carbone de substrats respiratoires putatifs et de CO_2 respiré est influencée par la forme d'azote fourni, et (ii) dans quelle mesure la voie anaplérotique (*via* PEPc) pourrait expliquer les différences isotopiques entre organes hétérotrophes et autotrophes sous différentes formes de nutrition azotée, deux espèces, le haricot (*Phaseolus vulgaris* L.) et l'épinard (*Spinacia oleracea* L.), ont été sélectionnées à partir d'une expérience préliminaire et ont été cultivées dans du sable avec divers rapports NH_4^+: NO_3^- dans l'azote fourni. La composition isotopique du C du CO_2 respiré par les feuilles et les racines à l'obscurité et dans des substrats respiratoires putatifs, y compris les sucres solubles et les acides organiques (malate et citrate), l'activité de la PEPc ainsi que les échanges gazeux foliaires ont été déterminés.

Les plantes ne présentaient aucun symptôme visuel de toxicité au NH_4^+ ni de suppression de la croissance, probablement en raison de la faible intensité lumineuse au cours de la période de culture, ce qui a dû atténuer l'effet toxique du NH_4^+. Aucune tendance particulière lelong du gradient NH_4^+: NO_3^- n'a été observée pour les paramètres d'échanges gazeux ni pour la biomasse chez aucune des espèces étudiées. Cependant, en accord avec notre hypothèse initiale, le CO_2 respiré par les feuilles était enrichi en ^{13}C sous nutrition avec NO_3^- et devenait progressivement appauvri en ^{13}C avec une quantité croissante de NH_4^+ dans le N fourni, tandis que la composition isotopique du C du CO_2 respiré par les racines restait inchangée quel que soit le rapport NH_4^+:NO_3^- Dans la solution nutritive. Les changements isotopiques du C des métabolites individuels et leurs quantités, ainsi que l'activité de la PEPc, ont montré des profils différents entre les deux espèces. Nous avons suggéré qu'une plus grande quantité de pools de C enrichis en ^{13}C fixés par la PEPc *via* la voie anaplérotique contribuait à la respiration dans les feuilles sous nutrition avec NO_3^-. Cependant, un effet similaire dans les racines attendu sous NH_4^+ était masqué en raison d'une refixation par la PEPc du CO_2 respiré (source de C appauvri en ^{13}C). L'écart isotopique entre le malate et le citrate, différent entre les 2 espèces et évoluant différemment selon le gradient de NH_4^+:NO_3^-, a confirmé la grande plasticité du cycle de TCA chez les plantes. Selon nos résultats, nous avons suggéré que, dans le cas du haricot le malate et le citrate ayant des signatures isotopiques presque similaires, le malate et même le citrate provenait principalement du pool de carbones fixés anaplérotiquement, mais que chez l'épinard le malate étant plus enrichi en ^{13}C que le citrate, les branches du malate et du citrate dans le TCA sont moins connectées que chez le haricot.

Nos résultats et notre discussion mettent en évidence le potentiel de l'écart isotopique malate/citrate (ou d'autres acides organiques abondants et pertinents) en tant que proxy valable pour le dépistage d'organisations métaboliques particulières de TCA parmi différentes espèces. Des expériences de double marquage (^{13}C et ^{15}N) sont nécessaires pour mieux comprendre la plasticité métabolique du TCA et son impact sur l'écart isotopique entre le malate et le citrate et sur la composition isotopique du CO_2 respiré chez différentes espèces.

CHAPTER 1 - General Introduction

Photosynthetic assimilation of inorganic carbon (i.e. atmospheric CO_2) provides the organic carbon source that plants depend on. The carbon fixed by the autotrophic organs (i.e. leaves) is partly used for synthesis of the structural materials for growth of both the autotrophic and heterotrophic organs, and partly for synthesis of different metabolic pools, which are then degraded by respiration during the day- and night-time releasing the energy needed for plant cell functions. Photosynthetic carbon, before being respired by plants, is directed towards the synthesis of carbohydrates, and other compounds and/or stored as reserves with different turnover rates in different cellular compartments, tissues or organs. Some compounds (or metabolic pools) are rapidly consumed by respiration (immediately or within few hours after assimilation), others more slowly (few days or even longer time after assimilation). Respiration, with its associated carbon metabolism, releases the energy stored in carbon compounds in a controlled manner for cellular use (Azcón-Bieto and Osmond, 1983). At the same time, it generates many carbon precursors for biosynthesis (organic and amino acids, fatty acids, secondary metabolites, etc.) (Noggle and Fritz, 1983). The carbon released by plant respiration is generally considered to come from the degradation of the recently formed photo-assimilates (i.e. carbohydrates). However, other reserves (i.e. organic acids, as well as lipids, and occasionally proteins) are also reported to be used as substrates for respiration (Nobel, 1983; Lambers, 1985), with their relative contributions depending on the species, pool sizes as well as environmental conditions (Tcherkez *et al.*, 2003; Nogués *et al.*, 2006). In addition, carbon atoms assimilated at different times can be mixed in metabolic pools in plant cells (Nogués *et al.*, 2004). Thus, the metabolic articulation between the assimilation of carbon and its use by respiration and the identification of the substrates or pools used for respiration are not easy to study.

In addition, C and N metabolisms are tightly interconnected mainly through the use of some intermediates of respiratory processes and associated pathways for biosynthesis of amino acids. NO_3^- is preferentially reduced and assimilated in leaves, while NH_4^+ tends to be assimilated in roots as much as possible. However, this picture probably varies substantially across species, and depends on NO_3^-/NH_4^+ concentrations involved. Regardless of the N type and the site of assimilation, N fixation involves the tricarboxylic acid (TCA) cycle to fuel glutamate/glutamine synthesis through the GS/GOGAT pathway. This diversion of intermediates from the TCA cycle

to amino acid synthesis requires anaplerotic activity (PEPc mainly) to supply C-skeletons to the cycle.

In this context, the analysis of C stable isotopes in individual metabolites (putative respiratory substrates) and in respired CO_2 is a powerful tool to study the metabolic origin of the respired carbon and thus the activities of metabolic pathways associated with respiration under varying N-source conditions. The use of stable isotopes to study the respiratory metabolism has made important progress during the past 15 years, with both natural ^{13}C abundance as well as ^{13}C-labelling experiments (e.g. labelling the photo-assimilates by feeding the leaves with ^{13}C-labelled CO_2, feeding leaves or roots with positionally labelled metabolites, etc.) as recently reviewed by Ghashghaie and Badeck (2014) and Bathellier *et al.* (2017). Huge variability in the C-isotope composition of both leaf- and root-respired CO_2 (relative to corresponding organic material) has been reported, depending on the species and environmental conditions (e.g. drought, temperature, light, etc.). However, to our knowledge, the studies on the impact of N-type nutrition on C-isotope composition of respiratory substrates together with that of respired CO_2 are scarce. Therefore, the present PhD work aimed at studying the impact of varying ratios of NH_4^+:NO_3^- in supplied N on the C-isotope composition of putative respiratory substrates as well as that of leaf- and root-respired CO_2 in two C_3 plant species, bean and spinach (as a NH_4^+-tolerant and a NH_4^+-sensitive species, respectively).

This Chapter describes (1) the main steps of plant respiration and associated pathways as well as their interconnections, (2) the basics of the use of stable isotopes as well as the C-isotope discrimination during both photosynthesis and respiration, and (3) the N-type assimilation (NH_4^+ *versus* NO_3^-) and its potential impact on C-isotope composition of respiratory substrates and of both leaf- and root-respired CO_2. Finally, the main objectives of this PhD work are presented at the end of this Chapter.

1.1 Major respiratory metabolism steps and associated pathways in plants

The oxidation of glucose can be grouped into four major processes: glycolysis, tricarboxylic acid cycle (i.e. TCA cycle) or Krebs cycle, oxidative pentose phosphate pathway (PPP) and oxidative phosphorylation (Rees, 1980). These pathways are not isolated, they are interconnected and interacted by exchanging metabolic intermediates at several levels (Dennis and Blakeley, 2000).

Substrates of respiration enter the respiratory process at different points of these pathways (Linka and Weber, 2010), as summarized in Figure 1.1 (Bathellier *et al.*, 2017).

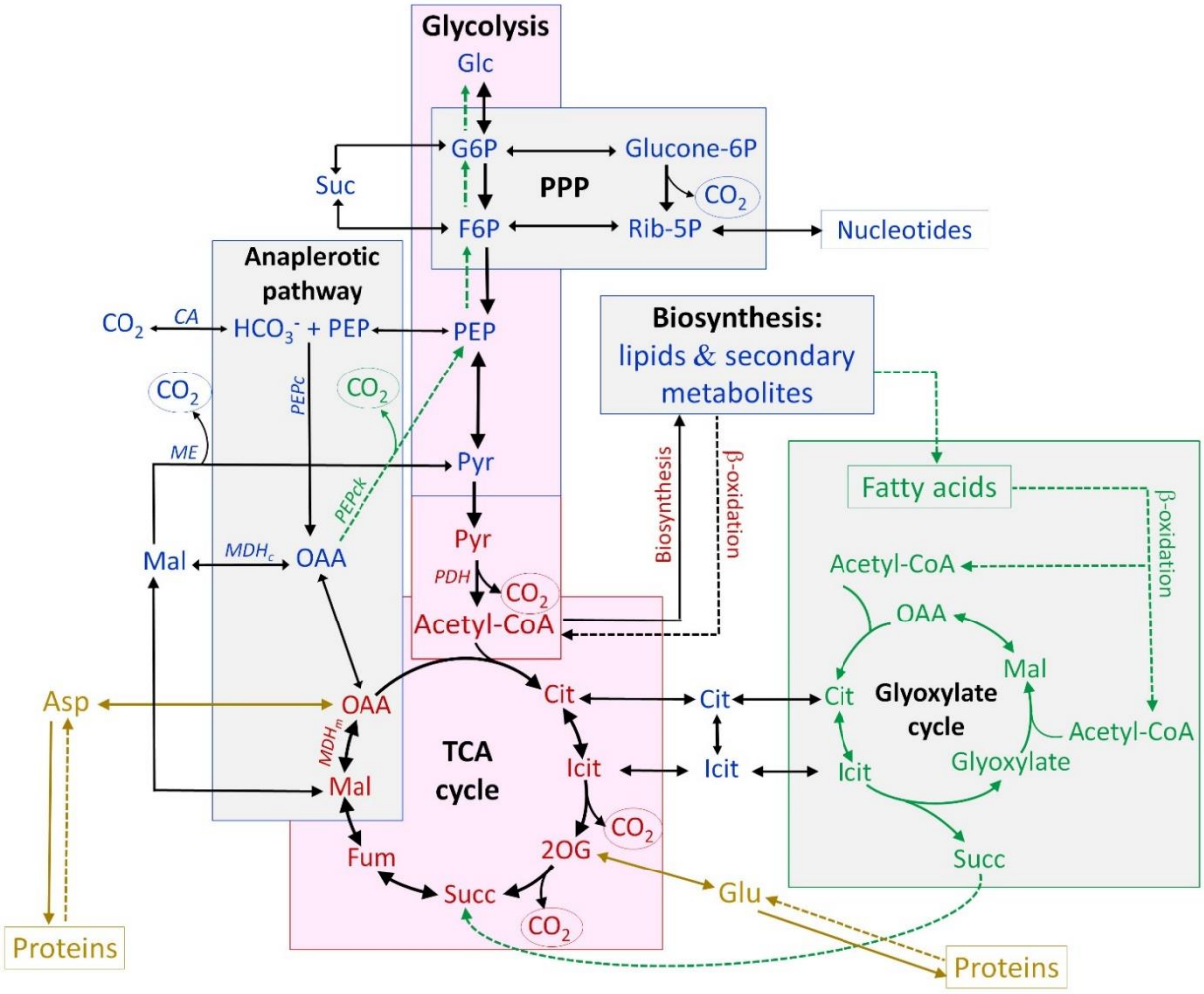

Figure 1.1. Simplified metabolic scheme of main respiratory pathways (pink boxes including glycolysis, translocation and decarboxylation of pyruvate and Krebs cycle) and associated pathways (grey boxes including pentose phosphate pathway, anaplerotic pathway, biosynthesis of lipids and secondary metabolites, and green box including glyoxylate pathway). Biosynthesis of proteins linked to the tricarboxylic acid (TCA) pathway are shown in light brown. Metabolites involved in processes occurring in the cytosol, mitochondrion, and glyoxysomes have their names in blue, red and green, respectively. Anabolic pathways are shown with solid-line arrows, while the catabolic ones with dashed-line arrows i.e. degradation of lipids, β-oxidation of fatty acids, and gluconeogenesis [from the incorporation of succinate (Succ) coming from the glyoxylic cycle into TCA pathway, and transformation of resulting OAA to PEP and finally to sugars (dashed-line arrows in green)]. The degradation of proteins to amino acids is also indicated by dashed-line arrows. Evolved CO_2 molecules are shown in ellipses. Pathways and enzymes are in bold letters: PPP (pentose phosphate pathway), PEPc (phospho*enol*pyruvate carboxylase), PDH (pyruvate dehydrogenase), PEPck (phospho*enol*pyruvate carboxykinase), MDH (malate dehydrogenase), ME (malic enzyme), CA (carbonic anhydrase). (Bathellier *et al.*, 2017)

During glucose oxidation, large amounts of free energy are released step wisely by mitochondrial electron transport. Nicotinamide adenine dinucleotide (NAD^+/NADH, mainly driving catabolism) and nicotinamide adenine dinucleotide phosphate ($NADP^+$/NADPH, mainly driving anabolism) are the most important organic cofactors (coenzymes) which store electron redox energy (Taiz and Zeiger, 2006; Igamberdiev and Bykova, 2018). NAD^+ and $NADP^+$ are the oxidized forms, while NADH and NADPH are relatively strong reductants (i.e., electron donors). In addition to these redox pairs, organic acids play a crucial role in numerous metabolic processes accompanied by transfer of electrons and protons (Igamberdiev and Bykova, 2018). These will be discussed in the following sub-sections.

1.1.1 Glycolysis

Glycolysis occurs in all living organisms, and is the cornerstone for anabolism by oxidizing hexoses to generate ATP, reductant (NADH), and pyruvate. In many plant species, sucrose is the main translocated sugar from leaves to roots, and therefore the major form of organic carbon source of most non-photosynthetic tissues. In the early steps of glycolysis, sucrose is split into glucose and fructose in the cytosol (Fig. 1.2). Subsequently, hexose is split into two triose phosphates, eventually forms phospho*enol*pyruvate (PEP), which is catalysed by pyruvate kinase (PK) to yield ATP and pyruvate – the precursor of acetyl-CoA, which is the substrate for the TCA cycle (Fernie *et al.*, 2004).

To be noted that, PEP can be metabolized in an alternative pathway, then the end-product of plant glycolysis will be malic acid (malate). In this pathway, with HCO_3^- fixation, PEP is carboxylated by the cytosolic enzyme PEP carboxylase (PEPc or PEPcase) to form oxaloacetate (OAA).

$$PEP + HCO_3^- \rightarrow OAA \qquad \text{(Eq 1.1)}$$

The OAA is then reduced to malate by the action of the enzyme malate dehydrogenase (MDH), which uses NADH as the source of electrons. The resulting malate can be stored in the vacuole or transported to the mitochondrion, where it can enter the TCA cycle (Davies, 1979; Zoglowek *et al.*, 1988; Plaxton, 1996).

Figure 1.2 Plant glycolysis. The enzymes that catalyze the numbered reactions are as follows:
1, hexokinase;
3, phosphoglucomutase;
4, phosphoglucose isomerase;
5, PFK;
6, ALD;
7, triose phosphate isomerase;
8, NAD-dependent GAPDH;
9, 3-PGA kinase;
10, phosphoglyceromutase;
11, enolase;
12, PK;
13, invertase;
14, sucrose synthase;
19, NADP-dependent GAPDH;
20, PEPase;
21, PEPc;
22, MDH;
23, ME.
Abbreviations are as in the text or as follows:
Glu-1-P, glucose-1-phosphate;
DHAP, dihydroxyacetone phosphate;
G3P, glyceraldehyde-3-phosphate;
1,3-DPGA, 1,3-diphosphoglycerate;
2-PGA, 2-phosphoglycerate;
OAA, oxaloacetate.
Note that the number of substrate and product molecules in all reactions from G3P to pyruvate should be doubled because two molecules of G3P are formed from one molecule of hexose (Plaxton, 1996).

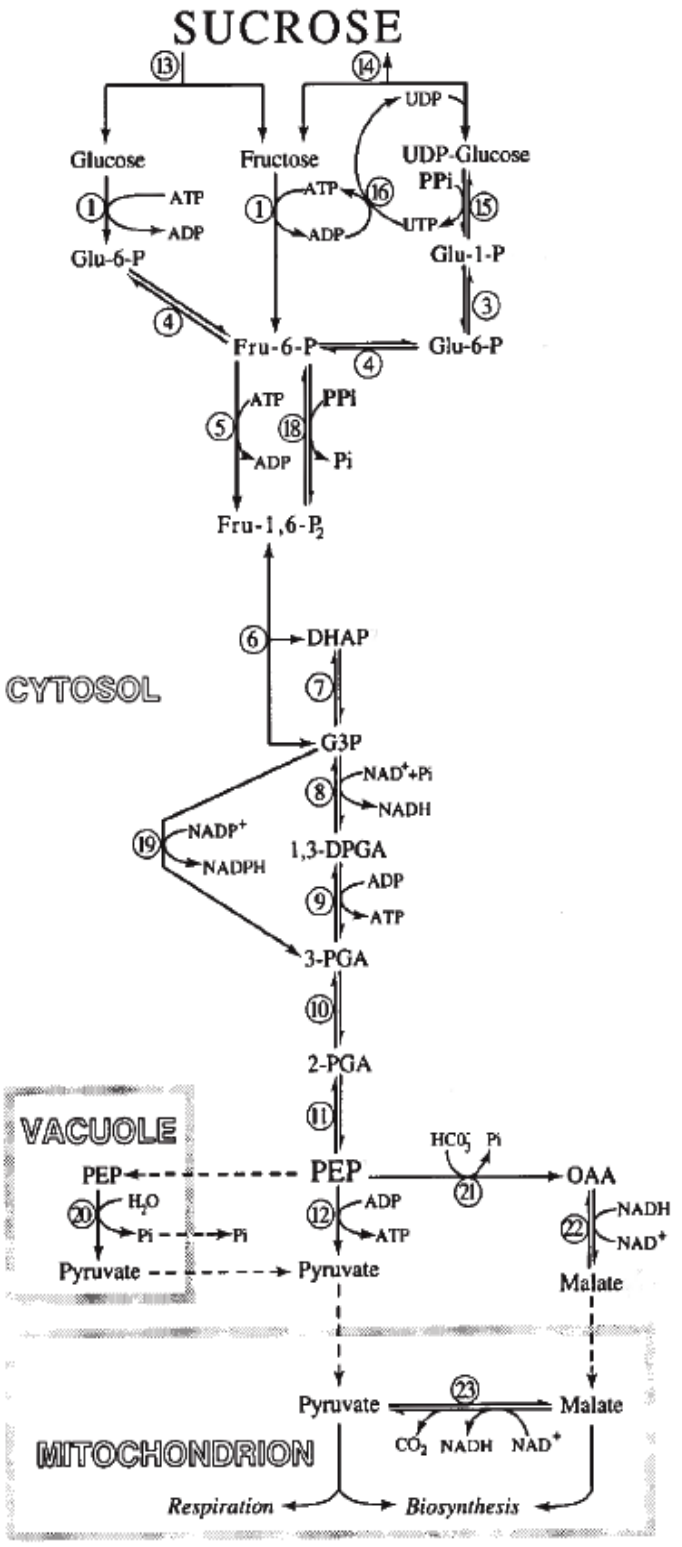

1.1.2 Pentose phosphate pathway

In addition to the glycolysis pathway, 10-25% of glucose is oxidized by the oxidative pentose phosphate pathway (also known as the hexose monophosphate shunt) in plants (Dieuaide-Noubhani *et al.*, 1995; Wamelink *et al.*, 2008). In plastids of non-photosynthetic cells and in chloroplasts functioning in the dark, the required NADPH is mainly provided by PPP: one glucose-6-phosphate (G6P) molecule, which is produced during glycolysis, is catalyzed by glucose-6-phosphate dehydrogenase (G6PDH) and 6-phosphogluconate dehydrogenase (6PGDH) successively, and completely oxidized to 5 CO_2 and 12 NADPH molecules (Fig. 1.3), which can supply reducing power for respiration, redox equilibration and biosynthetic reactions such as lipid biosynthesis and nitrite reduction during nitrate assimilation (Hoefnagel *et al.*, 1998; Shetty, 2004).

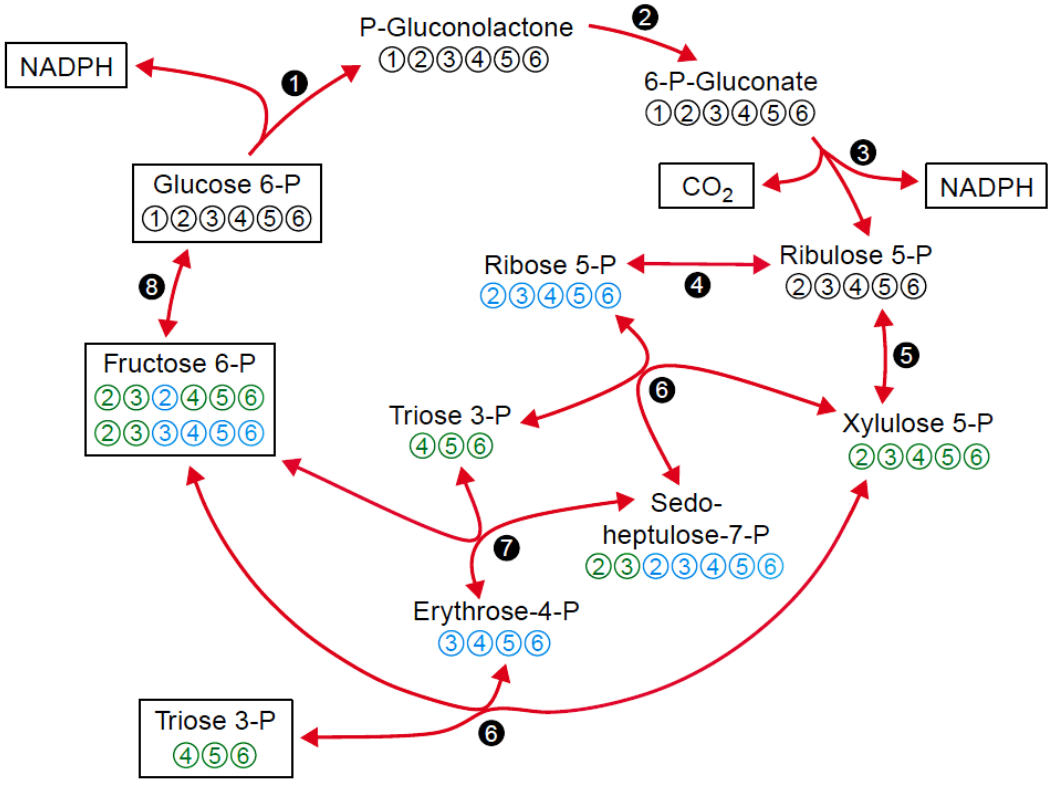

Figure 1.3 Conventional scheme of the operation of the pentose phosphate pathway. The numbers in the black circles correspond to the following enzymes: ① G6PDH, ② 6-Phophogluconolactonase, ③ 6PGDH, ④ Ribose-5P isomerase, ⑤ Ribose-5P 3-epimerase, ⑥ Transketolase ⑦ Transaldolase, ⑧ G6-P isomerase. The numbers under each of the compounds describe the fate of each of the carbons from G6-P. The colors show carbons from ribose 5-P (blue) or xylulose 5-P (green) (Kruger and von Schaewen, 2003).

Since the activity of G6PDH is markedly inhibited by a high ratio of NADPH/$NADP^+$, the PPP is regulated by cellular redox status. In the light, little operation of PPP is likely to occur in the chloroplast, because the G6PDH will be inhibited during photosynthesis by a high NADPH/$NADP^+$ ratio, as well as by a reductive inactivation involving the ferredoxin-thioredoxin system (Buchanan, 1991; Kruger and von Schaewen, 2003). Generally, PPP predominates in plastids of non-photosynthetic tissues, where the G6PDH of PPP is not sensitive to the reduction inactivation induced by ferredoxin-thioredoxin or NADPH (Kruger and von Schaewen, 2003).

1.1.3 Tricarboxylic acid cycle (TCA cycle)

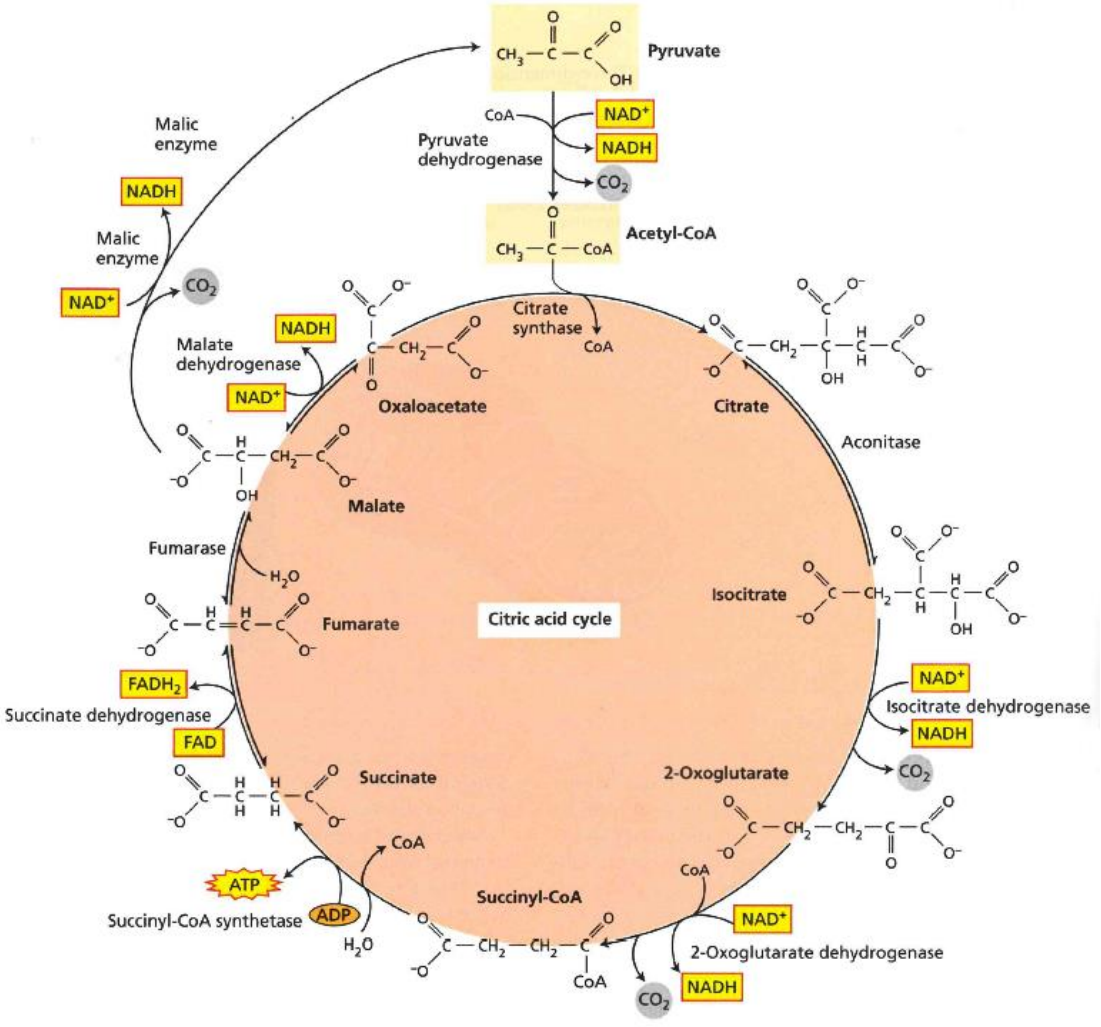

Figure 1.4. Reactions and enzymes of the plant TCA cycle. Pyruvate is completely oxidized to three molecules of CO_2 (Taiz and Zeiger, 2006).

Krebs cycle is also known as tricarboxylic acid (TCA) cycle, because of the importance of the tricarboxylic acids i.e. citric acid (citrate) and isocitric acid (isocitrate) as early intermediates. TCA cycle takes place in the mitochondrial matrix, and its operation requires pyruvate generated in the cytosol during glycolysis (Fernie *et al.*, 2004).

Inside the mitochondrial matrix (Fig. 1.4), pyruvate is firstly decarboxylated in an oxidation reaction catalyzed by the enzyme pyruvate dehydrogenase (PDH) and releases one molecule of CO_2. The product of PDH reaction, i.e. acetyl-CoA (2 C), combines with OAA molecule (4 C) forming citrate (6 C) that proceeds *via* a series of oxidative steps releasing two molecules of CO_2 (*via* oxidative decarboxylation of isocitrate and 2-oxoglutarate by enzymes isocitrate dehydrogenase (ICDH) and 2-oxoglutarate dehydrogenase (2-OGDH), respectively), and ends with the regeneration of OAA (Sweetlove *et al.*, 2010).

Generally, when TCA cycle operates in a cyclic mode, PDH, which inputs acetyl-CoA to TCA cycle, is thought to be a key regulatory point for fluxes into the cycle. This flux functions as the heart of mitochondrial respiratory metabolism, since the levels of all the intermediates involved in the cycle (citrate, isocitrate, 2-oxoglutarate, succinyl-CoA, succinate, fumarate, malate and OAA) have to be maintained constant for generating a large amount of free energy continuously.

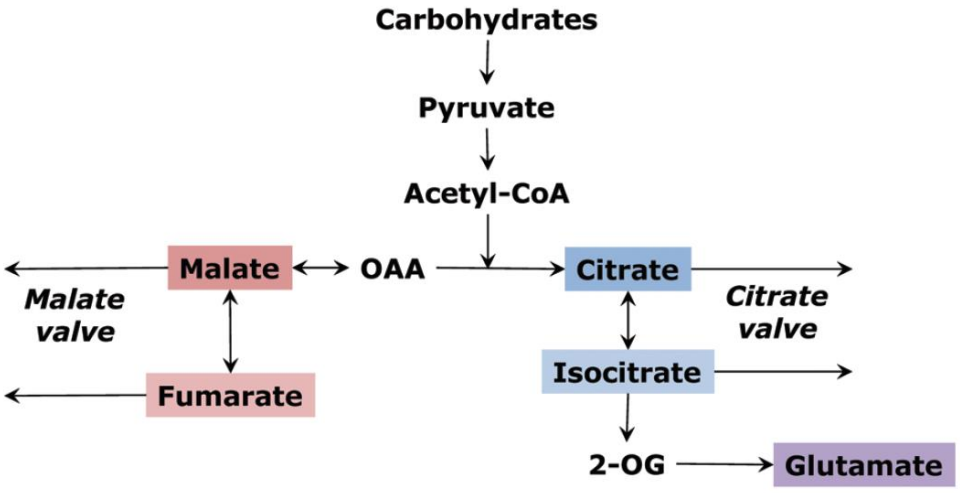

Figure 1.5 Operation of the TCA cycle as an open mode. Malate and citrate valves are the result of outflow of organic acids from the two branches. (Igamberdiev and Eprintsev, 2016).

However, it should be underlined that the TCA cycle is known to be especially plastic in plants, notably in leaves where its operating mode is now thought to vary together with day/night circadian cycles. In the light, leaf respiration (both glycolysis and TCA cycle) is highly reduced (for a review, see Atkin *et al.* (2000), because many enzymes involved (e.g. citrate synthase, CS; ICDH, 2-OGDH, succinate dehydrogenase, SDH; fumarase; ME and PK) are inhibited in the light (Hanning and Heldt, 1993; Tcherkez *et al.*, 2005). Labelling experiments have demonstrated that TCA cycle does not operate in the cyclic mode in the light, but as a 2-branched pathway (Fig. 1.5). The C-skeletons for the left-side branch (malate valve) are supplied as OAA/malate by PEPc (activated in the light), and for the right-side branch (citrate valve), which driven by the increase of redox potential under light, provides 2-OG mainly by the remobilization of the night-accumulated organic acids (Tcherkez *et al.*, 2009; Gauthier *et al.*, 2010); see also the review by Igamberdiev and Eprintsev (2016) and Igamberdiev and Bykova (2018).

In summary, TCA cycle does not always operate as a complete cycle as described above but also as an incomplete cycle, through malate and/or citrate valve (Hanning and Heldt, 1993; Gardeström *et al.*, 2002; Scheibe, 2004; Igamberdiev and Eprintsev, 2016). Indeed, not all the carbons that enter the respiratory pathway end up as CO_2. Many respiratory intermediates are the starting points for pathways such as assimilating inorganic nitrogen into organic form (e.g. amino acids), or synthesizing nucleotides and lipids, etc. (Foyer *et al.*, 2011).

1.1.4 Oxidative phosphorylation and mitochondrial electron transport chain (ETC)

ATP synthesis via oxidative phosphorylation is coupled to electron transport (see Fig. 1.6 a). During glycolysis and TCA cycle, NAD^+ accepts the electrons released by the respiratory substrate, and the released free energy is temporarily conserved in the NADH molecule. $NADP^+$/NADPH functions in redox reactions of PPP and mitochondrial metabolism. Eventually, electrons are transferred along the electron transport chain in mitochondrial internal membrane, consume O_2, and release a large amount of free energy, which is then converted to ATP to perform cell functions (Siedow and Umbach, 1995; Fernie *et al.*, 2004). When the respiratory pathway is considered as a whole, in addition to ATP synthesis, there are further functional processes of the respiratory

pathways which are integrated with ETC, such as the provision of carbon skeletons, regulation of cellular redox potential, etc. (Fig. 1.6 b, c).

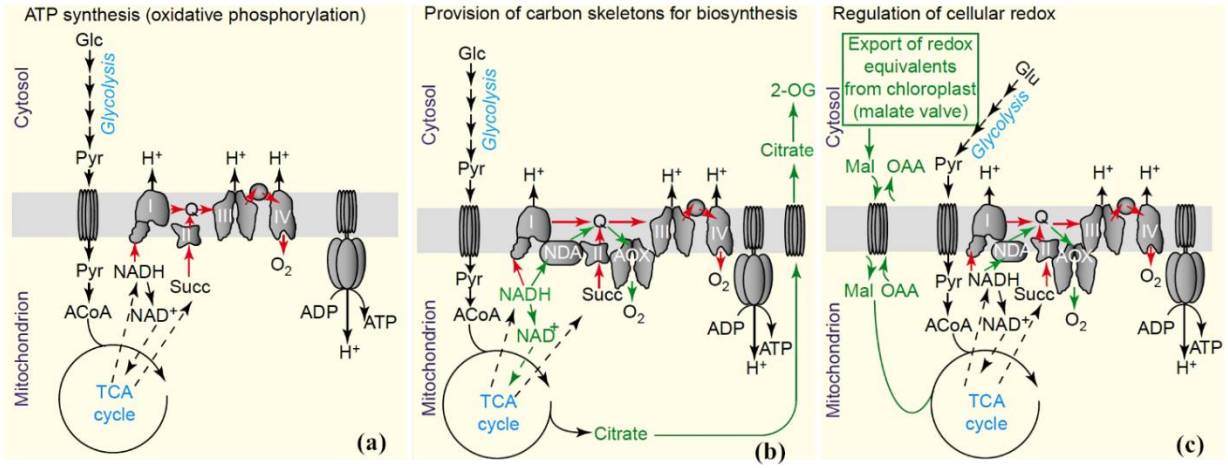

Figure 1.6 (a) ATP synthesis (i.e. oxidative phosphorylation). Pyruvate (Pyr) supplied by glycolysis is oxidized by the mitochondrial TCA cycle, and electrons from the resulting reductants (i.e. NADH and FADH2) are transferred through the electron transport chain with a chemiosmotically coupled synthesis of ATP. Complexes I–IV of the electron transport chain are shown. (b) Provision of carbon skeletons for biosynthesis. Withdrawal of TCA-cycle intermediates (the export of citrate to support nitrogen assimilation through 2-OG is illustrated) may necessitate a higher flux of portions of the TCA cycle and a higher rate of entry of electrons into the electron transport chain. These extra electrons may be accommodated by a non-proton-pumping pathway that consists of the internal NADH dehydrogenase and AOX (alternative oxidase), such that electron flow is not restricted by the rate of ATP synthesis. (c) Regulation of cellular redox. Photosynthesis requires a precise balance between the generation of NADH and ATP. One way in which this may be achieved is to export excess NADH *via* metabolite shuttles. The 'malate valve' exports excess chloroplastic reductants as malate and imports it into the mitochondrion *via* oxaloacetate (OAA) exchange. Mitochondrial malate dehydrogenase releases the NADH. The extent to which this NADH supports ATP synthesis depends on the route of electrons through the electron transport chain (red arrows represent the phosphorylating pathway; green arrows represent the non-phosphorylating pathway). (Fernie *et al.*, 2004).

Organic acids play a major role in the transformation of redox energy. Because most membranes of organelles are impenetrable to NADH, malate and citrate serve as the main substances establishing the redox state in organelles (Igamberdiev and Bykova, 2018). The export of malate from chloroplasts generates the catabolic reducing power (NADH) and drives mostly oxidative processes in cell compartments, the citrate valve generates anabolic reducing power (NADPH) and drives biosynthesis. (Fig. 1.6 b, c) (Fernie *et al.*, 2004).

1.1.5 Respiratory pathways are tightly coupled to other metabolic pathways

Glycolysis, PPP and TCA cycle are linked to several other important metabolic pathways (Noggle and Fritz, 1983; Linka and Weber, 2010). In fact, much of the reduced carbon, which is metabolized by TCA cycle is diverted to biosynthetic purposes and not oxidized to CO_2. Respiratory pathways supply carbon skeletons to the production of a wide variety of metabolites, including amino acids, lipids, and secondary metabolites (Fig. 1.7). The anaplerotic pathway refixes carbon for replenishing the TCA cycle. Acetyl-CoA, pyruvate and PEP represent the major control points of carbon flux through different pathways of primary- and/or secondary-metabolite synthesis.

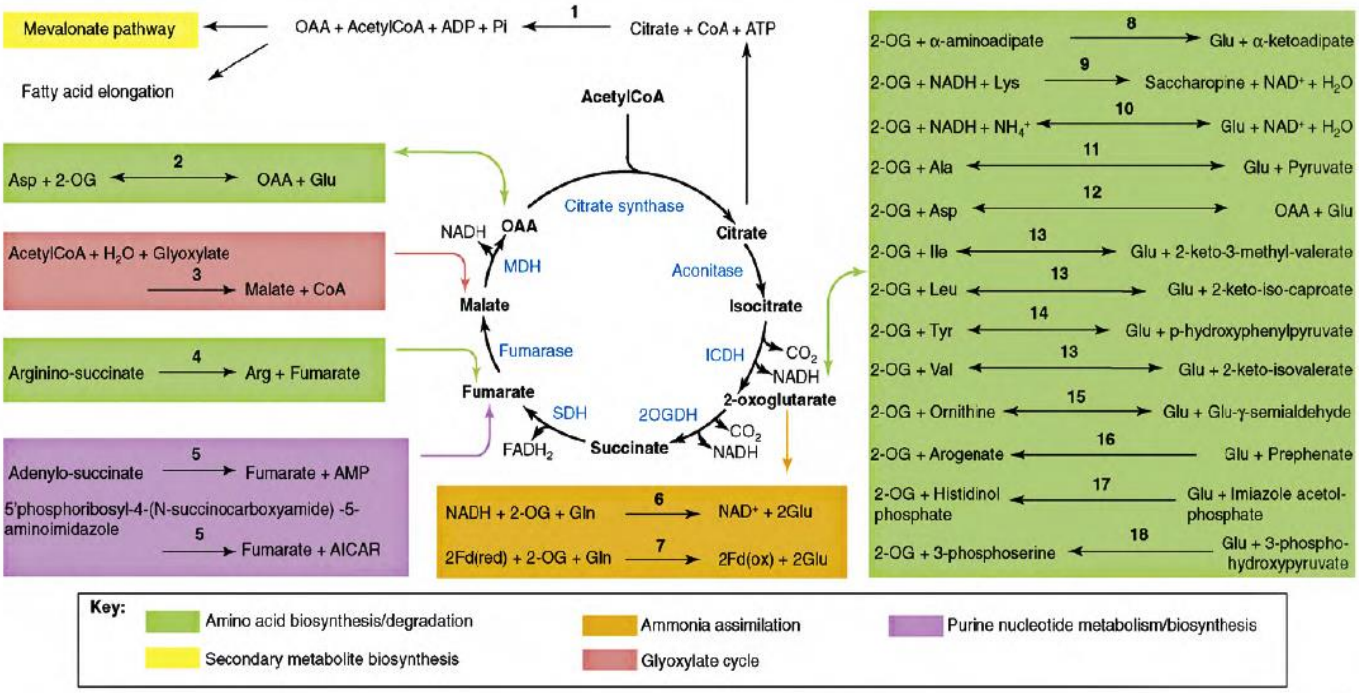

Figure 1.7 The TCA cycle is embedded in a larger metabolic network. Reactions are shown that consume or produce TCA cycle intermediates. For simplicity, co-enzymes are omitted from the TCA cycle. TCA cycle enzyme names are shown in blue. Abbreviations: ICDH, isocitrate dehydrogenase (NAD(P) dependent); MDH, malate dehydrogenase (NAD+ dependent); 2OGDH, 2-oxoglutarate dehydrogenase; PDH, pyruvate dehydrogenase; and SDH, succinate dehydrogenase. Metabolite abbreviations: AICAR, aminoimidazole carboxamide ribonucleotide; CoA, coenzyme A; Fd(ox), oxidised ferredoxin; Fd(red), reduced ferredoxin; 2-OG, 2-oxoglutarate; OAA, oxaloacetate; and Pi, inorganic phosphate. Numbered reactions are catalysed by the following enzymes: 1, ATP citrate lyase; 2, aspartate transaminase; 3, malate synthase; 4, arginosuccinate lyase; 5, adenylosuccinate lyase; 6, glutamate synthase (NADH); 7, glutamate synthase (ferredoxin); 8-18 are transaminases and aminotransferases (Sweetlove *et al.*, 2010).

1.1.5.1 Anaplerotic C-(re)fixation pathway

Synthesis of ATP is not the only function of the TCA cycle, since the cycle also provides carbon skeletons for biosynthetic processes. When the intermediates of the TCA cycle are used for biosynthesis, the anaplerotic pathways which can replenish intermediates in a metabolic cycle are believed to be of crucial importance to feed the TCA cycle (see Fig. 1.8) (Tcherkez *et al.*, 2012).

For example, export of 2-oxoglutarate for nitrogen assimilation in the chloroplast will cause a shortage of malate needed in the citrate synthase reaction (Melzer and O'Leary, 1987). The malate produced *via* PEPc and MDH, can replenish the TCA cycle by supplying the C-skeletons, which have been diverted for nitrogen assimilation (see Eq 1.1). Thus malate can enter the TCA cycle and supply the respiratory carbon skeletons without involving pyruvate delivered by glycolysis (Oliver, 1995). The C source for PEPc in the leaves during the day is mainly the atmospheric CO_2 because of open stomata. In the dark, the cyclic nature of the TCA is restored. Indeed, contrary to the light, leaf respiration is higher in the dark and is associated with the consumption of pyruvate by the TCA cycle regenerating thus the OAA molecules through the cycle (Gibbs and Beevers, 1955). The C source for PEPc in the leaves in the night is

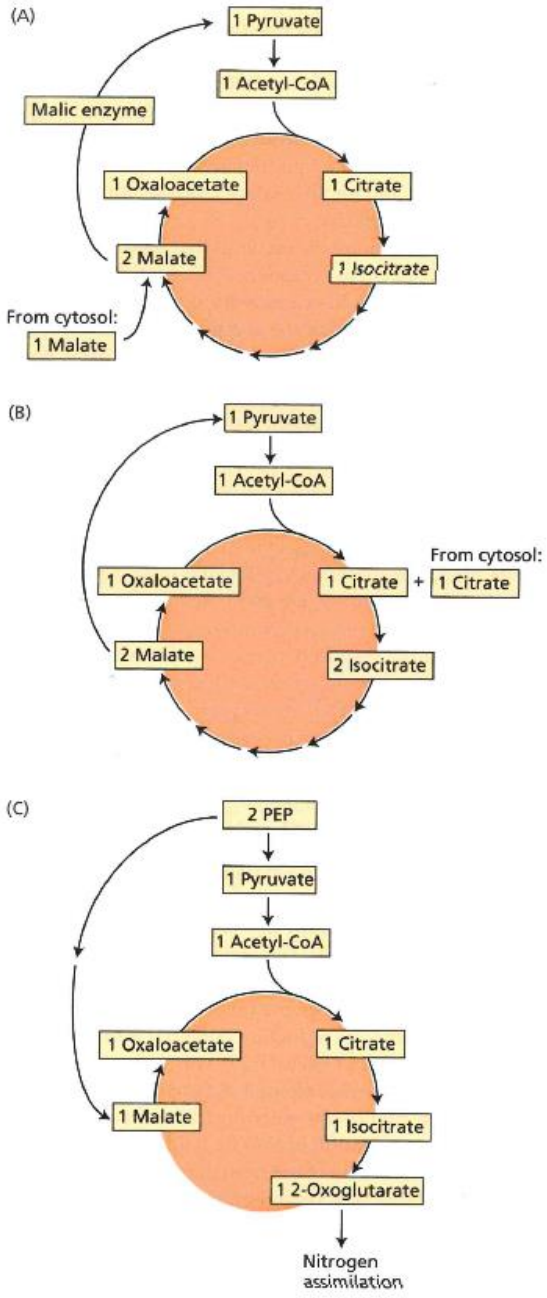

Figure 1.8 Malic enzyme converts malate to pyruvate and makes it possible for plant mitochondria to oxidize both malate (A) and citrate (B) without involving pyruvate delivered by glycolysis. PEPc and PK can convert glycolytic PEP to malate, then form 2-oxoglutarate, which is used for nitrogen assimilation (C). (Taiz and Zeiger, 2006).

mainly the leaf respired CO_2 because of closed stomata. This is also the case in roots during both the day and the night.

Pyruvate deficiency at the beginning of light-to-dark transition, can be replenished by malate, which generates pyruvate *via* mitochondrial NAD^+ malic enzyme (NAD^+-ME) and/or cytosolic $NADP^+$ malic enzyme (NADP-ME) (Eq 1.2) (Artus and Edwards, 1985).

$$\text{Malate} + \text{NAD(P)}^+ \rightarrow \text{pyruvate} + CO_2 + \text{NAD(P)H} \qquad \text{(Eq 1.2)}$$

Furthermore, many plant tissues store significant amounts of malate or other organic acids (e.g. citrate) in their vacuoles (Scheible *et al.*, 2000; Liu *et al.*, 2015; Igamberdiev and Eprintsev, 2016). The stored organic acid (e.g. citrate) can be remobilized for providing 2-OG for glutamate synthesis in illuminated leaves (Gauthier *et al.*, 2010).

1.1.5.2 Acetyl-CoA is a precursor to the biosynthesis of lipids

Fatty acid biosynthesis involves acetyl-CoA as precursor, and consists of the condensation of the two-carbon units in the plastids (Ohlrogge and Browse, 1995; Sasaki *et al.*, 1995). Only in specific situations, such as seed germination or starvation, storage lipids can be converted into carbohydrates (generally as glucose) for providing carbon sources and energy to root and shoot tissues (Poxleitner *et al.*, 2006). This process involves the oxidation of the fatty acids to produce acetyl-CoA (*via* β-oxidation) in glyoxysomes (Ohlrogge and Browse, 1995). The function of glyoxylate cycle is to convert acetyl-CoA to succinate, then to malate in mitochondria. The malate can be transported into the cytosol for supporting respiration *via* anaplerotic pathway or producing glucose *via* the gluconeogenic pathway (see Figs. 1.1 and 1.7).

1.1.5.3 Interrelationships between primary and secondary metabolism

A group of plant compounds known as secondary metabolites (secondary products, or natural products) defend plants against a variety of herbivores and pathogenic microbes. They can be divided into three chemically distinct groups: terpenes, phenolics, and nitrogen-containing compounds. Acetyl-CoA and pyruvate are necessary for terpene biosynthesis *via* the mevalonic acid pathway and the methylerythritol phosphate (MEP) pathway, respectively (Rodrıguez-Concepción and Boronat, 2002). PEP (derived from glycolysis) and erythrose-4-phosphate

(derived from PPP) provide carbohydrate precursors to the aromatic amino acids, finally yielding phenolics (lignin, flavonoids and tannins, etc.) in higher plants (Sasaki *et al.*, 1995).

1.1.6 Conclusion

Taken all together, the carbon metabolism of plants is considerably complex and the metabolic interactions among pathways of carbon assimilation and/or respiration, and the identification of respiratory substrates used for respiration are remaining deficient. In the past decades, the natural abundance of stable isotopes of the elements in plants (C, H, O, N, and S) has been widely used as a tracer or physiological marker to examine biochemical and eco-physiological mechanisms from the cell to the ecosystem scales. Carbon stable isotopes have been proved to be a powerful tool to investigate carbon primary metabolism and respiratory flux patterns (see review by Ghashghaie and Tcherkez, 2013). Furthermore, IRMS and site-specific NMR technology of the natural ^{13}C analysis are considerably developed, and used as a convenient tool to study carbon respiratory metabolism. Therefore, in the present work, we focused on using stable isotope techniques to study the effects of different carbon assimilation pathways on plant respiration and respiratory substrates.

1.2 Carbon Isotope Fractionation in Plants

Isotope fractionations during biophysical and biochemical processes are at the origin of natural differences in heavy-to-light isotope ratios (e.g. $^{13}C/^{12}C$, $^{2}H/^{1}H$, etc.) among biosphere components, metabolites and atomic positions within molecules (Ghashghaie and Tcherkez, 2013). Carbon isotope fractionation associated with plant respiration have received increasing attention because of their possible influences on efforts to elucidate factors associated with ecosystem carbon balances *via* carbon isotope analyses (Buchmann *et al.*, 1996; Yakir and Sternberg, 2000; Badeck *et al.*, 2005; Schmidt *et al.*, 2007; Ghashghaie *et al.*, 2016; Cornwell *et al.*, 2018).

Generally, isotope fractionation against heavy carbon (^{13}C) in C_3 plants occurs during photosynthetic CO_2 uptake leading to ^{13}C depletion in plant organic matter (OM) compared to air CO_2. The fractionation occurs mainly during CO_2 diffusion through stomata and during carboxylation by primary carboxylases, mainly ribulose-1,5-bisphosphate carboxylase/oxygenase (Rubisco, EC 4.1.1.39) in C_3 plants. Leaves were found to be in general ^{13}C depleted compared to all other organs (Badeck *et al.*, 2005). However, during respiration it has been shown that the CO_2

respired by leaves in the dark was ^{13}C enriched (Ghashghaie *et al.*, 2003; Tcherkez *et al.*, 2003), while it was ^{13}C depleted in the case of roots (Bathellier *et al.*, 2008) relative to their respective organs and soluble substrates (Ghashghaie and Badeck, 2014).

The following subsections will focus on the carbon isotope fractionation during photosynthesis and particularly respiratory processes, and the interactions in the carbon metabolic network.

1.2.1 Basics in isotopes

Elemental isotope composition is commonly expressed by the isotopic abundance. Isotopic abundance refers to the ratio of a particular isotope atom numbers to the total atom numbers in an isotope element mixture. Absolute abundance refers to the ratio of the existence of various elements or nuclei on the earth, also known as abundance of elements. Since the natural abundance of heavy isotopes is very low, their relative abundances are generally determined. The relative abundance of stable isotopes can be expressed as an isotope ratio (R), defined as the molar ratio of the heavy to light isotopes, e.g. for carbon, $R = {}^{13}C/{}^{12}C$. In biological and ecological research, as R values of natural material are very small (approximately 0.0112, O'Leary, 1988), it is generally more practical to express them as a deviation relative to an international standard, the isotopic composition δ. For carbon:

$$\delta^{13}C = (R_S - R_{PDB}) / R_{PDB} = (R_S / R_{PDB}) - 1 \qquad \text{(Eq 1.3)}$$

where, R_S and R_{PDB} are the isotope ratios of the sample and the PDB standard, respectively. PDB is a belemnite fossil coming from the geological formation Pee Dee in South Carolina, USA. Since the PDB is only slightly ^{13}C enriched ($R_{PDB} = 0.0112372$) compared to all organic and almost all inorganic materials, the $\delta^{13}C$ of biological samples are generally very small (expressed in per mil, ‰) and have negative values.

The differences in physical (e.g. coefficients for diffusion, dissolution, evaporation, etc.) and chemical properties (e.g. rate constants of a reaction) between the heavy and light isotopes in a given element are caused by the difference in their atomic masses. Most chemical and biochemical processes favour the initial incorporation of the lighter isotope in the product, leaving the substrate enriched in the heavy isotope (Hobbie and Werner, 2004). For a (bio)chemical reaction converting a substrate (S) into a product (P), the isotope effect can be expressed as: $\alpha = R_S/R_P$. Isotope

fractionation or discrimination (Δ) is more frequently used in biological research instead of isotope effect. Δ is defined as: $\Delta = \alpha - 1$. Otherwise, the isotope fractionation can be conveniently rearranged using δ values: $\Delta = (\delta_S - \delta_P) / (1 + \delta_P)$.

There are 2 types of fractionation: thermodynamic equilibrium fractionation, and kinetic disequilibrium fractionation. When the system is in isotopic equilibrium state, the fractionation of the isotopes between the two phases is called equilibrium isotope fractionation. As the fractionation coefficient is related to temperature, it is also called thermodynamic isotope fractionation. Kinetic disequilibrium fractionation refers to time-dependent fractionation that deviates from isotopic equilibrium, thus fractionation of isotopes between phases is constantly changing over time and reaction progress. It commonly happens during the one-way chemical reactions.

When dealing with *in vivo* isotopic fractionation (Δ) in a metabolic context (e.g. respiration), fractionating processes occur between different metabolites and also between the atoms within molecules. Kinetic isotope effects vary with the fraction of the substrate that is consumed by the reaction under different pathways. When the kinetic reaction is total, i.e. all the substrate is transformed to the product, there will be no fractionation and the product will have the same isotope composition as the substrate used. It is only when the substrate is partially consumed by the enzymatic reaction under consideration and/or another fraction of the substrate has an alternative fate (i.e. metabolic branching occurs) that the kinetic isotope effect will be expressed (Hayes, 2001; Bathellier *et al.*, 2017).

1.2.2 Carbon isotope fractionation during photosynthesis

Plant photosynthesis is the most important process in the natural world to produce carbon isotope kinetic fractionation. Photosynthetic fractionation can be estimated using either the $\delta^{13}C$ of bulk OM (integrated value during plant growth), $\delta^{13}C$ of sugars (integrates about 2-3 days of photosynthetic fractionation) or measured on-line during leaf CO_2 exchanges (instantaneous net photosynthetic fractionation under fixed conditions) (Brugnoli *et al.*, 1988). However, the photosynthetic fractionation and thus the ^{13}C content in photosynthetic products vary between plant species, plant developmental stages and environmental conditions.

$^{12}CO_2$ in the air can be more rapidly involved in the above-mentioned one-way reaction than $^{13}CO_2$ by photosynthetic enzymes. In other words, plant photosynthetic fractionation against ^{13}C

during fixation of CO_2 leads to ^{13}C depletion of both C_3 and C_4 plant organic matter (OM) compared to atmospheric CO_2 (Farquhar and Sharkey, 1982; Farquhar *et al.*, 1989). It is carried out in three steps:

(1) Diffusion of CO_2 from the atmosphere into the leaves through stomata. Carbon isotope fractionation during this diffusion process is as high as 4.4‰ against ^{13}C, thus the $\delta^{13}C$ value of intercellular CO_2 is lower than that of the extra-leaf atmospheric CO_2.

(2) Dissolution and hydration of CO_2 in leaf water. The CO_2 absorbed by plants is first dissolved in the cytoplasm. A fractionation of about 1.1‰ occurs against ^{13}C during dissolution. Then, the dissolved CO_2 is hydrated by carbonic anhydrase and C-isotope exchange occurs between CO_2 and water-soluble carbonate ions (HCO_3^-). Due to equilibrium isotope fractionation, HCO_3^- becomes ^{13}C enriched, while CO_2 becomes ^{13}C depleted (by about 9‰ at 25°C, O'Leary, 1981).

(3) Assimilation of CO_2 by carboxylation enzymes. Different photosynthetic pathways (C_3, C_4 and CAM) have different fractionation levels against ^{13}C, due to different fractionation mechanisms by different carboxylases (Rubisco and PEPc), and the temporal and spatial differences in carboxylation, resulting in distinctly different $\delta^{13}C$ values within different photosynthetic pathways.

The carbon isotope fractionation during photosynthesis in C_3 plants (Δ_{C3}) can usually be evaluated by the following model (Farquhar *et al.*, 1982):

$$\Delta_{C3} = a + (b - a) \cdot (C_i/C_a) \qquad \text{(Eq 1.4)}$$

where, a and b represent the isotope fractionation coefficients of the diffusion process (4.4 ‰) and of the Rubisco enzyme carboxylation process (29 ‰) (Roeske and O'Leary, 1984; Tcherkez, 2013), respectively, and C_i/C_a is the ratio of intercellular CO_2 (C_i) to air CO_2 (C_a) concentration. Since in C_3 plants, a small fraction of CO_2 is also fixed by PEPc, the "b" value is often taken around 27‰ (with about 5% CO_2 fixed by PEPc and 95% by Rubisco) rather than 29‰ (CO_2 fixed only by Rubisco) (Brugnoli *et al.*, 1988). Since Δ_{C3} can be approximated as the difference between the isotope compositions of the source carbon ($\delta^{13}C_{air}$) and that of the product ($\delta^{13}C_{C3\ plant}$), the equation can be written as follows:

$$\delta^{13}C_{C3\ plant} = \delta^{13}C_{air} - a - (b - a) \cdot (C_i/C_a) \qquad \text{(Eq 1.5)}$$

where, $\delta^{13}C_{C3\ plant}$ and $\delta^{13}C_{air}$ are the C-isotope composition of leaf OM (integrated value during plant growth) and the air outside the leaf, respectively. C_i/C_a value is an important eco-physiological parameter, reflecting the relative size of net photo-assimilation rate (CO_2 demand) and stomatal conductance (CO_2 supply). It is controlled by leaf photosynthetic carboxylase activity, leaf stomata movement and environmental factors, which regulate carbon metabolism involved in physiological processes. Therefore, $\delta^{13}C$ value of C_3 leaves is not only related to plant photosynthesis pathway, but also to a long-term integration of C_i/C_a ratio. From another perspective, it can be used to estimate the long-term water use efficiency of plants (Farquhar and Richards, 1984), and reflects the physiological and ecological characteristics of the plant throughout its growing season.

C_4 plants firstly fix CO_2 through PEPc in mesophyll cells and then transport the resulting C_4 acid (i.e. malate) to vascular bundle sheaths where CO_2 is released and assimilated by Rubisco. Therefore, the carbon isotope fractionation process during C_4 photosynthesis is distinct from C_3 plants, and generally can be evaluated by the following model (Farquhar, 1983):

$$\delta^{13}C_{C4\ plant} = \delta^{13}C_{air} - a - (b_4 + b_3 \cdot \Phi - s) \,.\, (C_i/C_a) \qquad \text{(Eq 1.6)}$$

where, b_4 is the carbon isotope fractionation coefficient of carboxylation reaction process by PEPc (about –5.7‰), b_3 is the fractionation by Rubisco (29‰), Φ is the rate of CO_2 leakage from photosynthetic bundle sheath cells to mesophyll cells, usually as 0.20~0.37 depending on the tightness of the bundle-sheath cell walls and s is the fractionation during dissolution and diffusion of CO_2 in the liquid phase in the cells (1.8‰). $\delta^{13}C_{OM}$ of C_4 leaves ranges from –9.2‰ to –19.3‰ (Hattersley, 1982), i.e. C_4 plants are ^{13}C enriched compared with C_3 plants. Since the $\delta^{13}C$ value of C_4 OM mainly depends on the Φ value (it controls the extent to which Rubisco fractionation is expressed) and not on C_i/C_a, and the value of $(b_4 + b_3 \cdot \Phi - a)$ is very close to 0, the formula can be simplified to: $\delta^{13}C_{C4\ plant} = \delta^{13}C_{air} - a$. Therefore, $\delta^{13}C$ of C_4 plant can be used to indirectly estimate the $\delta^{13}C$ value of atmospheric CO_2 (Hattersley, 1982; Ohsugi *et al.*, 1988; Brugnoli and Farquhar, 2000).

CAM plants can fix CO_2 through PEPc during the night with open stomata. CO_2 is then released during the day with closed stomata or alternatively is taken up during day-time with open stomata. Thus their $\delta^{13}C$ values are generally between –22‰ and –10‰. The formula for expression of the $\delta^{13}C$ value of CAM combines fractionation during the C_3 and C_4 phases of carbon

fixation at day and night, respectively. A simplified model to describe it was first published by (Farquhar *et al.*, 1989). The daytime fixation into carbohydrates of the nocturnally produced malic acid would not introduce any further ^{13}C discrimination if all the malic acid was to be consumed and all the liberated CO_2 refixed by Rubisco (see the review of Cernusak *et al.*, 2013).

In C_3 plants, CO_2 and O_2 are both competitive substrates of Rubisco to be fixed on ribulose-1,5-bisphosphate (RuBP), because carboxylation and oxygenation are both catalysed at the same active site.

The inherent kinetic properties of Rubisco depend on plant species and temperature, but the relative concentration of CO_2 and O_2 is the main determinant of the rates of photosynthesis *versus* photorespiration. CO_2 released by photorespiration is 12‰ ^{13}C depleted compared to the net photosynthetic fixed carbon changing thus the on-line photosynthetic fractionation measurements (Lanigan *et al.*, 2008). Additionally, net photosynthetic fractionation of ^{13}C is also affected by the anaplerotic CO_2 fixation pathway *via* PEPc (Tcherkez *et al.*, 2012). So that the overall fractionation between CO_2 and primary photosynthetic products is determined by all these concomitant processes together, thus varying between species and with environmental conditions. Equation 1.7 shows a more complete model of Farquhar for C_3 plants which includes the CO_2 gradient between intercellular spaces (C_i) and carboxylation sites in the chloroplasts (C_c), the fractionation during dissolution and diffusion of CO_2 in the chloroplast (s), as well as the carbon fluxes through photorespiration and day respiration and corresponding fractionations (included in term d):

$$\Delta = a\,(C_a - C_i)/C_a + s\,(C_i - C_c)/C_a + b\,(C_c/C_a) - d \qquad \text{(Eq 1.7)}$$

1.2.3 Post-photosynthetic carbon isotope fractionation

Carbon isotope composition of plant OM is generally considered to properly reflect the carbon isotope fractionation of a given photosynthesizing system during photosynthetic CO_2 assimilation. However, inter-organ isotopic differences have been repeatedly observed in plants, and leaves were shown to be generally more ^{13}C depleted compared to all other organs, suggesting that fractionating mechanisms do occur after photosynthetic CO_2 fixation in the leaves (Badeck *et al.*, 2005; Cernusak *et al.*, 2009; Ghashghaie and Badeck, 2014).

The first step of post-photosynthetic fractionation starts from the synthesis of hexoses. It is thus also called “post-carboxylation” fractionation (Gessler *et al.*, 2008). Triose phosphates, the

end-products of the Calvin cycle, are firstly used to form hexoses and synthesize the transitory starch during the daytime, the remaining triose-phosphates are transported to the cytoplasm to form sucrose. The first carbon isotope fractionation occurs by the enzyme aldolase during the synthesis of fructose-1,6-bisphosphate from trioses in the chloroplasts. During this equilibrium reaction catalysed by aldolase, the C-3 and C-4 atom positions of hexose molecules become ^{13}C enriched, while the trioses left behind in the chloroplasts become ^{13}C depleted. Indeed, intramolecular heterogeneity in ^{13}C distribution within glucose molecules has been demonstrated with C-3 and C-4 atom positions being ^{13}C enriched, while C-1, C-2, C-5 and mainly C-6 positions being ^{13}C depleted compared with the average $\delta^{13}C$ value of the molecule, in both C_3 and C_4 plants (Rossmann *et al.*, 1991; Gleixner and Schmidt, 1997; Tcherkez *et al.*, 2004; Gilbert *et al.*, 2011; Gilbert *et al.*, 2012). Importantly, the intramolecular ^{13}C pattern of glucose can be modified downstream the Calvin cycle by starch and sucrose metabolism, which are variable both spatially (among the different tissues of the plant) and temporally (day/night cycle, and seasonal cycle) (Bathellier *et al.*, 2017). Intramolecular isotopic heterogeneity has also been found in other primary and secondary metabolites, such as amino acids (Abelson and Hoering, 1961; Melzer and O'Leary, 1987), lipids (Monson and Hayes, 1982), and alkaloids (Romek *et al.*, 2015; Romek *et al.*, 2016).

Another consequence of post-photosynthetic fractionation is the differences in isotopic composition among metabolites, which is also the result of enzymatic fractionations (Brugnoli and Farquhar, 2000). The updated survey of available data shows that lipids, lignin and secondary metabolites (e.g. terpenes) are relatively ^{13}C depleted, while sucrose, cellulose, starch, protein and organic acids are relatively ^{13}C enriched compared to bulk OM (Bathellier *et al.*, 2017). Acetyl-CoA which is the substrate for synthesizing lipids is more ^{13}C depleted due to fractionation by PDH against ^{13}C, as a result, lipids have 5‰ depletion in ^{13}C (DeNiro and Epstein, 1977; Melzer and Schmidt, 1987; Schmidt and Gleixner, 1998). Amino acids are also found to be substantially ^{13}C depleted (by about 3.5‰), but this isotopic signature does not seem to be conserved in proteins (Bowling *et al.*, 2008). To be noticed, the isotope composition in metabolites can vary temporally. For example, phloem sugars are ^{13}C enriched during the night-time (because they come from transitory starch degradation), while day-time sugars originating from trioses are ^{13}C depleted (because they come from trioses left behind after aldolase reaction). Such a diel change in the ^{13}C content of phloem sugars modelled by Tcherkez *et al.* (2004) has been experimentally demonstrtaed by Gessler *et al.* (2008) in castor bean plants.

The above mentioned carbon isotope distribution within atom positions of the molecules and/or between the potential substrates of respiration, are basics for better understanding of overall plant respiratory fractionation processes and its interactions in the metabolic network.

1.2.4 Variation of respiratory fractionation in different respiratory pathways

Contrarily to photosynthetic discrimination, respiratory fractionation is more complex. Different respiratory pathways involve several enzymatic steps and reactions, which can change the ^{13}C signature of respiratory CO_2 depending on the relative commitment of the substrates at metabolic branching points. Moreover, the source carbon (i.e. respiratory substrate) used for the respiration changes with environmental conditions (e.g. drought, light or temperature, etc.), and its isotopic composition cannot be accurately determined. For all these reasons, the term 'apparent' respiratory fractionation (denoted Δ_R) is generally used (Ghashghaie *et al.*, 2003) to describe the overall discrimination during respiration by the isotopic difference between bulk OM taken as source carbon (or putative substrates mainly sugars) and the product (overall released CO_2).

It is now well known that the respiratory CO_2 released by leaves in the dark is ^{13}C enriched compared with the leaf bulk organic carbon, soluble sugars, starch or soluble proteins. This fractionation ranges between 2‰ and 6‰ on average (Ghashghaie *et al.*, 2003; Tcherkez *et al.*, 2003; Hymus *et al.*, 2005; Klumpp *et al.*, 2005; Prater *et al.*, 2006; Wingate *et al.*, 2007). By contrast, root-respired CO_2 was shown to be ^{13}C depleted relative to root OM and its soluble substrates (Bathellier *et al.*, 2008). Despite huge variability observed (more than 10‰) but in opposite direction in leaves *versus* roots, the same trend was found for all plant types (C_3 and C_4 plants), except for woody species for which both leaf- and root-respired CO_2 are ^{13}C enriched compared with their respective OM (Ghashghaie and Badeck, 2014), with some exception in each case (Fig. 1.9).

As mentioned above, not all the carbon that enters the respiratory pathway comes from the same source and ends-up as CO_2, because carbon flows into different metabolic pathways under different internal and external conditions. Generally, the isotope composition of leaf-respired CO_2 varies depending on species and environmental conditions, e.g. drought (Duranceau *et al.*, 1999; Ghashghaie *et al.*, 2001; Ghashghaie *et al.*, 2003), temperature (Tcherkez *et al.*, 2003; Schnyder and Lattanzi, 2005; Lehmann *et al.*, 2015), light intensity (Ocheltree and Marshall, 2004; Klumpp

et al., 2005), the nature of the substrate used (carbohydrates, lipids or proteins), pool seizes and the relative activity of metabolic pathways (Tcherkez *et al.*, 2003), while isotopic signal of root-respired CO_2 was shown to remain unchanged whatever the carbohydrate pool size (Bathellier *et al.*, 2009a).

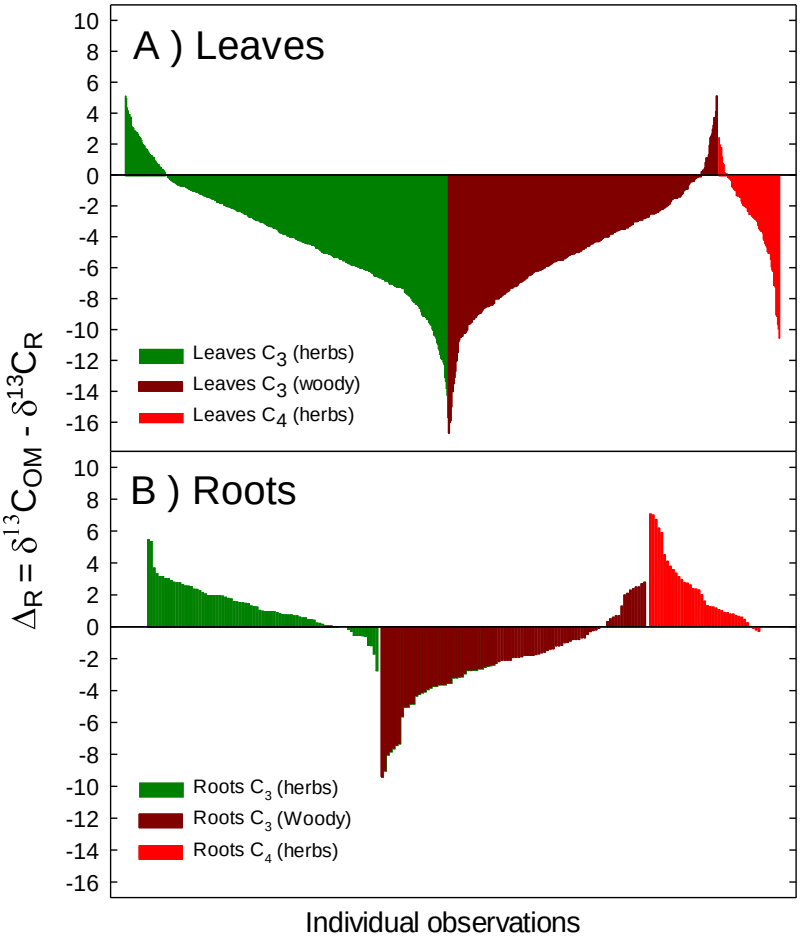

Figure 1.9 Compilation of the individual data from literature (> 900 data for leaves and > 600 data for roots) on the C-isotope discrimination during dark respiration (Δ_R) calculated as the difference between $\delta^{13}C$ of plant material (bulk OM or carbohydrates) and $\delta^{13}C$ of respired CO_2 for leaves (A) and roots (B) of C_3 herbs (green), C_4 herbs (red) and C_3 woody species (brown). Despite huge variability, in all plants, leaf-respired CO_2 is ^{13}C enriched, while root-respired CO_2 is ^{13}C depleted, except for woody species, for which root while root-respired CO_2 is^{13}C enriched. On the Y-axis, Δ_R=0 corresponds to no fractionation (i.e. $\delta^{13}C_{OM}$= $\delta^{13}C_R$). Some exceptions are observed for each case (updated and redrawn from Ghashghaie and Badeck, 2014).

Researches took lots of effort for explaining the determination for those phenomena. Tcherkez *et al.* (2003) found that dark-respired CO_2 of bean leaves became more and more ^{13}C depleted with increasing temperature and with increasing the time in darkness, while the respiratory

quotient (RQ, the ratio of respiratory CO_2 production to O_2 consumption) decreased accordingly (Fig. 1.10). They suggested that the main respiratory substrate shifted from carbohydrates to lipids when plants were subjected to high temperature and/or prolonged darkness i.e. starved. Contrarily to leaves, root-respired CO_2 was ^{13}C depleted and remained almost unchanged (Fig. 1.10).

In general, carbohydrates are the main carbon pool for respiration, but the water-soluble fraction (WSOM) which contains mostly the carbohydrates is usually taken as a reference for C-isotope composition of respiratory substrate pool (Bathellier *et al.*, 2017). However, WSOM is a mixture of carbohydrates and other compounds such as organic acids and amino acids which could influence its isotope composition.

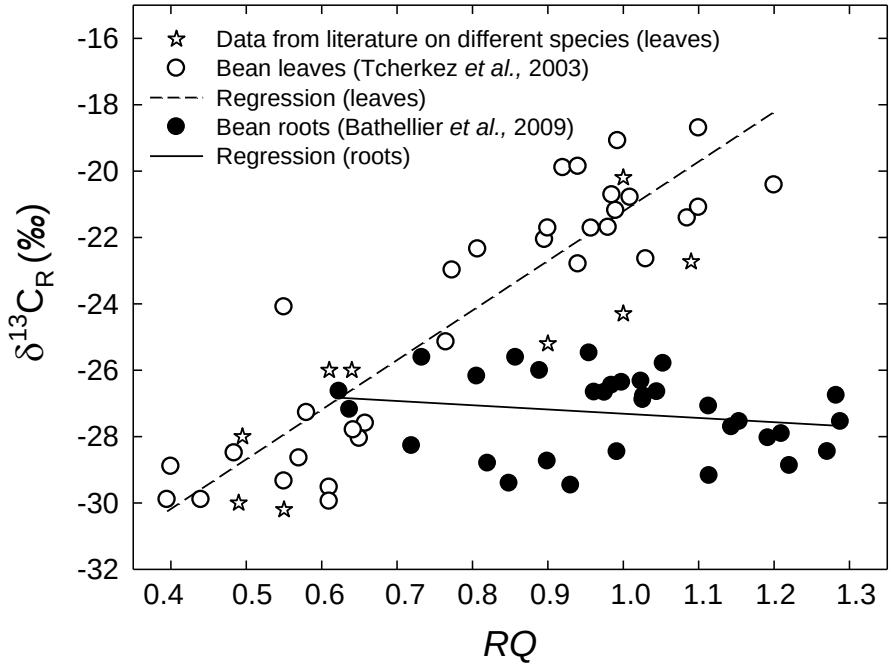

Figure 1.10 Variations of carbon isotope composition of CO_2 respired ($\delta^{13}C_R$) by attached leaves (open symbols) and washed attached roots (closed symbols) of *Phaseolus vulgaris* as a function of respiratory quotient (RQ = CO_2 evolved/O_2 consumed). Regression lines are also presented. Data points correspond to individual measurements on different plants. Leaf data are from Tcherkez *et al.* (2003) and root data from Bathellier *et al.* (2009). Additional data extracted from literature for several other plant species (tomato, castor bean, peanut, pea and radish) are indicated by stars (James, 1953; Park and Epstein, 1961; Smith and Epstein, 1971). From Ghashghaie and Badeck, 2014).

1.2.4.1 Respiratory fractionation in TCA cycle

There are 3 molecules of CO_2 released from the oxidation of pyruvate. The first one is produced by the enzyme PDH decarboxylating the C-1 of pyruvate, which originating from positions C-3 and C-4 of glucose is ^{13}C enriched compared to the average isotopic composition of the molecule, releasing thus a ^{13}C enriched CO_2 in this process (see Fig. 1.11). The remaining ^{13}C depleted carbon atoms (C-2 and C-3 of pyruvate, corresponding to C-2, C-5 and C-1, C-6 of glucose, respectively) are carried by acetyl-CoA into TCA cycle and released relatively ^{13}C depleted CO_2 *via* ICDH and 2-OGDH (Tcherkez *et al.*, 2003; Gilbert *et al.*, 2011; Gilbert *et al.*, 2012).

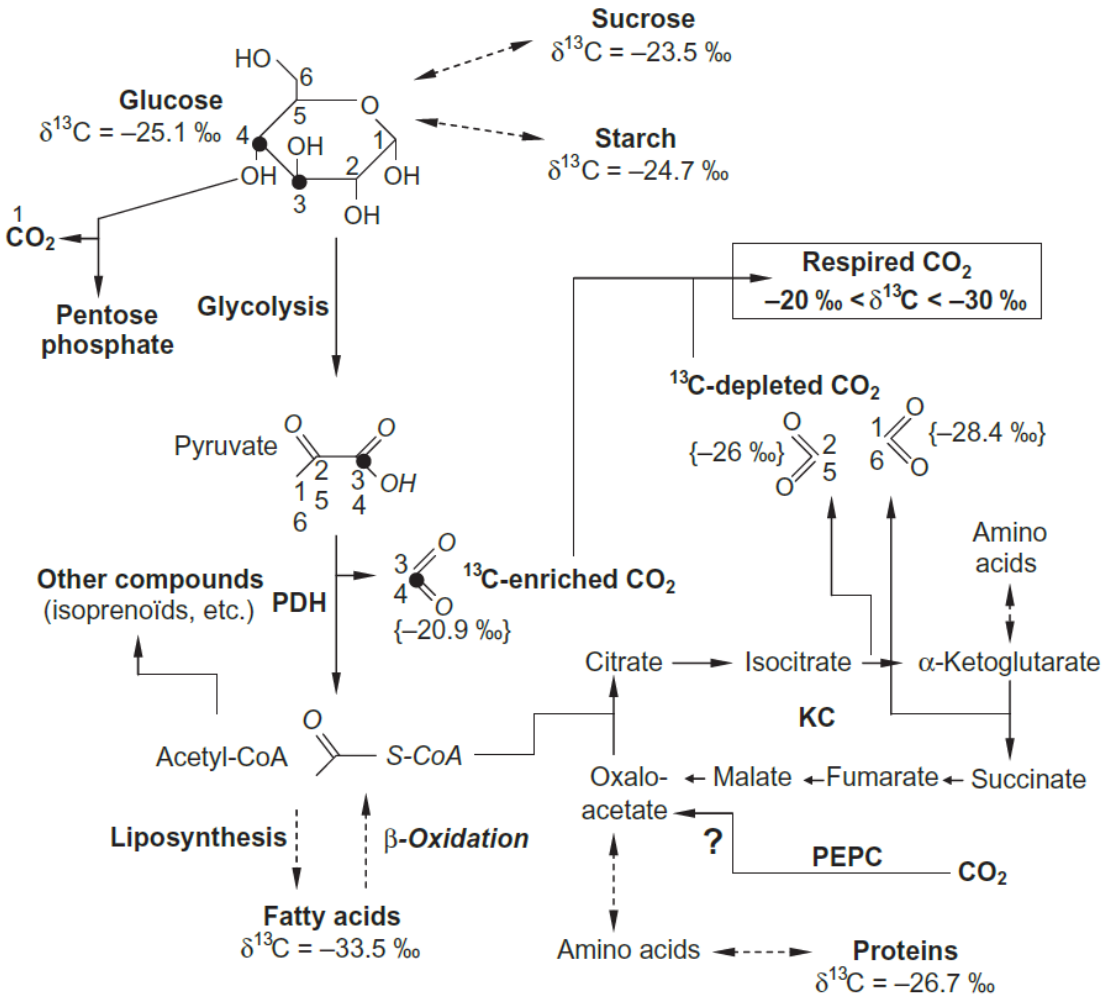

Figure 1.11 Carbon metabolism in darkness in relation to $\delta^{13}C$ of leaf-respired CO_2. $\delta^{13}C$ values of metabolites are those measured in French bean leaves. $\delta^{13}C$ of CO_2 in brackets are derived from positional $\delta^{13}C$ values in natural glucose as given by Rossmann *et al.* (1991). PEPC, phosphoenolpyruvate carboxylase; PDH, pyruvate dehydrogenase; KC, Krebs cycle. The symbol "?" points out the uncertainty about the amplitude of the PEPC reaction in darkness (Tcherkez *et al.*, 2003).

In the dark, the isotope composition of respiratory CO_2 ($\delta^{13}C_R$) is suggested to be determined by the relative magnitude of PDH and TCA decarboxylation (Badeck et al., 2005; Cernusak et al., 2009; Werner and Gessler, 2011; Ghashghaie and Badeck, 2014). In addition, most biosynthetic processes probably occur predominantly in the light (e.g. nitrogen assimilation), and consume carbon skeletons originating from TCA cycle, which functions in a non-cyclic mode. Thus the main substrate for leaf respiration can be influenced by the anaplerotic CO_2 fixation *via* PEPc, which supplies ^{13}C enriched malate into TCA cycle.

Bathellier *et al.* (2017) calculated that glycolysis and TCA cycle can only account for apparent fractionations in between about 5‰ and –2‰. However, respiratory CO_2 of leaves in the dark is 2-6‰ ^{13}C enriched compared with leaf bulk organic carbon or leaf soluble sugars. They suggested that there must be other processes, which can release more ^{13}C enriched CO_2 during leaf dark respiration.

As described above, organic acids accumulated in leaves in the light are the only obvious ^{13}C enriched pools and play the role in the maintenance of redox balance, production and consumption of ATP, support of protonic gradients on membranes, etc. Citrate and malate can be accumulated in the vacuole (Cheung *et al.*, 2014), then remobilized affecting the isotopic composition of the CO_2 released during the night. But non-cyclic TCA is less likely to occur in the dark because of energy limitations.

1.2.4.2 Respiratory fractionation in anaplerotic pathway

As noted above, the organic acids accumulated in the light constitute a ^{13}C enriched pool. On the other hand, organic acid synthesis is strongly supported by anaplerotic pathway. In this pathway, PEPc fixes ^{13}C enriched HCO_3^- in the cytoplasm for replenishing TCA cycle when the intermediates of this cycle are diverted for biosynthesis of amino acids (mainly 2-OG diverted for synthesizing glutamate/glutamine, and OAA for synthesizing aspartate/asparagine) (Marques *et al.*, 1983; Melzer and O'Leary, 1987; Salsac, 1987; Bittsanszky *et al.*, 2015; Hachiya and Sakakibara, 2016). As a result, OAA is ^{13}C enriched (in positions C-4 and C-1), leading to more ^{13}C enriched CO_2 evolved in the TCA cycle. Indeed, accounting for the isotope effect of the equilibrium between CO_2 and HCO_3^-, carbon fixation by PEPc discriminates in favour of ^{13}C by about 5.7‰ (Farquhar, 1983).

In the leaves, because the stomata are open in the light, the C source for PEPc is mostly the HCO_3^- originating from atmospheric CO_2, thus strongly enriching OAA and its derivatives, e.g. malate, fumarate, and aspartate (Melzer and O'Leary, 1987; Tcherkez *et al.*, 2011). Nevertheless, in the dark, when stomata are closed, PEPc likely refixes an important proportion of ^{13}C depleted respired-CO_2. No matter how large the flux is, its net isotope contribution will thus be small (Bathellier *et al.*, 2017).

In heterotrophic organs, the anaplerotic function of PEPc accounts for about 10% of respiratory efflux (Dieuaide-Noubhani *et al.*, 1995; Bathellier *et al.*, 2009a). However, HCO_3^- in cells should be more influenced by CO_2 pool in the soil (i.e. root- and soil-respired CO_2) instead of atmospheric CO_2. HCO_3^- fixed by PEPc would be expected to be more ^{13}C depleted compared to illuminated leaves with open stomata, although it will be dependent on their respiration rates (Ghashghaie *et al.*, 2015) and physiological conditions such as nitrogen availability (Chia *et al.*, 2000; Pracharoenwattana *et al.*, 2010).

1.2.4.3 Respiratory fractionation in PPP

During PPP, the key enzyme is G6PDH, which is regulated by the redox status of the cell. G6PDH fractionates by 16.5‰ against ^{13}C in the C-1 atom position of glucose (Hermes and Cleland, 1984), which is subsequently decarboxylated by 6PGDH releasing the ^{13}C depleted C-1 atom as CO_2. To be pointed out, 6PGDH is expected to make little impact on the fractionation, since it is a reversible enzyme, which discriminates 9.6‰ against ^{13}C in the direction of decarboxylation, but 4‰ in favour of ^{13}C reversibly (Rendina *et al.*, 1984; Bathellier *et al.*, 2017).

Root-respired CO_2 is on average more ^{13}C depleted and less variable than that of leaves in many species (Bathellier *et al.*, 2009a; Ghashghaie and Badeck, 2014). Experiments using the positionally labelled substrates (i.e. glucose and pyruvate) have shown a high activity of PPP in roots (22%), which could partly explain the ^{13}C depleted CO_2 respired by roots (Bathellier *et al.*, 2009a). Further work is still needed for exploring the existence of other ^{13}C depleted pools used for root respiration.

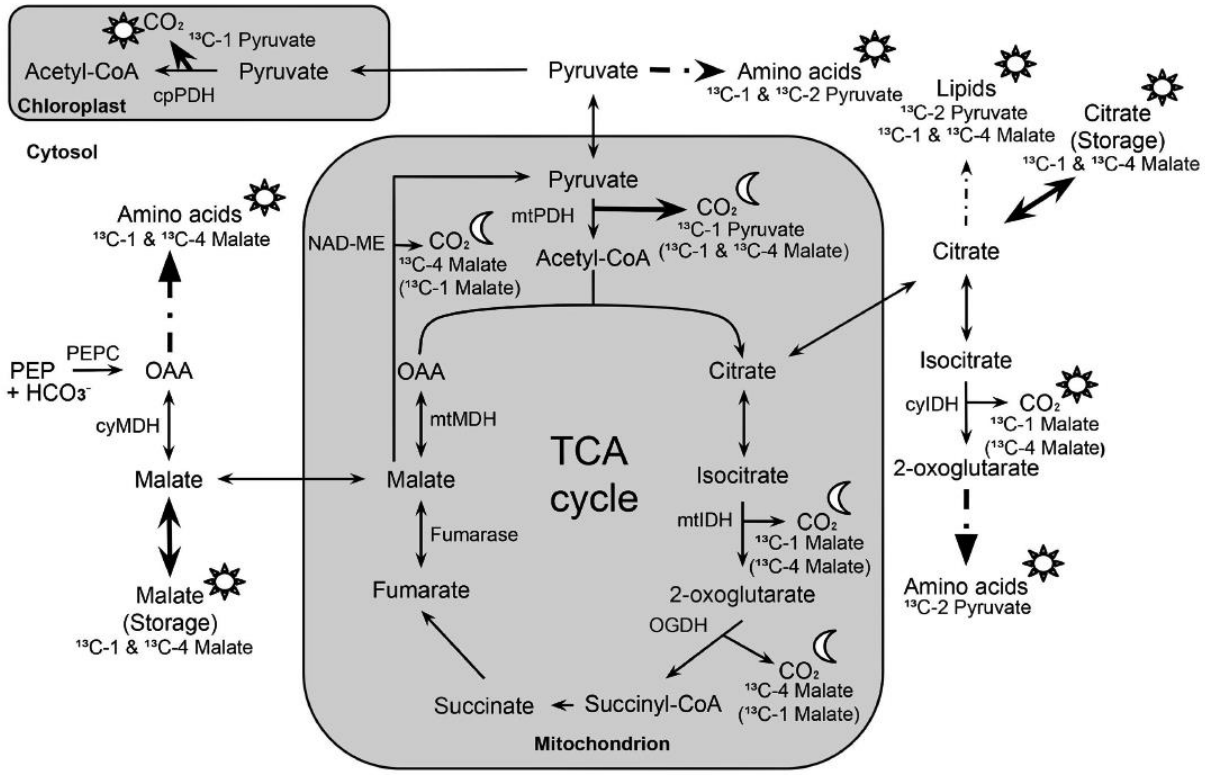

Figure 1.12 Overview of ^{13}C allocation from position-specific ^{13}C-labelled malate (^{13}C-1, ^{13}C-4) and pyruvate (^{13}C-1, ^{13}C-2) during light-to-dark transitions. Sun and half-moon symbols denote temporary ^{13}C allocation during light or dark periods (LEDR), respectively. Solid arrows indicate ^{13}C allocation of highest importance, while dashed arrows indicate reactions with intermediate steps. ^{13}C-labelled malate substrates in brackets denote alternative respiratory pathways due to the influence of NAD-ME (decarboxylation of C-4 position of malate) and fumarase (randomization of C-1 and C-4 position of malate). The following abbreviations are used: cyIDH and mtIDH, NADP-cytosolic and NAD-mitochondrial isocitrate dehydrogenase; cyMDH and mtMDH, cytosolic and mitochondrial malate dehydrogenase; NAD-ME, NAD-malic enzyme; OAA, oxaloacetate; OGDH, 2-oxoglutarate dehydrogenase; cpPDH and mtPDH, chloroplast and mitochondrial pyruvate dehydrogenase; PEPC, phosphoenolpyruvate carboxylase; TCAcycle, tricarboxylic acid cycle (Lehmann *et al.*, 2016).

1.2.4.4 The special case of light-enhanced dark-respiration (LEDR)

Light-enhanced dark-respiration (LEDR) occurs within 15-25 min of light-to-dark transition, accompanying a short peak of respiration rate with highly ^{13}C enriched leaf-respiratory CO_2 (in both C_3 and C_4 plants) compared with the values after longer periods of being in darkness (Barbour *et al.*, 2007; Gessler *et al.*, 2009; Priault *et al.*, 2009; Lehmann *et al.*, 2015; Ghashghaie *et al.*, 2016). For example, leaf-respired CO_2 at the beginning of the dark has been shown to be ^{13}C enriched more than 10‰ compared with leaf OM (i.e. $\delta^{13}C_R$ values around –15‰ in C_3 leaves and around –4‰ in C_4 leaves), while after 1-2 h of darkness the $\delta^{13}C_R$ values were around –21‰ or

more negative for C_3 leaf-respired CO_2 and around –13‰ for C_4 maize leaf-respired CO_2. LEDR has been attributed to a rapid consumption of ^{13}C enriched malate pool accumulated in the light, and the time-frame changes based on the photoperiod and temperature (Igamberdiev *et al.*, 1997; Atkin *et al.*, 1998). Labelling experiments have demonstrated that the subcellular origin of the malate pool involved in LEDR is mitochondrial (*via* fumarase) by TCA reactions or by NAD-ME (Lehmann *et al.*, 2016) (Fig. 1.12).

1.3 Nitrogen Metabolism in Plants

Most plant species can utilize inorganic nitrogen sources i.e. NH_4^+ and NO_3^- (Raven and Smith, 1976; Yin and Raven, 1998; Lasa *et al.*, 2002b). Nitrate is the major form of N in most aerated soils, whereas ammonium can be a dominant form in some acidic and/or anaerobic environments (Guo *et al.*, 2007; Roosta *et al.*, 2009; Masclaux-Daubresse *et al.*, 2010; Hachiya and Sakakibara, 2016; Sarasketa *et al.*, 2016).

Nitrate is reduced to ammonium by nitrate reductase (NR), and nitrite reductase (NiR) and its reduction requires eight moles of electrons per mole of nitrate. Thus, ammonium utilization greatly decreases the energy consumption required to synthesize organic N compounds (Salsac, 1987; Pate and Layzell, 1990). Ammonium is thus a preferable N source for the plants. However, high levels of ammonium in living tissues is toxic to both plants and animals. Plants assimilate ammonium near the site of absorption or generation and rapidly store any excess in their vacuoles, thus avoiding toxic effects on membranes and the cytosol (Raven and Smith, 1976; Salsac, 1987; Britto and Kronzucker, 2002; Esteban *et al.*, 2016). In contrast to ammonium, plants can store high levels of nitrate, or they can translocate it from tissue to tissue without deleterious effects (Raab and Terry, 1995).

1.3.1 Nitrogen uptake

Plant roots actively absorb both nitrate and ammonium *via* several high-affinity (HATS) and low-affinity (LATS) ion-proton cotransporters. HATS function dominantly in low level, while LATS function in high level of nitrogen supply (Crawford and Forde, 2002; Miller *et al.*, 2007; Masclaux-Daubresse *et al.*, 2010).

Since nitrate is negatively charged, the addition of negative electric charge into the cytosol imposes energy requirement for the transport of the nitrate ion at all concentrations. The energy is provided by a transmembrane pH and electrical potential gradients *via* $2H^+$:$1NO_3^-$ symporter (Miller *et al.*, 2007; Kraiser *et al.*, 2011) (see Fig. 1.13).

The major HATS for ammonium uptake into plants is AMT1 family, which can carry ammonium *via* $1H^+$:$1NH_4^+$ symporter (Ludewig *et al.*, 2007; Lanquar *et al.*, 2009; Ortiz-Ramirez *et al.*, 2011). LATS of ammonium is hypothesized to be identical or very similar to the K^+ uptake transporter. Its activity is not downregulated even at high ammonium concentration (toxic level), so that it leads to K^+ starvation and uncontrollable uptake of NH_4^+. To be noted that, NH_4^+ uptake is a passive process, while transport of NH_4^+ from the cytosol to the external medium must be energetically active, which may lead to high ATP consumption and respiration rate, resulting in a decline of plant growth.

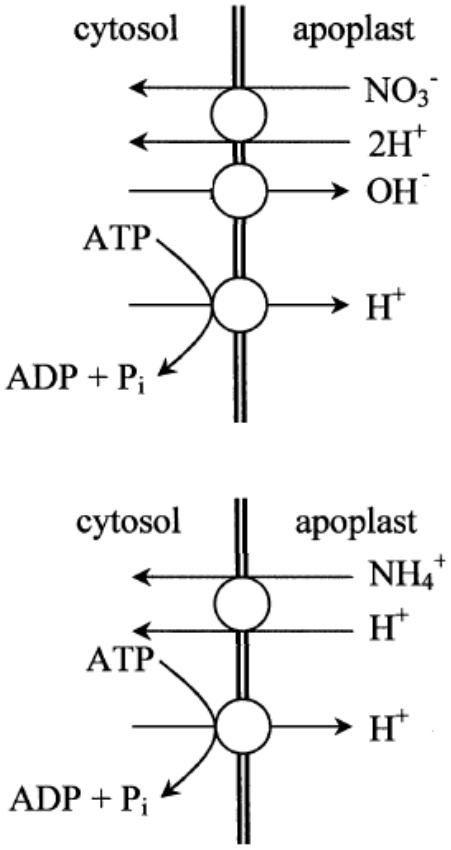

Figure 1.13 The role of proton transport as charge-balancer in inorganic nitrogen transport. Transport of NO_3^- and NH_4^+ across the plasma membrane, rectified by proton pumping by membrane ATPase (redrawn from Britto and Kronzucker, 2005).

1.3.2 Assimilation and translocation of different nitrogen sources

In leaves, nitrogen is mainly assimilated in the light as a result of the requirement for ATP and reductants of involved enzymes. In roots, nitrogen is assimilated either in the dark or in the light.

Plants eventually assimilate most of the absorbed nitrate into organic nitrogen compounds. The first step of this process is the reduction of nitrate to nitrite *via* the enzyme nitrate reductase (NR) in the cytosol (Mengel *et al.*, 1983; Warner and Kleinhofs, 1992; Oaks, 1994). Nitrite is a highly reactive and potentially toxic ion, thus plant cells immediately transport the generated nitrite from cytosol into chloroplasts in leaves and plastids in roots. In these organelles, the enzyme nitrite

reductase (NiR) reduces nitrite to ammonium (Eqs 1.8 and 1.9). NiR requires six moles of electrons per mole of nitrite, which accounts for 75% of the electrons consumed during nitrate reduction. Energy for the reduction is derived from photosynthetic electron transport and from NADPH generated by the oxidative PPP in non-green tissues.

$$NO_3^- + NAD(P)H + H^+ \rightarrow NO_2^- + NAD(P)^+ + H_2O \qquad \text{(Eq 1.8)}$$

$$NO_2^- + 6Fd_{red} + 8H+ \rightarrow NH_4^+ + 6Fd_{ox} + 2H_2O \qquad \text{(Eq 1.9)}$$

Fd is ferredoxin, and the subscripts *red* and *ox* stand for *reduced* and *oxidized*, respectively.

Nitrate transport is strongly regulated according to its availability. The enzymes required for NO_3^- transport, as well as for its assimilation, are induced in the presence of NO_3^- in the environment (Scheible *et al.*, 1997), but repressed if NO_3^- accumulates in the sink cells. Nitrate absorbed by roots can be stored or assimilated in the roots or transported to the shoot, where again it can be reduced or stored, such as in lettuce and spinach as reported, respectively, by Sindelar and Milkowski (2012) and Andrews *et al.* (2013). In many plants, when the roots receive small amounts of nitrate, it is reduced primarily in the roots. As the NO_3^- supply increases, a greater proportion of the absorbed NO_3^- is translocated to the shoots and assimilated there in herbaceous species (Marschner *et al.*, 1996; Scheurwater, 2002; Hachiya and Sakakibara, 2016). But even under similar condition of NO_3^- supply, the balance between root and shoot NO_3^- assimilation varies from species to species.

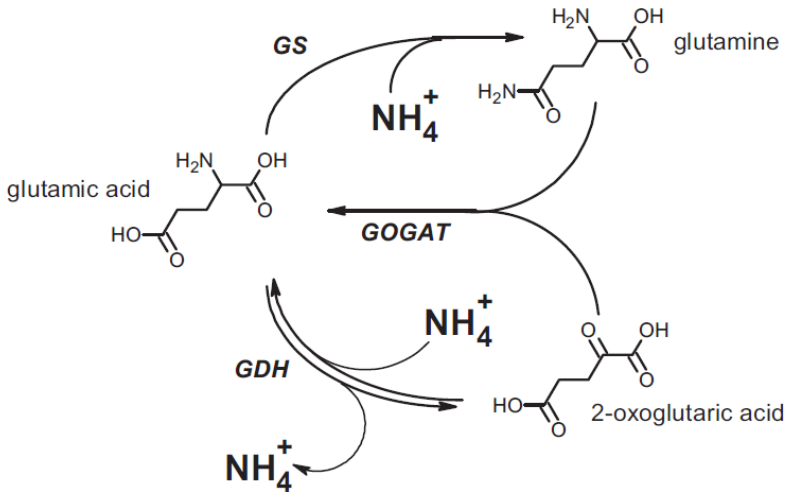

Figure 1.14 Key detoxification pathways of ammonium in plants. GS: glutamine synthetase; GOGAT: glutamate synthase (or glutamine 2-oxoglutarate aminotransferase); GDH: glutamate dehydrogenase (Bittsanszky *et al.*, 2015).

Plant cells avoid NH_4^+ toxicity by rapidly converting the NH_4^+ generated from NO_3^- assimilation or photorespiration into amino acids (Guo *et al.*, 2007; Andrews *et al.*, 2013). The primary pathway for this conversion is GS/GOGAT, which involves the sequential actions of glutamine synthetase (GS), and glutamate synthase (known as GOGAT or glutamine 2-oxoglutarate aminotransferase) (See Fig. 1.14).

$$\text{Glutamate} + NH_4^+ + \text{ATP} \rightarrow \text{glutamine} + \text{ADP} + P_i \qquad \text{(Eq 1.10)}$$

$$\text{Glutamine} + \text{2-oxoglutarate} + \text{NADH} + H^+ \rightarrow 2\ \text{glutamate} + NAD^+ \qquad \text{(Eq 1.11)}$$

$$\text{Glutamine} + \text{2-oxoglutarate} + Fd_{red} \rightarrow 2\ \text{glutamate} + \text{NAD} + Fd_{ox} \qquad \text{(Eq 1.12)}$$

Plants contain two different classes of both GS and GOGAT, one in the cytosol and the other one in root plastids or in the chloroplasts (Lam *et al.*, 1996; Vanoni, 2015). In the cytosol, the cytosolic GS forms (GS1) together with NADH-GOGAT assimilates NH_4^+ absorbed from the rhizosphere, or of glutamine translocated from roots or senescing leaves to vascular bundles of developing leaves. In root plastids or in the chloroplasts, GS2 with Fd-dependent GOGAT generates amides for local consumption in roots, or functions for NH_4^+ reassimilation during photorespiration in the chloroplast (Lam *et al.*, 1996; Suzuki and Knaff, 2005; Forde and Lea, 2007; Bittsanszky *et al.*, 2015).

Glutamate dehydrogenase (GDH) provides an alternative pathway for synthesizing or deaminating glutamate (Masclaux-Daubresse *et al.*, 2010). Its primary function is deaminating glutamate, which produces during the reallocation or under ammonium stress (Skopelitis *et al.*, 2006), thus GS-GOGAT pathway always plays the main N flux for ammonium assimilation.

When ammonium is used directly as N source, a high proportion of its assimilation occurs in the roots (Salsac, 1987; Britto and Kronzucker, 2002; Esteban *et al.*, 2016; Hachiya and Sakakibara, 2016). Low concentrations (mM magnitude) of ammonium can be converted to amino acids in the roots then loaded into the xylem *via* specific transporters (Tegeder, 2014). But if GS capacity in roots is exceeded by a large amount of ammonium, NH_4^+ may be directly loaded into the xylem and delivered to the shoots then stored out to the apoplast (Allen and Smith, 1986; Schjoerring *et al.*, 2002).

1.3.3 Interactions between nitrate and ammonium in plants

Many evidences have indicated that co-provision of nitrate and ammonium stimulates plant growth; NO_3^- responses can be affected by the co-provision of NH_4^+, and NH_4^+ responses are altered by NO_3^- (Cao and Tibbitts, 1993; Britto and Kronzucker, 2002; Siddiqi *et al.*, 2002).

During nutrient uptake, it was found that compared with NO_3^- alone, net NO_3^- uptake was significantly repressed by the co-provision of NH_4^+ involved in a major HATS (AtNRT2.1) (Kronzucker *et al.*, 1999a; Kronzucker *et al.*, 1999b; Cerezo *et al.*, 2001; Hachiya and Sakakibara, 2016). On the other side, when NO_3^- is present, net NH_4^+ uptake becomes higher, but the reason remains uncertain (Kronzucker *et al.*, 1999c; Hachiya and Sakakibara, 2016).

As a signal, NO_3^- stimulates gene expression, which is involved in glutamine loading in xylem. It was suggested that NO_3^- enhances NH_4^+ assimilation by accelerating amino acid biosynthesis (Ladwig *et al.*, 2012).

1.3.4 Metabolic regulations in response to different inorganic N sources

1.3.4.1 N source determines apoplastic pH regulation

Nitrogen source is known to be determinant for apoplastic pH. Nitrate and protons are co-transported into the cytosol *via* NRTs, whereas NH_4^+ uptake is accompanied by proton extrusion *via* the plasma membrane H^+-ATPase to maintain the charge balance (Meharg and Blatt, 1995; Britto and Kronzucker, 2005). Thus, the extracellular environments are alkalinized and acidified following the application of NO_3^- and NH_4^+, respectively.

For example, if the root medium is switched from NO_3^- to NH_4^+, there will be a rapid decrease in apoplastic pH (Schjoerring *et al.*, 2002), because of an excess H^+ generated during NH_4^+ uptake and assimilation. Excess H^+ must then be excreted or neutralized to maintain cytoplasmic pH. Otherwise, the disordered pH would be toxic for plant. H^+ generated in the roots is excluded into the soil (Raven and Smith, 1976; Andrews *et al.*, 2013). However, when GS capacity is overloaded by large amount of NH_4^+ supply, extra free NH_4^+ is distributed to the shoots, and visual symptoms would appear (e.g. necrotic lesions and very dark green leaves).

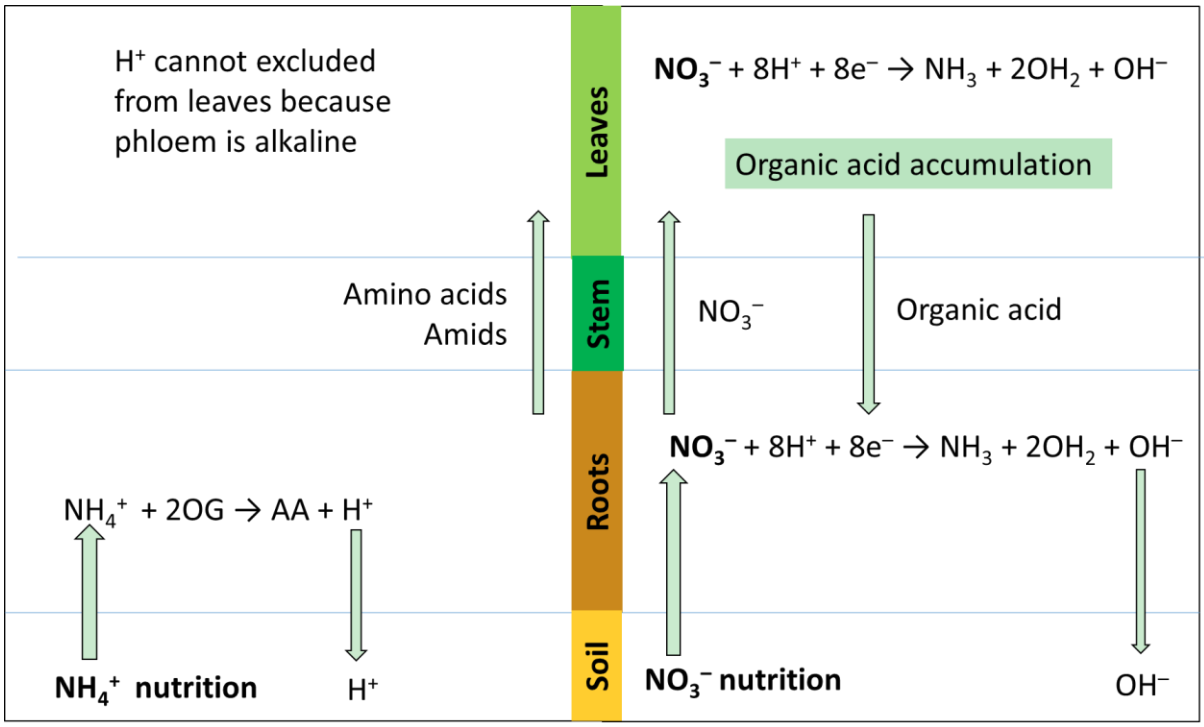

Figure 1.15 A simplified presentation of inorganic N absorption by the roots and its transport to the leaves and its assimilation into organic acids (NO_3^- is presented at the right side and NH_4^+ at the left-side.

By contrast, NO_3^- uptake results in a high consumption of H^+ and thus high production of OH^- (Raven, 1985). Similar to NH_4^+, excess OH^- can be excluded to the soil if it is generated in roots (Fig. 1.15). In the case of shoots, the classic biochemical pH-stat model presupposes that the excess OH^- generated in shoots is neutralized by the synthesis of organic acids (in particular, malate, which can be retained in the shoots or co-transported with K^+ from shoot to root), which is linked to OH^- excretion from the root to the soil (Andrews *et al.*, 2013) (Fig. 1.15). However, Britto and Kronzucker (2005) proposed another model, and they conceived that higher accumulation of malate in NO_3^--grown plants is for achieving electro-neutrality: the acidification by H^+/NO_3^- symporter of the cytosol results in a higher uptake of cations (especially K^+ and Ca^{2+}) in NO_3^--grown plants, and malate is a good and strong anion to neutralize charge-balancing.

1.3.4.2 Cellular redox status shifted by different N sources

The NADPH produced by the PPP usually provides energy for reducing NO_3^- to NH_4^+ in non-photosynthetic tissues (Esposito *et al.*, 2005). However, when NH_4^+ is supplied as N source alone,

there is no need for NO_3^- reduction. Under the condition where NO_3^- and NH_4^+ coexist, NO_3^- absorption is depressed by NH_4^+, thus the demand for NADPH decreases either. Therefore, the ratio of NADPH/$NADP^+$ increases with ammonium supplementation, then the flux of PPP accordingly decreases (Hachiya and Sakakibara, 2016).

1.4 N-Assimilation Impact on Carbon Metabolism and Isotope Fractionation

Because of the requirements of energy consumption, redox regulation and carbon skeleton for metabolite synthesis, respiration and nitrogen assimilation are intimately linked in plant cells. Plant growth and development depend on the metabolic pathways of carbon-nitrogen interactions (Lawlor, 2002; Foyer *et al.*, 2011; Igamberdiev and Eprintsev, 2016). Amino acid synthesis and anaplerotic pathway are thought to be the interfaces between C and N metabolism.

During generation of carbon skeletons for organic nitrogen compounds (e.g. amino acids), organic acids are synthesized through different pathways in response to different N types in different tissues (Raven and Farquhar, 1990). As respiratory substrates, organic acids play a key role to influence both the $\delta^{13}C_{OM}$ and respiratory $\delta^{13}CO_2$ in plants. Furthermore, the carbon sources for yielding organic acids (atmospheric CO_2, dissolved CO_2 or HCO_3^-) are the most important factors, which determine the final isotope signature of organic acids in plants. The relation between nitrogen assimilation, carbon metabolism and isotope fractionation are detailed below.

1.4.1 Amino acid biosynthesis links C and N metabolism

Plants synthesize approximately 20 amino acids. All carbon skeletons for biosynthesis of amino acids are derived from intermediates of glycolysis, PPP, or TCA cycle (see Fig. 1.16). Nitrogen enters these pathways mainly through 2-oxoglutarate (by forming glutamate and glutamine *via* GS/GOGAT) or OAA (by forming aspartate and asparagine *via* aspartate aminotransferase, Asp-AT and/or asparagine synthetase, AS) from TCA cycle. Once nitrogen is assimilated into glutamine and glutamate, it can then be incorporated into other amino acids *via* transamination reactions.

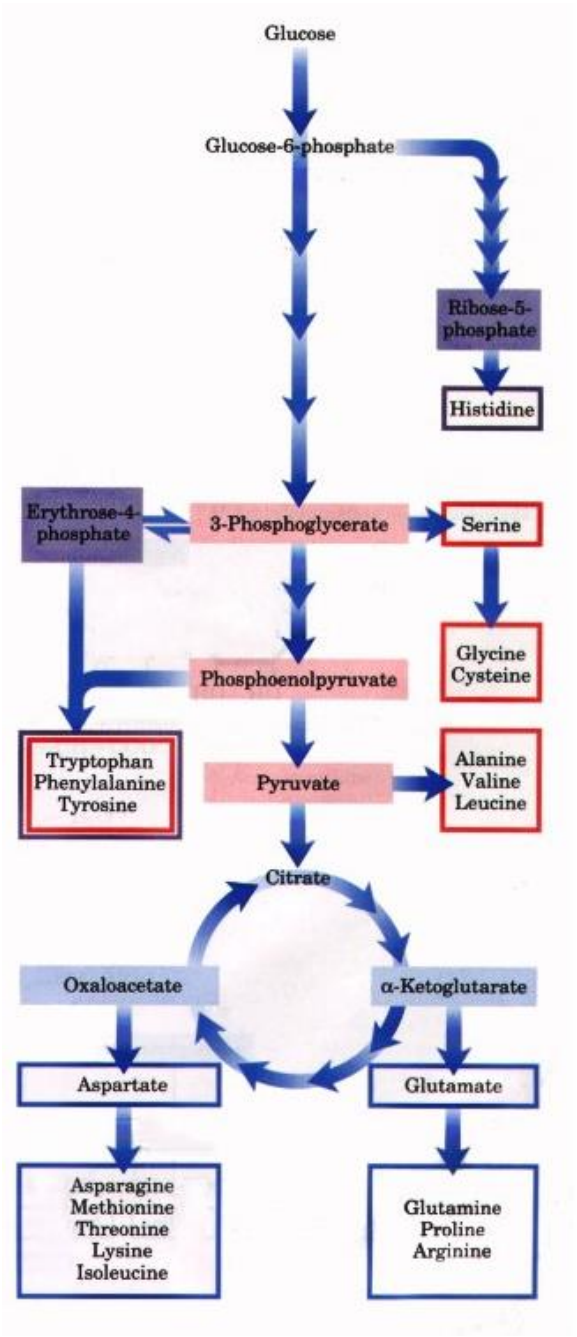

GS and AS consume energy generated during respiration. High-energy conditions (i.e., under light and high level of carbohydrates) stimulate GS and GOGAT, inhibit AS, and thus favour nitrogen assimilation into glutamine and glutamate for new plant material synthesis. In contrast, energy-limited conditions inhibit GS and GOGAT, stimulate AS, and thus favour nitrogen assimilation into asparagine for long-distance transport or long-term storage (Lam *et al.*, 1996).

In summary, during nitrogen assimilation, NR, NiR and GOGAT require reducing power as either Fd or NAD(P)H generated in PPP (Eq 3.1 to 3.5). ATP is essential for GS and AS reactions and carbon skeletons for amino acid synthesis, especially 2-oxoglutarate and OAA, generated through TCA cycle. It is thus believed that amino acid biosynthesis links C and N metabolism.

Figure 1.16 Overview of amino acid biosynthesis. Precursors from glycolysis (red), the citric acid cycle (blue), and the pentose phosphate pathway (purple) are shaded, and the amino acids derived from them are boxed in the corresponding colours (Lehninger *et al.*, 1993).

1.4.2 PEPc may be another interface linking C and N metabolism

PEPc is widely distributed in all photosynthetic and nonphotosynthetic organisms (Masumoto *et al.*, 2010). It is a multipurpose, highly regulated enzyme, subject to the pools of a wide range of metabolites (PEP, G6P, HCO_3^-, citrate, malate, aspartate, asparagine, glutamate, and glutamine,

etc.) (Britto and Kronzucker, 2005). Latzko and Kelly (1983) described its 11 possible functions in C_3 plants including replenishment of TCA intermediates and recapture of respired CO_2.

As described above, the carbon skeletons aminated to form amino acids are organic acids (more specifically 2-oxoglutarate and OAA), which also function as intermediates in the TCA cycle, and therefore their depletion must be counteracted. Hence, anaplerotic carbon (re)fixation is essential to be active (Britto and Kronzucker, 2005).

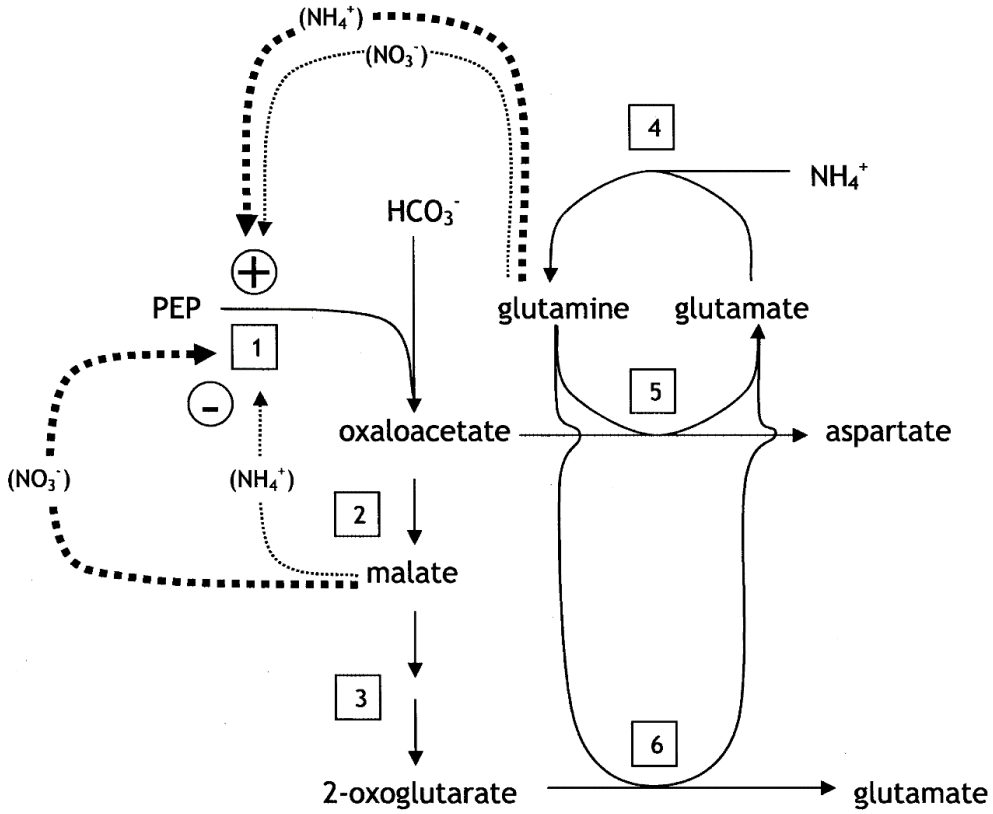

Figure 1.17 A model outlining a revised role of PEPc in inorganic N assimilation. Key enzymes or enzyme groups are indicated in boxed numbers as follows: (1) PEPc; (2) MDH; (3) TCA cycle enzymes; (4) GS; (5) Asp-AT; (6) GOGAT. Note the legend: bicarbonate (HCO_3^-) is produced by the activity of carbonic anhydrase. Dashed lines indicate feedback activities on PEP carboxylase by metabolic intermediates. Circled plus or minus signs indicate positive or negative feedback, respectively. Thickness of dashed lines indicates intensity of feedback, due to nitrogen source-dependent variations in pool sizes of feedback agents (Britto and Kronzucker, 2005).

At the end of glycolysis, plants have alternative pathways for metabolizing PEP. The operation of PK and PEPc can produce alternative organic acids – pyruvate or malate – both can be transported to the mitochondrion and enter TCA cycle (Fig. 1.17). When TCA cycle intermediates are withdrawn for nitrogen assimilation, in most non-photosynthetic tissues, PEPc

can perform a bypass reaction for generating OAA instead of pyruvate. The resulting malate (derived from OAA) then enters the mitochondria for ensuring a continuous functioning of the TCA cycle (Huppe and Turpin, 1994; Berveiller *et al.*, 2010). It has been proved that PEPc activity is positively correlated with the activity of GS (Koga and Ikeda, 2000; Lasa *et al.*, 2002b). Furthermore, the ratio of glutamine to glutamate can indicate anaplerotic efficiency. This ratio reflects the extent to which nitrogen has been incorporated into organic forms from organic acid pools (Britto and Kronzucker, 2005). At genome level, it was shown in maize leaves, that the exogenous nitrogen supply increased the expression of protein and mRNA for PEPc (Sugiharto and Sugiyama, 1992). Therefore, PEPc may be considered as an important interface between carbon and nitrogen metabolism.

In addition, NO_3^- reduction is accompanied by excess OH^- production. In the roots, OH^- may be directly excreted into the soil, while in the leaves, OH^- produced by NO_3^- assimilation cannot be excreted to the environment (Raven and Smith, 1976; Salsac, 1987; Raven and Farquhar, 1990). As described above, based on the classic biochemical pH-stat model of cytosolic pH regulation in plant cells, to avoid excessive alkalinisation in leaf cytosol when NO_3^- is reduced, the PEPc is activated resulting in the conversion of neutral sugars (G6P or F6P) to the relatively acidic malate, which thus counteracts the original pH increase (Latzko and Kelly, 1983; Salsac, 1987). However, this mode was challenged by its problem of calculation on proton transport accompanying the inorganic nitrogen transport (Britto and Kronzucker, 2005), as well as its low capacity and slow action rate for pH regulation (Gerendás and Ratcliffe, 2000). Britto and Kronzucker (2005) explained that the roots of NO_3^--grown plants tend to alkalinize the external medium, so that the uptake of nitrate is a cytosol-acidifying process. They listed the studies, which showed that NO_3^- transport stimulates a transient lowering of pH in cytosol. The accumulation of organic acids in NO_3^--grown plants, particularly malate, should be better explaind by achieving electroneutrality in plants, because NO_3^--grown plants accumulate cations in their tissue compared to the plants grown under NH_4^+.

1.4.3 Different N-type assimilation impacts carbon metabolism

Different N sources (NH_4^+ or NO_3^-) impact metabolic regulation associated with ATP consumption, pH regulation and redox control, which largely involve organic acid synthesis and circadian

dynamics, thus vary C-fixation pathways in generating the C skeletons during N assimilation (Raven and Farquhar, 1990; Sagi *et al.*, 1998; Lasa *et al.*, 2002b; Masclaux-Daubresse *et al.*, 2010; Hachiya and Sakakibara, 2016).

In illuminated leaves, nitrate reduces to nitrite and then to ammonium, requires ATP, reductants and carbon skeletons in the form of organic acids (mainly 2-OG). The reducing power is provided by ferredoxin system in chloroplasts. As described above, the TCA cycle does not operate in the cyclic mode since some involved enzymes are inhibited by light. Thus the carbon sources used for 2-OG synthesis are probably from reserves of organic acids (e.g. citrate), and not from the recent photoassimilates (Gauthier *et al.*, 2010). Two modes have been put forward in the literature concerning the involvement of citrate in N-assimilation in illuminated leaves (See Fig. 1.18). The first mode proposes that the mitochondrial oxidation of malate produces mainly citrate, which is exported to the cytosol to yield 2-OG *via* cytosolic aconitase and NADP-ICDH (Hanning and Heldt, 1993). The second mode proposes that the decarboxylation rate by PDH being decreased by about 30% in the light, and that the TCA cycle

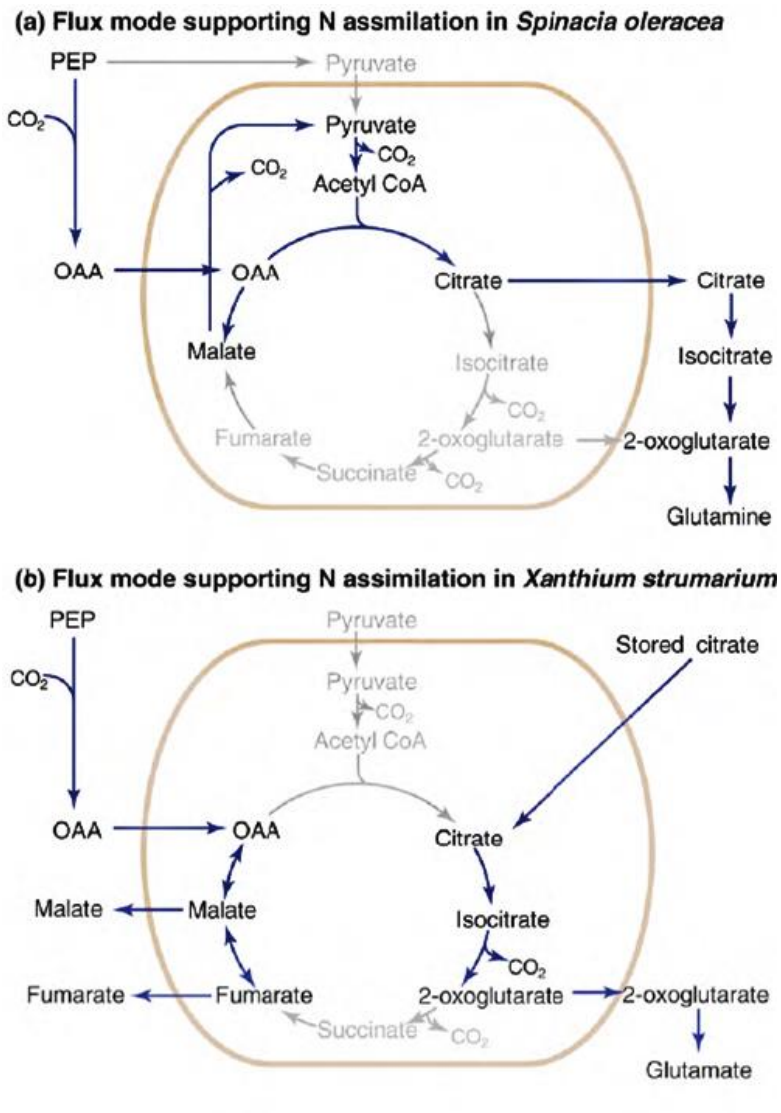

Figure 1.18 Flux modes of carboxylic acid metabolism in illuminated leaves. (a) Flux mode in *Spinacia oleracea* leaves proposed by (Hanning and Heldt, 1993). (b) Non-cyclic flux mode in *Xanthium strumarium* leaves proposed by (Tcherkez *et al.*, 2009). The mitochondrial limit is shown by brown lines. The figure is modified from (Sweetlove *et al.*, 2010).

functions as a two-branched system during the daytime. Carbon skeletons used for amino acid synthesis are in this case strongly dependent on the remobilization of stored citrate synthesized during the dark period (Tcherkez *et al.*, 2009; Gauthier *et al.*, 2010). For both modes, the consumed mitochondrial malate is supplemented by PEPc through anaplerotic pathway. Leaf NO_3^- reduction and assimilation mostly occurs in the light, a higher nitrate supply will thus lead to a higher C flux through anaplerotic pathway.

In non-photosynthetic tissues and in darkened leaves, the necessary reducing power for N assimilation is supplied by PPP, thus NH_4^+ nutrition leads to lower PPP flux since bypassing NO_3^- reduction (see details in 1.3.4.2). In this case, the TCA cycle functions in the cyclic mode. During nitrogen assimilation (NH_4^+ assimilation in roots and aspartate/asparagine synthesis, etc.), large amounts of organic acid precursers (e.g. 2-OG and OAA) are directly required from TCA cycle (Figure 1.15), then a substantial contribution of fixed C is required for filling TCA cycle (Marques *et al.*, 1983; Salsac, 1987; Bittsanszky *et al.*, 2015; Hachiya and Sakakibara, 2016). Anaplerotic pathway would thus have higher activity in non-photosynthetic tissues and in darkened leaves supplemented with NH_4^+ than with NO_3^- (Sugiharto and Sugiyama, 1992).

In summary, primary NH_4^+ assimilation takes place mostly in roots, most of NH_4^+ accumulation occurs in roots, and ammonium application leads to low PPP activity by bypassing NO_3^- reduction consumption of nitrogen assimilation. Therefore, it requires high levels of carbon skeletons thus increases the anaplerotic pathway *via* PEPc. Many researches have observed higher PEPc activity in roots of NH_4^+-grown plants (Schweizer and Erismann, 1985; Arnozis *et al.*, 1988; Lasa *et al.*, 2002b; Setien *et al.*, 2014; Sarasketa *et al.*, 2016). However, for the case of leaves, the associated anaplerotic requirement is more genetic-dependent, and it lies on the location of primary NO_3^- assimilation. Nevertheless, with increasing of NO_3^- assimilation, the PEPc activity increases at NO_3^- primary location. To be noted that, because of the interaction between NH_4^+ and NO_3^- (see 1.3.3), the net influence on carbon metabolism in the plants under different ratios of NH_4^+ and NO_3^- could not be simply estimated by their ratio.

1.4.4 Different N-type assimilation impacts on respiratory carbon isotope fractionation

Under extreme nitrogen source conditions (i.e. high nitrate or high ammonium supply), the variation of inorganic carbon source (atmospheric CO_2, dissolved CO_2 or HCO_3^-) contributing to

non-photosynthetic carbon fixation cannot be ignored. Carbon fixation pathway varies in different organs under different N source conditions, some of them using dissolved CO_2 (e.g. photosynthesis *via* Rubisco), while the others use HCO_3^- (e.g. anaplerotic pathway *via* PEPc) (Arnozis *et al.*, 1988; Raven and Farquhar, 1990; Vanlerberghe *et al.*, 1990; Britto and Kronzucker, 2005). Since the hydration of CO_2 by carbonic anhydrase discriminates in favour of ^{13}C (HCO_3^- is enriched in ^{13}C by about 9‰ compared with CO_2) and PEPc discriminates only by about 2.2‰ against ^{13}C, organic carbon compounds originating from anaplerotic pathway (e.g. OAA and malate) in the light are naturally more ^{13}C enriched than those originating from photosynthesis *via* Rubisco (Badeck *et al.*, 2005; Cernusak *et al.*, 2009; Ghashghaie and Badeck, 2014). It has already been shown that in different C_3 leaves, the higher the carbon fixation is in the dark (using ^{14}C-labelled CO_2), the more ^{13}C enriched is the leaf OM (Nalborczyk, 1978, Fig. 1.19).

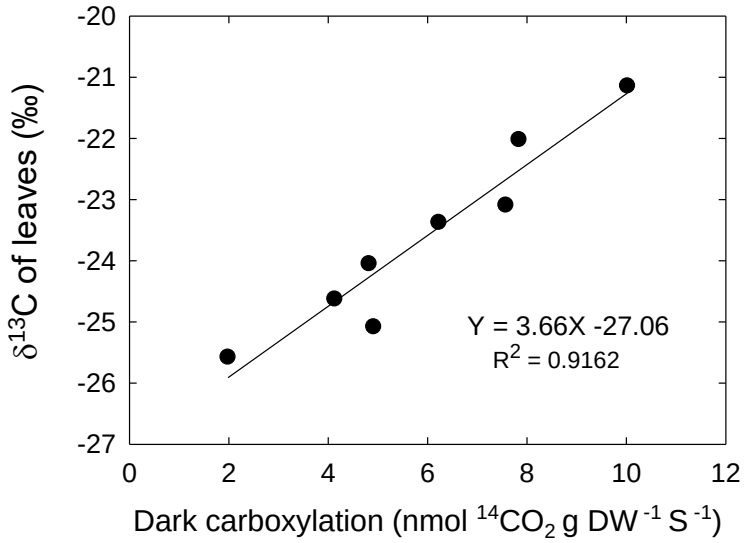

Figure 1.19 Carbon isotope composition ($\delta^{13}C$) of leaf bulk organic matter as a function of carboxylation rate in the dark measured using ^{14}C-labelled CO_2 on sunflower, tomato, rape, barley, rye, cucumber, wheat and lupine. $\delta^{13}C$ was determined in ambient air before labelling on plants grown under low light (redrawn by Ghashghaie and Badeck, 2014, using data from Nalborczyk, 1978).

As described above, because a high level of NH_4^+ accumulation is toxic to plants, plants assimilate NH_4^+ near the site of absorption or generation (roots) and rapidly convert it into amino acids or store any excess in their vacuoles, thus avoiding NH_4^+ toxicity effects on membranes and the cytosol. The physiological concentrations of NH_4^+ vary among species. For example, legumes are more tolerant to NH_4^+, but spinach is more sensitive (Allen and Smith, 1986; Esteban *et al.*, 2016). The primary pathway for NH_4^+ assimilation involves synthesizing glutamine from glutamate (GS-GOGAT pathway) or/and synthesizing asparagine from aspartate (Larsen *et al.*, 1981; Lasa *et*

al., 2002b; Masclaux-Daubresse *et al.*, 2010), so that large amounts of organic acid intermediates of TCA cycle (e.g. 2-OG and OAA) are diverted, then a substantial contribution of fixed C is required for replesnishing the TCA cycle (Marques *et al.*, 1983; Salsac, 1987; Bittsanszky *et al.*, 2015; Hachiya and Sakakibara, 2016). Theoretically, since ammonium is predominantly assimilated in roots, NH_4^+ nutrition should naturally enhance activity of anaplerotic pathway (carboxylation *via* PEPc), which incorporates more ^{13}C (through OAA and malate) into TCA cycle as substrates for respiration (Raven and Farquhar, 1990; Sagi *et al.*, 1998). Thus, in roots, more ^{13}C enriched respired CO_2 is expected under NH_4^+ nutrition compared with NO_3^- nutrition.

Different to ammonium, nitrate reduction takes place in both roots and leaves. Nitrate is firstly reduced to nitrite and then to ammonium with ATP consumption, but its influence on carbon flux is spatially separated from the place where nitrite reduction occurs (Masclaux-Daubresse *et al.*, 2010; Andrews *et al.*, 2013; Hachiya and Sakakibara, 2016). In leaves, NO_3^- reduction mianly occurs in the light, but because of the increase in redox level caused by photosynthesis and photorespiration, respiratory involved enzymes (e.g. ICDH, 2-OGDH, ME, etc.) in TCA cycle are inhibited, and thus TCA functions in a non-cyclic mode (Igamberdiev and Eprintsev, 2016; Igamberdiev and Bykova, 2018). Furthurmore, carbon fluxes manner in different ways in non-cyclic mode (Sweetlove *et al.*, 2010). If malate contributes to the synthesis of citrate (as was shown in Fig. 1.18a), which is exported to the cytosol to yield 2-OG as the precursor for GS-GOGAT pathway, citrate should also be ^{13}C enriched (but less than malate because citrate contains 2 additional C coming from acetyl-CoA). Accompanied with increased malate synthesis for ion charge and reduction equivalents balance under nitrate absorption (Britto and Kronzucker, 2002, 2005), higher levels of malate and citrate, higher carbon fluxes of anaplerotic pathway, more ^{13}C enriched respiratory intermediates in TCA, and more ^{13}C enriched dark respired CO_2 in illuminated leaves fed with NO_3^- than NH_4^+ are expected. While if TCA functions as in Figure 1.18b, citrate, used for providing carbon skeleton of nitrogen assimilation, will originate from remobilized cytosolic citrate which is less ^{13}C enriched (synthesized and stored during the night). Malate synthesis is still essential for maintenance of charge balance under NO_3^- nutrition, but will be less affected by amino acid synthesis. ^{13}C enriched OAA may synthesize and/or accumulate malate and/or fumarate, which are used for subsequent dark respiration. In this case, higher levels of malate and/or fumarate, higher carbon fluxes of anaplerotic pathway, more ^{13}C enriched respiratory intermediates in TCA cycle, and more ^{13}C enriched dark respired CO_2 in illuminated leaves fed

with NO_3^- than with NH_4^+ are expected. When NO_3^- reduction occurs in the roots, regardless of ATP consumption during nitrate reduction, it is considered to have the same impact on anaplerotic pathway activity as in plants fed with NH_4^+.

Taken all together, assimilation of different nitrogen sources changes anaplerotic carbon fixation flux in plants, and is thus expected to affect C-isotope composition of plants, especially respired CO_2 and respiratory substrates. As described above, in leaves, more ^{13}C enriched malate originating from anaplerotic pathway *via* PEPc will be synthesized for cellular homeostasis, when NO_3^- is supplied (compared to NH_4^+) as main N sources (Raven and Smith, 1976; Schweizer and Erismann, 1985; Lopes and Araus, 2006; Sarasketa *et al.*, 2016). It may also introduce higher level of more ^{13}C enriched citrate pool, which is for producing carbon skeleton for amino acid synthesis. Regardless of which carbon flux mode manners in the plants, more ^{13}C enriched intermediates as respiratory substrate are introduced in NO_3^--fed plant, thus subsequently carbon decarboxylation in the dark by ICDH and 2-OGDH will finally release more ^{13}C enriched CO_2. In roots, predominant sites of ammonium assimilation, TCA functions in a cyclic mode, thus higher N assimilation leads to higher anaplerotic pathway *via* PEPc and naturally incorporates more ^{13}C enriched organic acids as substrate for respiration. It is expected that NH_4^+ nutrition (compared to NO_3^-) enhances activity of anaplerotic pathway and enriches root-respired CO_2 in ^{13}C. However, PEPc-derived organic acids as well as respired CO_2 are expected to be less ^{13}C enriched in the roots than in the leaves, since the C source for PEPc in the roots mainly stems from respiratory CO_2 which is ^{13}C depleted compared with atmospheric CO_2. To be noted that, NO_3^- reduction in the roots is considered to have the same isotopic impact on root organic matter than in plants fed with the same amount of NH_4^+ (Raven and Farquhar, 1990). Theoretically, more ^{13}C enriched respiratory CO_2 and involved substrates are expected to be observed in roots of NH_4^+-fed and in leaves of NO_3^--fed plants.

1.5 Objectives and outline of this thesis

Carbon isotope fractionations associated with plant respiration have received increasing attention as indicator of metabolic responses, which can be non-destructively monitored, making it possible to elucidate factors associated with ecosystem carbon balances *via* carbon isotopic analysis. It is important to study the response of C_3 plants to ammonium and nitrate nutrition and its impact on C isotope composition of respired CO_2 because this information is needed to optimise fertilisation

in agriculture maximising yield and product quality while minimising losses of N to water bodies and the atmosphere. In natural ecosystems it serves to understand the role of N in the biogeochemical cycles and for species competition and biodiversity.

The general objective of this thesis is to study the responses of C_3 plants to ammonium and nitrate nutrition and the subsequent impact on C-isotope composition of leaf- and root-respired CO_2 and putative respiratory substrates. Nutrient solutions with different ratios of NH_4^+:NO_3^- were used for plant culture, to examine (*i*) in which extent the isotopic signature of putative respiratory substrates and respired CO_2 is affected by N-type nutrition in plants, and (*ii*) in which extent the anaplerotic pathway (*via* PEPc) is affected by N-type in leaves *versus* roots. This would allow a better understanding of the metabolic origin of the divergence in isotopic signature between heterotrophic and autotrophic organs**.**

Chapter 2 describes the material and methods of the experiments as well as the statistial analysis applied in this study.

Chapter 3 describes a pre-experiment on the amonium tolerance of 9 species in our specific culture conditions, which aimed in selection of suitable species for the subsequent more detailed experiments. Nutrient solutions with different ratios of NH_4^+:NO_3^-were used to examine which species can survive under extreme NH4+ in our culture conditions, which species are more tolerant, and which ones are more sensitive to NH_4^+: NO_3^- ratio gradient in terms of both plant growth, and $\delta^{13}C$ in plant organic mass.

Chapters 4 and 5, deal with our investigations on the two selected species, bean (more NH_4^+ tolerant) and spinach (more NH_4^+ sensitive), respectively. The changes in $\delta^{13}C$ values of respired CO_2 and of the main metabolic pools involved in respiration, as well as PEPc activity in both leaves and roots of plants fed with various NO_3^-:NH_4^+ ratios are presented. Gas exchanges and some other physiological traits were also investigated and discussed. The main objactives were to better understand (i) in which extent the isotopic composition of putative respiratory substrates and respired CO_2 is affected by N-type nutrition in plants, and (ii) in which extent the anaplerotic pathway (*via* PEPc) could explain isotope changes under N-type nutrition in heterotrophic and autotrophic organs. We showed that the leaf dark respired CO_2 was ^{13}C enriched under NO_3^- nutrition but became more and more ^{13}C depleted with increasing NH_4^+ amount in nutrient solution. However, in roots, nitrogen type did not significantly affect the isotope composition in root-

respired CO_2. The Chapter 4, is a paper manuscript on bean data, but the Chapter 5 on spinach data is not prepared as a paper mnuscript yet.

Finally, chapter 6 discusses the main findings of this thesis, compares differences of isotopic responses to different nitrogen sources between species, and provides an outlook for future research that could further stregthen our knowledge on the contribution of the metabolic origin of the divergence in isotopic signature between heterotrophic and autotrophic organs**.**

CHAPTER 2 - Materials and Methods

2.1 Plant species selection

As preliminary experiment, we tested the tolerance to ammonium of eight C_3 plant species (bean, soybean, pea, sunflower, tomato, castor bean, wheat and spinach) and one C_4 plant (maize), under our experimental conditions (Fig. 2.1). Five proportions of NH_4^+ as % of supplied N: 0%, 25%, 50%, 75%, and 100% (i.e. 100%, 75%, 50%, 25% and 0% of NO_3^-, respectively) were used for the preliminary experiment. The nutrient solutions (Tables 2.1 and 2.2) contained 6 mmol L^{-1} of N applied either as KNO_3, $Ca(NO_3)_2$, NH_4NO_3 or $(NH_4)_2SO_4$ at different ratios for different N-treatments (adapted from Arnozis *et al.*, 1988, by Ghiasi *et al.,* unpublished). Additional components were: 1 mmol L^{-1} $CaCl_2$, 0.25 mmol L^{-1} KH_2PO_4, 1 mmol L^{-1} $MgSO_4$, and trace elements (2 µmol L^{-1} $MnSO_4$, 2 µmol L^{-1} $ZnSO_4$, 0.5 µmol L^{-1} $CuSO_4$, 25 µmol L^{-1} $B(OH)_3$, 0.5 µmol L^{-1} Na_2MoO_4, 40 µmol L^{-1} Fe-EDTA). The pH of all the solutions was around 5.5. In addition, in 100% and 90% NH_4 treatment, 1 mmol L^{-1} K_2SO_4 was added to keep the K concentration constant.

Figure 2.1. Pots of 6 plant species from the first set of the preliminary experiment, for 5 N-type treatments (i.e. 5 different proportions of NH_4^+ as N source).

The preliminary (species-selecting) experiment was carried in two sets. The first set started from 27/11/2015, including bean, soybean, pea, maize, sunflower, tomato and castor bean. Plant seeds experienced 6-7 days of germination in the dark, in a plate filled with vermiculite humidified with tap water. The germinated seedlings were then transplanted to the pots of 8.3 cm top diameter, 5.5 cm bottom diameter and 11.0 cm of height, filled with vermiculite and watered with tap water under light for 7-18 days (depending on the species) until the cotyledons appeared out of the vermiculite. When cotyledons of dicotyledon plants or the first 2 leaves of monocotyledon plants emerged out of the vermiculite, different N-type treatments were applied for about 28-30 days. The second set started on 17/02/2016, including wheat and spinach. Plant seeds firstly experienced 5-7 days of germination in vermiculite with tap water in the dark; 2-3 days to let the cotyledons come out; then 21 days of N-treatments with different NH_4^+ proportions in nutrient solution. Daytime temperature was 25±3 °C (the night temperature was not recorded in the preliminary experiment) and the photoperiod was 10 h per day, for both sets. For preliminary experiment, 5 plants (n=5) for each species and each treatment were cultured and analysed. Pots with the same treatment were placed together in a plate. The positions of the plates in the culture room were random and changed every week.

Table 2.1. Composition of the nutrient solutions with various NH_4^+: NO_3^- ratios. The second solution (90% NH_4^+: 10% NO_3^-) was not used in the preliminary experiment).

NH_4^+: NO_3^- (% of total N)	Compounds (mmol/L)								
	Micronutrient	$CaCl_2$	$MgSO_4$	KH_2PO_4	K_2SO_4	$(NH_4)_2SO_4$	NH_4NO_3	$Ca(NO_3)_2$	KNO_3
100:0	1	1	1	0.25	1	3	-	-	-
90:10	1	1	1	0.25	1	2.4	0.6	-	-
75:25	1	1	1	0.25	-	2	0.5	-	1
50:50	1	1	1	0.25	-	0.5	2	-	1
25:75	1	1	1	0.25	-	-	1.5	1	1
0:100	1	1	1	0.25	-	-	-	2	2

Table 2.2. Composition of micronutrient stock solution.

Micronutrient	H_3BO_3	$MnSO_4$	$ZnSO_4$	$CuSO_4$	Na_2MoO_4	FeNa-EDTA
Concentration (μmol/L)	25	2.2	2.2	0.5	0.5	16.5 (mg/L)

2.2 Plant material and culture conditions in main experiments

Based on the results from the pre-experiment described in 2.1, French bean (*Phaseolus vulgaris* L.) cultivar Contender, and spinach (*Spinacia oleracea L.*) cultivar Géant d'Hiver (both species from Vilmorin, France) were selected for investigation in this study. French bean, as a legume (N_2-fixing), is more ammonium tolerant (Esteban et al., 2016) and well-studied by our group, while spinach is more ammonium sensitive and requires great amounts of nitrogen (Lasa *et al.*, 2002b; Cruz *et al.*, 2006).

Seeds of both bean and spinach were first germinated in vermiculate with tap water in a dark room. Similar-height seedlings of 7-d old were transplanted to pots (one plant per pot) filled with sand of Loire (previously washed with tap water and sterilized in autoclave). Since some tests showed that vermiculite progressively released CO_2, the plants were cultured in sand for the main experiments. The pots (the same as those used for preliminary experiment described above) were placed in the culture room in the greenhouse. The whole culture period was 33 d and 38 d for bean and spinach, respectively. Bean plants had one set of mature and one set of still-growing trifoliate leaves at the end of the culture period. Their cotyledonary leaves were mature but not senescent. Spinach had 3 pairs of euphylla.

The bean culture was performed during January 2017 under natural light, with supplementary light supplied by lamps (Metal Halide Lamps, HSI-THX, 400W, Sylvania) for 10 h per day, providing the maximum photosynthetic photon flux density (PPFD) of 140-160 μmol photons m^{-2} s^{-1} at plant height at midday (measured value). Air temperature was 23 ± 2 °C during the day and 17 ± 2 °C during the night. Humidity was 42 ± 8% during the day and 55 ± 15% during the night. Because of the technical problem in temperature controlling system of the culture room used for bean plants, spinach plants were cultured in another room, from July to August in 2017, with only artificial light source (Neon, Phillips Master 58W/965) of 200-210 μmol photons m^{-2} s^{-1} at plant height 16h per day. Temperature and humidity were the same as for bean culture. Carbon isotope composition of the ambient CO_2 in the culture rooms was not determined, but the C-isotope composition in leaf OM of maize plants (the 4^{th} and 5^{th} leaves) cultured in bean and spinach rooms was –11.74 ± 0.06‰ (n=6) and –16.43 ± 0.03‰ (n=5), respectively, i.e. air CO_2 was ^{13}C depleted in spinach culture room compared with bean culture room by about 4.6‰.

Plants were supplied with nutrient solutions with 6 different proportions of NH_4^+ as % of supplied N: 0%, 25%, 50%, 75%, 90% and 100% (i.e. 100%, 75%, 50%, 25%, 10% and 0% of NO_3^-, respectively, Table 2.1). One ppm of nitrification inhibitor (2-Chloro-6-trichloromethylpyridine) was added to the nutrient solutions for spinach culture. Indeed, even the sand was sterilized, it is difficult to avoid the influence of nitrifying bacteria from environment.

Pots with the same treatment were placed together in a plate, and their positions in the culture room were random and changed every week. Nutrient solutions were supplied for watering the plants only after the cotyledons came out of the sand and were not in touch with the top of the sand. We started with 750 mL solution $plate^{-1}$ d^{-1} (with 8 pots in each plate), increasing the amount during the plant growth. The amount of the solution was so that the pots were completely filled, then allowed to drain to the plates. During the last week before the harvest, the amount of the solution was approximately 1500 mL $plate^{-1}$ d^{-1}. Three bean plants (n=3) and 5 spinach plants (n=5) for each treatment were cultured and analysed.

2.3 Leaf Chlorophyll content and the nitrogen status

Chlorophyll and flavonol content indexes were measured by DUALEX SCIENTIFIC^{+TM} (ForceA, France) every 3 days. Nitrogen balance index (NBI), i.e. the ratio of chlorophyll to favonol contents, was regularly measured as an indicator to detect if the plants were going through N deficiency. All parameters were factory calibrated by DUALEX. For every measurement time and for each treatment, 5 leaves of 5 bean or 5 spinach plants were measured (one leaf from one plant for each case, n=5).

The Dualex instrument measures a chlorophyll index based on measurements of light transmission through the leaf blades and a leaf flavonoid index based on measurements UV-screening of chlorophyll fluorescence. The latter is performed by comparing UV-induced to red-induced (reference wavelength) chlorophyll fluorescence. The units of chlorophyll and flavonoid indices were factory calibrated. Cerovic et al. (2012) and Cartelat et al. (2005) have shown that the chlorophyll and flavonoid index values are linearly correlated with the chlorophyll content and flavonoid content per leaf area, respectively.

2.4 Leaf gas exchange and chlorophyll fluorescence measurements

One month after planting, gas exchange and chlorophyll fluorescence parameters of the leaves were measured using Licor 6400 with LCF chamber (LI-COR, Inc. USA) in the morning (9-12 am) during 3 successive days. One plant with mature euphylla was selected from each N-treatment for measurements on each day. Therefore, there were 3 replications and the measurement turns were random (for N-treatments) in different days. Three leaves from 3 independent bean or spinach plants (n=3) for each treatment were analysed.

Before measurements, plants were dark-adapted for 30 min, the minimum and maximum fluorescence yields in the dark (F_0 and F_m) were recorded, F_m was measured during a 1s saturating flash at 6000 mmol m^{-2} s^{-1}. The maximum PSII efficiency was calculated as F_v/F_m, where $F_v = F_m - F_0$. Then one mature euphylla was used for measurements (in the case of bean, only the middle trifoliate was used). During measurements, Licor conditions were set as follows: flow rate at 300 µmol s^{-1}, CO_2 concentration at 390 µmol mol^{-1} and PPFD at 400 µmol m^{-2} s^{-1} (with 10% blue light) for both species (for spinach, two PPFD levels were used: 200 and 400 µmol m^{-2} s^{-1}). Leaf temperature was fixed at 22 °C. Leaf net CO_2 assimilation rate (A_n), stomatal conductance (g_s) and the ratio of intercellular to ambient CO_2 concentrations (C_i/C_a) were automatically recorded every 3 min, reaching steady values after about 30 min. Three values at steady state were taken to get a mean value of these parameters for each plant.

After steady state reached, the minimal and maximal fluorescence yields in the light (F_0' and F_m'); F_m' were measured the same way as F_m. The relative quantum efficiency of photosystem II (PSII) electron transport (usually written as Φ_{PSII} or $\Delta F/F_m$') estimated from $(F_m' - F_s)/ F_m'$, where F_s is the steady-state fluorescence (Genty *et al.*, 1989). The efficiency of energy harvesting by oxidized (open) PSII reaction centres in the light was estimated from F_v'/F_m', where $F_v' = F_m' - F_0'$ (Andrews *et al.*, 1993). Parameters of photochemical quenching (QP) and non-photochemical quenching (NPQ) were calculated according to Oxborough and Baker (1997). The actual flux of electrons (µmol m^{-2} s^{-1}) originating from photosystem II can be inferred from chlorophyll fluorescence measurements. This is called electron transport rate (ETR), and is given by $\Phi_{PSII} \cdot f \, I \, \alpha_{leaf}$, where *f* is the fraction of absorbed quanta that is used by PSII, and is typically assumed to be 0.5 for C_3 plants, and 0.4 for some C_4 plants like maize (Earl and Tollenaar, 1998), I is incident photon flux density (µmol m^{-2} s^{-1}), and α_{leaf} is leaf absorbance.

2.5 Carbon isotope composition of respired CO_2

To ensure that plants had enough photo-assimilates as respiratory substrates, they were taken from the greenhouse after at least 4 h into the photoperiod. Then they were placed in the dark for 30 min to avoid the ^{13}C enrichment peak in respired CO_2 resulting from initial decarboxylation of malate, i.e. light-enhanced-dark-respiration (LEDR). For leaf-respired CO_2, one intact mature euphylla was cut off and put into a flask (50 mL) completely covered by aluminium foil (Fig. 2.2). The flask was flushed by CO_2-free air for 5 min (checked to be large enough to remove all CO_2 from the flasks), then sealed by septum and left for accumulation of CO_2 respired. CO_2 concentration was analysed by micro-GC (490 Micro GC, Agilent Technologies, USA). The needle of Micro-GC was automatically introduced into the flask through the septum (injection volume was 5 µl every 3 min).

When CO_2 concentration was above 1000 ppm (approximately after 12 min), air samples were manually collected from the flask by syringes (0.5 to 1 ml depending on CO_2 concentration) and then injected into a gas chromatograph (GC; HP 5890, Les Ulis, France) coupled to a stable isotope ratio mass spectrometer (Optima Isochrom-µG, Fisons Instruments, Manchester, UK), to measure C-isotope composition of respired CO_2 ($\delta^{13}C_R$). The syringes were flushed with helium five times and then with sample air inside a given flask 10 times before each injection. Each flask was sampled and measured 3 times to make sure the values were stable.

For root-respired CO_2, roots were first washed with tap water and dried with absorbing paper before incubation in the flasks. Since the respiration rate of roots was higher than that of leaves, bigger flasks (120 mL) were used for roots. Generally, measurements started from 10:00 to 16:00, on each day, and the turns of N-treatments were random.

The C-isotope composition of respired CO_2 was measured at the Écologie Fonctionnelle et Écotoxicologie des Agroécosystèmes (ÉcoSys), Laboratory of Claire Chenu (INRA Thiverval-Grignon) with the technical assistance of Cyril Girardin, for all the samples of this PhD work.

The leaves and roots used for respiration measurements were then plunged in liquid nitrogen and kept at –80 °C, then freeze-dried and finely ground for isotope analyses of bulk OM as well as water-soluble organic matter (WSOM) and individual metabolites. Three bean (n=3) and 5 spinach plants (n=5) from each treatment were used for analysis.

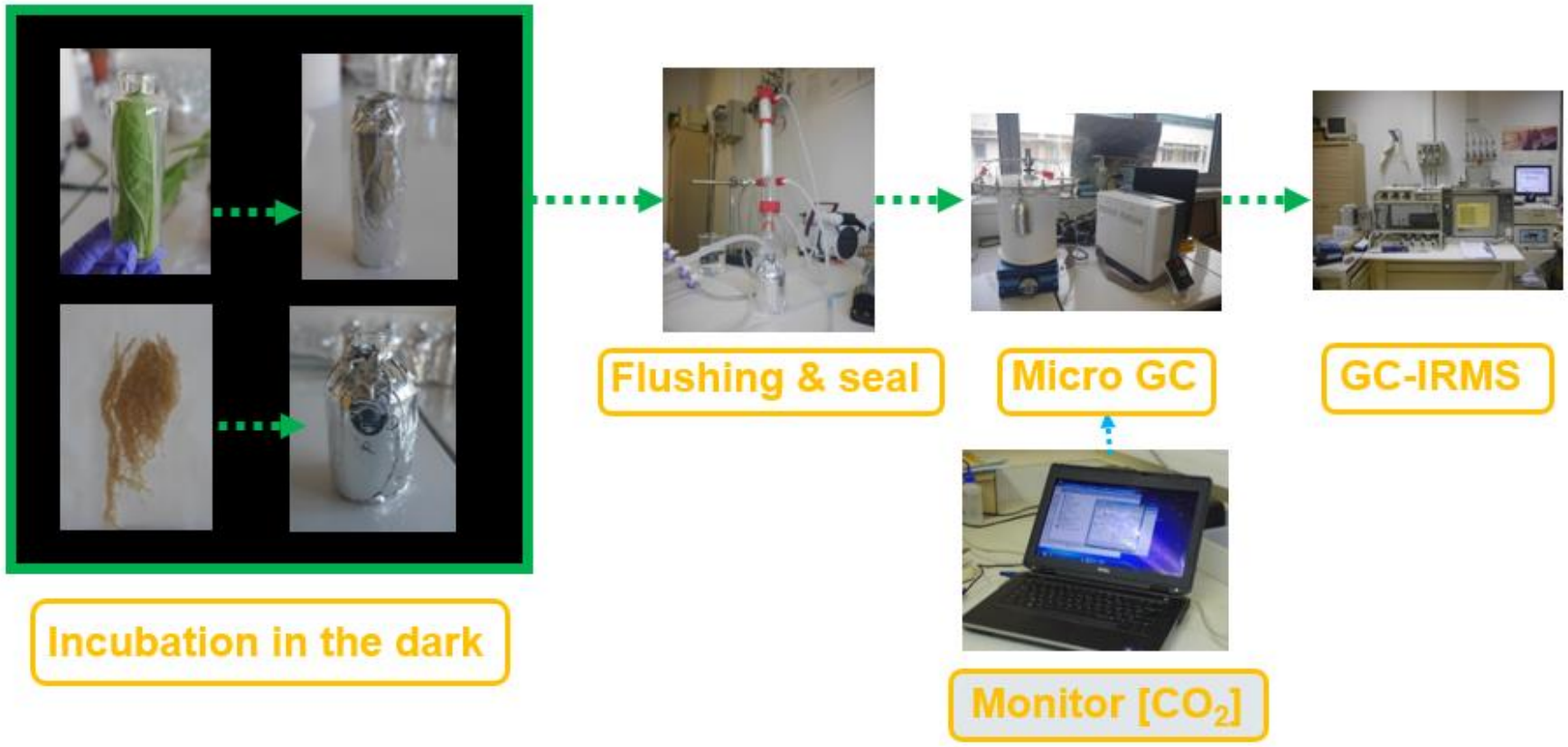

Figure 2.2. Measuring leaf- and root-respired CO_2 by GC-IRMS.

2.6 Carbon isotope composition of organic material

Carbon isotope composition of both bulk organic matter ($\delta^{13}C_{OM}$) and water-soluble organic matter ($\delta^{13}C_{WSOM}$) was determined on freeze-dried material. Dried samples were finely ground by a Retsch MM200 ball mill (Bioblock Scientific, Illkirch, France). An aliquot of 600-800 µg per sample powder was weighed in tin capsules (Courtage Analyse Service, Mont Saint-Aignan, France).

Samples of bean and spinach plants of both preliminary and main experiments were analysed at the Grassland Science Laboratory of Nina Buchmann (ETH, Zurich), with the technical assistance of Roland A. Werner and Annika Ackermann. An elemental analyser (Flash EA) coupled to a Deltaplus^{XP} isotope ratio mass spectrometer (IRMS) *via* a 6-port valve (Brooks *et al.*, 2003), and a ConFlo III interface (Finnigan MAT, Bremen, Germany, (Werner *et al.*, 1999), were used for these analyses. In order to avoid frequent exchange of the $Mg(ClO_4)_2$ of the conventional water trap, the Flash EA was additionally equipped with a custom-built Nafion^{TM} trap after the reduction tube. The positioning of samples, blanks and laboratory and quality control standards in a measurement sequence followed the scheme described in Werner and Brand (2001). Three leaves from 3 independent bean or spinach plants (n=3) from each treatment were used for analyses.

$\delta^{13}C_{OM}$ of maize, pea, castor bean, soybean, sunflower, tomato and wheat in preliminary experiment was analysed at the Plateforme Métabolisme-Métabolome, Institut des Sciences des Plantes, Université Paris-Sud, Université Paris-Saclay. An elemental analyser (Flash EA 1112 series, Thermo Electron, USA) coupled to an isotope ratio mass spectrometer (Optima, Micromass, Villeurbanne, France) were used for these analyses. Two blanks were set in the beginning of each sequence, and then the quality control standards (L-glutamate, USGS40, and sucrose, IAEA-C6) were set after the blanks at the beginning, every 18 samples and at the end of the sequence. Laboratory glutamate standards were inserted every 6 samples. The scheme of EA-IRMS system is demonstrated in Fig. 2.3.

C-isotope composition ($\delta^{13}C$) was calculated as deviation of the carbon isotope ratio ($^{13}C/^{12}C$, called R) from the international standard (Vienna Pee Dee Belemnite, V-PDB) according to (Farquhar *et al.*, 1989):

$$\delta^{13}C\ (‰) = [(R_{sample} - R_{V\text{-}PDB})/R_{V\text{-}PDB}] * 1000 \qquad \text{(Eq. 2.1)}$$

R_{sample} and $R_{V\text{-}PDB}$ are the C-isotope ratios of the sample and the V-PDB standard, respectively.

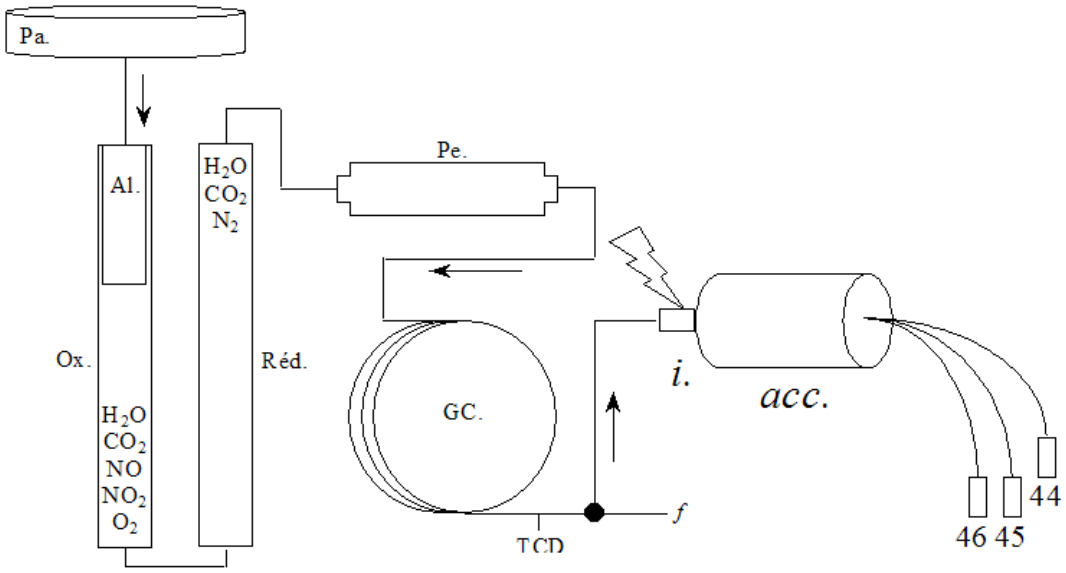

Figure 2.3. Scheme of the EA-IRMS used for analysing the isotope composition of organic matter. The tin cups containing the dry powder of organic material, falling individually from the auto-sampler (Pa) are first burned in the oxidation column (Ox), the molten tin being recovered in the quartz extension (Al). The oxidation products and excess oxygen are then reduced in the reduction column (Réd), and the produced water (if any) is absorbed by a magnesium perchlorate (Pe) trap. The CO_2 and N_2 are separated by gas chromatography (GC), after which a detector is installed to identify their output concentration (TCD). The gas of interest is directed to the IRMS for isotopic analysis (i, ionizer; acc, accelerator), and the other gas to the leak (f). The 3 collectors receive the 3 isotopologues for a given gas (44, 45 and 46 for CO_2, and 28, 29, 30 for N_2). The carrier gas is helium.

2.7 Extraction and C-isotope analyses of water-soluble fraction

The method of Tcherkez *et al.* (2003) was used for extraction of the water-soluble fraction from plant samples. Freeze-dried powder (50 mg) of a given sample was suspended in 1mL of cold distilled water in an Eppendorf vial and maintained on ice slurry for 60 min except when removed to agitate in a vortex mixer every 10 min. After centrifugation at 14,000 g at 5 °C for 15 min, the supernatant (containing soluble sugars, organic and amino acids and soluble proteins) was separated from the pellets. It was heated at 100 °C for 5 min (it should be boiled) and then kept on ice for 30 min to precipitate the heat-denatured proteins, which were then removed by centrifugation at 14,000 g for 15 min at 5 °C. The final supernatant, i.e. water-soluble fraction of

organic matter (WSOM), was conserved at –20 °C for isotopic analysis, but before any further use, it was centrifuged again to remove precipitations, which can be observed after freezing.

Aliquots of 200 µl of protein-free WSOM were poured into tin cups and oven-dried at 50 °C for isotope analysis ($\delta^{13}C_{WSOM}$) with EA-IRMS as explained in 2.5. Three leaves or roots of 3 independent bean or spinach plants (n=3) from each treatment were used for analysis.

2.8 Carbon isotope composition of individual metabolites

Before separation of soluble sugars and organic acids from the water soluble extract, cation exchangers (Dionex OnGuard II H 1.0 cc Cartridges, Thermo Scientific, Sunnyvale, CA, USA) were conditioned with 10 ml distilled water, and anion exchangers (Dionex OnGuard II A 1.0 cc Cartridges, Thermo Scientific, Sunnyvale, CA, USA) were conditioned firstly with 10 ml 0.5 M HCl, then10 ml distilled water.

The protein-less water-soluble fraction of organic matter (WSOM, described above) was diluted to 100 ng/µL (pH was adjusted to 7), then 4 mL of the diluted solution passed through cation and anion exchangers, to retain amino acids and organic acids, respectively, and thus to drain and collect the soluble sugars (Fig. 2.4). The first 2 mL were discarded, and the last 2 mL were collected in 2 amber silanized glass vials of 1.5 mL (Vial short tread, VWR International, USA) as purified soluble sugars. Organic acids were eluted from anion exchangers using 4 mL 0.5 M HCl. Again, the first 2 mL were discarded, and the last 2 mL were collected in 2 amber glass vials of 1.5 mL (HPLC/GC Certified Kit, VWR International, USA). Collected bulk sugars and bulk organic acids were used for compound specific C-isotope analysis with HPLC coupled to IRMS, as follows.

A ThermoFinnigan LC-IsoLink system (Ultimate 3000, Dionex, Part of Thermo Fisher Scientific, USA) coupled to a Delta V Advantage (Thermo Fisher Scientific, USA) was used for analysing carbon isotope composition of individual soluble sugars (sucrose, glucose and fructose) and organic acids (only malate and citrate were determined, the amounts of oxaloacetate and succinate were too small to be detected). Separation of sugars was in water as solvent, through the column NUCLEOGEL Sugar 810 Ca, length 300 mm, internal diameter 7.8 mm (MACHEREY-NAGEL GmbH & Co. KG, Germany). Organic acids were separated by the column Prevail Organic Acid, 150 mm x 4.6 mm, 5µ (Grace Davison Discovery Sciences, USA) with 25 mM KH_2PO_4 (pH=2.5) as solvent. The system was controlled with Chromeleon 7.2 software (Thermo

Electron). These extractions and analayses were perforemd at the Max Planck Institute in the Biogeochemistry Laboratory of Gerd Gleixner (Jena, Germany), with the technical assistance of Steffen Ruehlow.

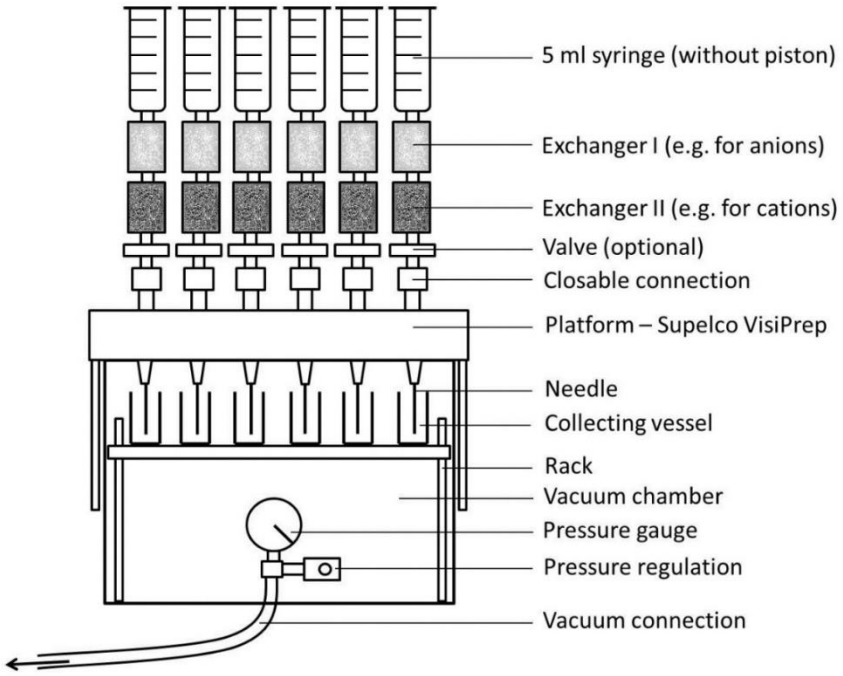

Figure 2.4. Extraction system for seperation of bulk sugars, and bulk organic acid and bulk amino acids from water soluble fraction of plant samples. Bulk amino acids were not analysed yet.

The amounts [C] and the $\delta^{13}C$ values of the individual sugars were used to calculate the C-isotope composition of the total soluble sugars ($\delta^{13}C_{Sug}$) using a simple mass balance:

$$\delta^{13}C_{Sug} = (\delta^{13}C_{Glc} \,.\, [C]_{Glc} + \delta^{13}C_{Suc} \,.\, [C]_{Suc} + \delta^{13}C_{Fru} \,.\, [C]_{Fru}) / ([C]_{Glc} + [C]_{Suc} + [C]_{Fru}) \quad \text{(Eq. 2.2)}$$

Similarly, using the amounts and the $\delta^{13}C$ values of individual sugars and organic acids, we calculated an estimated C-isotope composition of the total water soluble fraction ($\delta^{13}C_{Est.\,WSOM}$) to compare with the measured values ($\delta^{13}C_{WSOM}$). Three leaves or roots of 3 independent bean or spinach plants (n=3) from each treatment were used for analysis and calculation.

2.9 Biomass

Plants used for measurements of $\delta^{13}C$ of respired CO_2 ($\delta^{13}C_R$) were harvested for biomass determination of different organs of both species (i.e. bean and spinach). Whole plants were divided into leaves, stems and roots, plunged into liquid nitrogen for temporary conservation, and then moved to freezer-dryer before determination of dry weights. Three bean plants (n=3) and 5 spinach plants (n=5) from each treatment were used for analysis.

2.10 PEP carboxylase (PEPc) activity determination

Other plants, from the same culture set used for respiration analysis, were used for PEPc activity determination. Three leaves or roots of 3 bean or spinach plants (n=3) for each treatment were used for analysis. Samples used for PEPc activity measurements were harvested during the morning (from 10:00 am to 12:00 am) and conserved at –80 °C. 150 mg of each frozen root or leaf sample (without petioles and midribs) were completely ground in a mortar (on a plate containing liquid nitrogen to maintain the sample frozen) with 100 mg sand, then 1 ml extraction buffer was added (4 °C). The extraction buffer contained HEPES 50 mM; $MgCl_2$ 10 mM; EDTA 1 mM; EGTA 1 mM; BSA 0.025% (w/v); glycerol 10% (w/v); DTT 5 mM; and protease inhibitor. Thereafter, the mix was agitated in a vortex for 2 seconds, defrosted completely on ice and agitated again in the vortex for 5 sec, and centrifuged at 10,000 rcf at 4 °C for 10 min.

PEPc activity was measured by coupling the reaction to the NADH-oxidation mediated by malate dehydrogenase (MDH). The standard assay buffer contained: 100 mM Tricine (pH 8.0), 10 mM $NaHCO_3$, 20 mM $MgCl_2$, and 0.05% Triton. 40 µl assay buffer, 20 µl 20 mM PEP, 20 µl 0.5 mM NADH, 2 µl 1 u mL^{-1} MDH, 98 µl distilled water and 20 µL extract were added in a 96-well plate. Two technical replicates for each sample were set for the NR measurements. The 96-well plate was placed in a microplate spectrophotometer (PowerWave HT, BioTek, USA) to record the first 20 min oxidation of NADH at 340 nm.

Even when no PEP had been added to the reaction mixture, NADH was oxidized at a rate corresponding to 1 to 30 % of its rate after PEP addition. Endogenous NADH oxidation rate remained stable for several hours. After addition of small amounts of PEP, the oxidation rate initially rose rapidly but returned quickly to the endogenous level after exhaustion of PEP (Arnozis

et al., 1988). Accordingly, PEP replaced by H_2O was designed as control assay, and the PEPc activity has been calculated as the difference in NADH oxidation rate before and after the addition of PEP.

2.11 Nitrate reductase (NR) activity determination

Frozen leaf or root samples which were kept in –80℃ freezer (around 100 mg) were ground in liquid nitrogen and the resulting powder dissolved in 1 mL of 50 mM HEPES-NaOH buffer, pH 7.6, containing 0.1% Triton X-100, 5 mM $MgCl_2$, 10 µM leupeptin, 0.5 mM AEBSF [4-(2-aminoethyl)-benzenesulfonyl fluoride], 3 mM DTT, 1% polyvinylpolypyrrolidone, 3% polyethylene glycol 4000, and 19.2 µM flavine adenine dinucleotide (FAD). The mix was centrifuged for 10 min at 13,000 g (Fresneau *et al.*, 2007). NR activities were carried out on the supernatant in the presence of ethylenediaminetetraacetic acid (EDTA) as total NR activity (NR-EDTA) and in the presence of Mg^{2+}, as active (actual) NR activity (NR-Mg) following the method described by (Foyer *et al.*, 1998). Briefly, the reaction mixture contained 250 µL of 50 mM HEPES-NaOH buffer, pH 7.6, 50 µL of 100 mM KNO_3, and 50 µL of 2 mM nicotinamide adenine dinucletide reduced form (NADH). The reaction was initiated by adding 50 µL of extract and incubated at 30 °C for 30 min. The reaction was stopped by adding 50 µL of 1 M $ZnSO_4$, 7 H_2O. The nitrite ions produced were assayed after diazotization with 500 µL of 1.5% (w/v) sulfanilamide and 500 µL of 0.02% (w/v) N-(1-Naphthyl) ethyl-Enediamine (NEDD). Then, the solution was again centrifuged at 8,000 g for 10 min and the absorbance of the supernatant was measured at 540 nm. The activities of both NR-EDTA and NR-Mg were estimated as µmol NO_2^- formation per mg fresh biomass and per hour. The percentage of activation of NR was determined by the ratio of NR-Mg to NR-EDTA and expressed in percent. Three leaves or roots of 3 bean plants (n=3) for each treatment were used for analysis.

2.12 Statistical analyses

Differences between NH_4^+:NO_3^- ratios of preliminary experiment were tested with one-way ANOVA and Tukeys HSD test with $p < 0.05$. Statistical analyses of correlation, and ANCOVA for main experiments on bean and spinach were performed using STATISTICA 8.0 (StaSoft Inc.,

Tulsa, USA). Mean comparisons were performed with the 'LSD' test with $p < 0.05$. Linear regression were carried out with SigmaPlot 12.0 (Systat Software, Inc., San Jose, California,USA). When representing three or more measurements, data are presented as mean values ± SE.

Correlation and regression analyses as well as PCA were done with R (R core team, 2018). Regression of all traits on the fraction of NH_4^+ in the nutrient solution was performed as linear regression and as regression with log-transformed fraction of NH_4^+, emphasizing a more pronounced change at low fractions of NH_4^+. Furthermore, regression on the log-transformed fraction of NO_3^- (i.e., 100 – NH_4^+), emphasizing a more pronounced change at high fractions of NH_4^+ and the absolute difference of fractions of NH_4^+ from 25, 50 and 75%, respectively were done. Between-trait correlations were calculated and ordered with hierarchical clustering.

CHAPTER 3 - Impact of varying NH_4^+: NO_3^- ratios in nutrient solution on biomass and C-isotope composition of leaf- and root-OM of several species.

3.1 Introduction

A preliminary experiment was performed to study the impact of varying NH_4^+: NO_3^- ratios in nutrient solution on carbon isotope composition of leaf- and root-organic matter. NH_4^+ is generally considered to be toxic to plants, but contradictory results have been reported in the literature on the plant tolerance to ammonium, which varies among species and experimental conditions. Effects of NH_4^+: NO_3^- ratio gradients on growth were well studied for many years, while less is known about how NH_4^+ to NO_3^- ratio gradients may affect $\delta^{13}C$ in plant organic matter. Raven and Farquhar postulated that the N metabolism may affect natural abundance of isotopes of carbon in plants (Raven and Farquhar, 1990). Some studies explored the influence of N deficiency stress on carbon isotopes composition (Condon *et al.*, 1992; Livingston *et al.*, 1999), some studies tested the isotopic effect by only supplying NH_4^+ or NO_3^- as sole N source (Guo *et al.*, 2002; Lasa *et al.*, 2002b), and only few studies added also NH_4^+:NO_3^-=1:1 treatment (Yin and Raven, 1998; Lopes and Araus, 2006). However, to our knowledge, no reference is available in the literature on the effects of various NH_4^+:NO_3^- ratio gradients on carbon isotope fractionation during respiration.

The aim of the preliminary experiment was to select suitable species for the subsequent, more detailed study. Nutrient solutions with different ratios of NH_4^+:NO_3^- were used in the preliminary experiment for 9 species (Fig. 3.1), to examine which species can survive under pure NH_4^+ nutrition in our culture condition, which are more tolerant, and which are more sensitive to NH_4^+: NO_3^- ratio gradient in terms of both plant growth, and $\delta^{13}C$ in plant organic mass.

3.2 Material and Methods

3.2.1 Plant material and culture conditions: See Chapter 2 (2.1)

3.2.2 C- and N-isotope composition of organic material: See Chapter 2 (2.6)

3.3 Results

3.3.1 Effect of N-type gradient supply on plant growth

Biomass is the most comprehensive parameter used to evaluate plant performance in response to a long-term stressful situation. In this preliminary experiment, 9 species: French bean (*Phaseolus vulgaris* L.), soybean (*Glycine max* (L.) Merr.), pea (*Pisum sativum* L.), maize (*Zea* mays L.), sunflower (*Helianthus annuus* L.), tomato (*Lycopersicon esculentum* Mill.), castor bean (*Ricinus communis* L.), wheat (*Triticum aestivum* L.) and spinach (*Spinacia oleracea* L.) performed differently along the NH_4^+ to NO_3^- ratio gradient (Fig. 3.1). Interestingly, total plant dry mass (DM) of all 9 species did not significantly differ between the 100% NH_4^+ and 0% NH_4^+ (100% NO_3^-) treatments, and no chlorosis of leaves (typical ammonium toxicity symptom) was observed in the plants under 100% NH_4^+ treatment. Maximum total DM generally occurred at mixtures of NH_4^+ and NO_3^-: in 25% NH_4^+ (bean, soybean, tomato and wheat), 50% NH_4^+ treatment (maize, pea, Castor bean and spinach), or in 75% NH_4^+ (sunflower). There were no significant differences in total DM along the NH_4^+ to NO_3^- ratio gradient in most species. A significant decrease ($p < 0.05$) under 100% NH_4^+ treatment (minimum) compared to 50% NH_4^+ treatment (maximum) in maize and a significant increase ($p < 0.05$) under 25% NH_4^+ treatment (maximum) compared to 0, 75 and 100% NH_4^+ treatments in wheat were observed (Fig. 3.2).

Shoot DM responded to the NH_4^+:NO_3^- ratio gradient in all 9 species in a similar manner as did total DM. One exception was observed in spinach shoots where DM in the 100% NH_4^+ treatment (minimum) was significantly smaller than in the 25%, 50% and 75% NH_4^+ treatments (Fig. 3.3). Root biomass accumulation was approximately 10 times smaller than shoot mass accumulation among all 9 species. However, root DM followed different patterns in response to the NH_4^+ to NO_3^- ratio gradient. There was no root DM reduction under 100% NH_4^+ treatment compared to other treatments in spinach. Except 50% NH_4^+ treatment in maize roots and 25% NH_4^+ treatment in wheat roots, which presented a significant increase compared to maize roots at 100% NH_4^+ treatment and wheat roots at 50%, 75% and 100% NH_4^+ treatments ($p < 0.05$), respectively, no more significant differences were observed among root DM (Fig. 3.4).

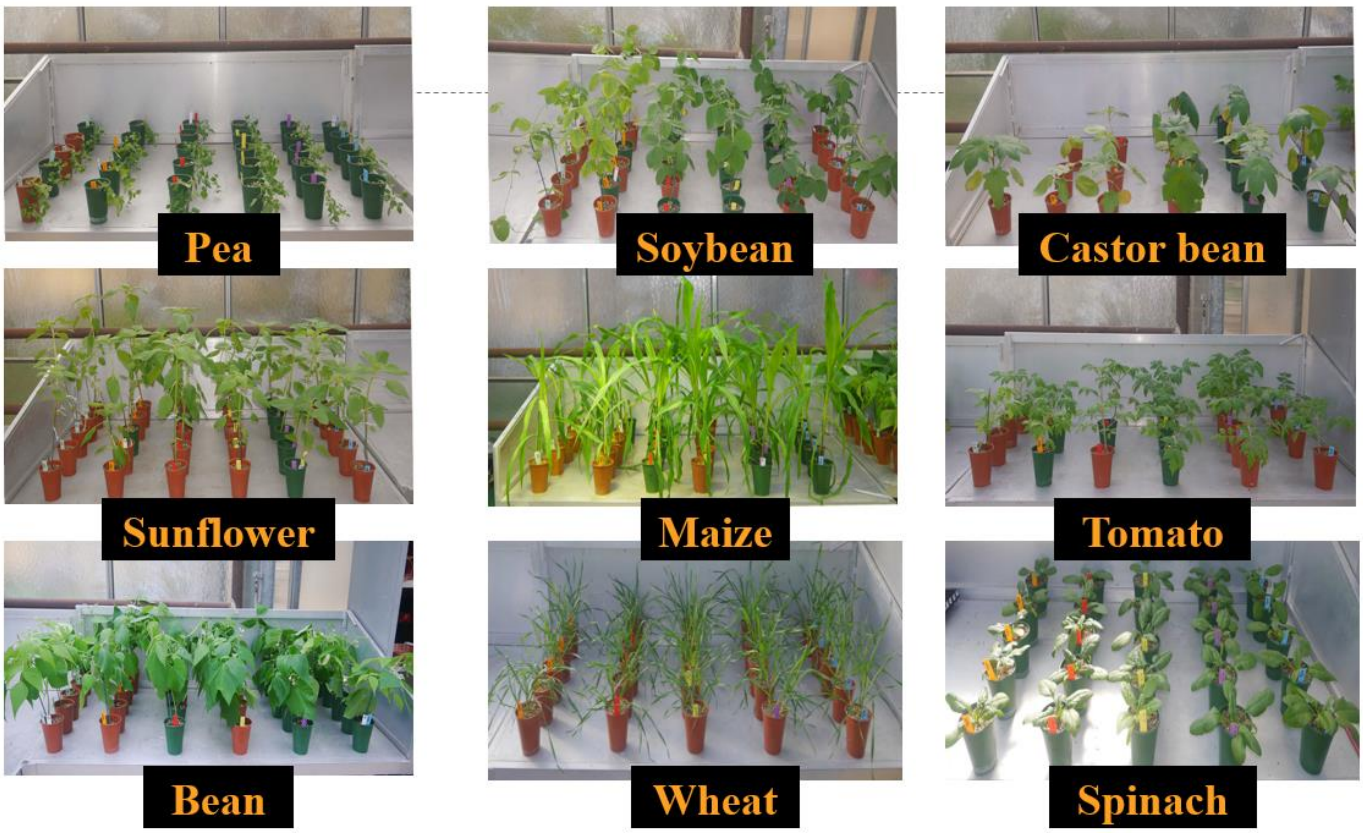

Figure 3.1 Nine species (bean, soybean, pea, maize, sunflower, tomato, castor bean, wheat and spinach) cultured under different % of NH_4^+ and NO_3^- as N source in nutrient solutions. Each row of pots represents a given ratio of NH_4^+: NO_3^- corresponding from left to right to 100%, 90%, 75%, 50%, 25% and 0%. The first rows for pea, soybean, castor bean, sunflower, maize, tomato and bean were the usual nutrient solution provided by the greenhouse, which were set as control. Photos were made on the harvesting days.

Plant root to shoot DM ratios of the 9 species were quite stable without significant differences along the NH_4^+ to NO_3^- ratio gradient in bean, pea, castor bean, sunflower and tomato. In spinach, root/shoot ratio positively correlated with NH_4^+%, increasing from 0.21 at 0% NH_4^+ to 0.42 at 100% NH_4^+. The 100% NH_4^+ treatment particularly showed a significant increase compared to other treatments. Contrarily, root/shoot ratio of wheat decreased from 0.46 at 0% NH_4^+ to 0.37 at 100% NH_4^+. The 100% NH_4^+ treatment presented a significant decrease compared to the 0% NH_4^+ and 25% NH_4^+ treatments (Fig. 3.5). The maximum value of root/shoot ratio in maize and soybean appeared in 25% NH_4^+ and 75% NH_4^+ treatments, respectively.

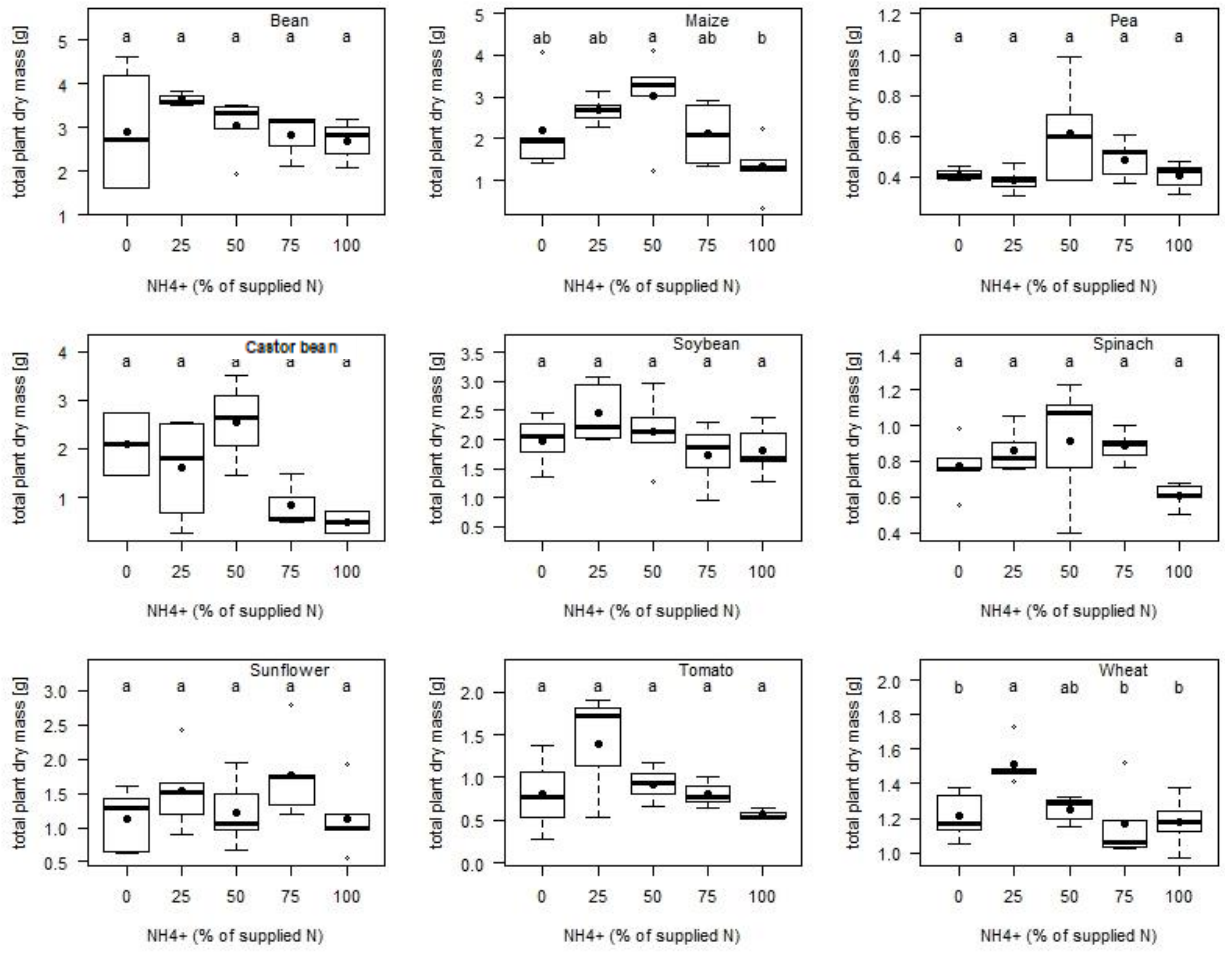

Figure 3.2 Total dry mass of bean, soybean, pea, maize, sunflower, tomato, castor bean, wheat and spinach cultured under different % of NH_4^+ and NO_3^- as N source in nutrient solutions used for watering the pots. On the X-axis, 0 and 100 correspond to 0% NH_4^+ (i.e. 100% NO_3^-) and 100% NH_4^+ (i.e. 0% NO_3^-) as % of supplied N in the nutrient solutions, respectively. Box and whisker plots show the distribution of the data where the line within the box stands for the median. Filled circles represent the mean (n=5). The box range includes the second and third quartile and the whiskers are located at the maximum and minimum values or at 1.5 times the interquartile range. If more extreme values are present, these are then shown with open circles. Same lowercase letters indicate results that are not significantly different at $p < 0.05$.

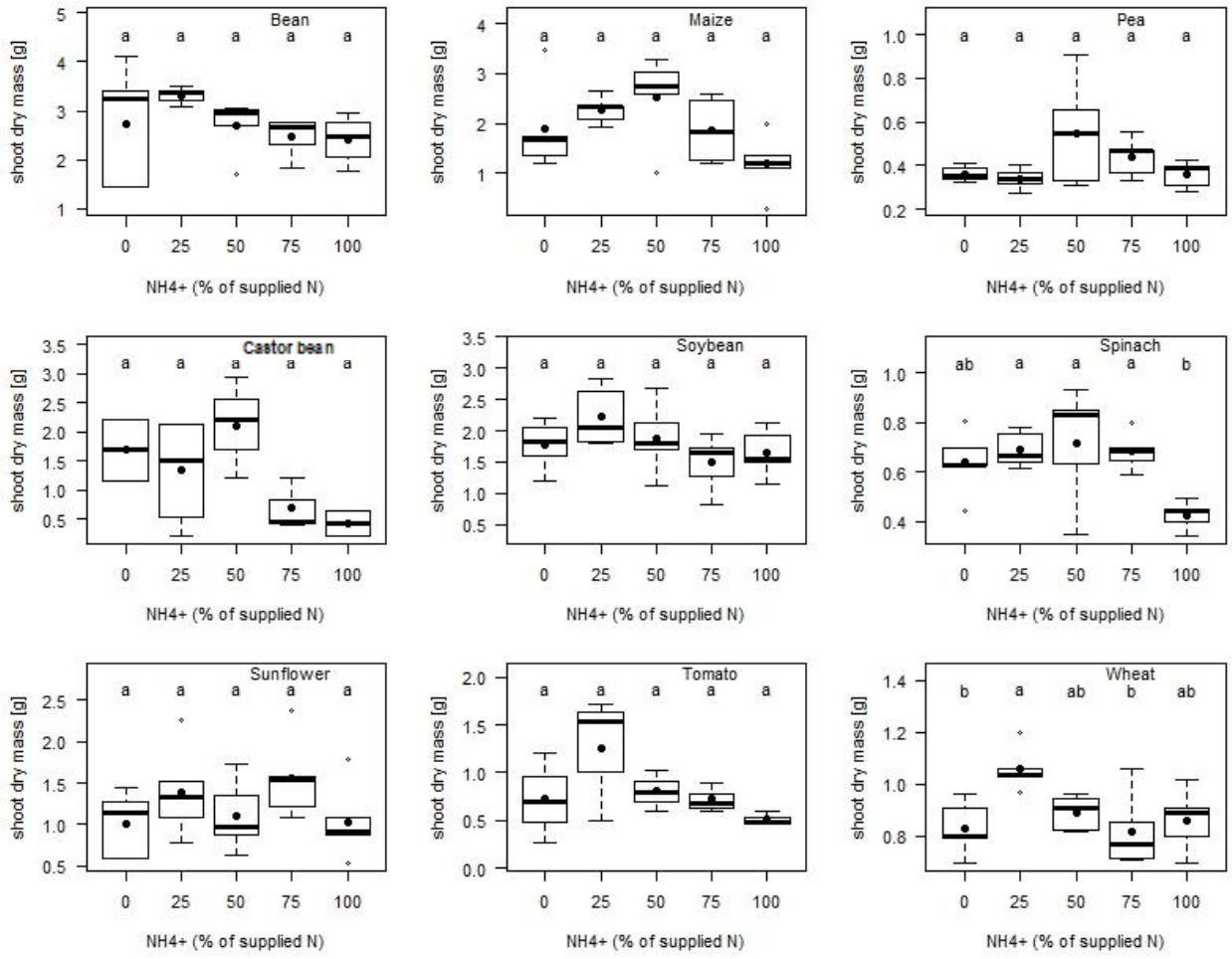

Figure 3.3 Shoot dry mass of bean, soybean, pea, maize, sunflower, tomato, castor bean, wheat and spinach cultured under different % of NH_4^+ and NO_3^- as N source in nutrient solutions used for watering the pots. On the X-axis, 0 and 100 correspond to 0% NH_4^+ (i.e. 100% NO_3^-) and 100% NH_4^+ (i.e. 0% NO_3^-) as % of supplied N in the nutrient solutions, respectively. Box and whisker plots show the distribution of the data where the line within the box stands for the median. Filled circles represent the mean (n=5). The box range includes the second and third quartile and the whiskers are located at the maximum and minimum values or at 1.5 times the interquartile range. If more extreme values are present, these are then shown with open circles. Same lowercase letters indicate results that are not significantly different at $p < 0.05$.

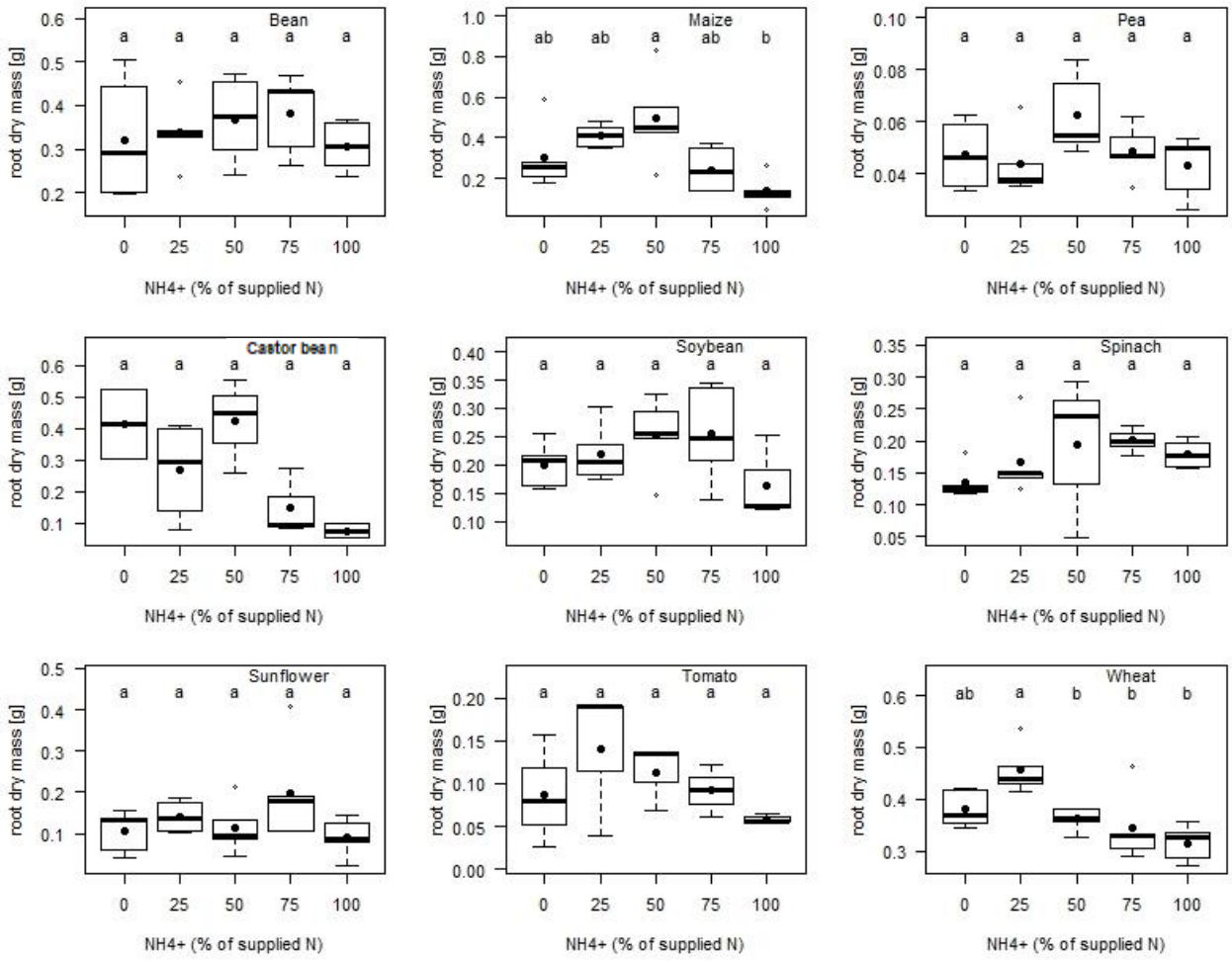

Figure 3.4 Root dry mass of bean, soybean, pea, maize, sunflower, tomato, castor bean, wheat and spinach cultured under different % of NH_4^+ and NO_3^- as N source in nutrient solutions used for watering the pots. On the X-axis, 0 and 100 correspond to 0% NH_4^+ (i.e. 100% NO_3^-) and 100% NH_4^+ (i.e. 0% NO_3^-) as % of supplied N in the nutrient solutions, respectively. Box and whisker plots show the distribution of the data where the line within the box stands for the median. Filled circles represent the mean (n=5). The box range includes the second and third quartile and the whiskers are located at the maximum and minimum values or at 1.5 times the interquartile range. If more extreme values are present, these are then shown with open circles. Same lowercase letters indicate results that are not significantly different at $p < 0.05$.

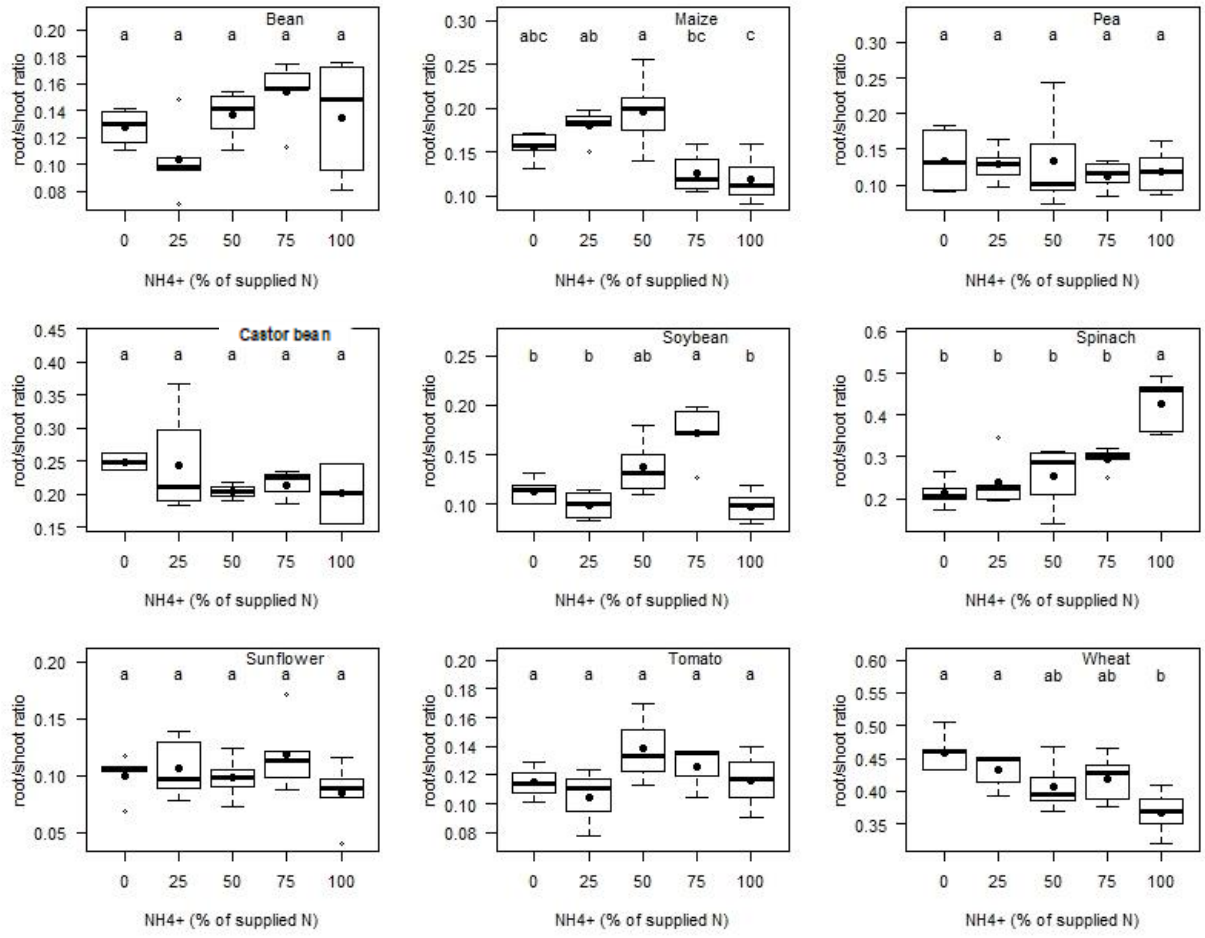

Figure 3.5 Root to shoot dry mass ratio of bean, soybean, pea, maize, sunflower, tomato, castor bean, wheat and spinach cultured under different % of NH_4^+ and NO_3^- as N source in nutrient solutions used for watering the pots. On the X-axis 0 and 100 correspond to 0% NH_4^+ (i.e. 100% NO_3^-) and 100% NH_4^+ (i.e. 0% NO_3^-) as % of supplied N in the nutrient solutions, respectively. Box and whisker plots show the distribution of the data where the line within the box stands for the median. Filled circles represent the mean (n=5). The box range includes the second and third quartile and the whiskers are located at the maximum and minimum values or at 1.5 times the interquartile range. If more extreme values are present, these are then shown with open circles. Same lowercase letters indicate results that are not significantly different at $p < 0.05$.

In this experiment, the final plant biomass was positively related to the initial seed mass in 8 species (bean, soybean, maize, sunflower, tomato, castor bean, wheat and spinach), but pea was an exception (Fig. 3.6). Seed mass represents the amount of reserves to start the first life stages. It is one of the most important traits influencing the early phases of the plant life cycle, including germination, growth rate and survival of seedlings. For example, larger seeds produce larger seedlings, which have larger shoots and more extensive roots to capture more light and water

(Green and Juniper, 2004; Quero *et al.*, 2007). Here, the average seed mass of pea was larger than that of tomato, spinach, wheat and sunflower, its total dry mass was the smallest among all 9 species. Furthurmore, the ratio of initial seed mass to total dry mass in pea is the largest (29.0%). Other legumes showed also relatively larger ratios, 17.1% and 13.9% in soybean and bean, respectively. In castor bean seeds, which contain more reserves, it accounted for 25.3% of the total dry mass. Spinach, wheat and sunflower, which had smaller initial seed mass, showed also smaller ratios to total dry mass (1.3% 3.0% and 2.8%, respectively). The smallest initial seed mass to total dry mass ratio was found in tomato; only 0.1% of initial seed mass to total dry mass.

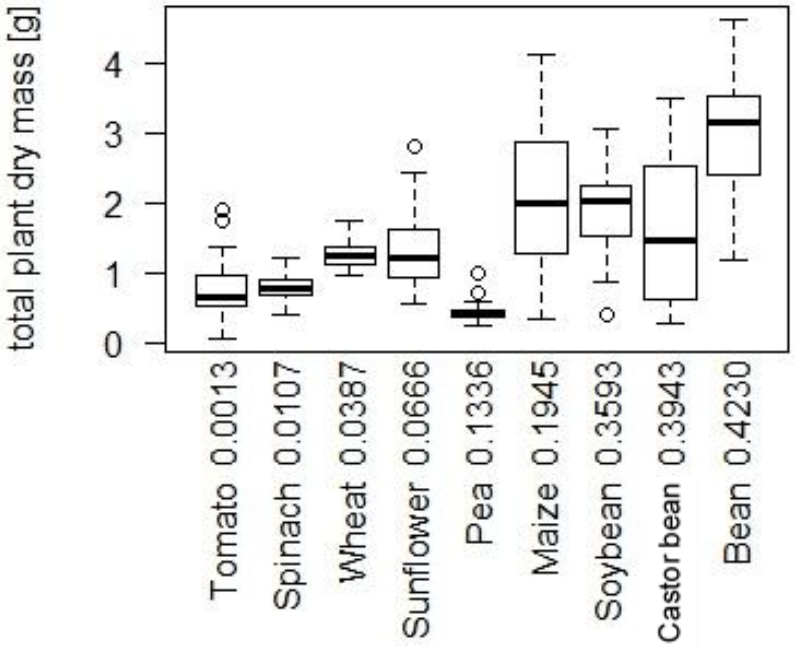

Figure 3.6 Seed initial mass and plant biomass relationships for bean, soybean, pea, maize, sunflower, tomato, castor bean, wheat and spinach cultured under different % of NH_4^+ and NO_3^- as N source in nutrient solutions used for watering the pots. The initial seed mass was determined on seeds other than those used for the culture. For soybean, castor bean and bean, the dry mass was determined as the mean of 20 seeds, for pea, wheat, tomato, spinach and sunflower, it was the mean of 50 seeds, and for maize it was the mean of 30 seeds. X-axis is ordered by the initial seed dry mass and its label shows the species name and the initial seed dry mass. Box and whisker plots show the distribution of the data where the line within the box stands for the median. The box range includes the second and third quartile and the whiskers are located at the maximum and minimum values or at 1.5 times the interquartile range. When more extreme values are present, these are then shown with open circles.

3.3.2 Effect of N-type gradient supply on C-isotope composition of organic matter in plants

Figure 3.7 shows leaf bulk carbon isotope composition in the 9 species (bean, soybean, pea, maize, sunflower, tomato, castor bean, wheat and spinach) grown along nitrogen type gradient as the N source. Obviously, $\delta^{13}C_{OM}$ of C_3 plant leaves (–28.3 to –33.9‰) were more ^{13}C depleted than C_4 plant leaves (–11.1 to –12.6‰), and among C_3 plants, leaves of soybean (–28.1 to –30.9‰) and castor bean (–27.8 to –31.1‰) were more ^{13}C enriched than those of other species, while pea (–31.8 to –33.6‰) and sunflower (–30.9 to –34.9‰) showed the most ^{13}C depleted values. Along the NH_4^+ to NO_3^- ratio gradient, species responded differently. $\delta^{13}C_{OM}$ of monocotyledonous plants (maize and wheat) increased from –11.9‰ (at 0% NH_4^+) to –11.5‰ (at 75% NH_4^+) and from –31.6‰ (at 0% NH_4^+) to –30.8‰ (at 100% NH_4^+) in maize and wheat, respectively. However, the responses of castor bean and spinach leaves were inverse, $\delta^{13}C_{OM}$ became more and more ^{13}C depleted with increase of NH_4^+ supply; it decreased from –28.3 (0% NH_4^+) to –30.3‰ (75% NH_4^+) and from –30.1 (0% NH_4^+) to –31.9‰ (100% NH_4^+), respectively. Interestingly, $\delta^{13}C_{OM}$ in leaves under 100% NH_4^+ did not follow the overall trend in maize and castor bean. A significant difference between 100% NH_4^+ and 0% NH_4^+ treatment was only observed in wheat and spinach. Leaf-$\delta^{13}C_{OM}$ in bean, soybean, sunflower and tomato was stable along NH_4^+ to NO_3^- ratio gradient, $\delta^{13}C_{OM}$ of 50% NH_4^+ and 75% NH_4^+ treatment showed significant ^{13}C depletion compared to 25% NH_4^+ and 100% NH_4^+ treatments, but no trend was found.

OM in C_3 plant roots was ^{13}C enriched compared to their corresponding leaves, but not for C_4 plants (Fig. 3.8). Similar to leaves, root-$\delta^{13}C_{OM}$ of C_4 plants (–11.2 to –12.4‰) was more ^{13}C enriched than that of C_3 plants (–27.0 to –33.0‰). Sunflower roots were the most ^{13}C depleted (–29.0 to –33.0‰) among the 8 C_3 plant species, while soybean roots were the most ^{13}C enriched in this experiment (–26.4 to –30.6‰). $\delta^{13}C_{OM}$ in wheat and spinach roots responded to NH_4^+ to NO_3^- ratio gradient in the same manner as they did in leaves. Root-$\delta^{13}C_{OM}$ of wheat became more and more ^{13}C enriched when higher fractions of N were supplied as NH_4^+. $\delta^{13}C_{OM}$ under 100% NH_4^+ treatment was significantly more ^{13}C enriched compared to 0% NH_4^+ treatment. On the contrary, root-$\delta^{13}C_{OM}$ of spinach had a negative relationship with % of NH_4^+ supply. Root-$\delta^{13}C_{OM}$ under 100% NH_4^+ was significantly more ^{13}C depleted compared to 0% NH_4^+ treatment. Root-$\delta^{13}C_{OM}$ in castor bean and tomato also showed negative relationships with NH_4^+% supply. There were no significant differences among treatments. In summary, apart from wheat and spinach, no significant differences of $\delta^{13}C_{OM}$ between 100% NH_4^+ and 0% NH_4^+ treatment were observed in roots.

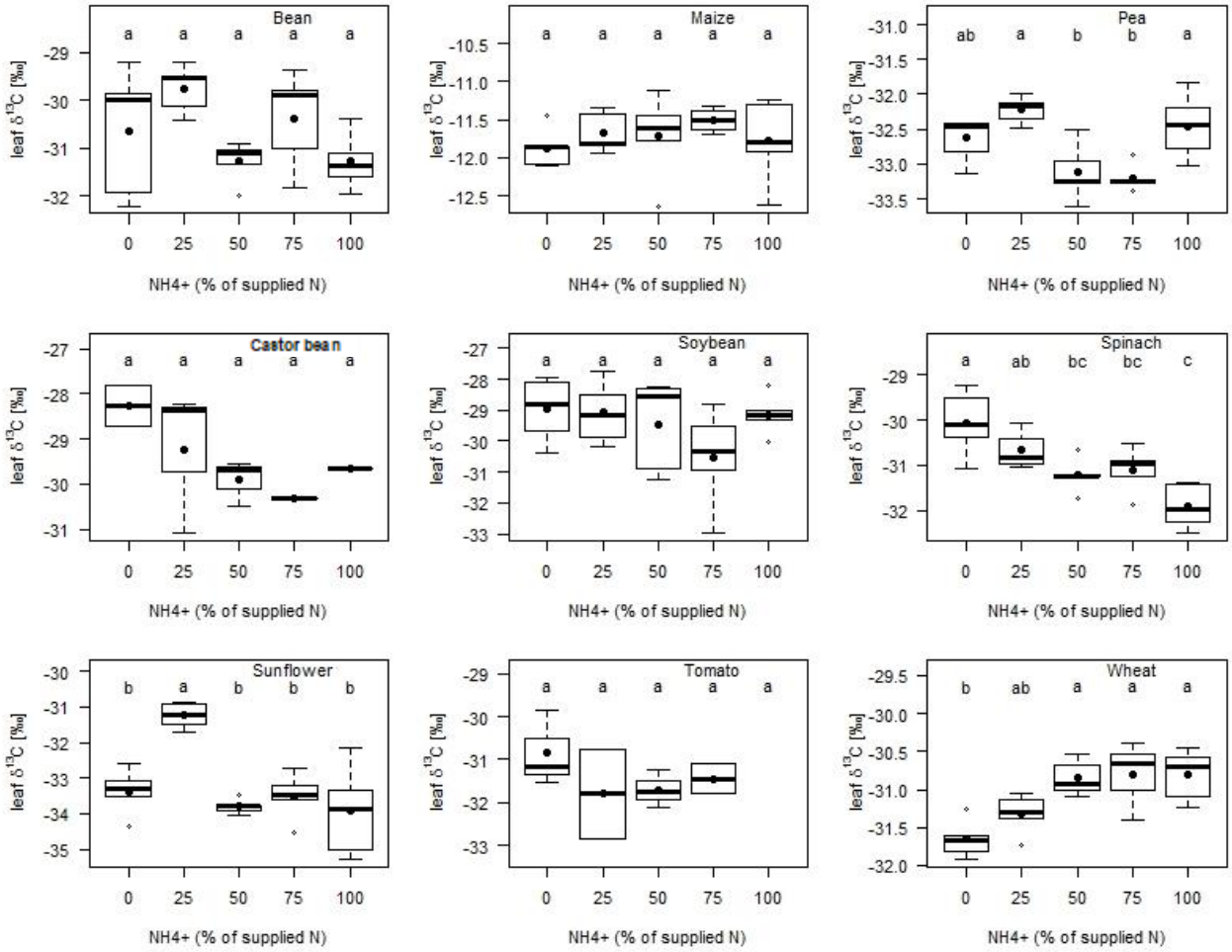

Figure 3.7 $\delta^{13}C$ of leaf organic matter ($\delta^{13}C_{OM}$) of bean, soybean, pea, maize, sunflower, tomato, castor bean, wheat and spinach grown with nutrient solutions containing different % of NH_4^+ and NO_3^- as N source. On the X-axis, 0 and 100 correspond to 0% NH_4^+ (i.e. 100% NO_3^-) and 100% NH_4^+ (i.e. 0% NO_3^-) as % of total N in the nutrient solutions, respectively. Box and whisker plots show the distribution of the data where the line within the box stands for the median. Filled circles represent the mean (n=5). The box range includes the second and third quartile and the whiskers are located at the maximum and minimum values or at 1.5 times the interquartile range. If more extreme values are present, these are then shown with open circles. The value for tomato 100% NH_4^+ treatment was missing because the dry matter was too small to meet the isotope analysis requirement. Same lowercase letters indicate results that are not significantly different at $p < 0.05$. Notes of the missing point of $\delta^{13}C_{OM}$ of tomato leaves in 100% NH_4^+ treatment: the material was too less for isotopic analysis.

Differences between root-$\delta^{13}C_{OM}$ and leaf-$\delta^{13}C_{OM}$ were less affected by NH_4^+ to NO_3^- ratio gradient (Fig. 3.9). Maize, as a C_4 plant, on average performed negative values and few changes (–0.19‰ to –0.35‰) with no significant differences among treatments. Among C_3 plants, pea had the largest $\delta^{13}C$ differences between roots and leaves (2.17‰ to 3.23‰), while spinach had the smallest differences, from 0.00 to 0.12‰, castor bean performed slightly higher differences and stronger variation (0.38‰ to 1.68‰). The between-organ $\delta^{13}C_{OM}$ differences in bean, soybean, sunflower, tomato and wheat ranged from 0.87‰ to 2.38‰. There were no significant differences of root-leaf $\delta^{13}C_{OM}$ between 100% NH_4^+ and 0% NH_4^+ treatments in none of the 9 species.

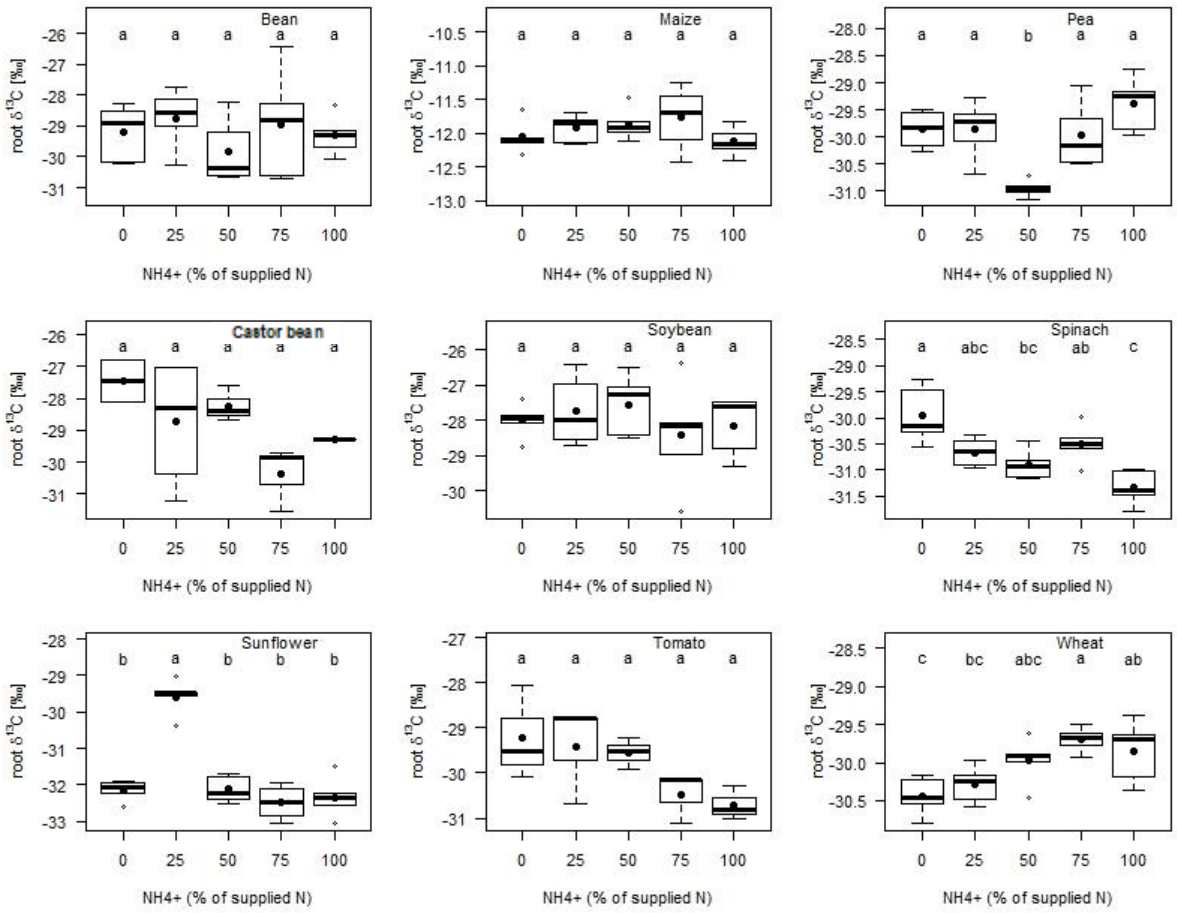

Figure 3.8 $\delta^{13}C$ of root organic matter ($\delta^{13}C_{OM}$) of bean, soybean, pea, maize, sunflower, tomato, castor bean, wheat and spinach grown with nutrient solutions containing different % of NH_4^+ and NO_3^- as N source. On the X-axis, 0 and 100 correspond to 0% NH_4^+ (i.e. 100% NO_3^-) and 100% NH_4^+ (i.e. 0% NO_3^-) as % of total N in the nutrient solutions, respectively. Box and whisker plots show the distribution of the data where the line within the box stands for the median. Filled circles represent the mean (n=5). The box range includes the second and third quartile and the whiskers are located at the maximum and minimum values or at 1.5 times the interquartile range. If more extreme values are present, these are then shown with open circles. Same lowercase letters indicate results that are not significantly different at $p < 0.05$.

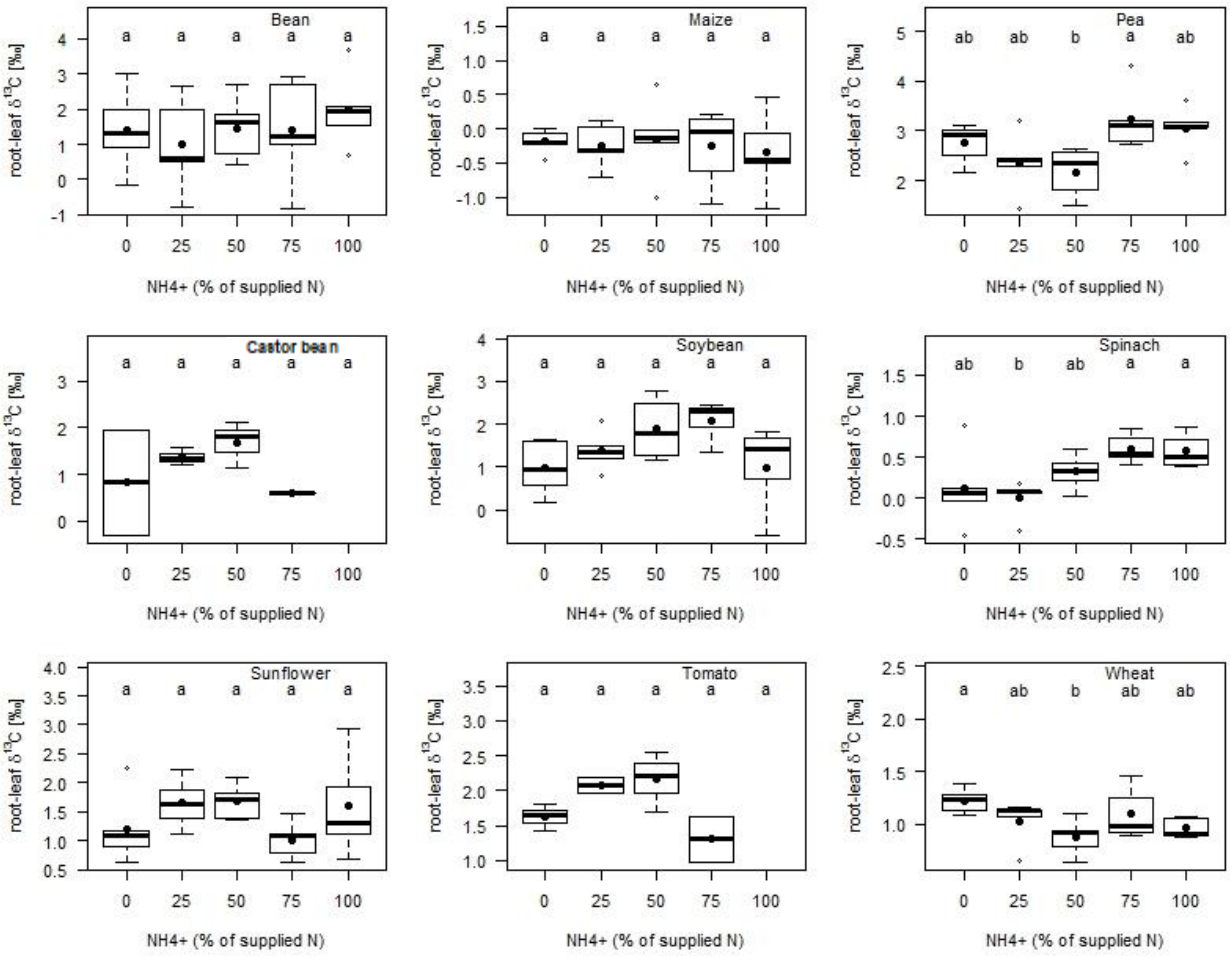

Figure 3.9 Variations in $\delta^{13}C$ difference between root and leaf of bean, soybean, pea, maize, sunflower, tomato, castor bean, wheat and spinach grown with nutrient solutions containing different % of NH_4^+ and NO_3^- as N source. On the X-axis, 0 and 100 correspond to 0% NH_4^+ (i.e. 100% NO_3^-) and 100% NH_4^+ (i.e. 0% NO_3^-) as % of total N in the nutrient solutions, respectively. The value for tomato 100% NH_4^+ treatment was missing because the dry matter was too small to meet the isotope analysis requirement. Box and whisker plots show the distribution of the data where the line within the box stands for the median. Filled circles represent the mean (n=5). The box range includes the second and third quartile and the whiskers are located at the maximum and minimum values or at 1.5 times the interquartile range. If more extreme values are present, these are then shown with open circles. Same lowercase letters indicate results that are not significantly different at $p < 0.05$. $\delta^{13}C_{OM}$ values for castor bean and tomato leaves are missing under 100% NH_4^+ treatment.

3.3.3 Correlation between C-isotope composition of organic matter and plant dry mass along NH_4^+ to NO_3^- ratio gradient

Total plant dry mass was positively related to $\delta^{13}C$ of whole plant ($\delta^{13}C_{plant}$) in all C_3 species, but slightly negatively in maize (C_4 plant). It was not correlated with the NH_4^+ to NO_3^- ratio gradient (Table 3.1, Fig. 3.10). $\delta^{13}C$ of the whole plant was calculated by: $\delta^{13}C_{plant} = ((\delta^{13}C_{root} \cdot \text{root mass}) + (\delta^{13}C_{leaf} \cdot \text{leaf mass})) / \text{total plant mass}$. In bean and soybean, which yielded higher total plant biomass, the positive relation between plant dry mass and $\delta^{13}C_{plant}$ was significant ($p_{mass} = 0.002$, and $p_{mass} = 0.028$, respectively). For sunflower and tomato, positive but non-significant relations were observed ($p_{mass} < 0.1$). The NH_4^+ to NO_3^- ratio in the nutrient solution had no significant impact on $\delta^{13}C_{plant}$ (Table 2.1). The relationship between individual leaf-$\delta^{13}C$ and individual leaf biomass, and between individual root-$\delta^{13}C$ and individual root biomass followed similar trends as the relationships between individual $\delta^{13}C$ of whole plant and individual total plant biomass (Fig. 3.10).

Table 3.1 Multiple regression of $\delta^{13}C$ of whole plant versus total plant biomass and different % of NH_4^+ and NO_3^- as N source. p_{mass} stands for the p value of the factor plant dry mass; p_{Nperc} stands for the p value of the factor of NH_4^+ to NO_3^- ratio; $p_{interact}$ stands for the interaction term of plant dry mass and NH_4^+ to NO_3^- ratio; p presents the p value for the full regression model which is associated with the R^2. Slope denotes the slope of $\delta^{13}C$ of whole plant versus biomass.

Species	Intercept	Slope	p_{mass}	p_{Nperc}	$p_{interact}$	R^2	p
Bean	–33.2041	0.9434	0.0019	0.3120	0.2481	0.4481	0.0068
Castor bean	–30.9130	1.3290	0.1324	0.5695	0.2013	0.6514	0.1265
Maize	–11.4780	–0.1669	0.2377	0.2166	0.0881	0.1632	0.3020
Pea	–32.5398	0.6759	0.7992	0.5350	0.4734	0.1789	0.2574
Soybean	–32.6392	1.6702	0.0265	0.7675	0.7585	0.4561	0.0045
Spinach	–31.2344	1.2618	0.2802	0.5503	0.7328	0.6140	0.0001
Sunflower	–34.1747	1.4258	0.0592	0.6569	0.5581	0.4174	0.0089
Tomato	–32.2402	1.4709	0.0954	0.9187	0.7948	0.5767	0.1368
Wheat	–31.9288	0.5901	0.3680	0.1709	0.3978	0.4865	0.0025

Figure 3.10 Relationship between $\delta^{13}C$ values and biomass of individual plants (A, whole plant, B, leaves and C, roots) of different 9 species (bean, soybean, pea, maize, sunflower, tomato, Castor bean, wheat and spinach) grown with nutrient solutions containing different % of NH_4^+ and NO_3^- as N source. In the legend box, different symbols correspond to different species, cross presents bean, asterisk presents castor bean, white circle presents maize, black square presents pea, inverted diamond with cross presents soybean, inverted triangle presents spinach, black circle presents sunflower, regular triangle presents tomato and white square present wheat. Each data point corresponds to individual measurement on independent plant.

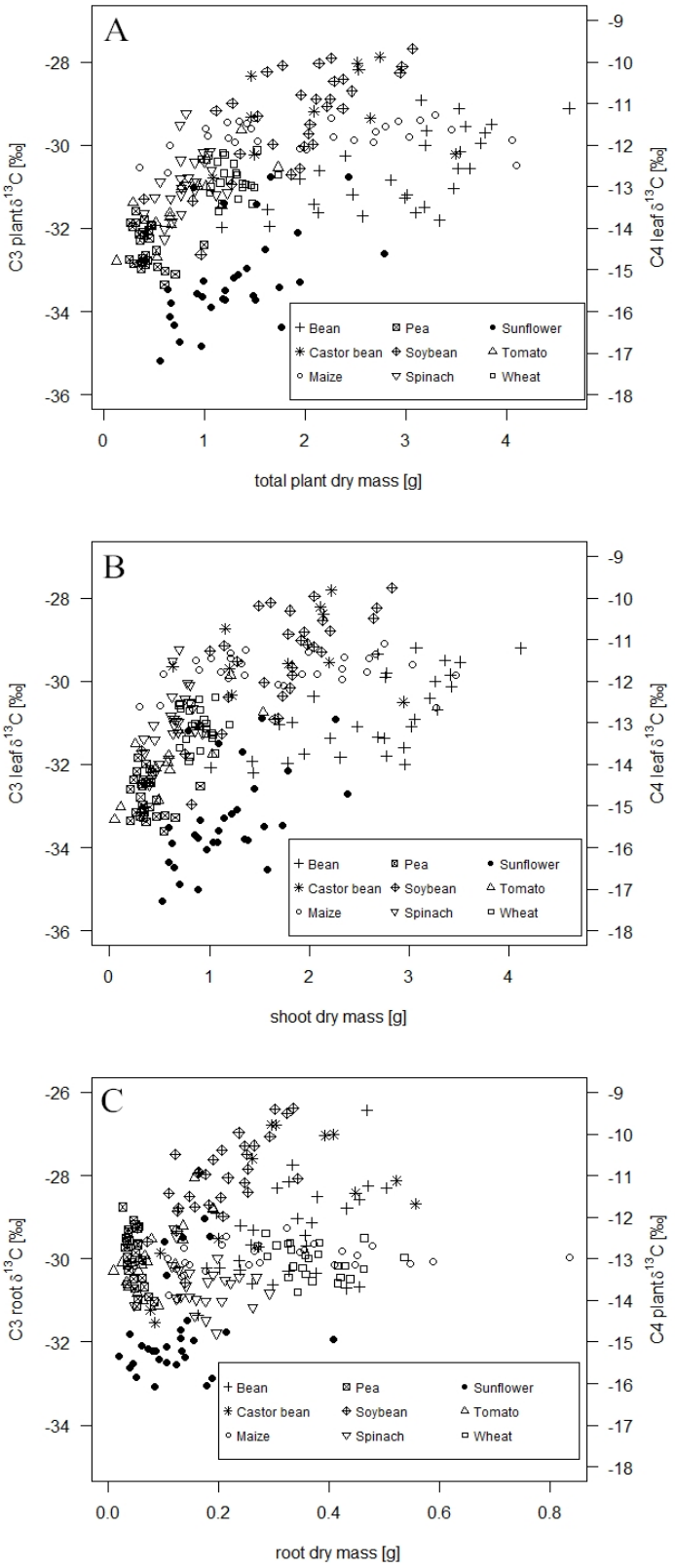

3.4 Discussion

3.4.1 Effect of N-type gradient supply on plant growth

Our results did not show significant effect of NH_4^+ to NO_3^- ratio gradient on plant growth. The manner of different species varied slightly. Certain plant species (e.g. maize, castor bean, spinach and wheat) were relatively more sensitive to high NH_4^+ concentrations, while legumes (e.g. bean, soybean and pea) were more tolerant to NH_4^+. The other species were little affected by NH_4^+ to NO_3^- ratio gradient. Those results are simillar to former researches including tomato (Magalhaes and Huber, 1989; Feng and Barker, 1992; Cruz *et al.*, 2006), castor bean (Allen and Smith, 1986), wheat (Cramer and Lewis, 1993a), maize (Cramer and Lewis, 1993b; Cramer *et al.*, 1993), bean (Guo *et al.*, 2002) and spinach (Elia *et al.*, 1998; Lasa *et al.*, 2002a, b; Cruz *et al.*, 2006). However, in some experiments, legumes were more sensitive when NH_4^+ was applied as sole N source, such as bean (Chaillou *et al.*, 1986) and pea (Bligny *et al.*, 1997). Such variations in NH_4^+ tolerance can be caused by different experimental conditions, for example, NH_4^+ concentrations, pH regimes, concentration of other supplied nutrients (calcium, phosphorus, potassium, etc.), light intensity, temperature, different developmental stages of plants (Gerendás *et al.*, 1997; Britto and Kronzucker, 2002), and also the duration of the NH_4^+-treatment. In addition, the highest biomass always occurred in mixed NH_4^+ and NO_3^- and not under 100% NO_3^- nor 100% NH_4^+ condition. That is probably a consequence of the interactions between NO_3^- and NH_4^+ during nitrogen uptake, allocation or assimilation. Similar results were found by other researchers (Magalhaes and Huber, 1991; Cao and Tibbitts, 1993). Little suppression of growth between 0% NH_4^+ (100% NO_3^-) and 100% NH_4^+ among the 9 species may be attributed to low light intensity during the culture period in the present experiment (Seel *et al.*, 1993; Zhu *et al.*, 2000).

There was not a general response of root/shoot ratio along NH_4^+ to NO_3^- ratio gradient among species, with three types of trends: increasing in spinach, decreasing in wheat, and no changes in other species. Those results confirmed the findings in former researches (Chaillou *et al.*, 1986; Magalhaes and Huber, 1991; Cramer and Lewis, 1993a; Cramer *et al.*, 1993; Raab and Terry, 1994; Guo *et al.*, 2002; Lasa *et al.*, 2002a, b; Sarasketa *et al.*, 2016). The symptoms of NH_4^+ toxicity on spinach is mainly reflected in the reduction of leaf DM, but in root DM of wheat. Possible mechanisms of ammonium toxicity in plants have been explained including depletion of carbon supply, damaged chloroplast ultrastructure, deficiency of mineral cations, disruptions in hormonal homeostasis and in photosynthesis, energy-demanding, futile trans-membrane ammonium cycling,

increased proton efflux, inhibition of the enzyme GDP-mannose pyrophosphorylase, oxidative stress, shifting the cellular pH to intolerable levels, uncoupling of photophosphorylation, and higher root carbon allocation to amino acid synthesis under NH_4^+ nutrition, etc. (Britto and Kronzucker, 2002; Lasa *et al.*, 2002a; Andrews *et al.*, 2013; Bittsanszky *et al.*, 2015). Unfortunately, we cannot determine the possible toxicity mechanism on spinach and wheat from the data obtained in this experiment. However, it is known that during plant growth, shoots provide carbon and roots provide nutrients and water. Plants with a higher proportion of roots can compete more effectively for nutrients, while those with a higher proportion of shoots can collect more light energy from photosynthesis (Agren and Ingestad, 1987). Our results support the hypothesis that high concentration of NH_4^+ may inhibit carbon fixation of leaves in spinach and reduce nutrient absorption ability of the root system in wheat. Therefore, spinach leaves and wheat roots were more sensitive to, and legumes were more tolerence of NH_4^+ in our experimental conditions.

3.4.2 Effect of N-type gradient supply on C-isotope composition of organic matter in plants

The $\delta^{13}C$ values in our experiment confirmed two common findings: C_4 plants (maize) were more ^{13}C enriched in both leaves and roots than C_3 plants; leaves were more ^{13}C depleted compared with roots. These $\delta^{13}C$ values are consistent with already published data and theory. Phospho*enol*pyruvate carboxylase (PEPc) in mesophyll cells of C_4 plants captures more ^{13}C enriched CO_2 than Rubisco does in C_3 plants, leading to a more ^{13}C enriched values of organic matter in C_4 plants than in C_3 plants (Farquhar, 1983). The isotopic difference between autotrophic and heterotrophic organs has frequently been observed and hypotheses on potential causes were summarized by Badeck *et al.* (2005). Furthermore, isotopic composition of C_3 plants varies largely among species, between –21‰ and –35‰ (Badeck *et al.*, 2005). The results in our experiments are consistent with this. It is well known that the $\delta^{13}C$ value of plant organic matter is highly related to the atmospheric $\delta^{13}CO_2$, and culture condition such as light, humidity and temperature, which may affect stomatal conductance thus leading to differences in $\delta^{13}C_{OM}$ values. Therefore, in the same species, different $\delta^{13}C_{OM}$ values between our results and other experiments were observed: wheat was 1‰ ^{13}C depleted relative to the results of Lopes and Araus (2006); spinach was 2‰ ^{13}C depleted relative to the results of Lasa *et al.* (2002b); bean was 1.5‰, 2‰ and 3‰ ^{13}C depleted relative to the results of Bathellier *et al.* (2008), Guo *et al.* (2002) and Tcherkez *et al.* (2003),

respectively; and maize was more ^{13}C enriched compared with the results of Werth and Kuzyakov (2005).

Turning now to the response of $\delta^{13}C_{OM}$ values along the NH_4^+ to NO_3^- ratio gradient, our observation from 9 different species showed that $\delta^{13}C_{OM}$ values of spinach and wheat were more strongly affected by the NH_4^+ to NO_3^- ratio gradient in both leaves and roots, while the other species were less sensitive to it. In both leaves and roots, wheat was more ^{13}C depleted in the NO_3^- than in the NH_4^+ treatment, which is similar to the results of Lopes and Araus (2006), but different from the results of Yin and Raven (1998). As opposed to wheat, spinach was more ^{13}C depleted in the NO_3^- than in the NH_4^+ treatment, in agreement with the data reported by Lasa *et al.* (2002b). The latter study also confirmed that pea, as a legume, was little affected by the N type source. Moreover, Guo *et al.* (2002) observed that bean roots were 1.05‰ ^{13}C enriched but leaves were 0.08‰ ^{13}C depleted when NH_4^+ was applied as sole N source compared to NO_3^-. However, there are no data in the literature on the responses to NH_4^+ to NO_3^- ratio gradient of those species in terms of $\delta^{13}C_{OM}$. In addition, similar to the results on biomass, the most ^{13}C enriched or ^{13}C depleted values of $\delta^{13}C_{OM}$ generally occurred in NH_4^+ and NO_3^- mixture treatment but not in 100% NO_3^- or 100% NH_4^+ conditions. This implies that the interactions between NO_3^- and NH_4^+ may affect carbon isotope fractionation during nitrogen uptake, allocation or assimilation.

3.4.3 Effect of plant growth on C-isotope composition of organic matter

The relationship between $\delta^{13}C$ of whole plant and total plant biomass was positive for all C_3 species but little effect was found for C_4 plants (Table 3.1 and Fig. 3.10) If higher biomass production were due to higher photosynthesis and higher C_i/C_a, $\delta^{13}C_{plant}$ would be negatively correlated with total plant biomass. The ratio of intercellular to ambient CO_2 concentrations (C_i/C_a) generally determines biomass: when C_i/C_a is high, stomata are more open and photosynthetic activity is higher, finally plants yield more biomass. On the other hand, according to the model proposed by Farquhar *et al.* (1982), $\delta^{13}C_{plant}$ of C_3 plant is negatively correlated to C_i/C_a; higher C_i/C_a will lead to more negative values of $\delta^{13}C_{plant}$. However, interestingly, C_3 plants in this experiment showed opposite trends. There are four potential explanations for this observation.

The first possibility involves the activity of the anaplerotic pathway *via* PEPc. Higher PEPc activity brings more ^{13}C enriched carbon to plant organic matter (see Figure 1.19 redrawn from

Nalborczyk, 1978) and the carbon fixed *via* anaplerotic pathway could also increase biomass. This is consistent with the results from this experiment, especially in roots. However, the capacity of carbon fixation *via* anaplerotic pathway is limited. More model calculations are necessary to see how much the impact of PEPc would account for the change of $\delta^{13}C_{plant}$.

The second possibility relates to the heritage of seed traits among species. According to seedling effect, bigger initial seeds will yield larger biomass, even after longtime growth (Paz and MartÍnez-Ramos, 2003). Seed mass of pea accounted for 29% of total biomass (Fig 3.6), and $\delta^{13}C_{plant}$ values were strongly affected by seed heritable carbon isotope composition but not the carbon fixed *via* photosynthesis. Generally, bigger seeds also bring more grain reserves to plants and thus contribute more on $\delta^{13}C_{plant}$, for example, bean and soybean seeds, which are bigger and contain more starch or proteins, bring more ^{13}C enriched organic carbon to plants and lead to more ^{13}C enriched plant OM. However, it was not the case in castor bean, which had bigger seeds and with more lipids (^{13}C depleted), but yielded more ^{13}C enriched plants with larger biomass. Probably, the remobilization of the seed reserves varies among species. On the other hand, on the contrary, $\delta^{13}C_{plant}$ of plants, which had smaller seeds was more affected by the isotope composition of photosynthetic carbon (e.g. tomato and sunflower).

Furthurmore, C_i/C_a values may vary between different growth stages. If stomata opened more in early growth stages when plants were small for accelerating carbon fixation, $\delta^{13}C_{plant}$ would be more ^{13}C depleted. If, then, at advanced growth stages, stomata opened less, more ^{13}C enriched organic carbon would be assimilated. Thus, bigger plants can be composed of a relatively higher share of ^{13}C enriched organic carbon. Sampling across growth stages and plant sizes could thus result in a positive correlation between dry mass and $\delta^{13}C_{plant}$.

Finally, $\delta^{13}C$ is positively correlated with water use efficiency, WUE (Farquhar and Richards, 1984). When the stomatal conductance and transpiration are low, WUE increases because the decrease in conductance does lead to a less than proportional decrease in net assimilation. Low WUE makes plants grow better. Plants may experience periods of intermittent drought. Then "water spenders" use up the water in the pot with high stomatal conductance and thus more negative δ13C than "water savers" that keep stomata a bit more closed even when there is ample water availability. When drought develops, the "water spenders" have to close stomates and produce less, while the "water savers" can go on assimilating with the water they had consumed less before. This

interpretation implies that the type of stomatal regulation is different between the plants that grew better and those that grew less well.

For C_4 plants, $\delta^{13}C_{plant}$ has little relationship with total plant biomass. Because $\delta^{13}C_{plant}$ is mainly determined by the leakage of CO_2 from bundle sheath cells to mesophyll but not by the changes in stomatal conductance. Therefore, C_i/C_a values affect little the $\delta^{13}C_{plant}$.

It should be noted that the present results do not reveal the mechanism of ammonium toxicity, and that we focus only on the survival of plants under extreme NH_4^+ in our culture conditions and on the effect of NH_4^+ to NO_3^- ratio gradient on plant carbon isotope fractionation.

3.5 Conclusion

According to our results, varying responses to NH_4^+:NO_3^- ratio gradient in different species were observed, but some broad generalizations are possible: (i) there was no significant effect of NH_4^+:NO_3^- ratio gradient on plant growth among all species, (ii) $\delta^{13}C$ of spinach leaves and wheat roots were more sensitive and legumes were more tolerent to NH_4^+, and (iii) $\delta^{13}C$ of whole plant was positively related to the total plant biomass in all C_3 species but not in C_4 maize plants.

Biomass and ammonium sensitivity are the two factors for our final species selection. DM of wheat in our experimental conditions was too small to support subsequent biochemical or isotope analysis. Several researchers chose pea and spinach in their studies and indicated that these two species responded to ammonium with different metabolic strategies (Lasa *et al.*, 2002b, a; Cruz *et al.*, 2006). However, similar to wheat, the DM of pea was too small for furthur analysis. Alternatively, bean is another legume, which has been well studied in our group for its respiratory carbon isotope fractionation (Tcherkez *et al.*, 2003; Nogués *et al.*, 2004; Bathellier *et al.*, 2008; Bathellier *et al.*, 2009a; Bathellier *et al.*, 2009b). In addition, the studies on the influence of NH_4^+ versus NO_3^- on carbon isotope fractionation are rare, particularly, there is no former study on the N-type effect on respiratory carbon isotope fractionation. Therefore, familiar species are preferable for our subsequent experiments.

We finally chose bean and spinach for more in-depth analysis, exploring the impact of varying NH_4^+:NO_3^- ratios in nutrient solution on carbon isotope composition of leaf- and root-respired CO_2 and putative respiratory substrates.

CHAPTER 4 - Impact of varying NH_4^+:NO_3^- ratios in supplied N on C-isotope composition of leaf- and root-respired CO_2 and putative respiratory substrates in *Phaseolus vulgaris* L.

Yang Xia[1*], Franz-W. Badeck[2], Camille Bathellier[3], Cyril Girardin[4], Gerd. Gleixner [5], Roland A. Werner [6], Chantal Fresneau[1], Shiva Ghiasi[5], Mélodie Faucon[1], Karen Cosnier[1], Jaleh Ghashghaie[1]

[1] *Ecologie Systématique Evolution, Université Paris-Sud, CNRS, AgroParisTech, Université Paris-Saclay, 91400, Orsay, France.*

[2] *Genomics research centre, Council for Agricultural Research and Economics (CREA- GPG), Fiorenzuola d'Arda (PC), Italy.*

3 Elementar, 69003-Lyon, France

[4] *INRA, UMR 1402, ECOSYS, Campus AgroParisTech, F-78850 Thiverval Grignon, France.*

[5] *Max-Planck-Institute for Biogeochemistry, P.O. Box 100164, 07701 Jena, Germany.*

[6] *Institute of Agricultural Sciences, ETH Zurich, CH-8092 Zurich, Switzerland.*

E-mail addresses:

*Corresponding author: yang.xia@u-psud.fr

franz@badeck.eu
camille.bathellier@gmail.com
cyril.girardin@inra.fr
gerd.gleixner@bgc-jena.mpg.de
rwerner@ethz.ch
chantal.fresneau@u-psud.fr
shiva.ghiasi@usys.ethz.ch
melodie.faucon@u-psud.fr
Karen.cosnier@u-psud.fr
Jaleh.ghashghaie@u-psud.fr

Abstract

C-isotope composition of leaf- and root-respired CO_2 in the dark and that of putative respiratory substrates including soluble sugars and organic acids (malate and citrate), PEPc and NR activities, as well as leaf gas exchanges were investigated on bean plants grown in sand with varying ratios of NH_4^+:NO_3^- in supplied N. No particular trend was observed for gas exchange parameters, except a significant decrease in photosynthesis under pure NH_4^+ nutrition. In agreement with our initial hypothesis, leaf-respired CO_2 was ^{13}C enriched under NO_3^- nutrition and became progressively ^{13}C depleted with increasing amount of NH_4^+ in supplied N, while C-isotope composition of root-respired CO_2 remained unchanged across N-type gradient. Malate and citrate were highly ^{13}C enriched compared to sugars in leaves. Although, no particular change in C-isotope composition of individual metabolites was observed across N-type gradient, isotope composition of respired CO_2 was positively correlated with that of total water soluble organic matter in leaves. A higher contribution of anaplerotically ^{13}C enriched C fixed by PEPc to the leaf-respired CO_2 of plants under NO_3^- nutrition was concluded. Indeed, both PEPc and NR activities were high in leaves under NO_3^- and significantly decreased but were low in roots and slightly increased with increasing NH_4^+ in nutrient solution. In roots, the expected ^{13}C enrichment under NH_4^+ nutrition was not observed probably because the C source for PEPc stems from root respiration and is thus ^{13}C depleted. The isotopic gap between malate and citrate was low and changed only slightly across N-type gradient in both organs, malate being slightly ^{13}C enriched compared to citrate at high NO_3^- and *vice versa*. Considering that only 4/6 C of citrate originate from malate, we suggested a higher contribution of anaplerotically fixed C to citrate pool in bean. Our results also confirmed a highly plastic TCA cycle.

Keywords: inorganic N form, leaf gas exchange, ^{13}C, respiratory metabolism, anaplerotic pathway, PEPc activity, malate, citrate.

1. Introduction

Plants discriminate against the heavy isotope of carbon (^{13}C) during photosynthetic CO_2 assimilation. Plant organic material (OM) becomes thus ^{13}C depleted compared with source carbon (i.e. atmospheric CO_2) by about 20‰ on average in C_3 plants. This discrimination occurs mainly during CO_2 diffusion from the ambient air into the leaf through stomata and during its fixation by primary carboxylases, mainly by ribulose-1,5-bisphosphate carboxylase/oxygenase, (Rubisco, EC 4.1.1.39) in C_3 plants. Therefore, the ^{13}C content of C_3-leaf organic material changes with plant species and with environmental conditions affecting stomatal conductance and/or photosynthetic capacity, e.g. water deficit, light intensity, and air humidity (reviewed by Brugnoli and Farquhar, 2000). C-isotope composition ($\delta^{13}C$) of leaf bulk OM is thus often used as reference for photosynthetic discrimination in both plant and ecosystem level studies (Yakir and Sternberg, 2000; Bowling et al., 2008), and as a proxy for water use efficiency (WUE) of plant genotypes in breeding programs (Condon et al., 2004).

However, it is now well known that fractionation during post-photosynthetic processes (e.g. respiratory and related pathways, mainly those fixing or releasing CO_2) downstream the photosynthetic fixation of CO_2 in the leaves occurs altering the $\delta^{13}C$ of different metabolic pools and respired CO_2. This arises due to the spatial and metabolic complexity in plants (i.e. combination of enzymatic discrimination with metabolic branching points and compartmentalization in plant cells). Respiration and the associated metabolic network being quite plastic in plants, environmental parameters substantially affect respiratory fractionation as has been shown in various conditions.

Opposite respiratory fractionation has been reported in leaves *versus* roots, changing with plant developmental stages, and with factors affecting relative activity of metabolic pathways and metabolite pool sizes, e.g. temperature (reviewed by Ghashghaie and Badeck 2014; Bathellier et al., 2017). These reviews clearly showed that leaf-respired CO_2 is in general ^{13}C enriched compared with leaf OM in both C_3 and C_4 herbs and in woody species. By contrast, root-respired CO_2 is often ^{13}C depleted compared with root OM in C_3 and C_4 herbs but not in woody plants. Opposite respiratory fractionation in leaves *versus* roots could be one of the causes of the between-organ isotopic differences observed in all plant types (reviewed by Badeck et al., 2005; Bowling et al., 2008; Cernusak et al., 2009; Werner and Gessler, 2011; Ghashghaie and Badeck 2014; Bathellier et al., 2017).

Changes in $\delta^{13}C$ of bulk OM and/or putative respiratory substrates and respired CO_2 (in leaves and/or roots of different species) have already been investigated under different conditions. For instance, isotopic effects of drought (Duranceau et al., 1999; Ghashghaie et al., 2001, Lehmann et al., 2015), temperature (Tcherkez et al., 2003; Schnyder and Lattanzi, 2005; Lehmann et al., 2015), light intensity (Ocheltree and Marshall, 2004; Klumpp et al., 2005), plant developmental stage (Bathellier et al., 2008), carbohydrate pool size (Tcherkez et al., 2003; Bathellier et al., 2009), temporal dynamics both at diurnal and seasonal scales (Werner et al., 2007, 2009; Gessler et al., 2008; Wegener et al., 2010; Dubbert et al., 2012; see also the review by Werner and Gessler, 2011), have been demonstrated. Some data in the literature also reported the impact of N nutrition on $\delta^{13}C$ of plant material (Raven et al., 1984; Yin and Raven 1998; Martinez-Carrasco et al., 1998; Lopes et al., 2004; Lu et al., 2005; Lopes and Araus 2006). In a review, Raven and Farquhar (1990) analysed the potential impact of NO_3^- *versus* NH_4^+ nutrition on $\delta^{13}C$ of plant organic matter. They predicted that the flux through carboxylation reactions other than Rubisco and the plant organ in which the carboxylation occurs would leave an imprint on the isotopic composition of plant organic matter. Relative to an exclusive assimilation of CO_2 through Rubisco, ^{13}C of OM should then vary between about 0.25‰ enrichment in ^{13}C for NH_4^+ assimilation in roots and 2.48‰ enrichment for NO_3^- reduction and assimilation plus retention of free organic acids in the plant in shoots. Raven and Farquhar (1990) also pointed to the potential effects of the type of N nutrition on stomatal conductance, photosynthetic capacity and thus on intercellular to ambient CO_2 concentration ratio (C_i/C_a), which will lead to variations in carbon isotope discrimination. Both increased and decreased stomatal conductance and C_i/C_a under decreasing NO_3^-:NH_4^+ ratio have been documented in the literature.

Yet, the impact of inorganic N-type nutrition (i.e. NO_3^-: NH_4^+ ratio) on $\delta^{13}C$ of plant metabolites together with dark-respired CO_2 in leaves *versus* roots, has not been investigated so far (Ghiasi *et al.,* unpublished), although it is known that it has pervading effects on C and N metabolism as well as on the redox and pH homeostasis and turgor maintenance in cells. N-type nutrition influences (photo)respiration, anaplerotic C-fixation by phospho*enol*pyruvate carboxylase (PEPc, EC 4.1.1.31), as well as organic and amino acid synthesis/consumption (Schweizer and Erismann, 1985; Masclaux-Daubresse et al., 2010; Bittsanszky et al., 2015; Sarasketa et al., 2016). Therefore, it could affect the $\delta^{13}C$ of plant metabolites and that of respired CO_2. The isotopic effect of N-type nutrition is expected to be different between organs, depending

on if the N assimilation takes place mainly in leaves or in roots, and depending on the isotopic composition of the source C used for anaplerotic pathway (i.e. CO_2 coming from the atmosphere or from the respired CO_2 or mix of them).

NO_3^- is preferentially reduced and assimilated in leaves, while NH_4^+ tends to be assimilated mainly in roots. However, this picture probably varies substantially across species, and depending on NO_3^-/NH_4^+ concentrations involved. Regardless of the N type and site of assimilation, N fixation involves the tricarboxylic acid (TCA) cycle and requires anaplerotic activity (PEPc mainly) to fuel glutamate/glutamine synthesis through the GS/GOGAT pathway.

Approximately 70% of all ions acquired by plants consist of N. Thus, the form of N supply (negatively charged NO_3^- *versus* positively charged NH_4^+) exerts a strong influence on the charge balance and therefore ion homeostasis (Gerendas et al., 1997).

Once taken up by the roots, NO_3^- can be assimilated in the roots but mainly transported to the leaves, where it is reduced to NH_4^+ before its assimilation. The reduction takes place mainly in the light, with reducing power being supplied by photosynthesis. The N assimilation in the leaves is also linked to photorespiration. NO_3^- is absorbed together with cations as counter-charge (mainly K^+ and Ca^{2+}), and since NO_3^- reduction liberates OH^-, NO_3^- nutrition requires pH and charge balancing reactions, which are provided by organic acids (Raven and Smith, 1976). Indeed, the TCA cycle is involved in regulation of redox and energy balance in the cells and supplies C-skeletons for amino acid synthesis through the malate and citrate valves.

TCA cycle is known to be especially plastic in plants, notably in leaves where its operating mode is now thought to vary together with day/night circadian cycles. In the light, leaf respiration (both glycolysis and TCA cycle) is highly reduced (for a review, see Atkin et al., 2000), because many enzymes involved (e.g. CS, 2-OGDH, ME and PK) are inhibited under light (Hanning and Heldt, 1993; Tcherkez et al., 2005). In the light, the elevation of the redox potential during photosynthesis transforms the TCA cycle to an open structure (Igambardiev and Bykova, 2018). Labelling experiments have indeed demonstrated that the TCA cycle does not operate as a closed cycle in the light, but as a 2-branched pathway. The C skeletons for one branch are supplied as OAA/malate by PEPc (activated in the light) and for the other branch provided as 2-OG mainly by the remobilisation of the night-accumulated organic acids (Tcherkez et al., 2009; Gauthier et al., 2010; see also the review by Igambardiev and Eprintsev, 2016).

In the dark, the cyclic nature of the TCA is restored. Indeed, contrary to the light, leaf respiration is higher in the dark and is associated with the consumption of pyruvate by the TCA cycle regenerating thus the OAA molecules through the cycle (Gibbs and Beevers, 1955).

Since the C fixation by PEPc discriminates in favour of ^{13}C by about 5.7‰ compared to the source C, the accumulated malate, fixed by PEPc in the light, is expected to be ^{13}C enriched (compared to sugars coming from C-fixation by Rubisco). Moreover, the stomata being open in the light, the C source for PEPc is mainly the atmospheric CO_2, which is ^{13}C enriched compared to respired CO_2 (i.e. C source in the dark because of closed stomata). The PEPc-derived ^{13}C enriched malate could also enrich citrate and thus the released CO_2 in the dark. This is thus expected in leaves of plants under NO_3^- nutrition. The C-isotope signature of malate and citrate pools, which will be decarboxylated in the dark by the enzyme ME and the TCA cycle, respectively, will also depend on their synthesis pathways (Raven and Farquhar, 1990), which could vary depending on the species and environmental conditions.

Contrarily to NO_3^-, NH_4^+ is preferentially assimilated in the roots, and then transported to the leaves as amino acids or amides, etc. The pathway of N assimilation is the same for NO_3^- and NH_4^+ as N source, except that in the case of NH_4^+ no prior reduction is needed. NH_4^+ is taken up together with anions as counter-charge, thus the uptake of cations (mainly K^+ and Ca^{2+}) is reduced under NH_4^+ nutrition. However, this is not the case under NO_3^-, which when arrived in the leaves is reduced and its counter-ion for the cations is replaced by organic acids. Contrarily to NO_3^-, NH_4^+ leads to the acidification of the cytosol, but the H^+ resulting from NH_4^+ assimilation can be excreted into the soil. Since, NH_4^+ is mainly assimilated in the roots and probably only a small fraction of NH_4^+ is directly transported to the leaves, a higher PEPc activity is expected in the roots but a lower activity in the leaves of plants fed with NH_4^+ (Sagi *et al.*, 1998). However, a lower ^{13}C enrichment in PEPc-derived organic acids as well as in respired CO_2 is expected in the roots of plants under NH_4^+ nutrition, because the C source for PEPc in the roots mainly stems from root-respired CO_2.

Thus, because of the strong link between N assimilation and respiratory metabolism, notably the TCA cycle, inorganic N type is expected to affect respiratory fractionation, in particular through the strong ^{13}C enriching potential of PEPc. Besides, as explained above, leaves and roots are expected to be differently affected.

Therefore, we investigated the changes in the $\delta^{13}C$ of respired CO_2 and of the main metabolic pools involved in respiration in both leaves and roots of plants fed with various NO_3^-:

NH_4^+ ratios. We conducted the experiments on bean plants, because NH_4^+ nutrition does not induce oxidative stress in legumes, thus they are known to be relatively tolerant to ammonium (Dominguez-Valdivia *et al*., 2008; Esteban *et al*., 2016) and because we have already studied the respiratory C-isotope fractionation on this plant species and demonstrated some metabolic origin of the opposite respiratory fractionation in leaves *versus* roots as well as of its variability (see the references cited above). The main objectives of the present work were to determine: (i) if the N-type gradient in nutrient solution would change the $\delta^{13}C$ of plant OM, as well as respired CO_2 and its putative substrates, (ii) if its impact would be different in leaves and roots, and (iii) if the isotopic changes could be linked to PEPc activity.

2. Material and methods

2.1 Plant material and culture conditions

French bean (*Phaseolus vulgaris* L.), cultivar Contender, seeds were germinated in vermiculate with tap water in a dark room. Seedlings of 7-d old were transplanted to pots (one plant per pot) filled with sand of Loire (previously washed with tap water and sterilised in autoclave). The pots had 8.3 cm of top diameter, 5.5 cm of bottom diameter and 11.0 cm of height and placed in the culture room in the greenhouse. The whole culture period was 33 d. In addition to cotyledonary leaves, the plants had one set of mature and one set of still growing 3 trifoliate at the end of the culture period. The cotyledonary leaves were mature but not senescent.

The plant culture was performed during January 2017 under natural light, with supplementary light supplied by lamps (Metal Halide Lamps, HSI-THX, 400W, Sylvania) for 10 h per day, providing a photosynthetic photon flux density (PPFD) of 140-160 μmol photons m^{-2} s^{-1} at plant height (average value during daytime). Air temperature was 23 ± 2 °C during the day and 17 ± 2 °C at night. Humidity was 42 ± 8% during the day and 55 ± 15% at night. Carbon isotope composition of the ambient CO_2 in the culture room was not determined but the C-isotope composition in leaf OM of maize plants (the 4th and 5th leaves) cultured in the same room was –11.74 ± 0.06‰ (n=6).

Plants were supplied with nutrient solutions with 6 different proportions of NH_4^+ as N source: 0%, 25%, 50%, 75%, 90% and 100% NH_4^+ (i.e. 100%, 75%, 50%, 25%, 10% and 0% of NO_3^-, respectively). In the Figures, the numbers for N-treatments correspond to the % of NH_4^+ in the total N supplied. The nutrient solutions contained 6 mmol L^{-1} of N applied either as KNO_3,

$Ca(NO_3)_2$, NH_4NO_3 or $(NH_4)_2SO_4$ at different ratios for different N-treatments (adapted from Arnozis *et al*., 1988, by Ghiasi *et al.*, unpublished). Additional components were: 1 mmol L^{-1} $CaCl_2$, 0.25 mmol L^{-1} KH_2PO_4, 1 mmol L^{-1} $MgSO_4$, and trace elements (2 µmol L^{-1} $MnSO_4$, 2 µmol L^{-1} $ZnSO_4$, 0.5 µmol L^{-1} $CuSO_4$, 25 µmol L^{-1} $B(OH)_3$, 0.5 µmol L^{-1} Na_2MoO_4, 40 µmol L^{-1} Fe-EDTA). The pH of all the solutions was around 5.5. In addition, in 100% and 90% NH_4^+ treatments, 1 mmol L^{-1} K_2SO_4 was added to keep K concentration constant.

Pots with the same N-treatment were placed together in a plate, and their position in the culture room were random and changed every week. Nutrient solutions were used for watering the plants only after the cotyledons came out of the sand and were no more in touch with it. The amount of the solution was so that the pots were completely filled, then allowed to drain to the plates. It was initially 750 mL $plate^{-1}$ d^{-1} (with 8 pots in each plate), and then increased with plant growth reaching 1500 mL $plate^{-1}$ d^{-1} during the last week before the harvest. Chlorophyll content and chlorophyll/flavonols ratio, i.e. nitrogen balance index (NBI) were measured every 3 days using a portable DUALEX SCIENTIFIC^{+TM} (Force A, Orsay, France) to ensure that plants were not going through N deficiency. Three plants (n=3) for each treatment were cultured and analysed.

2.2 Leaf gas exchange parameters

One month after planting, the gas exchange and chlorophyll fluorescence were measured by Licor 6400 with LCF chamber (LI-COR, Inc. USA) in the morning (9-12h) during 3 successive days. One plant with mature euphylla was selected from each treatment for measurements on each day. Therefore, there were 3 replications for gas exchange measurement, and the measurement turns were random (for N-treatments) in different days. Three leaves (one leaf from each plant, n=3) for each treatment were used for measurements.

Before measurements, plants were dark-adapted for 30 min, then one mature euphylla (the middle one) was used for measurements. Minimum and maximum chlorophyll fluorescence values were first determined on dark-adapted leaves, and then the gas exchange and chlorophyll fluorescence parameters were measured under PPFD of 400 µmol m^{-2} s^{-1} (with 10% blue light). The flow rate was fixed at 300 µmol s^{-1}, CO_2 concentration at 390 µmol mol^{-1}, and the leaf temperature at 22 °C. Leaf net CO_2 assimilation rate (A_n), stomatal conductance for CO_2 (g_s) and the ratio of intercellular to ambient CO_2 concentrations (C_i/C_a) data were automatically recorded

every 3 min, reaching steady values after about 30 min. Three values at steady state were taken to get a mean value for each plant.

2.3 Carbon isotope composition of respired CO_2

To ensure that plants had enough photoassimilates as respiratory substrates, they were taken from the greenhouse after at least 4 h into the photoperiod for dark-respired CO_2 measurements. Then they were placed in the dark for 30 min to avoid the light-enhanced-dark-respiration (LEDR) effect. One intact mature euphylla was cut off and put into a flask (50 mL) completely covered by aluminium foil. The flask was flushed with CO_2-free air for 5 min, then sealed by septum and left for respired-CO_2 accumulation in the dark. CO_2 concentration was analysed by a Micro-GC (490 Micro GC, Agilent Technologies, USA). The needle of Micro-GC was automatically introduced into the flask through the septum (injection volume was 5 µl every 3 min).

When CO_2 concentration was above 1000 ppm (approximately after 12 min incubation), air samples were manually collected from the flask by syringes (0.5 to 1 ml depending on CO_2 concentration), then injected into a gas chromatograph (GC; HP 5890, Les Ulis, France) coupled to a stable isotope ratio mass spectrometer, IRMS (Optima Isochrom-µG, Fisons Instruments, Manchester, UK), to measure the C-isotope composition of respired CO_2 ($\delta^{13}C_R$). The syringes were flushed with helium five times and then with sample air inside a given flask 10 times before each injection (the needle of the syringe was kept inside the flask when flushing it with the sample air). Each flask was sampled and measured 3 times to make sure the values were stable. For root-respired CO_2, roots were first washed with tap water and then dried with absorbing paper before incubation in the flasks. Since the respiration rate of roots was higher than that of leaves, bigger flasks (120 mL) were used for roots. Generally, measurements started from 10:00 to 16:00, on each day, and the turn of N-treatments was random.

The leaves and roots used for analysing respired CO_2 were collected immediately after $\delta^{13}C_R$ analysis and conserved in –80 °C before freeze-drying. Dried samples were finely ground by a Retsch MM200 ball mill (Bioblock Scientific, Illkirch, France) and the dry powder was then used for C-isotope analyses of bulk organic matter, water-soluble fraction and individual compounds as described below. Three plants (n=3) for each treatment were used for analysis.

2.4 Extraction of water-soluble fraction of organic matter

Water-soluble fraction of plant samples was extracted using the method described by Tcherkez et al. (2003). Freeze-dried powder (50 mg) of a given sample was suspended in 1mL of cold distilled water in an Eppendorf vial and maintained on ice slurry for 60 min except when removed to agitate in a vortex mixer every 10 min. After centrifugation at 14,000 g at 5 °C for 15 min, the supernatant (containing soluble sugars, organic and amino acids and soluble proteins) was separated from the pellets. It was heated at 100 °C for 5 min (it should be boiled) and then kept on ice for 30 min to precipitate the heat-denatured proteins, which were then removed by centrifugation at 14,000 g for 15 min at 5 °C. The final supernatant, i.e. water-soluble fraction of organic matter (WSOM), was conserved at –20 °C for isotopic analysis, but before any further use, it was centrifuged again to remove precipitations, which can be observed after freezing. Three leaves or roots (one leaf and root from each plant, n=3) for each treatment were used for analyses.

2.5 Carbon isotope composition of bulk organic matter and water-soluble fraction

Carbon isotope composition of bulk organic matter ($\delta^{13}C_{OM}$) was determined on plant dry material. Aliquots of dry powder (600-800 µg per sample), weighed in stain capsules (Courtage Analyse Service, Mont Saint-Aignan, France), were analysed using an elemental analyser (Flash EA) coupled to a Deltaplus^{XP} isotope ratio mass spectrometer *via* a 6-port valve (Brooks et al., 2003) and a ConFlo III interface (Finnigan MAT, Bremen, Germany) (see Werner et al., 1999). In order to avoid frequent exchange of the $Mg(ClO_4)_2$ of the conventional water trap, the Flash EA was additionally equipped with a custom-built Nafion^{TM} trap after the reduction tube. The positioning of samples, blanks and laboratory- and quality-control standards in a measurement sequence for all analyses followed the scheme described in Werner and Brand (2001). Carbon isotope composition ($\delta^{13}C$) was calculated according to Farquhar *et al.* (1982), as deviation of the carbon isotope ratio ($^{13}C/^{12}C$, called R) from the international standard (Vienna Pee Dee Belemnite):

$$\delta^{13}C\ (‰) = [(R_{sample} - R_{V\text{-}PDB})/R_{V\text{-}PDB}] * 1000$$

R_{sample} and $R_{V\text{-}PDB}$ are the isotope ratios of the sample and the V-PDB standard, respectively.

Aliquots of 200 µl of protein-free WSOM were poured into the tin cups and oven-dried at 50 °C for isotope analysis ($\delta^{13}C_{WSOM}$) similarly to bulk OM ($\delta^{13}C_{OM}$) as described above. Three leaves or roots (one leaf and root from each plant, n=3) for each treatment were used for analyses.

2.6 Biomass

Plants used for measurements of $\delta^{13}C$ of respired CO_2 ($\delta^{13}C_R$) were harvested for biomass determination of different organs. Whole plants were divided into leaves, stems and roots, plunged into liquid nitrogen for temporary conservation, and then moved to freeze-dryer before determination of the biomasses of organs of each plant. Three plants (n=3) for each treatment were used for analysis.

2.7 Carbon isotope composition of individual metabolites

The protein-free WSOM of the samples used for respiration measurements were used for compound specific C-isotope analyses. Before separation of soluble sugars and organic acids from WSOM, cation exchangers (Dionex^{TM} OnGuard II H 1.0 cc Cartridges, Thermo Scientific, Sunnyvale, CA, USA) were conditioned with 10 ml distilled water, and anion exchangers (Dionex^{TM} OnGuard II A 1.0 cc Cartridges, Thermo Scientific, Sunnyvale, CA, USA) were conditioned firstly with 10 ml 0.5 M HCl, then with 10 ml distilled water.

The protein-free WSOM (described in 2.4) was diluted to 100 ng/μL (pH was adjusted to 7), then 4 mL diluted solution passed through cation and anion exchangers to retain amino acids and organic acids, respectively, and thus to drain and collect the soluble sugars. The first 2 mL were discarded and the last 2 mL were collected in 2 amber silanised glass vials of 1.5 mL (Vial short tread, VWR International, USA) as purified soluble sugars. Organic acids were eluted from anion exchangers using 4 mL 0.5 M HCl. Again, the first 2 mL were discarded and the last 2 mL were collected in 2 amber glass vials of 1.5 mL (HPLC/GC Certified Kit, VWR International, USA). Collected bulk sugars and bulk organic acids were used for C-isotope analysis of individual compounds as follows.

A ThermoFinnigan LC-IsoLink system (Ultimate 3000, Dionex, Part of Thermo Fisher Scientific, USA) coupled to a Delta V Advantage (Thermo Fisher Scientific, USA) was used for analysing C-isotope composition of individual soluble sugars (sucrose, glucose and fructose) and organic acids (only malate and citrate were determined, but OAA and succinate amounts were too low to be measured). Separation of sugars was in distilled water as solvent, through the column NUCLEOGEL Sugar 810 Ca, length 300 mm, and internal dimater 7.8 mm (MACHEREY-NAGEL GmbH & Co. KG, Germany). Organic acids were separated by the column Prevail Organic Acid, 150 mm x 4.6 mm, 5μ (Grace Davison Discovery Sciences, USA) with 25 mM

KH_2PO_4 (pH 2.5) as solvent. The system was controlled with Chromeleon 7.2 software (Thermo Electron).

The amounts, [C], and the $\delta^{13}C$ values of individual sugars were used to calculate the C-isotope composition of the total soluble sugars ($\delta^{13}C_{Sug}$) using a simple mass balance:

$$\delta^{13}C_{Sug}\ (‰) = (\delta^{13}C_{Glc} * [C]_{Glc} + \delta^{13}C_{Suc} * [C]_{Suc} + \delta^{13}C_{Fru} * [C]_{Fru})/ ([C]_{Glc} + [C]_{Suc} + [C]_{Fru})$$

Similarly, using the amounts and the $\delta^{13}C$ values of individual sugars and organic acids, we calculated an estimated C-isotope composition of the total water-soluble fraction ($\delta^{13}C_{Est.\ WSOM}$) to compare with the measured values ($\delta^{13}C_{WSOM}$). Three leaves or roots (one leaf and root from each plant, n=3) for each treatment were used for analyses and calculations.

2.8 Assessing PEP carboxylase activity

Other plants, from the same culture set used for respiration analysis, were used for PEPc activity determination. The samples were harvested from plants in the greenhouse under light (in the morning (from 10:00 to 12:00) and conserved at –80 °C. 150 mg of frozen roots or leaves (without petioles and midribs) were completely ground in a mortar (on a plate containing liquid nitrogen to maintain the sample frozen) with 100 mg sand, then 1 ml extraction buffer was added (4 °C) to the freezed powder. The extraction buffer contained HEPES 50 mM, $MgCl_2$ 10 mM, EDTA 1 mM, EGTA 1 mM, BSA 0.025% (w/v), glycerol 10% (w/v), DTT 5 mM, and protease inhibitor. Thereafter, the mix was agitated in a vortex for 2 sec, defrosted completely on ice and agitated again in the vortex for 5 sec and centrifuged at 10,000 rcf at 4 °C for 10 min.

PEPc activity was measured by coupling the reaction to the NADH-oxidation mediated by malate dehydrogenase (MDH). The standard assay buffer contained 100 mM Tricine (pH 8.0), 10 mM $NaHCO_3$, 20 mM $MgCl_2$, and 0.05% Triton. 40 µl assay buffer, 20 µl 20 mM PEP, 20 µl 0.5 mM NADH, 2 µl 1 u mL^{-1} MDH, 98 µl distilled water and 20 µL extract were added in a 96-well plate. Two technical replicates for each sample were set for the NR measurements. The 96-well plate was placed in a microplate spectrophotometer (PowerWave HT, BioTek, USA) to record the first 20 min oxidation of NADH at 340 nm.

Even when no PEP had been added to the reaction mixture, NADH was oxidised at a rate corresponding to 1 to 30 % of its rate after PEP addition. Endogenous NADH oxidation rate

remained stable for several hours. After addition of small amounts of PEP, the oxidation rate initially rose rapidly but returned quickly to the endogenous level after exhaustion of PEP (Arnozis et al. 1988). Accordingly, PEP replaced by H_2O as control assay, and the PEPc activity was calculated as the difference in NADH oxidation rate before and after addition of PEP.

2.9 Assessing nitrate reductase (NR) activity

The same samples used for PEPc assessment, were also used for NR activity measurement. Leaf samples (around 100 mg) were ground in liquid nitrogen and the resulting powder dissolved in 1 ml of 50 mM HEPES-NaOH buffer (pH 7.6) containing 0.1% Triton X-100, 5 mM $MgCl_2$, 10 µM leupeptin, 0.5 mM AEBSF [4-(2-aminoethyl)-benzenesulfonyl fluoride], 3 mM DTT, 1% polyvinylpolypyrrolidone, 3% polyethylene glycol 4000 and 19.2 µM flavine adenine dinucleotide (FAD). The mix was centrifuged for 10 min at 13,000 g (Fresneau *et al.*, 2007). Measurements of total NR activity, in the presence of ethylenediaminetetraacetic acid, EDTA (NR-EDTA) and active or actual NR activity, in the presence of Mg_2^+ (NR-Mg), were carried out on the supernatant following the method described by. Briefly, the reaction mixture contained 250 µl of 50 M HEPES-NaOH buffer (pH 7.6), 50 µl of 100 mM KNO_3, and 50 µl of 2 mM nicotinamide adenine dinucletide (NADH). The reaction was initiated by adding 50 µl of the extract, which was then incubated at 30 °C for 30 min. The reaction was stopped by adding 50 µl of 1 M $ZnSO_4$ 7 H_2O. The nitrite ions were produced after we assayed diazotization with 500 µl of 1.5% (w/v) sulfanilamide and 500 µl of 0.02% (w/v) N-(1-Naphthyl) ethyl-Enediamine (NEDD). Then, the solution was again centrifuged at 8,000 g for 10 min and the absorbance of the supernatant was measured at 540 nm. The catalytic activity of both NR-EDTA and NR-Mg were estimated as µmol NO_2^- formation per mg protein and per hour. The specific activity of NR was determined as the ratio of NR-Mg to NR-EDTA and expressed in percent.

2.10 Statistical analyses

Statistical analyses of ANCOVA were performed using STATISTICA 8.0 (StaSoft Inc., Tulsa, USA), mean comparisons were performed with the 'LSD' test with $p < 0.05$. When representing three or more measurements, data are presented as mean values ± SE.

Correlation and regression analyses as well as PCA were done with R (R core team, 2018). Regression of all traits on the fraction of NH_4^+ in the nutrient solution was performed as linear

regression and as regression with log-transformed fraction of NH_4^+, emphasizing a more pronounced change at low fractions of NH_4^+. Furthermore, regression on the log-transformed fraction of NO_3^- (i.e., 100 – NH_4^+), emphasizing a more pronounced change at high fractions of NH_4^+ and the absolute difference of fractions of NH_4^+ from 25, 50 and 75%, respectively were done. Between-trait correlations were calculated and ordered with hierarchical clustering.

3. Results

No NH_4^+ toxicity symptoms (e.g. extremely dark green leaves, necrotic spots, stunted roots, and stunted leaves) were observed in none of the N-type treatments in the present experiment.

3.1 Effect of N-type supply on plant growth, C% and N%

Only bean plants fed with 100% NO_3^- (i.e. 0% NH_4^+) showed significant ($p < 0.05$) increase in leaf biomass as well as in total biomass compared with plants fed with nutrient solutions containing >25% NH_4^+ (Fig. S1). However, the root/shoot biomass ratio was stable, varying between 0.25 and 0.3, with no significant change across N-type gradient (Fig. S2). C and N contents were higher in leaves compared to roots (Fig. S3). Carbon content in leaves and N content in roots remained stable along the N-type gradient. The C content in roots increased with increasing fraction of NH_4^+ in the nutrient solution (r = 0.94), while N% in leaves increased under 50% NH_4^+ and significantly ($p < 0.05$) decreased at high NH_4^+.

3.2 Effect of N-type supply on respiration and leaf gas-exchange parameters

Root respiration rate was slightly but not significantly higher than leaf respiration. No significant change in respiration rate along the N-type gradient was observed for none of the organs (Fig. S4).

Leaf net CO_2 assimilation (A_n) values varied non-significantly between 13.6 and 15.1 µmol m^{-2} s^{-1} across N-type gradient except a significant ($p < 0.05$) decrease to 11.6 µmol m^{-2} s^{-1} at 100% NH_4^+ (Fig. 1A). However, stomatal conductance (g_s) did not follow the same trend; the lowest value was observed at 25% NH_4^+ (Fig. 1B). C_i/C_a increased from 0.67 to 0.75 with increasing NH_4^+ from 50% to 100% (Fig. 1C). However, no significant difference in C_i/C_a was observed between 100% NH_4^+ and 0% NH_4^+ (i.e. 100% NO_3^-) treatments. The ratio A_n/C_i remained almost stable around 0.06 along N-type gradient, except a significant decrease ($p < 0.05$) observed at 100% NH_4^+ reaching almost 0.04 (Fig. S5).

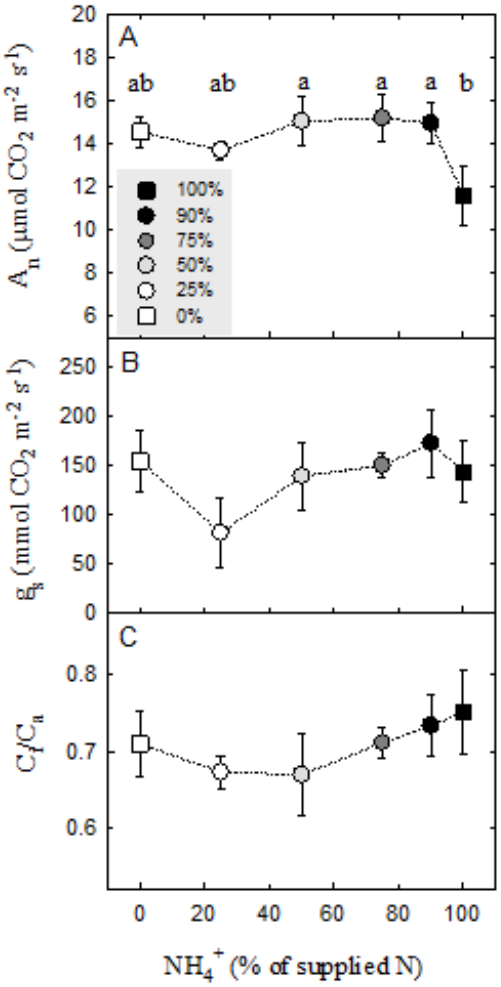

Figure 1. Changes in leaf net CO_2 assimilation rate, A_n (A), stomatal conductance for CO_2 diffusion, g_s (B), and the ratio of intercellular to ambient CO_2 concentrations, C_i/C_a (C) of bean plants cultured under different proportions of NH_4^+ *versus* NO_3^- as N sources in nutrient solutions used for watering the pots. On the X-axis (and in the legend box), 0% and 100% correspond to 0% $NH4^+$ (i.e. 100% NO_3^-, white squares) and 100% $NH4^+$ (i.e. 0% NO_3^-, black squares) as % of total N in the nutrient solutions, respectively. The other N-treatments are shown by circles, as a gradient of increasing NH_4^+ in the solutions, from low NH_4^+ (white) to medium NH_4^+) (grey) and high NH_4^+ (black). Values are means ± SE (n=3). Significant differences (p < 0.05) are shown by different lowercase letters.

3.3 Effect of N-type supply on C-isotope composition of OM, WSOM and respired CO_2

OM was ^{13}C depleted in leaves compared to roots whatever the N-type nutrition (Fig. 2A), while WSOM was ^{13}C enriched in leaves compared with roots under lower NH_4^+ supply and ^{13}C depleted under higher NH_4^+ supply (Fig. 2B). $\delta^{13}C_{OM}$ did not show any significant change along N-type gradient in none of the organs (Fig. 2A). OM was ^{13}C depleted compared with WSOM in leaves, but not in roots (Fig. 2A, B). In leaves, $\delta^{13}C_{WSOM}$ was negatively correlated with NH_4^+ fraction in supplied N ($R^2 = 0.97$, $p < 0.0001$), while in roots, there was no significant relationship between $\delta^{13}C_{WSOM}$ and N-type gradient (Fig. 2B). The isotopic difference between WSOM and OM was close to zero in roots, increasing only slightly, but not significantly, from –0.10‰ to +0.15‰ with increasing NH_4^+ fraction in supplied N from 0% to 100% (Fig. 3). Therefore, when $\delta^{13}C_{OM}$ was plotted against $\delta^{13}C_{WSOM}$, root data were on the 1:1 line (Fig. S6, B). Contrarily to roots, the isotopic

difference between WSOM and OM in leaves was the highest (+1.8‰) under pure NO_3^- nutrition, and significantly decreased with increasing NH_4^+ fraction in supplied N ($R^2 = 0.97$), reaching the lowest value (+0.3‰) under pure NH_4^+ nutrition (Fig. 3). Accordingly, the $\delta^{13}C_{OM}$ *versus* $\delta^{13}C_{WSOM}$ values were below the 1:1 line in leaves, with a clear change along N-type gradient (Fig. S6, A).

Leaf-respired CO_2 was ^{13}C enriched compared to root-respired CO_2, and negatively correlated with NH_4^+ % in supplied N (Fig. 2C). Leaf-respired CO_2 became more and more ^{13}C depleted changing from –20.4‰ at 0% NH_4^+ to –24.2‰ at 100% NH_4^+ (Fig. 2C). Contrarily to leaves, root-$\delta^{13}C_R$ remained low (around –28‰) and unchanged along the N-type gradient. It slightly but not significantly increased with increasing NH_4^+ supply reaching around –27‰ at 100% NH_4^+ (Fig. 2C).

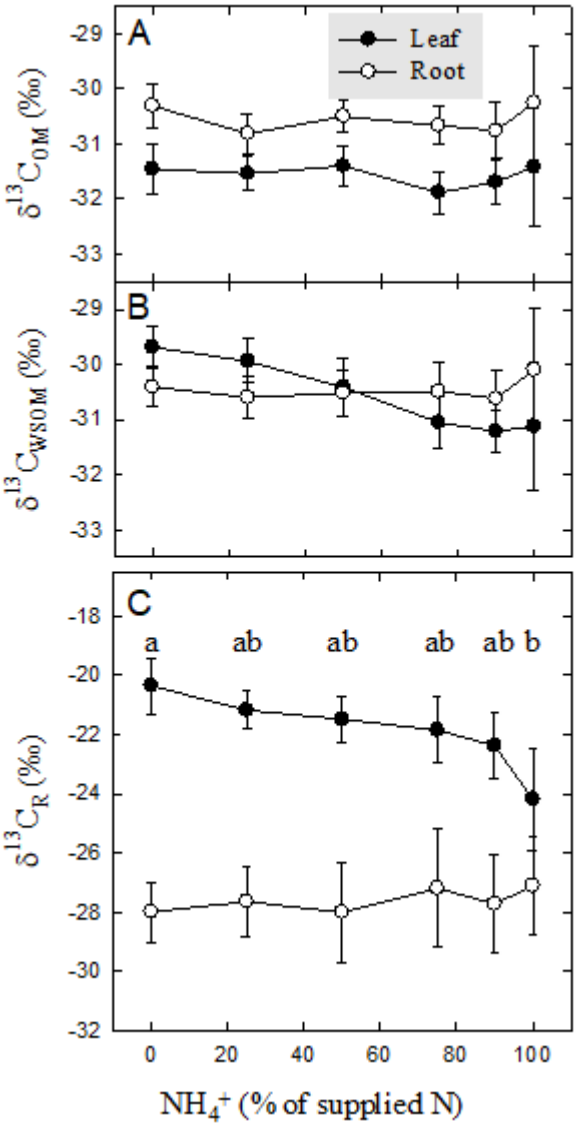

Figure 2. $\delta^{13}C$ of organic matter ($\delta^{13}C_{OM}$; **A**), water-soluble fraction ($\delta^{13}C_{WSOM}$; **B**), and respired CO_2 ($\delta^{13}C_R$; **C**) in leaves (black symbols) and roots (white symbols) of bean plants grown with nutrient solutions containing different % of NH_4^+ and NO_3^- as N source. On the X-axis, 0 and 100 correspond to 0% NH_4^+ (i.e. 100% NO_3^-) and 100% NH_4^+ (i.e. 0% NO_3^-) as % of total N in the nutrient solutions, respectively. Values are means ± SE (n=3). Only significant differences ($p < 0.05$) are shown by different letters (leaves only). Note that the respired CO_2 being ^{13}C enriched compared to both OM and WSOM, the scale used for respired CO_2 is different from that for WSOM and OM.

3.4 Effect of N-type supply on soluble-sugar contents and $\delta^{13}C$

Sugars were ^{13}C enriched in roots compared to leaves (Fig. 4), except for sucrose showing almost superimposed $\delta^{13}C_{Suc}$ values in leaves and roots (Fig. 4A). The isotopic difference between organs was the highest in glucose (Fig. 4B). In leaves, the $\delta^{13}C$ values of all sugars were almost stable across N-treatments, but showed a slight decrease under 50% NH_4^+. In roots, the individual sugars, and thus the total sugars, were ^{13}C enriched at 100% NH_4^+ compared with other N-treatments (Fig. 4A-D).

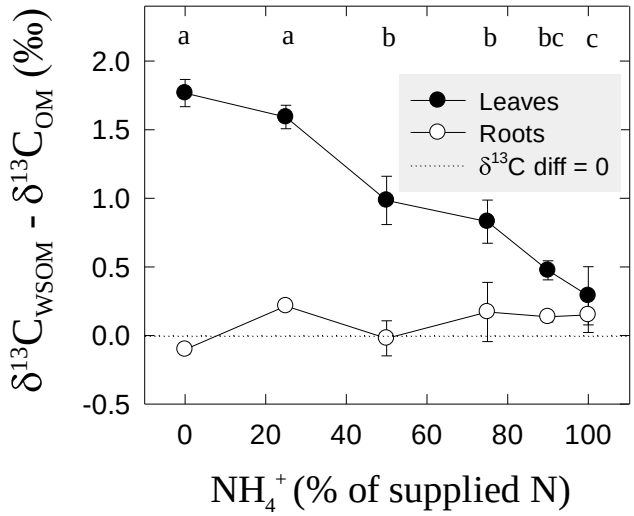

Figure 3. Variation in $\delta^{13}C$ difference between WSOM and OM ($\delta^{13}C_{WSOM-OM}$) in leaves (black circles) and roots (white circles) of bean plants cultured under different % of NH_4^+ and NO_3^- as N source in nutrient solution used for watering the pots. On the X-axis, 0 and 100 correspond to 0% NH_4^+ (i.e. 100% NO_3^-) and 100% NH_4^+ (i.e. 0% NO_3^-) in nutrient solution, respectively. Each data point corresponds to means ± SE (n=3). The dotted line corresponds to ($\delta^{13}C_{WSOM} = \delta^{13}C_{OM}$). Significant differences ($p < 0.05$) are shown by different letters for leaves (there was no significant difference for roots).

The sugar contents were higher in roots than in leaves, mainly sucrose and fructose in all N-treatments (Fig. 4E, G), glucose in higher NH_4^+ supply (Fig. 4F), and thus total sugars (Fig. 4H). Sugar contents increased in roots with increasing NH_4^+ supply (Fig. 4E-H). High NH_4^+ treatments (i.e. 90% and 100% NH_4^+) showed significant ($p < 0.05$) increase in sugar contents compared to other treatments. Plants fed with 100% NH_4^+ had the highest sugar contents compared to the plants fed with NO_3^-; there was 150% increase in sucrose, 290% increase in glucose, 310% increase in fructose and finally 210% increase in total sugars at 100% NH_4^+ compared with 100% NO_3^- treatment (Fig. 4E-H). By contrast, no significant change was observed in leaves.

3.5 Effect of N-type supply on organic acid contents and $\delta^{13}C$

Contrary to soluble sugars, the organic acids (malate and citrate) were ^{13}C enriched in leaves compared to roots (Fig. 4I, J), but with no significant difference among N-treatments in none of the organs (except citrate, which was significantly ^{13}C enriched in roots of plants fed with 100% NH_4^+ compared with roots of plants fed with 100% NH_4^+, Fig. 4J). Citrate became more ^{13}C enriched (although not significantly) with increasing NH_4^+ % (mainly at 100%) by about 1.02% and 1.04% in leaves and roots, respectively (Fig. 4I, J).

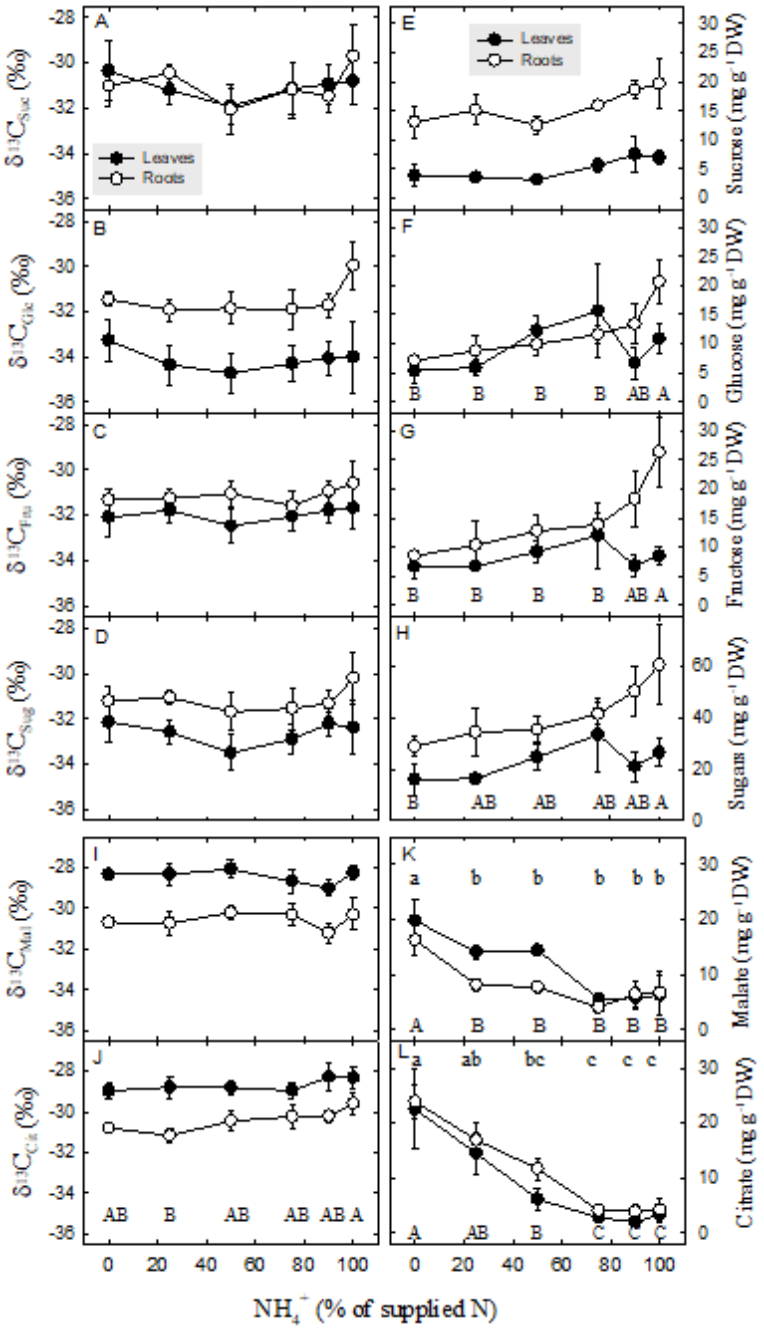

Figure 4. $\delta^{13}C$ of sucrose ($\delta^{13}C_{Suc}$; **A**), glucose ($\delta^{13}C_{Glc}$; **B**), fructose ($\delta^{13}C_{Fru}$; **C**), soluble sugars, i.e. sucrose, glucose and fructose ($\delta^{13}C_{Sug}$; **D**), malic acid ($\delta^{13}C_{Mal}$; **I**), citric acid ($\delta^{13}C_{Cit}$; **J**), and their amounts (**E, F, G, H, K, L**), in leaves (black symbols) and roots (white symbols) of bean plants grown with nutrient solutions containing different % of NH_4^+ and NO_3^- as N source. On the X-axis, 0 and 100 correspond to 0% NH_4^+ (i.e. 100% NO_3^-) and 100% NH_4^+ (i.e. 0% NO_3^-) as % of total N in the nutrient solutions, respectively. Values are shown as means ± SE (n=3). Note that the scale for total sugar concentration is different. Significant differences ($p < 0.05$) are shown by different letters (lowercase letters for leaves and uppercase letters for roots).

In contrast to C-isotope composition, malate and citrate contents sharply and significantly decreased ($p < 0.05$) with increasing % of NH_4^+ in supplied N, both in leaves and roots (Fig. 4K, L). Malate decreased from 20

to 6 mg g^{-1} DW in leaves and from 16 to 7 mg g^{-1} DW in roots (Fig. 4K). Similarly, citrate declined from 23 to 4 mg g^{-1} DW in leaves and from 24 to 5 mg g^{-1} DW in roots (Fig. 4L).

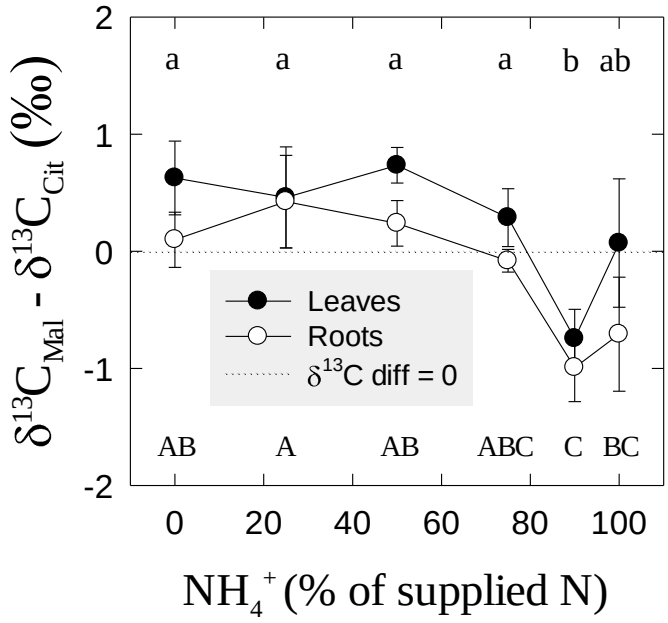

Figure 5. ^{13}C-difference between malate ($\delta^{13}C_{Mal}$) and citrate ($\delta^{13}C_{Cit}$) in leaves (black symbols) and roots (white symbols) of bean plants grown with nutrient solutions containing different % of NH_4^+ and NO_3^- as N source. On the X-axis, 0 and 100 correspond to 0% NH_4^+ (i.e. 100% NO_3^-) and 100% NH_4^+ (i.e. 0% NO_3^-) as % of total N in the nutrient solutions, respectively. Values are shown as means ± SE (n=3). Significant differences ($p < 0.05$) are shown by different letters (lowercase letters for leaves and uppercase letters for roots).

The isotopic difference between malate and citrate revealed 2 groups in both leaves and roots (Fig. 5). At lower NH_4^+ supply, the $\delta^{13}C$ difference was positive, while at higher NH_4^+ supply, it was negative or near zero for both organs. In leaves, it varied between +0.46‰ and +0.74‰ at lower NH_4^+ treatments (0-50% NH_4^+) and between 0‰ and –0.75‰ at higher NH_4^+ treatments (NH_4^+ >75%), it was +0.29‰ at 75% NH_4^+. Roots followed a similar trend but the values were always below those observed for leaves, being less positive (between +0.10 and +0.43‰) at N-treatments <50% NH_4^+, and more negative at higher NH_4^+ treatments (–0.99‰ and –0.71‰ at 90% and 100% NH_4^+, respectively). The more negative isotopic differences between malate and citrate were observed at 90% NH_4^+ treatment in both organs (Fig. 5).

3.6 Effect of N-type supply on apparent ^{13}C fractionation

The C-isotope differences between individual compounds and bulk OM (as apparent ^{13}C fractionation in metabolites), as well as between respired CO_2 and bulk OM (as apparent respiratory

fractionation) along the N-type gradient are compiled in Figure 6A and B, for leaves and roots, respectively. Both leaf- and root-respired CO_2 were ^{13}C enriched compared to OM and all individual metabolites in corresponding organs, but the enrichment was much higher in leaves than in roots. In leaves (Fig. 6A), glucose and fructose were ^{13}C depleted compared to OM, but sucrose (except at 50% NH_4^+ supply), WSOM and mainly organic acids were ^{13}C enriched compared to leaf bulk OM. In roots (Fig. 6B), all soluble sugars (and WSOM) were ^{13}C depleted compared to root OM (or had similar values), as well as organic acids, except slight ^{13}C enrichment in citrate at higher NH_4^+ supply.

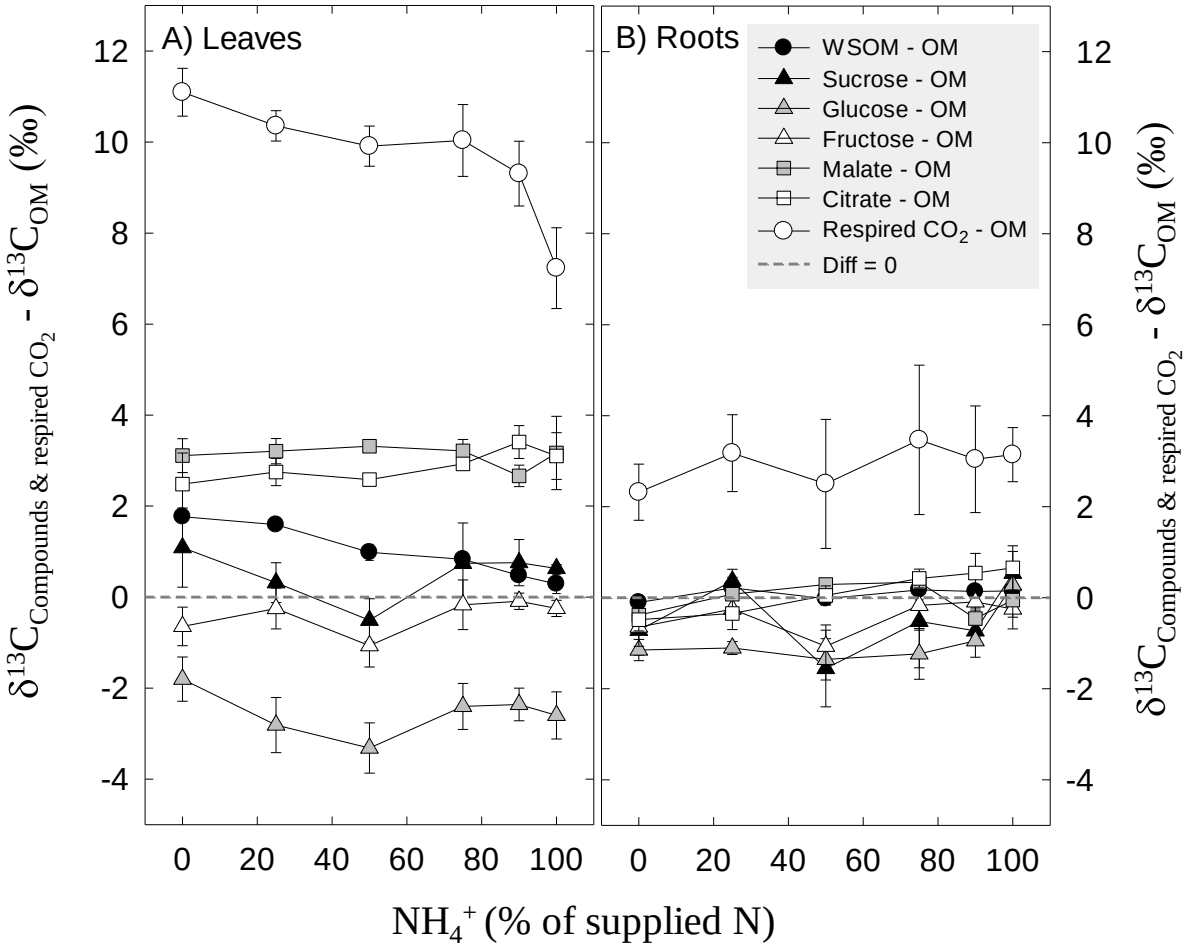

Figure 6. Changes in $\delta^{13}C$ of respired CO_2 (white circles), water soluble organic matter (WSOM, black circles, from **Figure 3**), sucrose (black triangles), glucose (grey triangles), fructose (white triangles), malic acid (grey squares) and citric acid (white squares), in leaves (**A**) and roots (**B**) relative to the $\delta^{13}C$ of respective organs (i.e. $\delta^{13}C$ of metabolites – $\delta^{13}C$ of OM) of bean plants grown with nutrient solutions containing different % of NH_4^+ and NO_3^- as N source. The grey dashed lines correspond to the reference value (i.e. isotopic difference with OM = 0) On the X-axis, 0 and 100 correspond to 0% NH_4^+ (i.e. 100% NO_3^-) and 100% NH_4^+ (i.e. 0% NO_3^-) as % of total N in the nutrient solutions, respectively. Values are means ± SE (n=3).

Sucrose was the most ^{13}C enriched sugar mainly in leaves. The ^{13}C difference between sucrose and OM oscillated between +1‰ and –1.5‰ in leaves and roots, respectively. Glucose was the most ^{13}C depleted compound analysed, with more negative values in leaves compared with roots. Fructose was ^{13}C depleted compared to OM in both organs, with the ^{13}C difference ranging between –0.1‰ and –1‰ along N-type gradient, in both leaves and roots. Contrarily to soluble sugars, the ^{13}C differences between organic acids and bulk OM were always highly positive in leaves remaining almost stable, but slightly below or above zero in roots across the N-type gradient.

3.7 Effect of N-type supply on NR and PEPc activities

Leaves of plants fed with low amounts of NH_4^+ (< 50% NH_4^+) had higher NR and PEPc activities (Fig. 7) compared with those fed with high NH_4^+ amounts in supplied N (> 50% NH_4^+). In roots, NR and PEPc activities were stable except in 100% NH_4^+-fed plants, with on average 200% higher activities than in other treatments. In addition, a high linear relationship between NR and PEPc activities was observed in bean leaves ($R^2 = 0.73$) but not in roots (not shown).

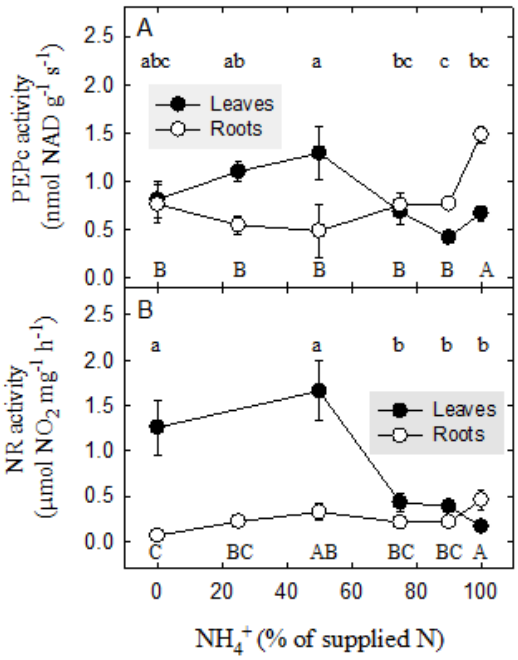

Figure 7. Changes in leaf (black symbols) and root (white symbols) enzyme activities, PEPc (**A**) and NR (**B**), of bean plants cultured under different % of NH_4^+ and NO_3^- as N source in nutrient solution used for watering the pots. On the X-axis, 0 and 100 correspond to 0% NH_4^+ (i.e. 100% NO_3^-) and 100% NH_4^+ (i.e. 0% NO_3^-) as % of total N in the nutrient solutions, respectively. Values are shown as means ± SE (n=3). Significant differences ($p < 0.05$) are shown by different letters (lowercase letters for leaves and uppercase letters for roots). The calculation of the enzyme activities is based on fresh weight of organic material.

3.8 Change of traits across the N-gradient and between-trait correlations

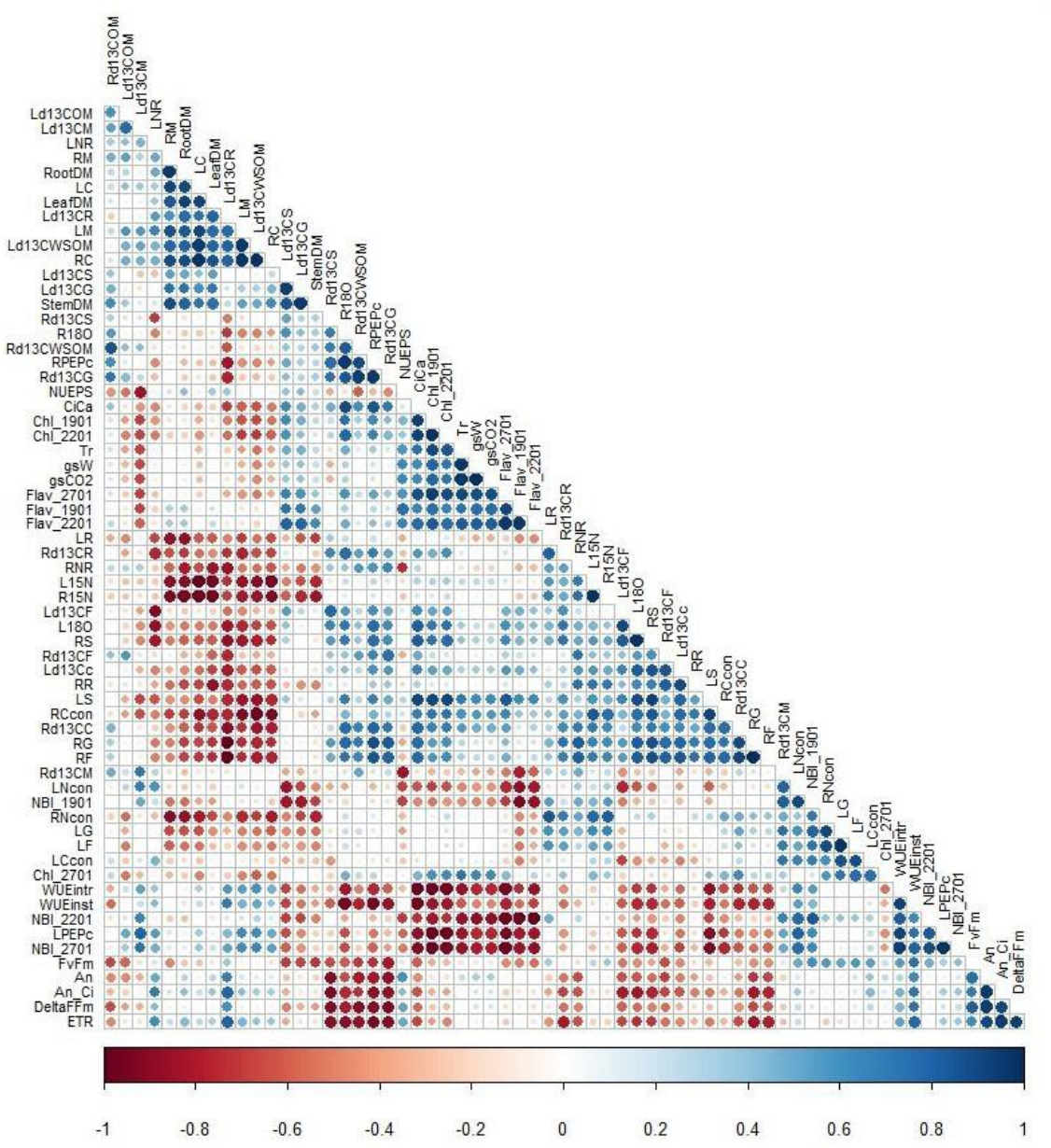

Figure 8. Matrix of between trait correlation coefficients. In general correlations with |r| > 0.8 are significant, i.e. the ones represented by dark coloured big circles. The matrix was ordered with hierarchical clustering.

PCA axis 1 and 2 explained 41.04 and 25.66 % of the variation in the full set of measured traits. PCA1 separated treatments with ≤ 50% NH_4^+ from those with > 50% NH_4^+. PCA2 separated treatments with 25 and 100 % NH4+ from the remaining treatments. Table S1 for every trait reports the PCA axis on which the trait loaded most. Several traits that loaded most strongly on PCA1 were significantly correlated with the N-type nutrition gradient (see Table S1): $\delta^{13}C$ of leaf respired CO_2,

$\delta^{13}C$ of leaf WSOM, leaf malate concentration, leaf dry mass and root citrate concentration were all negatively related to the N-type gradient. They also had elevated correlation coefficients for between trait correlations (Fig. 8). As opposed to this, the root sugars and root C content were positively related with the N gradient and positively correlated between each other.

4. Discussion

The main objective of the present work was to examine the impact of varying ratios of NH_4^+:NO_3^- in supplied N on the C-isotope composition of leaf- and root-respired CO_2 as well as in putative respiratory substrates in bean plants. We expected a higher anaplerotic activity of PEPc in leaves under high NO_3^- nutrition and in roots under high NH_4^+ nutrition. Accordingly, we expected more ^{13}C enriched respiratory substrates and thus respired CO_2 in leaves of NO_3^--fed plants and more ^{13}C depleted in leaves of NH_4^+-fed plants. Eventual interactions with effects of N nutrition on stomatal conductance, C_i/C_a, and growth needed to be scrutinized.

4.1 No major change in biomass production across N-type nutrition gradient

No major change in biomass production and no significant change in root/shoot ratio was observed across the N-type nutrition gradient in the present work. This result putatively is due to the specific growth conditions applied in the current experiment, especially low light (average PPFD of about 150 µmol m^{-2} s^{-1}), medium N concentrations and non-excessively acid pH of the growth medium. A minor contradiction to this hypothesis is the fact that pure NO_3^- grown plants produced more than the other treatments. Note that most of the literature reporting the negative impact of NH_4^+ nutrition on plant growth mainly compared the plants fed with pure NO_3^- to those fed with pure NH_4^+. In the present work, when only pure NO_3^- was compared to pure NH_4^+ the conclusion was a reduction in plant growth due to NH_4^+ by about 28%.

In previous experiments conducted on bean plants cultured under higher light levels, reductions in growth under NH_4^+ relative to NO_3^- nutrition of 52% (Chaillou *et al*., 1986), 23% (Volk *et al*., 1992), 30% (Zhu *et al*., 2000) and 18% (Guo *et al*., 2002) were reported. Enhanced growth by 21% and 7% relative to NO_3^- nutrition was obtained with NH_4^+:NO_3^- ratios of 1:2 and 2:1, respectively. Under low light (150 µmol m^{-2} s^{-1} PPFD, similar to PPFD level in the present work), a slight non-significant reduction of 5% compared with high light conditions (550 µmol m^-

^{2} s^{-1} PPFD) was found by Zhu *et al*. (2000), with root/shoot ratio unchanged, while it significantly decreased under high light.

Furthermore, in experiments with other crops, all kinds of growth responses were observed, passing from enhanced growth under NH_4^+ nutrition in sugar beet (Harada *et al*., 1968), wheat (Cox and Reisenauer, 1973), rice (Magalhaes and Huber, 1991) and tomato (Horshani *et al*., 2010) through no change in grasses (Høgh-Jensen and Schjoerring, 1997), corn (Magalhaes and Huber, 1991) and pea and barley (Kandlbinder *et al*. 1997), to decreased growth in wheat (Cox and Reisenauer, 1973), tomato (Clark, 1936; Magalhaes and Huber, 1991), spinach (Lasa *et al*., 2001; Xing *et al*., 2015), barley (Lopes *et al*., 2004), bean (Brück and Guo, 2006) and tobacco (Ghiasi *et al*., unpublished). Harada *et al*. (1968) in tomato observed a cross-over in the growth response to different N forms with higher and lower growth under NH_4^+ nutrition at low and high nutrient concentrations, respectively. Tsabarducas *et al*. (2017) also found a lowered biomass (both in leaves and roots) of young olive plants of 1-year old under NH_4^+ compared with NO_3^- but the highest biomass was under mixed nutrition.

Accordingly, contradictory results were also reported on the root/shoot biomass ratio. Horshani *et al*. (2010) observed a significantly higher root/shoot ratio in tomato plants fed with NH_4^+ compared with those fed with NO_3^-. They suggested that the higher photosynthetic activity of NH_4^+-fed plants not only covered the need for C-skeletons required for NH_4^+ assimilation but also the carbohydrates for root growth. This is not the case in the present work. Tsabarducas *et al*. (2017) found a lower root/shoot ratio in young olive plants fed with NH_4^+ compared with those fed with NO_3^-.

In a preliminary experiment under similar conditions, NO_3^- and NH_4^+ grown plants (9 species including bean) did not differ but a rather common growth enhancement under mixed N-type nutrition was observed (data not shown). Only the substrate was different; vermiculite in the preliminary experiment *versus* sand in the present work. A higher growth in mixed N-types in nutrient solution compared with pure NO_3^- or pure NH_4^+ was also reported in the literature (Hogeman, 1984; Lopes *et al*., 2004). We did not follow the pH in the pots after watering with nutrient solutions. In addition to light level, the impact of pH in the soil as well as the concentrations of nutrients have been reported to affect the N-responses of plants (Cox and Reisenauer, 1973; Fenn *et al*., 1987). Thus, there is no *a priori* expected growth response to N-type nutrition, changing

with experimental conditions and genetic material (Cruz *et al*., 2003). Rather, it needs to be defined within a spectrum of multidimensional environmental conditions (Britto and Kronzucker, 2013).

4.2 Photosynthesis decreased only at pure NH_4^+ and respiration rate did not significantly change along N-type gradient

Slight changes in leaf photosynthetic activity as well as in carboxylation efficiency (A_n/C_i) observed across the N-type gradient are in agreement with biomass data. Except that biomass increase was significant only at pure NO_3^-, while the decrease in photosynthesis and A_n/C_i was significant only at pure NH_4^+ compared to other treatments. The respiration rate did not significantly change along the N-type gradient. Enhancement in respiratory CO_2 flux has been reported to be a typical response to high NH_4^+ supply (Britto and Kronzucker, 2002). Respiration of primary leaves was higher in NH_4^+ grown (affected by premature senescence) than in NO_3^- grown *P. vulgaris* (Marques *et al*., 1983). Hachiya *et al*. (2010) found that the NH_4^+ levels in *A. thaliana* shoots were positively correlated with the rates of respiratory O_2 uptake under varying ratios of NO_3^-: NH_4^+. Hachiya and Sakakibara (2016) suggested that the NH_4^+-dependent increase in respiration rate might be related to the energetic demand of intracellular pH regulation, because the futile cycling of NH_4^+ across the plasma membrane requires a large amount of ATP. Our respiration rate data do not match the above reports, but are in agreement with our biomass data.

Since NO_3^- is absorbed together with K^+ as counter-charge, the lack of K^+ in plants fed with NH_4^+ could affect both stomatal conductance and photosynthesis. Indeed, Lips *et al*. (1990) have observed that biomass production and transpiration of wheat and tomato plants grown under NH_4^+ increased with increased concentration of K^+ in nutrient solution. In addition, since NO_3^- nutrition increases inorganic phosphate concentration in cytosol, and simultaneously decreases the accumulation of phosphate in vacuole, the decrease in photosynthesis of 100% NH_4^+-fed plants could be related to the lack of inorganic phosphate in the cytosol. This causes inhibition of triose-phosphates removal from chloroplasts, breaking the balance between source and sinks of photosynthesis, thus perturbing photosynthetic processes in 100% NH_4^+-fed plants (Salsac 1987). Xing *et al*. (2015) observed significant decrease in both photosynthesis and stomatal conductance of spinach leaves with increasing NH_4^+:NO_3^- ratio in nutrient solution. In the present work, the negative impact of NH_4^+ on photosynthesis is obvious only under pure NH_4^+ nutrition, suggesting that even a small amount of NO_3^- could be enough to maintain the phosphate balance for

photosynthetic activity. Our results on photosynthetic activity are in agreement with this observation. Similar trends were observed in previous studies on spinach and durum wheat (Lasa *et al*. 2002; Lopes and Araus 2006). Lopes *et al*. (2004) found the lowest photosynthesis and stomatal conductance under NH_4^+ and the highest under mixed NO_3^-: NH_4^+ nutrition in barley, and Tsabarducas *et al*. (2017) in young olive plants. However, Zhu *et al*. (2000) observed no N-type effect on stomatal conductance, photosynthesis (measured as oxygen evolved), neither on the maximum photosystem II efficiency in bean plants. Similarly, the electron transport and carboxylation capacity of barley leaves were less affected under NH_4^+ nutrition (Lopes *et al*., 2004), suggesting that the lowered stomatal conductance was the main cause of the decrease in photosynthesis. Brück and Guo (2006) observed that the light-saturated rates of CO_2 assimilation (A_{max}) per unit leaf area of bean plants were higher under NH_4^+ compared to NO_3^- supply while they found no significant effects of N-type nutrition on quantum yield and A_{max} per unit leaf weight and chlorophyll. Horshani *et al*. (2010) reported rather a higher photosynthesis in tomato plants fed with NH_4^+ compared with those fed with NO_3^-. As for biomass, the N-type impact on photosynthesis and stomatal conductance seems to change from experiment to experiment. In the current study, A_n was only weakly positively correlated with g_s ($r = 0.33$, $p = 0.52$) across the N-nutrition gradient. Thus, net photosynthesis varied mainly in response to factors other than the change in stomatal conductance. One of these factors is indicated by the drop in A_n, $\Delta F/F_m$, A_n/C_i by about 20% under 100% NH_4^+ relative to 90% NH_4^+ accompanied by only a small change in g_s (Table S1, regression results for ETR and A_n/C_i). These observations indicate a reduction of photosynthetic capacity at 100 % NH_4^+ as the most likely candidate for the drop in assimilation rate.

C_i/C_a changed slightly but not significantly with N-type gradient. The $\delta^{13}C$ values of photosynthetic products were estimated by using C_i/C_a values in Farquhar's simple model. The estimated $\delta^{13}C$ values roughly represent the carbon isotope composition of photoassimilates produced from photosynthetic fractionation affected by stomatal conductance. In this experiment, the estimated values were higher compared to those measured on individual sugars and even compared with $\delta^{13}C$ of WSOM (see Fig. S9). Note that we used the leaf-$\delta^{13}C_{OM}$ of maize plants grown in the same culture room, to estimate the $\delta^{13}C$ of air CO_2 assuming a photosynthetic discrimination of 3-4‰ for maize leaves (which gives a $\delta^{13}C$ value for CO_2 in the culture room of about –8‰ on average). Only when a lower discrimination for maize leaves around 2‰ (i.e.

estimated $\delta^{13}C$ of the air of –10‰) was assumed that the estimated $\delta^{13}C$ values were closer to the measured $\delta^{13}C_{WSOM}$, but still higher than those of all individual sugars (Fig. S9). Since the C_i/C_a is probably not constant and changes during plant growth, while it was determined instantaneously only at the end of the culture period in the present work, it cannot reflect the integrated C_i/C_a during the whole plant growth. In addition, not only C_i/C_a influences the fractionation by Rubisco against ^{13}C thus adding ^{13}C depleted C to OM, but also the anaplerotic carboxylation (e.g. by PEPc) introduces ^{13}C enriched carbon to OM (Raven and Farquhar, 1990). We did not observe any significant change in $^{13}C_{OM}$ across N-gradient. The effects of C_i/C_a and carboxylation by PEPc could have cancelled each other leaving no detectable impact on bulk OM. On the other hand, the C fixed by PEPc (C-4 of malate), which should be highly ^{13}C enriched, can be either decarboxylated by ME enriching in ^{13}C the respired CO_2 or stored in the vacuole enriching the reserves in ^{13}C, which could be respired later.

We did not determine leaf internal (mesophyll) conductance in our plants. However, any impact of N-type nutrition on mesophyll conductance lowering CO_2 concentration in the chloroplasts relative to C_i should have decreased the photosynthetic isotope discrimination leading to even more ^{13}C enriched expected values compared with those estimated using C_i.

Opposed to expectations based on the simple model for discrimination during photosynthesis, C_i/C_a was positively but not significantly correlated with $\delta^{13}C$ of leaf and root sugars (Fig. 8). Instead, C_i/C_a was negatively correlated with PEPc-activity in leaves, i.e. high PEPc activity was associated with low C_i/C_a and thus ^{13}C depleted CO_2 left behind by PEPc in the leaf internal CO_2 pool should have had a dampening effect on $\delta^{13}C$ of the leaf internal CO_2 pool, the substrate for carboxylation by Rubisco. When PEPc activity was low, i.e. at N nutrient mixtures dominated by NH_4^+ the $\delta^{13}C$ of the leaf internal CO_2 pool mainly depended on Rubisco activity.

4.3 No significant change across the N-type gradient in $\delta^{13}C$ of leaf and root OM

The observed ^{13}C enrichment in root OM compared with leaf OM by about 1 to 1.5‰ is in agreement with the general pattern reported in the literature (see the review by Badeck *et al*., 2005). However, the N-type gradient in nutrient solution did not significantly change the $\delta^{13}C_{OM}$ of bean in none of the organs. As for biomass, contradictory data are also reported in the literature on the N-type nutrition impact on $\delta^{13}C$ values of plant OM. Guo *et al*. (2002) observed a more ^{13}C depleted leaf OM in bean plants grown under NH_4^+ compared with those grown under NO_3^- nutrition. They

suggested that a higher stomatal conductance (i.e. higher photosynthetic discrimination) under NH_4^+ nutrition was the main reason of the observed ^{13}C depletion in leaves in this treatment in accordance with higher C_i measured in the NH_4^+ grown plants. Similarly, Raven *et al*. (1984) concluded a higher C_i/C_a to explain the lower WUE and the ^{13}C depletion of 2.1‰ observed in leaves of NH_4^+-grown *Ricinus communis* plants compared to NO_3^- ones. The findings of Høgh-Jensen and Schjoerring (1997) and Brück and Guo (2006) are in agreement with the observation of Guo *et al*. (2002) and Raven *et al*. (1984), but those of Yin and Raven (1998) are opposite. In the latter case, the $\delta^{13}C_{OM}$ values of leaves, stubble and roots were always higher in NH_4^+-grown wheat and maize plants compared to those grown under NO_3^-, or mixed N nutrition. Martinez-Carrasco *et al*. (1998) also reported more than 2‰ higher $\delta^{13}C_{OM}$ values for leaves of young trees (< 1-year old) of *Casuarina equisetifolia* under NH_4^+ compared to NO_3^- nutrition. Because of a higher water use efficiency (WUE) observed under NH_4^+ nutrition, they suggested decreased stomatal to carboxylation conductance in this condition. In addition, ontogeny-dependant changes in photosynthetic discrimination has been reported in well-watered *Trifolium repens* (Høgh-Jensen and Schjoerring, 1997). These authors observed a higher discrimination (i.e. more negative $\delta^{13}C_{OM}$) in plants grown under NH_4^+ compared with those grown under NO_3^- nutrition at 54 DAS, but opposite trend at 96 DAS. In the present work, the $\delta^{13}C_{OM}$ was determined only at the end of the culture period (on 1-month old plants), but it was not followed during the 3-week N-treatments. The changes in $\delta^{13}C_{OM}$ during ontogeny under NH_4^+ or NO_3^- nutrition reported in the literature could be due to physiological changes (e.g. stomatal conductance, photosynthetic capacity, etc.) during ontogeny under different N-treatments and/or due to the duration of the N-treatment.

4.4 $\delta^{13}C$ of leaf-respired CO_2 changed across N-type gradient but not that of root-respired CO_2

Leaf-respired CO_2 was ^{13}C enriched compared with leaf OM and all compounds analysed, whatever the N-type treatment was. This is in agreement with our earlier data and those of literature. However, it was more negative in plants grown under NH_4^+ compared with those fed with NO_3^-. This is in agreement with the initial hypothesis developed in the introduction that a higher anaplerotic activity in leaves of plants fed with NO_3^- should enrich in ^{13}C the respiratory substrates and thus the leaf-respired CO_2, compared with plants fed with NH_4^+, because NO_3^- assimilation takes place mainly in the leaves.

Although the root-respired CO_2 was ^{13}C depleted compared with leaf-respired CO_2, it was surprisingly ^{13}C enriched compared with root OM, WSOM and all compounds analysed, and remained stable across N-type gradient. This is opposed to the general pattern reported in the literature (see Reviews by Ghashghaie and Badeck, 2014 and Bathellier *et al*., 2017) on herbaceous roots, including the earlier results of Bathellier *et al*. (2008) who observed a ^{13}C depleted root-respired CO_2 compared with root OM in bean plants. These authors suggested the prevalence of the pathways releasing ^{13}C depleted CO_2 in roots, e.g. the pentose phosphate pathway (PPP), known to be more active in roots (Dieuaide-Noubhani *et al*., 1995) compared with leaves. Since the decarboxylating enzyme involved in PPP highly discriminates against ^{13}C, this pathway contributes to further ^{13}C depletion in root-respired CO_2 (Bathellier *et al*., 2009).

In the present work, the ^{13}C enrichment in root-respired CO_2 is surprising. However, in agreement with the present data, ^{13}C enriched values of root-respired CO_2 have also been reported for different wheat genotypes including hydrides (Aranjuelo *et al*., 2009, 2013; Aljazairi *et al*., 2014). Further studies are needed to determine its metabolic origin.

4.5 Change in $\delta^{13}C$ of respired CO_2 is not correlated with changes in $\delta^{13}C$ of respiratory substrates across N-type gradient

Since the changes in $\delta^{13}C$ of individual compounds analysed did not parallel those of leaf-respired CO_2, only weak correlations were observed between these parameters across the N-type gradient in both organs (data not shown). The R^2 values were however higher between leaf-$\delta^{13}C_R$ and $\delta^{13}C$ of individual sugars (R^2 = 0.47, 0.52, 0.33 for Suc, Glc and Fru, respectively), and much lower between leaf-$\delta^{13}C_R$ and $\delta^{13}C$ of organic acids (R^2 = 0.37 for Mal and 0.11 for Cit). Our results are in contrast with those reported by Lehmann *et al*. (2015; 2016) who observed a high correlation between leaf-$\delta^{13}C_R$ and $\delta^{13}C$ of malate pool under high/low temperature and drought/wet conditions. They suggested that malate was the main substrate for respiration in their experiments. Similarly, Ghiasi et al. (unpublished) found a strong relationship between changes in leaf-$\delta^{13}C_R$ and leaf-$\delta^{13}C$ of organic acids (mainly citrate) in tobacco plants grown under varying NH_4^+:NO_3^- nutrition conditions, but not with $\delta^{13}C$ of leaf sugars. The N-treatment duration was 45 days in their experiment and only 21 days in the present work, which could have impacted the $\delta^{13}C$ values.

We rather observed a strong correlation between changes in leaf-$\delta^{13}C_R$ and in concentration of organic acids, but less so in carbohydrates (Covariance set 1, Table 1). In addition, the best

correlation was found between changes in leaf-$\delta^{13}C_R$ and changes in leaf-$\delta^{13}C_{WSOM}$ ($R^2 = 0.79$, $p = 0.05$) as well as with $\delta^{13}C_{(WSOM-OM)}$ ($R^2 = 0.82$, $p = 0.05$, Fig. S7). The calculated values of $\delta^{13}C_{WSOM}$ (using a mass balance) were also lower than the measured ones in both organs (Fig. S8), and since WSOM represents a mix of all soluble compounds (even those not analysed in the present work), therefore, the change in $\delta^{13}C$ of leaf-respired CO_2 across N-type gradient probably was caused by a change in the mix of substrates used for respiration.

4.6 Malate and citrate storage

High concentrations of organic acids indicate storage in vacuoles in both organs. Storage in vacuoles needs to be invoked to explain the observed malate and citrate contents in leaves and in roots under higher NO_3^- nutrition. Their contents decreased across the N-type gradient with increasing fraction of NH_4^+. Clark (1936) reported leaf, stem and root malate and citrate contents that were an order of magnitude lower in NH_4^+ as compared to NO_3^--grown plants. Ben-Zioni *et al*. (1970) showed that under NO_3^- nutrition malate accumulated in leaves of corn, barley and tobacco. A greater stability of labelled (^{14}C) malate under NO_3^- nutrition, while its amount decreased with time in plants under NH_4^+ nutrition, suggested the accumulation of malate in vacuole under NO_3^- (Ben-Zioni *et al*., 1970). This trend is in accordance with the role of organic acids in counterbalancing excess inorganic cations under nitrate nutrition (see also the review by Britto and Kronzucker, 2005). Pierce and Appleman (1943) showed that organic acids content and excess inorganic cations were positively correlated across 11 species with 2.5 mM NO_3^- nutrition. These results are consistent with the ca. 6-fold higher incorporation of ^{14}C into malate of NO_3^--grown compared to NH_4^+-grown *P. vulgaris* after a short labelling pulse of 60 s (Marques *et al*., 1983).

Indeed, as mentioned in the introduction, approximately 70% of all ions acquired by plants consist of N. Thus, the form of N supply (negatively charged NO_3^- *versus* positively charged NH_4^+) exerts a strong influence on the charge balance and therefore ion homeostasis (Gerendas *et al*., 1997). In the case of NH_4^+, its uptake decreases the absorption of other cations especially K^+ and Ca^{2+} compared to nutrition with NO_3^-. In the case of NO_3^- this problem does not exist, however arrived in the leaves, NO_3^- is reduced to NH_4^+ but its role as cation counter-ion is replaced by organic acids.

4.7 What is the relation between the $\delta^{13}C$ of OA and respired CO_2 across the N-gradient in leaves?

Malate and citrate, derived from anaplerotic replenishment, were ^{13}C enriched relative to total soluble sugars. This ^{13}C enrichment was higher in leaves (ca. 3‰) than in roots (less than 1‰), which is expected based on a much higher contribution of atmospheric CO_2 to the C source mixture for PEPc in leaves than in roots. Organic acids have multiple roles in metabolism. In our case, malate and citrate were the organic acids found with major concentrations. They are employed in providing C-skeletons for NH_4^+ assimilation in GS/GOGAT, but also in osmoregulation, acid/base and ion balances and transport of reduction power between organelles. In addition, it is known that they occur in different ratios in different plant species and their concentrations vary in different manners at diurnal time scales. $\delta^{13}C$ of anaplerotically introduced C should differ between day and night-time in leaves, because of higher contribution of atmospheric CO_2 to C source during the day (open stomata) and of respired CO_2 during the night (closed stomata).

From a metabolic point of view, the way organic acids contribute to CO_2 efflux in darkened leaves is still largely unclear. In recent years, labelling and modelling approaches have shown that the TCA in illuminated leaves generally does not keep its cyclic nature (see Tcherkez *et al*., 2009 for a review). The current hypothesis is that it operates in flux modes where glutamate synthesis for N assimilation is essentially decoupled from OAA and malate synthesis. The latter is thus mainly fueled by PEPc activity, which probably supports fluxes larger than commonly thought (up to 10% of net photosynthesis, Abadie and Tcherkez, 2019). As mitochondrial CS is strongly inhibited in the light, the supply of carbon to the "citrate branch" towards glutamate has been shown to come mostly from remobilized pools (notably stored citrate in *Xanthium*, Tcherkez *et al*., 2009), although the origin of remobilized metabolites remains partly unclear, and probably varies across species (Abadie *et al*., 2017).

In any case, under this scenario PEPc mainly fuels OAA and malate (and potentially fumarate) synthesis in the light, so that a stronger ^{13}C enrichment is expected in these metabolites compared to other organic acids, especially citrate. Consistently, a significant malate/citrate isotopic gap was reported in leaves for various species (cotton, Whelan *et al*., 1970; potato, Gleixner *et al*., 1998). However, this is probably not a general rule, as contrasted data have been reported for tobacco (Ghashghaie *et al*., 2001, Lehmann *et al*., 2019), and a recent study on conifers shows that the isotopic gap between malate and citrate can vary with species, but also seasonally

(Churakova *et al*., 2019). In fact, in the present study, the ^{13}C enrichment relative to soluble sugars for malate and citrate in leaves was very similar (ca. 3‰; Fig. 6), regardless of the N forms supplied. This suggests that PEPc contribution to citrate accumulation in the light was similar (if not higher, as citrate has 2 more carbon atoms than malate) to that towards malate, which is incompatible with a TCA flux mode in the light where malate and citrate branches are fully independent, and stored citrate is remobilized to fuel glutamate synthesis.

In fact, it is highly likely that other flux modes exist (see Sweetlove *et al*., 2010 for a review). In sunflower, a species that exhibits a low citrate content and accumulates fumarate, glutamate synthesis has been shown to derive largely from OAA and Acetyl-CoA, and not from citrate remobilization, thus involving some CS activity (Abadie *et al*., 2017). The origin of Acetyl-CoA in this case is still unclear, but could involve the conversion of malate and/or OAA into pyruvate by NAD-ME in the mitochondria, according to the flux mode proposed by Hanning and Heldt (1993). In this framework, PEPc contribution to citrate synthesis (and potentially accumulation) in the light could well be higher than that towards malate, thus lowering the isotopic gap between the two OA, as is observed in this study. Clearly then, it appears that disentangling the precise contribution of citrate and/or malate to the observed ^{13}C enrichment in respired CO_2 is not a straightforward issue, and cannot be easily tackled without undertaking studies throughout the diurnal cycle.

4.8 $\delta^{13}C$ of individual sugars differed systematically

Sugar concentrations followed an inverse pattern relative to organic acids across the N-type gradient with increasing concentration of NH_4^+ in supplied N. The increase was slight in leaves and marked in roots. Such an increase in sugar concentrations with NH_4^+ nutrition was not always found in previous experiments. Britto and Kronzucker (2002) cited several experiments in which sugar concentrations declined in parallel to organic acid concentrations.

While sugar contents increased with increasing NH_4^+ fraction in the nutrient solution, the C-isotope signature of leaf soluble sugars remained almost stable, except a slight decrease at 50% NH_4^+. Leaf sucrose was less ^{13}C depleted than glucose and fructose. Similar results were found by Ghashghaie *et al*. (2001) for leaves of well-watered tobacco and sunflower plants. As in the current experiment the sampling for sugar extraction was done concomitantly with measurements of dark respiration. In potato leaves, Gleixner *et al*. (1998) found the opposite pattern with sucrose more

^{13}C depleted than glucose and fructose as well as starch. In their experiment, samples were taken on a bright July day at 10 am, i.e. several hours into the daylight period. We hypothesize that these results can be explained by the fractionation between assimilates directed to starch storage within the chloroplast and those exported to the cytosol as triose phosphates as already suggested by Gleixner *et al*. (1998) in combination with storage of glucose and fructose in the vacuole. When leaves are photosynthetically active, relatively ^{13}C depleted sucrose is synthesized and used for export from the leaves. Sucrose is also transported to the vacuole where it is hydrolysed to glucose and fructose. Acid invertase discriminates against ^{13}C, leading to enriched sucrose and depleted hexoses (Mauve *et al*., 2009). Thus, hexose storage within vacuoles can result in hexoses depleted in ^{13}C relative to sucrose. The overall ratio of $\delta^{13}C$ in hexoses *versus* sucrose will finally depend on the relative fluxes to export from leaves, starch and sugar storage. The results reported by Lehmann *et al*. (2015) are consistent with these considerations. Sucrose concentration increased during day-time and sucrose was more ^{13}C depleted. At night sucrose concentration decreased and it became slightly more ^{13}C enriched than the hexoses. Thus, while the day-time measurements of sugar $\delta^{13}C$ reported by Gleixner *et al*. (1998) are putatively a result of sucrose export from the leaf and residual hexose storage from night-time starch mobilisation, in the case of the current experiment the night-time measurements (after 30 min in the dark) putatively reflect sucrose export from starch mobilisation while glucose and fructose may still mainly reflect day-time storage in the vacuoles. Further experiments, tracing the changes in concentrations and isotopic composition as well as labelling studies to trace the fluxes are required to confirm or reject these hypotheses.

While the sugar concentrations were relatively constant across the N-type gradient in leaves, they increased with increasing NH_4^+ fraction in roots. This results in replacement of the contribution of decreasing organic acid levels to the root osmotic potential by increasing sugar levels.

4.9 N-type nutrition effect on plant $\delta^{13}C$ could be related to anaplerotic activity of PEPc

PEPc activity was higher in leaves compared with roots at lower NH_4^+ nutrition, and the tendency reversed at higher NH_4^+ nutrition. These data are in agreement with the initial hypothesis that the PEPc activity is in general induced in roots under high NH_4^+ nutrition, while in leaves, higher PEPc activity is expected when NO_3^- is the main N-source (see introduction). The observed ^{13}C enriched leaf-respired CO_2 could mainly reflect the use of ^{13}C enriched PEPc-derived substrates under

higher NO_3^- nutrition, decreasing with increasing NH_4^+ fraction in nutrient solution. This effect is masked in roots because of the ^{13}C depleted C source (respired CO_2) fixed by PEPc in roots. Similarly, Ghiasi et al. (unpublished) observed a clear decrease in enzyme activities (PEPC, NR and ME) with increasing NH_4^+/NO_3^- ratio in supplied N on tobacco leaves.

A higher NR activity under NO_3^- nutrition compared with NH_4^+ nutrition has been reported on tomato plants (Horshani et al., 2010). This is in agreement with other data confirming that NR activity is positively regulated by NO_3^- concentration (Stitt, 1999). Plant response to NH_4^+ also depends on the tissue NH_4^+ concentration, but we did not measure the NH_4^+ concentration in our plants. NH_4^+ tolerance may also be related to the efficiency of species to sequestrate NH_4^+ in vacuoles mainly in root cells (Cruz *et al*., 2006). This could prevent the transport of NH_4^+ to the shoots which are more sensitive (Schjoerring *et al*., 2002).

5. Conclusions

C-isotope composition of plant organic material is in general considered to be a result of photosynthetic C-isotope discrimination, changing with species, as well as with environmental conditions affecting stomatal conductance and/or photosynthetic capacity, e.g. water availability in the soil, air humidity, light intensity, temperature, and N availability. However, post-photosynthetic C-isotope discriminations have also been shown to change the C-isotope composition of plant organic material, mainly during dark respiration. Our results as well as analysis of literature data show that the N source (i.e. NO_3^- *versus* NH_4^+) should also be added to the environmental factors affecting plant C-isotope composition, as well as that of leaf-respired CO_2.

The initial hypothesis of the present work was to examine the impact of varying ratios of NO_3^-:NH_4^+ in supplied N on C-isotope composition of leaf- and root-respiratory substrates as well as in respired CO_2 in bean plants. Although no major effect of N-type nutrition was observed on leaf gas exchange parameters neither on the C-isotope composition of plant organic compounds in none of the organs, leaf-respired CO_2 was more ^{13}C enriched under NO_3^- than under NH_4^+ nutrition. The linear relationship between C-isotope composition of leaf-respired CO_2 and that of WSOM suggested the use of a mix of substrates for respiration, with a higher contribution of anaplerotically fixed ^{13}C enriched C to leaf respiration in NO_3^--fed compared with NH_4^+-fed plants, in agreement with the observed higher PEPc and NR activities in leaves of the former plants.

Accordingly, we expected more ^{13}C enriched malate in leaves of NO_3^--fed compared with leaves of NH_4^+-fed plants, but the values remained unchanged across N-type nutrition. Interestingly, the isotopic gap between malate and citrate was low, malate being slightly ^{13}C enriched compared to citrate at high NO_3^- and slightly ^{13}C depleted at high NH_4^+ nutrition. This suggested a higher contribution of anaplerotically fixed ^{13}C enriched C to citrate pool. These data unambiguously illustrate the metabolic plasticity around the TCA in plants that has recently emerged (i.e. open *versus* closed mode functioning of TCA, and connection between malate and citrate valves), although it still remains poorly understood, notably regarding the central role played by organic acids (see Tcherkez, 2017 for a discussion). This warrants further work to explore the physiotype landscape of organic acid metabolism in plants. Interestingly, the above discussion highlights the potential of the malate/citrate (or other relevant abundant organic acids) ^{13}C-isotopic gap as a valuable proxy to screen for peculiar metabolic TCA organisations across species.

Acknowledgements

YX wishes to thank China Scholarship Council (CSC) for her PhD scholarship funding. The authors are grateful to Laboratoire d'Ecologie, Systématique et Evolution, ESE (University of Paris-Sud, Orsay, France) for the financial support of the experiments; Laboratory of ECOSYS (INRA, Grignon) for training on and assistance in isotope analyses of respired CO_2; Annika Ackermann and Institute of Agricultural Sciences (ETH Zürich) for isotope analyses of organic material; Steffen Ruehlow and Max Planck Institute (Jena, Germany) for training on and assistance in LC-C-IRMS analyses of sugars and organic acids; Guillaume Tcherkez for helpful discussion; Marlène Lamothe-Sibold for training on EA-IRMS; and the gardeners of ESE for helping in plant culture/care.

Supplementary materials for Chapter 4

Table S1. Results of regression of traits on the fraction of NH_4^+ in supplied nitrogen (% of supplied N). Regression type: If linearly correlated with NH_4^+ (% of supplied N), – for negatively and + for positively correlated, log for regression on log transformed NH_4^+ (% of supplied N), log inv for regression on log transformed NO_3^- (i.e. 100 – NH_4^+) % of supplied N. For regressions on abs (NH_4^+ (% of supplied N)-extremum) with extremum at 25 (50, 75) %, min 25 (50, 75) % for minimum and max 25 (50, 75) % for maximum.

Trait	Regression type	R^2	Significance	Loading most on PCA axis
$\delta^{13}C$ of leaf respiration	–	0.8	$p < 0.017$	PCA1
	log	0.97	$p < 0.001$	
$\delta^{13}C$ of leaf WSOM	–	0.96	$p < 0.001$)	PCA1
[leaf malate]	–	0.9	$p < 0.005$	PCA1
[root sucrose]	+	0.68	$p < 0.044$	PCA1
	log inv	0.77	$p < 0.021$	
[root glucose]	+	0.74	$p < 0.028$	PCA1
	log inv	0.99	$p < 0.001$	
[root fructose]	+	0.78	$p < 0.021$	PCA1
	log inv	0.99	$p < 0.001$	
[root citrate]	–	0.95	$p < 0.001$	PCA1
root C%	+	0.89	$p < 0.005$	PCA1
leaf dry mass	–	0.76	$p < 0.025$	PCA2
	log	0.93	$p < 0.003$	
[leaf sucrose]	min 25%	0.84	$p < 0.011$	PCA1
$\delta^{18}O$ of leaf respiration	log inv	0.71	$p < 0.035$	PCA1
root PEPc activity	log inv	0.81	$p < 0.016$	PCA1
$\delta^{13}C$ of root citrate	min 25%	0.89	$p < 0.006$	PCA1
C_i/C_a	min 25%	0.82	$p < 0.014$	PCA1
WUE_{intr}	max 25%	0.79	$p < 0.019$	PCA1
WUE_{inst}	max 25%	0.69	$p < 0.040$	PCA1
Chl 19.01	min 25%	0.75	$p < 0.025$	PCA1
Chl 22.01	min 25%	0.77	$p < 0.023$	PCA1
NBI 27.01	max 25%	0.71	$p < 0.035$	PCA1
$\delta^{13}C$ of leaf sucrose	min 50%	0.92	$p < 0.003$	PCA2
$\delta^{13}C$ of leaf glucose	min 50%	0.72	$p < 0.032$	PCA2

leaf N%	max 50%	0.72	$p < 0.034$	PCA2
Fv/Fm	min 50%	0.66	$p < 0.051$	PCA6
NBI 19.01	max 50%	0.65	$p < 0.053$	PCA2
Flav 22.01	min 50%	0.67	$p < 0.047$	PCA2
[leaf citrate]	min 75%	0.918	$p < 0.003$	PCA2
$\delta^{15}N$ of leaf OM	max 75%	0.864	$p < 0.008$	PCA2
	log	0.9	$p < 0.004$	
[root malate]	min 75%	0.864	$p < 0.008$	PCA2
	log	0.92	$p < 0.003$	
root N%	max 75%	0.818	$p < 0.014$	PCA2
$\delta^{15}N$ of root OM	max 75%	0.849	$p < 0.009$	PCA2
	log	0.95	$p < 0.001$	
root DM	max 75%	0.734	$p < 0.030$	PCA2
	log	0.95	$p < 0.002$	
$\delta^{13}C$ of root glucose	log inv	0.71	$p < 0.037$	PCA3
stem DM	log	0.71	$p < 0.037$	PCA2
Carboxylation efficiency	log inv	0.66	$p < 0.050$	PCA3
Electron transport rate	log inv	0.69	$p < 0.040$	PCA3

Not significantly correlated with NH_4^+ (% of supplied N): $\delta^{13}C$ of leaf citrate, Leaf respiration rate, leaf PEPc activity, leaf NR activity, $\delta^{13}C$ of leaf OM, $\delta^{13}C$ of leaf fructose, $\delta^{13}C$ of leaf malate, [leaf glucose], [leaf fructose], leaf C content, root respiration rate, root NR activity, $\delta^{13}C$ of root respiration, $\delta^{13}C$ of root OM, $\delta^{13}C$ of root WSOM, $\delta^{13}C$ of root sucrose, $\delta^{13}C$ of root fructose, $\delta^{13}C$ of root malate, $\delta^{18}O$ of root respiration, [leaf citrate], Net photosynthesis, photosynthetic NUE, leaf transpiration rate, stomatal conductance, DF/Fm, ETR, Flav 19.01., NBI 22.01, Chl 27.01, Flav 27.01.

Supplementary Figures for Chapter 4

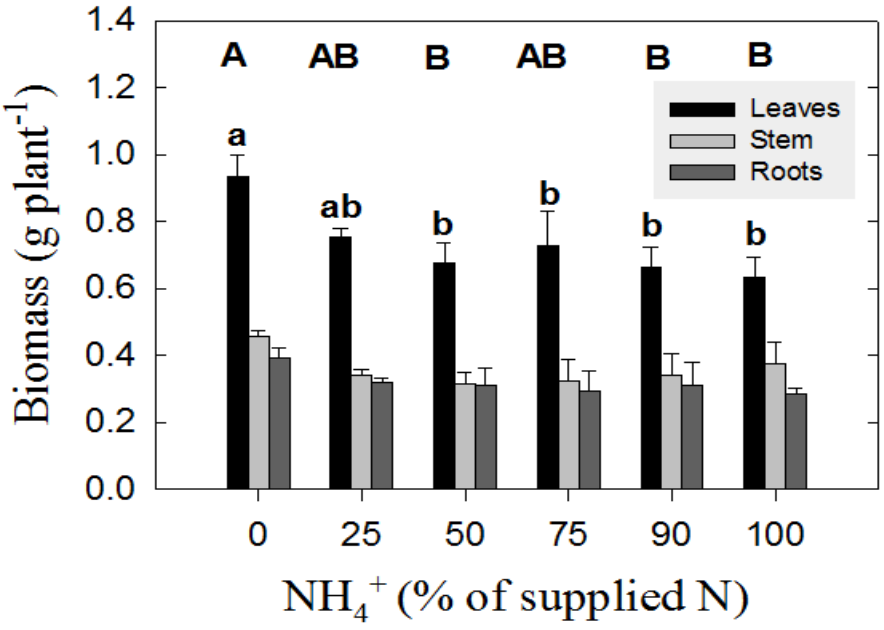

Figure S1. Biomass of different organs (leaves, stem and roots) of bean plants cultured under different % of NH_4^+ and NO_3^- as N source in nutrient solutions used for watering the pots. On the X-axis, 0 and 100 correspond to 0% NH_4^+ (i.e. 100% NO_3^-) and 100% NH_4^+ (i.e. 0% NO_3^-) as % of supplied N in the nutrient solutions, respectively. Values are means ± SE (n=3). Different letters (lowercase letters for leaves and capital letters for total biomass) indicate significant differences ($p < 0.05$).

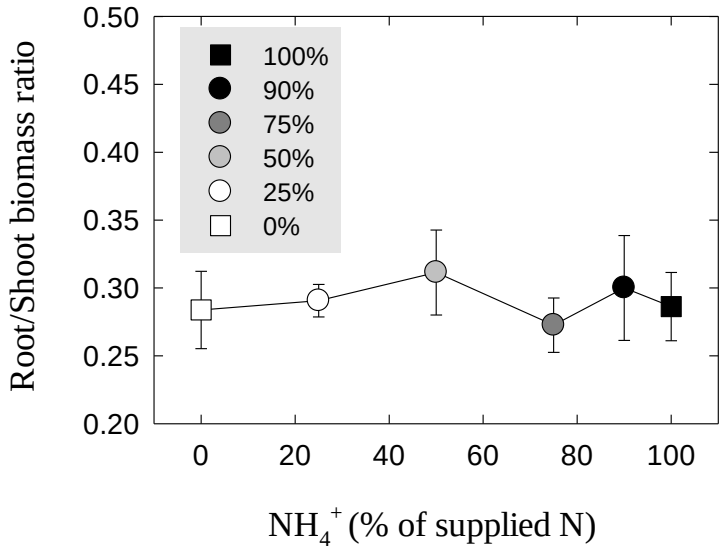

Figure S2. Root to shoot biomass ratio of bean plants cultured under different % of NH_4^+ and NO_3^- as N source in nutrient solutions used for watering the pots. On the X-axis (and in the legend box), 0% and 100% correspond to 0% $NH4^+$ (i.e. 100% NO_3^-, white squares) and 100% $NH4^+$ (i.e. 0% NO_3^-, black squares) as % of total N in the nutrient solutions, respectively. The other N-treatments are shown by circles, as a gradient of increasing NH_4^+ fraction in supplied N, from low NH_4^+ (white) to medium NH_4^+ (grey) and high NH_4^+ (black). Values are means ± SE (n=3). N-type gradient had no significant effect on the root/shoot biomass ratio.

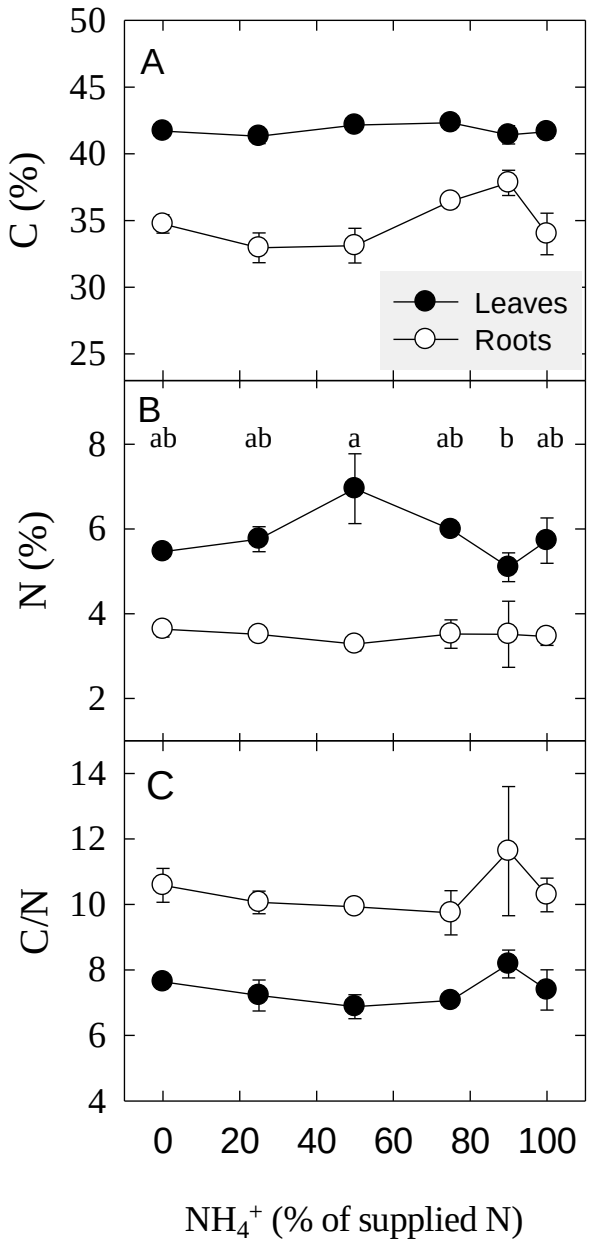

Figure S3. Percentages of carbon (A) and nitrogen (B) and the ratio C/N (C) in bulk OM of leaves (black symbols) and roots (white symbols) of bean plants grown with nutrient solutions containing different ratios of NH_4^+ and NO_3^- as N source. On the X-axis, 0 and 100 correspond to 0% NH_4^+ (i.e. 100% NO_3^-) and 100% NH_4^+ (i.e. 0% NO_3^-) as % of total N in the nutrient solutions, respectively. Values are shown as means ± SE (n=3). Only significant differences ($p < 0.05$) are shown by different letters for leaf N% (because there was no significant difference for roots).

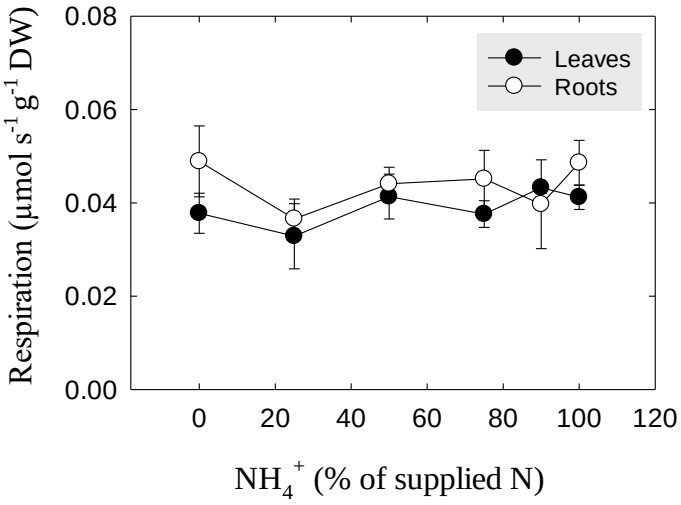

Figure S4. Respiration rates of leaves (black circles) and roots (white circles) of bean plants grown with nutrient solutions containing different ratios of NH_4^+ and NO_3^- as N source. On the X-axis, 0 and 100 correspond to 0% NH_4^+ (i.e. 100% NO_3^-) and 100% NH_4^+ (i.e. 0% NO_3^-) as % of total N in the nutrient solutions, respectively. The respiration rates were measured during CO_2 collection on samples in the darkened flasks before respired CO_2 isotopic analyses. Values are shown as means ± SE (n=3). No significant change in respiration rate along the N-type gradient was observed for none of the organs.

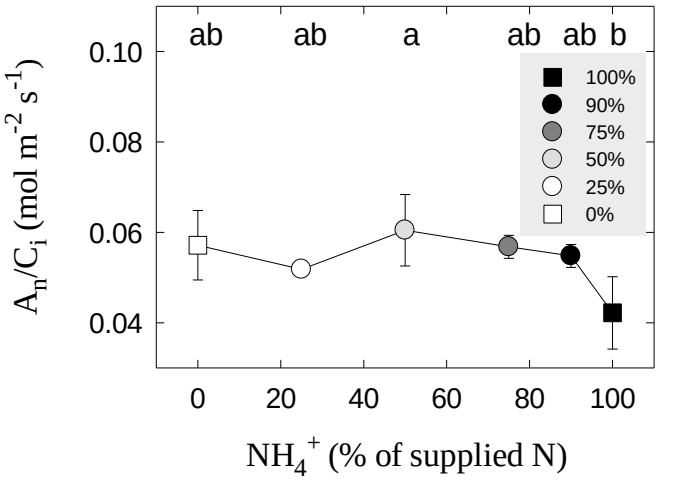

Figure S5. Changes in the carboxylation efficiency, calculated as the ratio of net CO_2 assimilation (A_n) to the intercellular CO_2 concentration (C_i), of bean plants cultured under different proportions of NH_4^+ *versus* NO_3^- as N sources in nutrient solutions used for watering the pots. Data are taken from **Figure 1.** On the X-axis (and in the legend box), 0% and 100% correspond to 0% $NH4^+$ (i.e. 100% NO_3^-, white squares) and 100% $NH4^+$ (i.e. 0% NO_3^-, black squares) as % of total N in the nutrient solutions, respectively. The other N-treatments are shown by circles, as a gradient of increasing NH_4^+ in the solutions, from low NH_4^+ (white) to medium NH_4^+) (grey) and high NH_4^+ (black). Means values ± SE (n=3) are presented. Significant differences ($p < 0.05$) are shown by different letters.

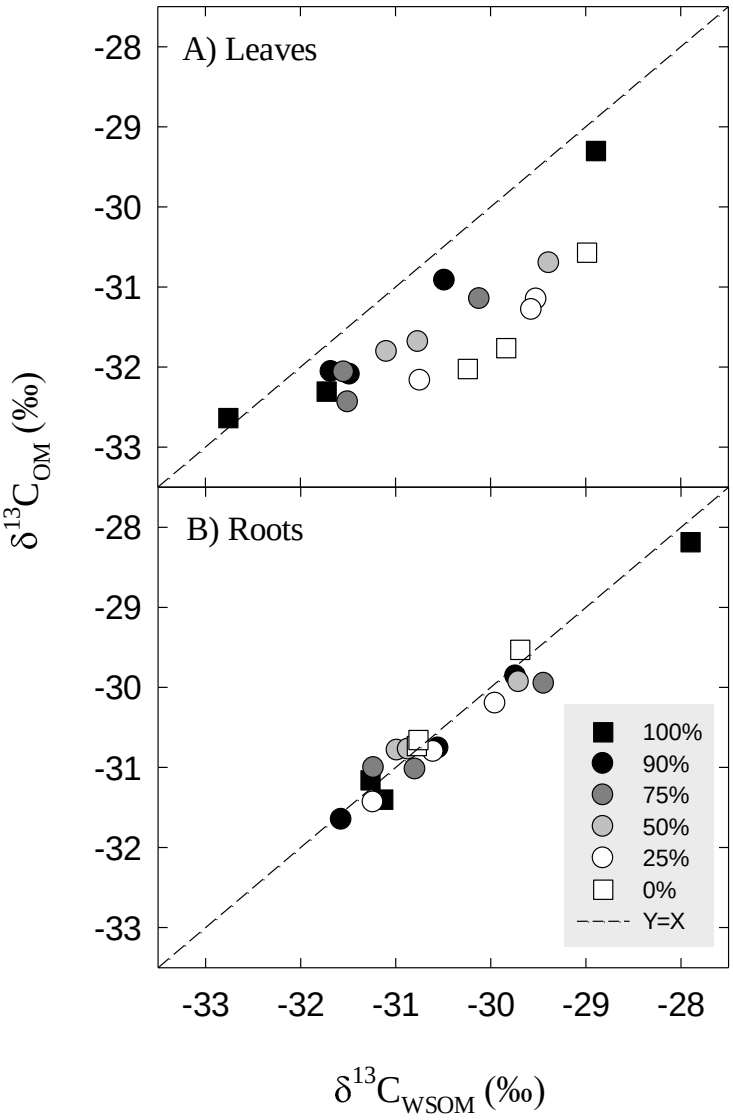

Figure S6. Relationship between $\delta^{13}C$ of bulk OM ($\delta^{13}C_{OM}$) and that of WSOM ($\delta^{13}C_{WSOM}$) in leaves (A) and roots (B) of bean plants cultured under different % of NH_4^+ and NO_3^- as N source in nutrient solution used for watering the pots. The white squares correspond to 0% NH_4^+ (i.e. 100% NO_3^-) and black squares to 100% NH_4^+ (i.e. 0% NO_3^-) in nutrient solutions. The other N-treatments are shown by circles, as a gradient of increasing NH_4^+ in the solutions from white (low NH_4^+) to grey (medium NH_4^+) and black (high NH_4^+) circles. The 1:1 relationship (Y=X) are also presented by dashed lines. Each data point corresponds to individual measurement on independent plant (three replicates for each N-treatment).

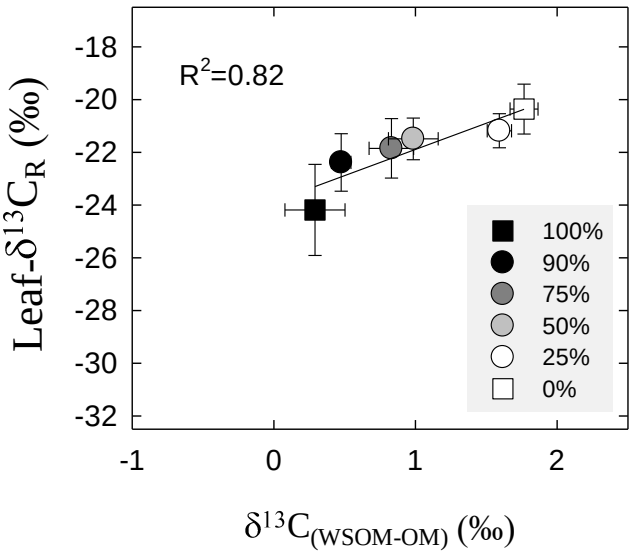

Figure S7. Variation in $\delta^{13}C$ of respired CO_2 as a function of ^{13}C-difference between WSOM and OM ($\delta^{13}C_{WSOM-OM}$) in leaves of bean plants cultured under different % of NH_4^+ and NO_3^- as N source in nutrient solution used for watering the pots. In the legend box, 0% and 100% correspond to 0% $NH4^+$ (i.e. 100% NO_3^-, white squares) and 100% $NH4^+$ (i.e. 0% NO_3^-, black squares) as % of total N in the nutrient solutions, respectively. The other N-treatments are shown by circles, as a gradient of increasing NH_4^+ fraction in supplied N, from low NH_4^+ (white) to medium NH_4^+ (grey) and high NH_4^+ (black). Values are means ± SE (n=3).

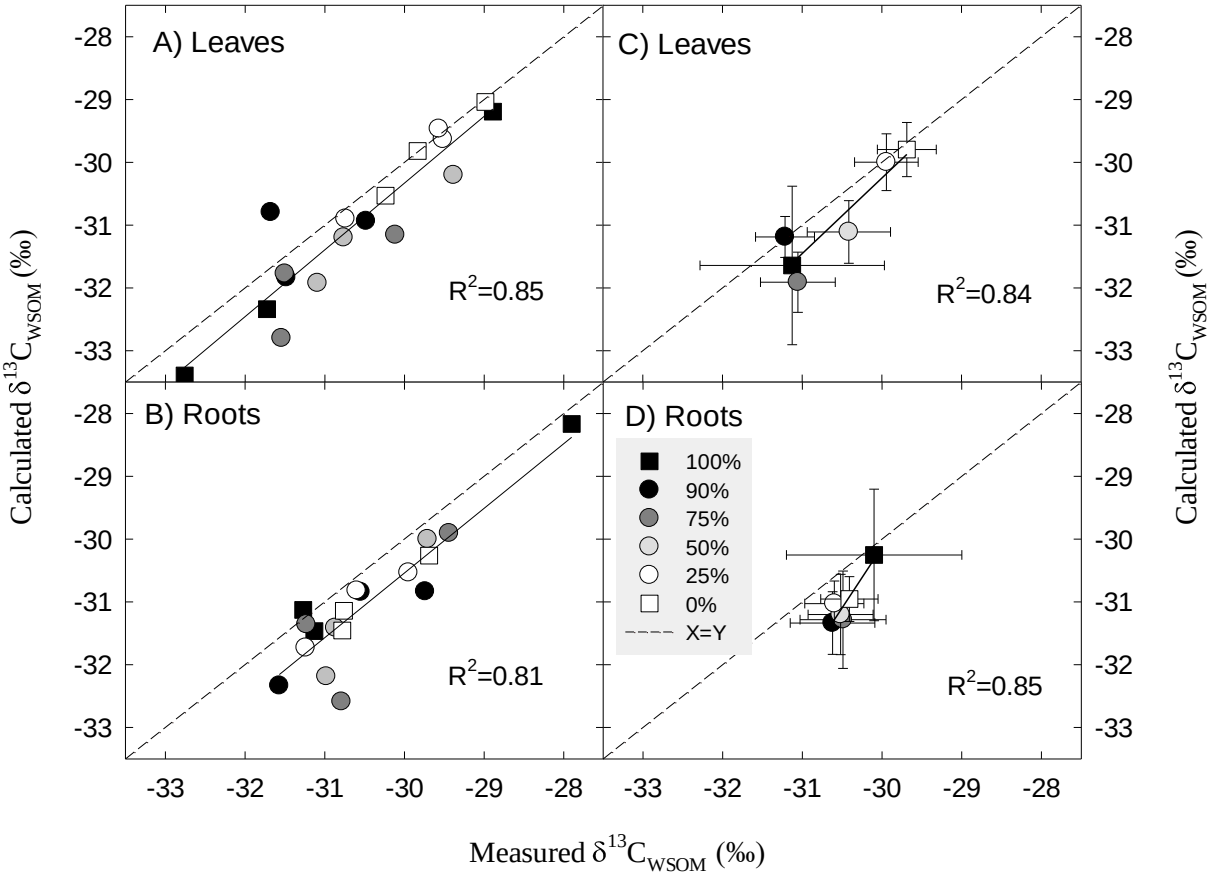

Figure S8: Expected values of $\delta^{13}C_{WSOM,}$ calculated using the amounts and $\delta^{13}C$ values of individual compounds analysed in this study (sugars and organic acids) versus the measured $\delta^{13}C_{WSOM}$ values in leaves (A, C) and roots (B, D) of bean plants cultured under different % of NH_4^+ and NO_3^- as N source in nutrient solutions used for watering the pots. In the legend box, 0% and 100% correspond to 0% $NH4^+$ (i.e. 100% NO_3^-, white squares) and 100% $NH4^+$ (i.e. 0% NO_3^-, black squares) as % of total N in the nutrient solutions, respectively. The other N-treatments are shown by circles, as a gradient of increasing NH_4^+ in the solutions, from low NH_4^+ (white) to medium NH_4^+) (grey) and high NH_4^+ (black). Individual data are presented in A and B and mean ± SE (n=3) values in C and D.

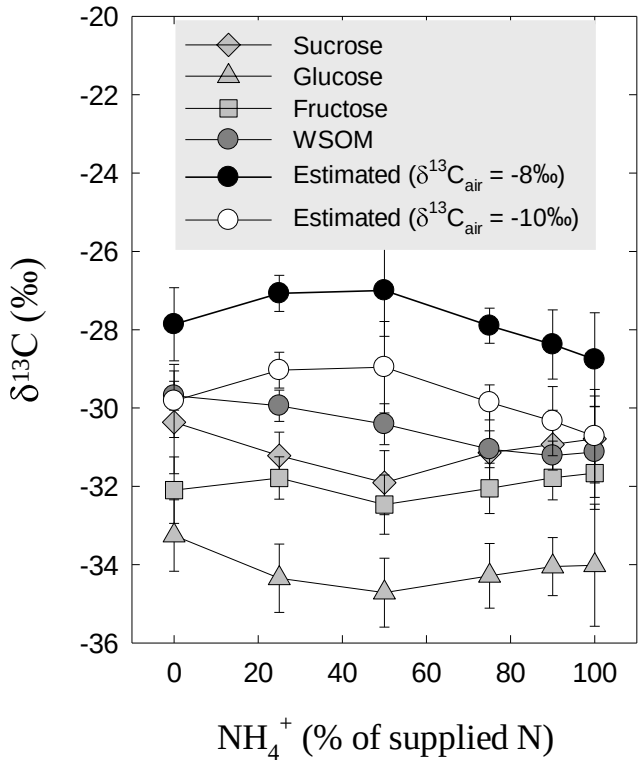

Figure S9. Estimated $\delta^{13}C$ values (black and withe symbols) of the photosynthetic products compared with measured values (grey symbols) of leaf-$\delta^{13}C_{WSOM}$ (dark-grey circles), leaf-$\delta^{13}C_{Suc}$ (light-grey diamonds), leaf-$\delta^{13}C_{Glc}$ (light-grey triangles), and leaf-$\delta^{13}C_{Fru}$ (light-grey squares), as a function of N-treatment in bean plants. On the X-axis, 0 and 100 correspond to 0% NH_4^+ (i.e. 100% NO_3^-) and 100% NH_4^+ (i.e. 0% NO_3^-) in nutrient solutions, respectively. Estimated $\delta^{13}C$ values are calculated using the C_i/C_a values from **Figure 1C** and the simple C_3 model of Farquhar et al. (1982) with a = 4.4‰ and b=27‰. Means ±SE are presented (n=3). $\delta^{13}C$ of ambient CO_2 in the culture room was estimated to be around –8‰, using the leaf-$\delta^{13}C_{OM}$ of maize plants cultured in the same room, assuming a photosynthetic discrimination of 4‰ for maize leaves (black circles). When maize discrimination is taken around 2‰, thus air CO_2 ca. –10‰ that the estimated values (white circles) were close to measured $\delta^{13}C_{WSOM}$ values, but did not match the values of none of the sugars.

CHAPTER 5 - Impact of varying NH_4^+:NO_3^- ratios in supplied N on C-isotope respiratory fractionation in *Spinacia oleracea* L.

5.1 Introduction

In previous experiment described in Chapter 4, we investigated the changes in the $\delta^{13}C$ of respired CO_2 and of the main metabolic pools involved in respiration in both leaves and roots of French bean plants fed with various NO_3^-:NH_4^+ ratios. We observed that leaf-respired CO_2 was highly ^{13}C enriched under NO_3^- nutrition and became progressively ^{13}C depleted with increasing amount of NH_4^+ in supplied N, while C-isotope composition of root-respired CO_2 remained unchanged across N-type gradient. In both organs, respired CO_2 remained ^{13}C enriched compared with plant organic material and all metabolites analysed across N-type nutrition gradient. The linear relationship between C-isotope composition of leaf-respired CO_2 and that of WSOM partially reflected a higher flux through the anaplerotic pathway (which fixes ^{13}C enriched carbon) of NO_3^--fed compared to NH_4^+-fed plants in leaves, but not in roots. More malate in leaves of NO_3^--fed compared with leaves of NH_4^+-fed plants was observed, but with no significant carbon isotopic differences among N-type nutrition. Furthermore, intrestingly, unexpected organic acid ^{13}C-isotopic gaps (malate/citrate) which involes two weakly connected branches operating in opposite directions in non-cyclic TCA were observed in leaves. The plasticity of TCA flux in the light is indeed expected to affect the concentration and $\delta^{13}C$ values of organic acids, which are key C sources of leaf dark-respired CO_2. To our knowledge, no literature is available on how the N type can affect isotopic signature of putative respiratory substrates (mainly carbohydrates and organic acids) and that of respired CO_2. Further works are necessary to explore the potential role of organic acid metabolism on ^{13}C-isotopic fractionation in other species.

According to our preliminary experiment described in Chapter 3, we selected bean and spinach for in-depth studies. In the present chapter, the response of plants to ammonium and nitrate nutrition and the subsequent impact on C-isotope composition of leaf- and root-respired CO_2 and putative respiratory substrates was investigated in spinach, which is a more ammonium-sensitive plant species than bean (Britto and Kronzucker, 2002; Lasa *et al.*, 2002a, b; Esteban *et al.*, 2016). Plants were grown under varying ratios of NH_4^+:NO_3^- in supplied N (the same used for bean culture), to examine in which extent the isotopic signature of putative respiratory substrates and

respired CO_2 is affected by N-type nutrition in this plant species, and in which extent the anaplerotic C-(re)fixation pathway (*via* PEPc) is affected by N-type in roots *versus* leaves. This would allow a better understanding of the metabolic origin of the divergence in isotopic signature between heterotrophic and autotrophic organs**.**

5.2 Material and Methods

Plant material studied in this experiment was *Spinacia oleracea* L. Most of the methods and experimental protocols in this experiment are the same as those used for bean (see details in Chapter 2 and in bean manuscript Chapter 4).

To be recalled that, the differences between spinach and bean experimental conditions were: (i) light intensity was slightly higher for spinach with only artificial light source with 200-210 µmol photons m^{-2} s^{-1} at plant height (while for bean there was also natural light in the culture room); (ii) the photoperiod was longer (16 h per day) than for bean (10 h per day); (iii) because of a lower growth rate, the culture period was longer for spinach (36 d) than for bean (28 d) as well as the N-treatment duration (29 d and 21 d, respectvely), (iv) 1 ppm nitrification inhibitor (2-Chloro-6-trichloromethylpyridine) was added to the nutrient solutions in spinach but not in bean culture; (v) two PPFD levels were used for gas exchange measurements (200 and 400 µmol m^{-2} s^{-1}) for spinach (only 400 µmol m^{-2} s^{-1} for bean).

5.3. Results and Discussion

5.3.1 Effect of N-type supply on plant growth

As in the experiment on bean, chlorosis was not observed on spinach leaves during the whole culture period. Similar to the results from the preliminary experiment (Chapter 3), there were no significant differences ($p < 0.05$) along the N-type gradient in total plant biomass neither in biomass of individual organs (Fig. 5.1). Intrestingly, the lowest biomass values for all the organs were observed in 75% NH_4^+ treatment but not in 100% NH_4^+. The root/shoot biomass ratio was stable with mean values around 0.4 along N-type gradient and decreased only, but not significantly, at 100% NH_4^+ reaching values below 0.3 (Fig. 5.2). This ratio was lower in bean (≤ 0.3) but did not significantly change across N-type nutrition gradient.

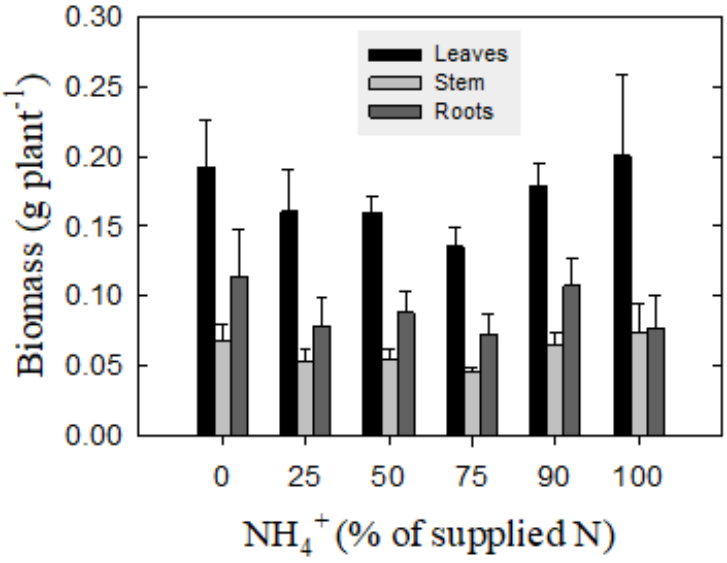

Figure 5.1 Biomass of different organs (leaves, stem and roots) of spinach plants cultured under different % of NH_4^+ and NO_3^- as N source in nutrient solutions. On the X-axis, 0 and 100 correspond to 0% NH_4^+ (i.e. 100% NO_3^-) and 100% NH_4^+ (i.e. 0% NO_3^-) as % of supplied N in the nutrient solutions, respectively. Values are means ± SE (n = 5). Different letters on the top of the bar charts indicate significant differences (p = 0.05).

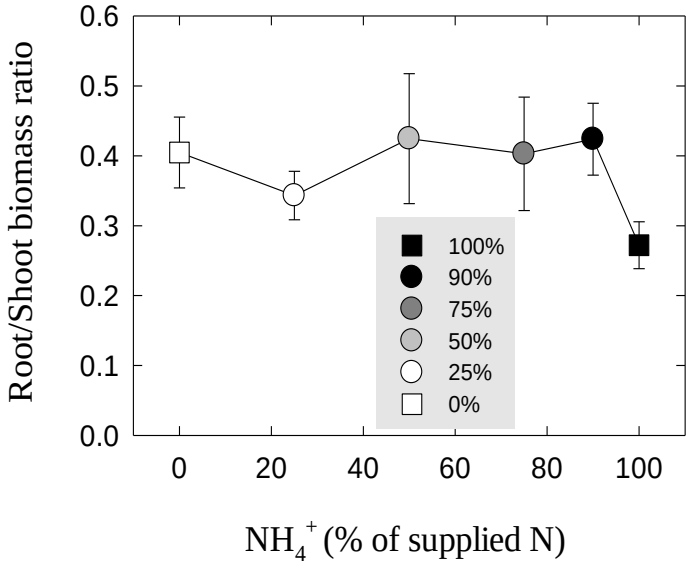

Figure 5.2 Root to shoot biomass ratio of spinach plants cultured under different % of NH_4^+ and NO_3^- as N source in nutrient solutions used for watering the pots. On the X-axis (and in the legend box), 0% and 100% correspond to 0% $NH4^+$ (i.e. 100% NO_3^-, white squares) and 100% $NH4^+$ (i.e. 0% NO_3^-, black squares) as % of total N in the nutrient solutions, respectively. The other N-treatments are shown by circles, as a gradient of increasing NH_4^+ in the solutions, from low NH_4^+ (white) to medium NH_4^+) (grey) and high NH_4^+ (black). Values are means ± SE (n=5).

Chlorosis of leaves, overall suppression of growth and root/shoot ratio decrease are the general visual symptoms of NH_4^+ toxicity (Britto and Kronzucker, 2002; Bittsanszky *et al.*, 2015; Esteban *et al.*, 2016). However, in the present work, there was no significant decrease in biomss or in root/shoot ratio with increasing NH_4^+ fraction in supplied N. As we discussed in Chapters 3 and 4, the tolerance for NH_4^+ varies with multiple experimental conditions such as NH_4^+ concentrations, pH, concentration of other supplied nutrients (calcium, phosphorus, potassium, etc.), light intensity,

temperature, etc. (Gerendás *et al.*, 1997; Britto and Kronzucker, 2002). In our study, the alleviation of NH_4^+ toxicity effect should be due to low light intensity (Gerendás *et al.*, 1997; Zhu *et al.*, 2000; Britto and Kronzucker, 2002; Guo *et al.*, 2007; Bittsanszky *et al.*, 2015; Esteban *et al.*, 2016) during plant culture (140-160 and 200-210 μmol photons m^{-2} s^{-1} in bean and spinach, respectively). The high variability in plant biomass and root/shoot ratio among species and experiments reported in the literature are also visible when comparying our data of the pre-experiment and the main experiments (see Appendix 1 and 2 , respectively).

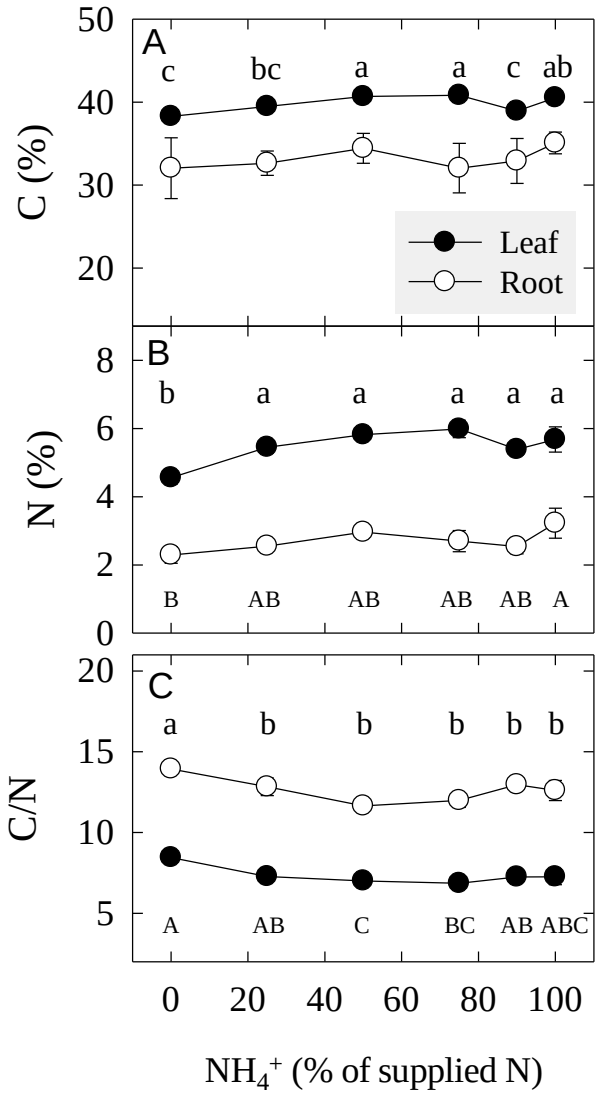

Figure 5.3 Percentages of carbon (A) and nitrogen (B) and the ratio C/N (C) in bulk OM of leaves (black symbols) and roots (white symbols) of spinach plants grown with nutrient solutions containing different ratios of NH_4^+ and NO_3^- as N source. On the X-axis, 0 and 100 correspond to 0% NH_4^+ (i.e. 100% NO_3^-) and 100% NH_4^+ (i.e. 0% NO_3^-) as % of total N in the nutrient solutions, respectively. Values are shown as means ± SE (n=3). Significant differences ($p < 0.05$) are shown by different letters (lowercase letters for leaves, uppercase letters for roots).

C and N contents were higher in leaves compared to roots, but C/N ratio was different (Fig. 5.3). Spinach fed with 0% NH_4^+ had the lowest C and N contents but the highest C/N ratio in leaves. In roots, nitrogen content of 0% NH_4^+ was significantly ($p < 0.05$) lower than that of 100% NH_4^+, while there was no significant difference in C/N ratio between 0% and 100% NH_4^+ treatments.

5.3.2 Effect of N-type supply on respiration and leaf gas exchange parameters

Root respiration rate was about 3 times higher than leaf respiration (Fig. 5.4). No significant changes in respiration rate along the N-type gradient was observed in roots, but respiration rate of leaves in 0% NH_4^+ (100% NO_3^-) was significantly smaller than in 100% NH_4^+ (Fig. 5.4). High respiratory rates were commonly, but not always, observed with NH_4^+ nutrition compared with NO_3^- nutrition in many plants (see the review of Britto and Kronzucker, 2002; Hachiya and Sakakibara, 2016). The plausible explanation was thought to be the energy-demanding active efflux of cytosolic NH_4^+ during membrane trasportation of NH_4^+ from the cytosol to the external medium (detoxification stragety).

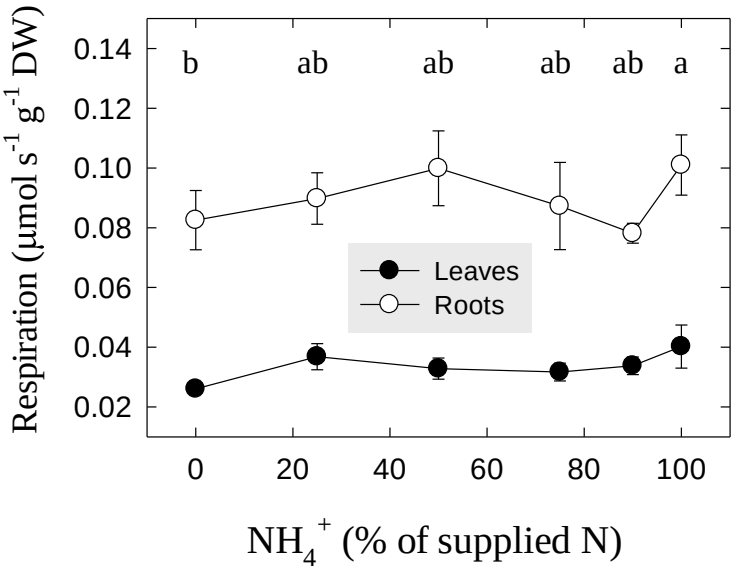

Figure 5.4 Respiration rates of leaves (black circles) and roots (white circles) of spinach plants grown with nutrient solutions containing different ratios of NH_4^+ and NO_3^- as N source. On the X-axis, 0 and 100 correspond to 0% NH_4^+ (i.e. 100% NO_3^-) and 100% NH_4^+ (i.e. 0% NO_3^-) as % of total N in the nutrient solutions, respectively. The respiration rates were measured during CO_2 collection on samples in the darkened flasks before respired CO_2 isotopic analyses. Values are shown as means ± SE (n=5). Significant differences ($p < 0.05$) are shown by different lowercase letters for leaves. There is no significant difference for root data.

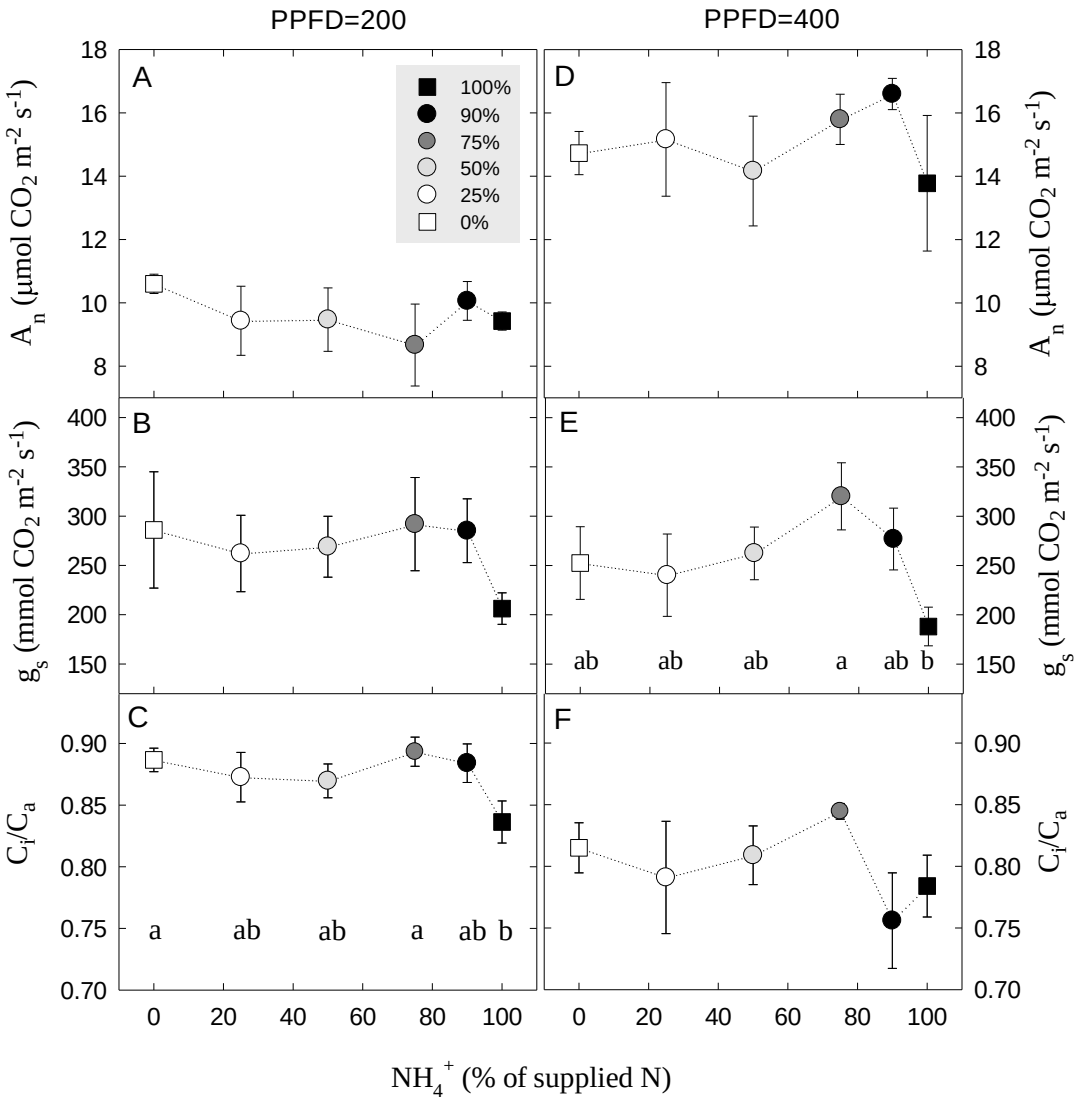

Figure 5.5 Changes in leaf net CO_2 assimilation rate, A_n (A, D), stomatal conductance for CO_2 diffusion, g_s (C, E), and the ratio of intercellular to ambient CO_2 concentrations, C_i/C_a (C, F) of spinach plants cultured under different proportions of NH_4^+ *versus* NO_3^- as N sources in nutrient solutions used for watering the pots. On the X-axis (and in the legend box), 0% and 100% correspond to 0% $NH4^+$ (i.e. 100% NO_3^-, white squares) and 100% $NH4^+$ (i.e. 0% NO_3^-, black squares) as % of total N in the nutrient solutions, respectively. The other N-treatments are shown by circles, as a gradient of increasing NH_4^+ in the solutions, from low NH_4^+ (white) to medium NH_4^+) (grey) and high NH_4^+ (black). The measurements were conducted under PPFD of 200 (left side panels) and 400 µmol m^{-2} s^{-1} (right side panels). Values are means ± SE (n=3). Only significant differences ($p < 0.05$) are shown by lowercase letters.

Different to bean, we used two levels of PPFD for gas exchange measurements in spianch, the low level (200 µmol photons m^{-2} s^{-1}) aimed to mimic the light intensity during spinach growth, and the higher level (400 µmol photons m^{-2} s^{-1}) was set to be similar to that used for gas exchange experiment on bean plants. Leaf net CO_2 assimilation (A_n) values measured at low PPFD were

lower (varying between 9 and 10.5 µmol m^{-2} s^{-1}) than at high PPFD (varying between 14 and 17 µmol m^{-2} s^{-1}) but with no significant changes across N-type gradient (Fig. 5.5A, D). The ranges of stomatal conductance (g_s) were simillar between the two PPFD levels (Fig. 5.5B, E), 100% NH_4^+ treatment exhibiting the smallest values among all N-treatments, with significant ($p < 0.05$) decrease compared to 75% NH_4^+ treatment, but only at high PPFD. C_i/C_a values at 400 PPFD were lower than those at 200 PPFD (Fig. 5.5C, F), 100% NH_4^+ treatment showing a significant ($p < 0.05$) decrease as compared with 75% NH_4^+ and 0% NH_4^+ (100% NO_3^-) treatments but only at 200 PPFD. In the case of bean, the N-type gradient had no significant impact on g_s and C_i/C_a (see Fig. 1 in Chapter 4).

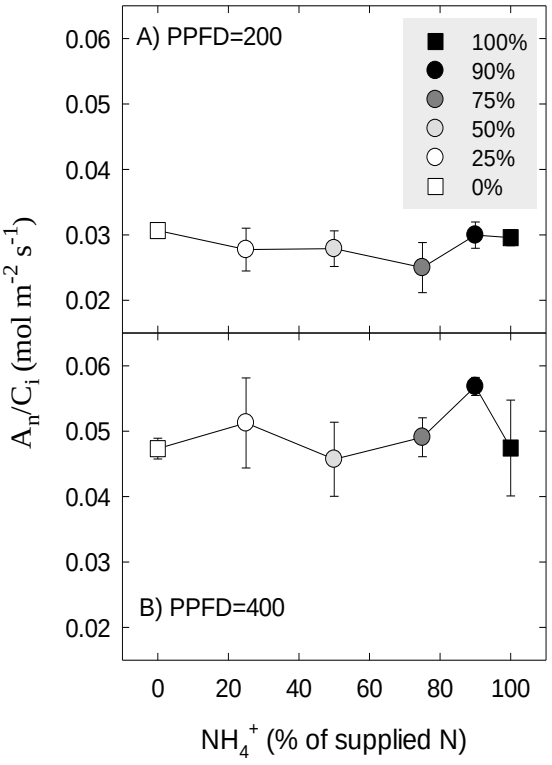

Figure 5.6 Changes in the carboxylation efficiency, calculated as the ratio of net CO_2 assimilation (A_n) to the intercellular CO_2 concentration (C_i) of plants cultured under different proportions of NH_4^+ *versus* NO_3^- as N sources in nutrient solutions. On the X-axis (and in the legend box), 0% and 100% correspond to 0% $NH4^+$ (i.e. 100% NO_3^-, white squares) and 100% $NH4^+$ (i.e. 0% NO_3^-, black squares) as % of total N in the nutrient solutions, respectively. The other N-treatments are shown by circles, as a gradient of increasing NH_4^+ in the solutions, from low NH_4^+ (white) to medium NH_4^+) (grey) and high NH_4^+ (black). The measurements were conducted under PPFD of 200 (upside panels) and 400 µmol m^{-2} s^{-1} (bottom side panels). Means values ± SE (n=3) are presented.

In addition, the carboxylation efficiency (A_n/C_i) remained stable in both PPFD levels (around 0.03 and 0.05 mol m^{-2} s^{-1}, respectively) along N-type gradient, with no significant changes (Fig. 5.6).

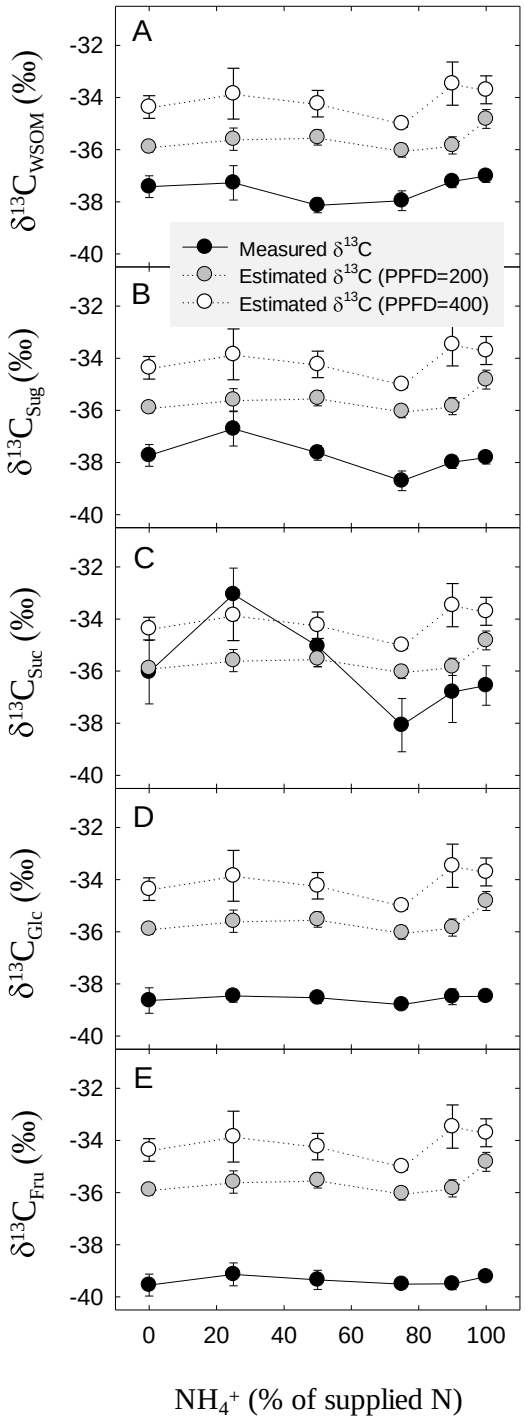

Figure 5.7 Measured values (black symbols) and estimated values according to Farquhar model (grey and white symbols at PPFD=200 and 400, respectively) of leaf-$\delta^{13}C_{WSOM}$ (A), leaf-$\delta^{13}C_{sug}$ (B), leaf-$\delta^{13}C_{Suc}$ (C), leaf-$\delta^{13}C_{Glc}$ (D), and leaf-$\delta^{13}C_{Fru}$ (E), as a function of N-treatment in bean plants. On the X-axis, 0 and 100 correspond to 0% NH_4^+ (i.e. 100% NO_3^-) and 100% NH_4^+ (i.e. 0% NO_3^-) in nutrient solutions, respectively. Estimated values of $\delta^{13}C$ are calculated using simple model of Farquhar et al. (1982) using the C_i/C_a values, and taking a=4.4‰ and b=27‰. Means ±SE are presented (n=3). $\delta^{13}C$ value of the ambient CO_2 in the culture room (–12.33‰) was estimated using the leaf-$\delta^{13}C_{OM}$ of maize plants grown in the same room together with spinach plants, and assuming a photosynthetic discrimination by maize leaves of 4‰ against ^{13}C.

Similar to bean, the stable values of A_n and A_n/C_i observed across the N-type gradient in spinach are in agreement with biomass data. In Chapter 4, we discussed in detail the contrasting responses to N-type of different species under different culture conditions found in the literature. Our results of A_n and g_s in spinach are consistent with those in wheat (Cramer and Lewis, 1993b;

Lopes and Araus, 2006), strawberry and raspberry (Claussen and Lenz, 1999), and spinach (Xing *et al.*, 2015), but different from those in blueberry (Claussen and Lenz, 1999), bean (Guo *et al.*, 2002) and even from those of bean in our previous experiment (Chapter 4). Different from bean, A_n was more stable in spinach, while g_s decreased at higher NH_4^+ nutrition and under both PPFD levels (in 100% NH_4^+ at PPFD=200, and in 100% and 90% NH_4^+ at PPFD=400). In spinach, the negative impacts of NH_4^+ on photosynthesis were low at low PPFD compared with high PPFD. These results support our conclusion that low light can alleviate NH_4^+ toxicity, and also corroborate our hypothesis that a small amount of NO_3^- could be enough to maintain the phosphate balance for photosynthetic activity.

As for bean, only slight changes in gas exchange and fluorescence parameters in response to varying NH_4^+ to NO_3^- ratios were observed (see Appendix 3 and 4 for fluorescence and Dualex data of both species). C_i/C_a decreased under both PPFD levels, exhibiting more sensitive response to NH_4^+ in spinach (Fig. 5.5C, F) than in bean, in agreement with the results of Lopes and Araus (2006) and Cramer and Lewis (1993b) in wheat. By using C_i/C_a values in Farquhar's simple model, we estimated the $\delta^{13}C$ values of photoassimilates which mainly affected by photosynthetic fractionation. The $\delta^{13}C$ value of the air CO_2 in spinach culture room was estimated using the leaf-$\delta^{13}C_{OM}$ of maize plants grown in the same culture room together with spinach and assuming a photosynthetic discrimination of 4‰ against ^{13}C for maize leaves (see Fig. 5.7). Whatever the PPFD level used for gas exchange measurements, and similar to bean, the estimated $\delta^{13}C$ values of photosynthetic products were higher compared to those measured on individual sugars and even compared with $\delta^{13}C_{WSOM}$, except for sucrose at lower NH_4^+ conditions. Only if a lower discrimination value for maize leaves is assumed (about 2‰, rather than 4‰) that the estimated $\delta^{13}C$ values of photosynthetic products will match the measured values on sugars, mainly at low PPFD (not shown). In bean, all sugars were more ^{13}C depleted than the estimated values even with assuming a lower photosynthetic discrimination for maize leaves (see Fig. S9 in Chapter 4).

5.3.3 Effect of N-type supply on C-isotope composition of OM, WSOM and respired CO_2

Similar to bean, leaf-$\delta^{13}C_R$ was ^{13}C enriched compared to root-$\delta^{13}C_R$, and negatively correlated with NH_4^+% in supplied N in spinach plants (Fig. 5.8C). In leaves, $\delta^{13}C_R$ became more and more ^{13}C depleted with increasing NH_4^+% in nutrient solution, from –23.2‰ at 0% NH_4^+ to –27.7‰ at 100% NH_4^+ (3‰ ^{13}C depleted compared with bean, because of the more ^{13}C depleted air CO_2 in

spinach culture room compared with bean culture room). The results verified our initial hypothesis once again, namely that a higher amount of more ^{13}C enriched carbon pools are introduced *via* anaplerotic pathway during NO_3^- assimilation in leaves of NO_3^--fed compared to NH_4^+-fed spinach plants and then used as respiratory substrates. Root-$\delta^{13}C_R$ showed the same pattern as in bean, remaining unchanged between –28 and –30‰ (1-2‰ more depleted than in bean roots) along the N-type gradient (Fig. 5.8C).

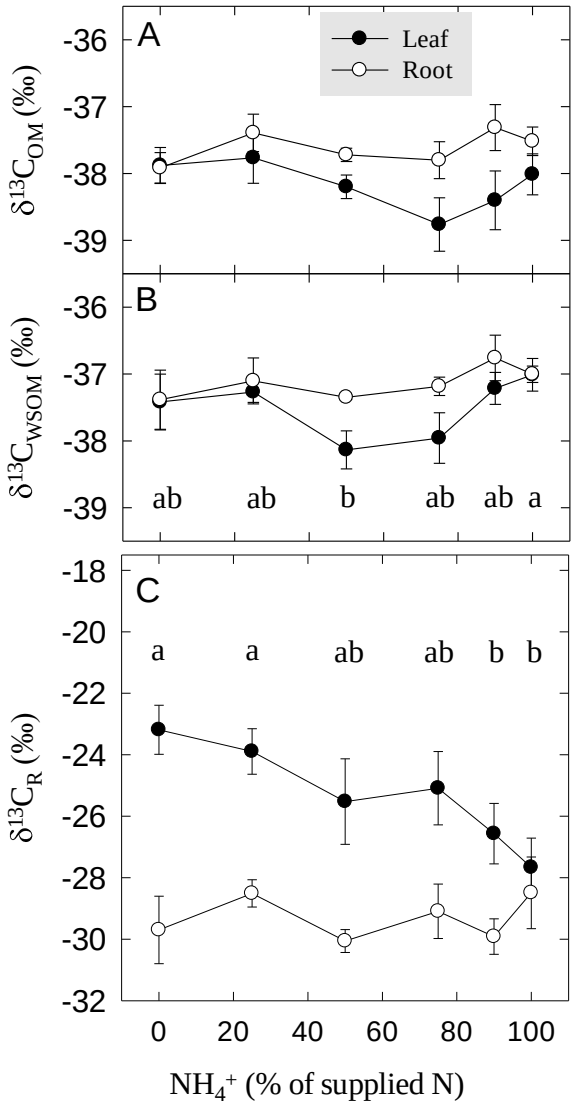

Figure 5.8 $\delta^{13}C$ of organic matter ($\delta^{13}C_{OM}$; **A**), water soluble fraction ($\delta^{13}C_{WSOM}$; **B**), and respired CO_2 ($\delta^{13}C_R$; **C**) of leaves (black symbols) and roots (white symbols) of spinach plants grown with nutrient solutions containing different % of NH_4^+ and NO_3^- as N source. On the X-axis, 0 and 100 correspond to 0% NH_4^+ (i.e. 100% NO_3^-) and 100% NH_4^+ (i.e. 0% NO_3^-) as % of total N in the nutrient solutions, respectively. Values are means ± SE (n=5 for respired CO_2 and n=3 for OM and WSOM). Only significant differences ($p < 0.05$) for leaves are shown by different lowercase letters (there is no significant difference for root data). Note that the respired CO_2 being ^{13}C enriched compared to both OM and WSOM, the scale used for respired CO_2 is different from that for WSOM and OM.

Again, as in bean, root-respired CO_2 was ^{13}C enriched compared with root OM (by about 7‰), WOSM and all potential respiratory substrats analysed in spianch. As we discussed in Chapter 4, although some similar results have been reported in wheat (Aranjuelo *et al.*, 2009;

Aranjuelo *et al.*, 2013), for the moment, the mechanisms responsible for this ^{13}C enrichment in root-respired CO_2 are not elucidated yet.

Similar to bean, OM of spinach was ^{13}C depleted in leaves compared to roots (by about 0.5 to 1‰) in most of the N-type nutrition except in 0% NH_4^+, where similar values were observed in leaves and roots (Fig. 5.8A). $\delta^{13}C_{WSOM}$ exhibited similar trend as $\delta^{13}C_{OM}$; WSOM being ^{13}C depleted in leaves compared with roots, while at 0% NH_4^+ and 100% NH_4^+, $\delta^{13}C$ values of leaves and roots were similar (Fig. 5.8B). Furthermore, there was no significant differences in $^{13}C_{OM}$ of leaves or roots along N-type gradient, but $\delta^{13}C_{WSOM}$ of leaves at 100% NH_4^+ was significantly more ^{13}C enriched compared to 50% NH_4^+ treatment (Fig. 5.8B). Neither $\delta^{13}C_{OM}$ nor $^{13}C_{WSOM}$ showed significant changes along N-type gradient in roots (Fig. 5.8A).

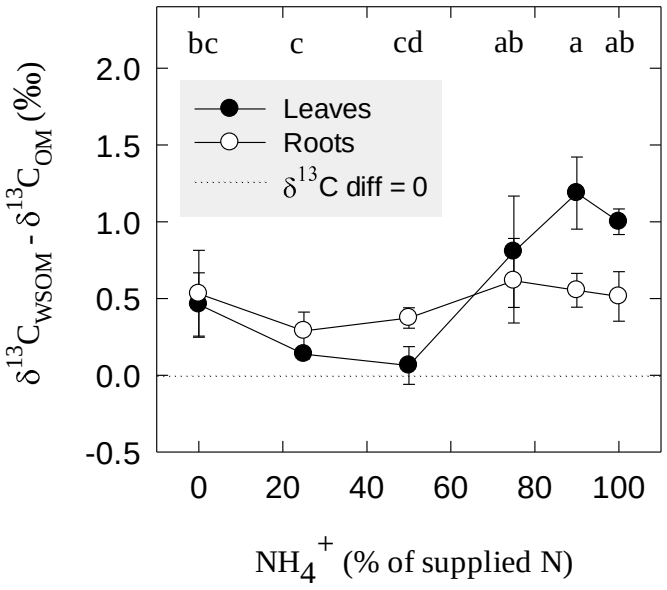

Figure 5.9 Variation in $\delta^{13}C$ difference between WSOM and OM ($\delta^{13}C_{WSOM-OM}$) in leaves (black circles) and roots (white circles) of spinach plants cultured under different % of NH_4^+ and NO_3^- as N source in nutrient solution used for watering the pots. On the X-axis, 0 and 100 correspond to 0% NH_4^+ (i.e. 100% NO_3^-) and 100% NH_4^+ (i.e. 0% NO_3^-) in nutrient solution, respectively. Each data point corresponds to means ± SE (n=3). The dotted line corresponds to ($\delta^{13}C_{WSOM}$ = $\delta^{13}C_{OM}$). Only significant differences ($p < 0.05$) for leaves are shown by different lowercase letters (no significant difference for root data).

The relatively negative $\delta^{13}C$ values of OM, WSOM and respired CO_2 are presumably a result of growth in a ^{13}C depleted CO_2 environment (–12.33‰, calculated based on leaf-$\delta^{13}C_{OM}$ of maize plants grown together with spinach). However, the $\delta^{13}C$ of source CO_2 was the same for all plants grown with different N sources, so the discussion can still be carried out to determine the effect of N-type gradient on C-isotope composition of OM, WSOM, respired CO_2 and putative substracts which will be discussed below.

As discussed in Chapter 4, differences in $\delta^{13}C$ values of OM under NH_4^+ or NO_3^- nutrition were generally observed (Yin and Raven, 1998; Guo *et al.*, 2002; Lasa *et al.*, 2002b; Lopes and

Araus, 2006), and stomatal conductance, C_i/C_a, ontogeny, and genetic materials were considered to determine the temporal value of $\delta^{13}C_{OM}$ in plants.

In roots, the isotopic differences between OM and WSOM ($\delta^{13}C_{(WSOM-OM)}$) were stable across all N-treatments as in bean, but the values were above zero in spinach (between 0.3‰ and 0.6‰, Fig. 5.9) while they were around zero in bean. For leaves, the trend in spinach was quite different from that in bean, with changes in opposite direction compared with bean. Contrary to bean, the $\delta^{13}C_{(WSOM-OM)}$ values revealed 2 groups in spianch leaves (Fig. 5.9): at lower NH_4^+ supply (≤ 50% NH_4^+), $\delta^{13}C_{(WSOM-OM)}$ values were lower than in roots, but at higher NH_4^+ supply (> 50% NH_4^+), they were higher. The highest isotopic differences were observed at 90% $NH4^+$ and 100% NH_4^+ treatments (up to 1.2‰ and 1.0‰, respectively) and significantly ($p < 0.05$) higher than at 25% and 50% NH_4^+ treatments. Therefore, contrarily to bean leaves for which a strong significant relationship was found between $\delta^{13}C_R$ and $\delta^{13}C_{(WSOM-OM)}$ (Fig. 3, Chapter 4), suggesting the use of mixed substrates for respiration, no such a relationship was observed in spinach leaves. In spinach roots, both $\delta^{13}C_R$ and $\delta^{13}C_{(WSOM-OM)}$ remained unchanged across N-type gradient.

5.3.4 Effect of N-type supply on PEPc activities

Leaf tissues had much higher PEPc activity compared with roots (more than 4 times), but no significant changes along NH_4^+ gradient were observed in none of the organs (Fig. 5.10). PEPc activity was only slightly (1.02- and 1.58-fold) higher in NO_3^--fed plants compared to plants fed with 100% NH_4^+, in leaves and in roots, respectively, but this was not significant.

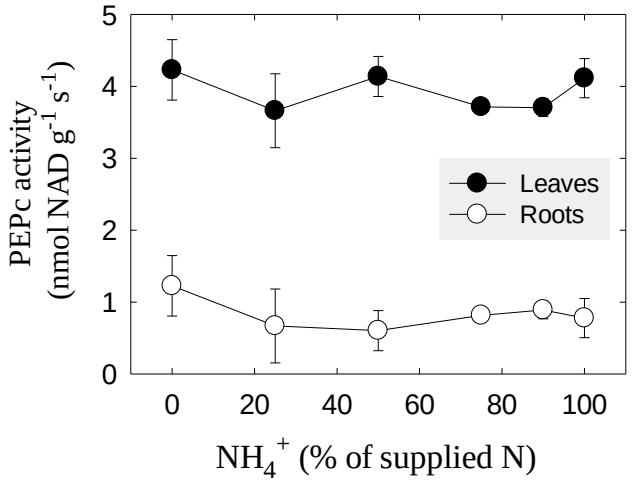

Figure 5.10 Changes PEPc activity in leaf (black symbols) and root (white symbols) of spinach plants cultured under different % of NH_4^+ and NO_3^- as N source in nutrient solution used for watering the pots. On the X-axis, 0 and 100 correspond to 0% NH_4^+ (i.e. 100% NO_3^-) and 100% NH_4^+ (i.e. 0% NO_3^-) as % of total N in the nutrient solutions, respectively. Values are shown as means ± SE (n=3).

It has been found that PEPc activity can be induced by NH_4^+ in both leaves and roots (Lepiniec *et al.*, 2003). Since the shoot is considered to be more sensitive to ammonium than the root, spinach, which is highly sensitive to ammonium nutrition, assimilates NH_4^+ preferentially in the shoots (Lasa *et al.*, 2002b), so that the large differences of PEPc activities between leaves and roots were observed. Our data are in agreement with the previous studies on ammonium sensitive species, such as spinach (Lasa *et al.*, 2002b) and wheat (Arnozis *et al.*, 1988). Lasa *et al.* (2002b) even observed a higher PEPc activity in spinach leaves grown under NH_4^+ compared with those grown under NO_3^- nutrition.

However, the responses of PEPc activity along NH_4^+ gradient in both organs were not as expected by our initial hypothesis, especially in roots. In fact, Lasa *et al.* (2002b) found 10-fold higher PK (pyruvate kinase) activity in spinach roots under NH_4^+ nutrition compared to legumes, and they believed that the carbon skeletons required for ammonium assimilation in spinach was mainly provided *via* PK instead of PEPc in roots. But their hypothesis is controversial, because the pyruvate produced *via* PK can sustainably feed the TCA only if TCA is functioning in the closed mode, without extraction of substrates as 2-oxoglutarate.

In summary, a larger decrease in C_i/C_a and a higher PEPc activity observed in leaves under high NH_4^+ nutrition indicated more NH_4^+ sensitivity of spinach compared to bean. PEPc activity was stimulated by ammonium in both leaves and roots in spinach, and their stable values can explain the stable $\delta^{13}C$ values of OM and WSOM in both organs. But unfortunately, it could not be responsible for the observed shift of $\delta^{13}C_R$ along NH_4^+ gradient in leaves. The possible reason maybe that PK plays a major role for providing carbon skeletons to TCA *via* pyruvate instead of PEPc, thus the ^{13}C enrichment driven by PEPc in spinach roots could not be observed.

5.3.5 Effect of N-type supply on soluble sugar contents and $\delta^{13}C$

The amounts of glucose, fructose and total sugars were higher in roots than in leaves (Fig. 5.11F-H), as was the case in bean. Sucrose was not detected in spinach roots. In addition, under 75% NH_4^+ treatment, fructose content was significantly ($p < 0.05$) higher than under 25% NH_4^+, but no significant change was observed in none of the organs (Fig. 5.11E-H).

In their review, Britto and Kronzucker (2002) showed that sugar and starch contents of plants generally decrease in NH_4^+ compared with NO_3^- nutrition condition. However, Xu *et al.* (1994) observed the accumulation of starch, fructose and glucose, but no change in sucrose content of

soybean leaves supplied with nitrate compared to those fed with ammonium. They concluded that these changes were mainly caused by the decrease in net photosynthesis rate (per leaf area) by inhibition of Rubisco activity under NO_3^- nutrition. In spinach, our results were closer to what we observed in bean (see Chapter 4), but the increased amounts of sugars under NH_4^+ nutrition were not significant in spinach. As the samples for sugar extraction were collected after measurements of dark respiration, we hypothesize that a too low sucrose content in roots (below detection limit) can be the result of depletion of the sucrose which had been stored during photosynthesis, while the starch-degraded sucrose has not reached the roots yet.

Glucose and fructose were more ^{13}C enriched in roots compared to leaves (by about 1.4‰ and 1.8‰, respectively) (Fig. 5.11A-C). The isotopic difference in $\delta^{13}C_{Suc}$ values between organs was low (Fig. 5.11D). In leaves, sucrose was more ^{13}C enriched than glucose and fructose, as it was the case in bean. Sucrose and total sugars were more ^{13}C enriched at lower NH_4^+ supply, and at 25% NH_4^+ they were significantly ($p < 0.05$) ^{13}C enriched compared with 75% NH_4^+ treatment. While the $\delta^{13}C$ values of glucose and fructose were stable, as in bean. In roots, similar to bean, the $\delta^{13}C$ values of glucose, fructose and total sugars showed no significant differences across N-treatments (Fig. 5.11A-D), but the between-organ isotopic differences for total sugars in spinach were very small. Howerver, highly ^{13}C depleted values of glucose in bean were not observed in spinach.

These results confirmed our hypotheses postulated in Chapter 4, that after 30 min in the dark, the leaf sucrose putatively started to be a mix of both day-time storage and that exported from starch degradation, especially at lower NH_4^+ supply (0%, 25% and 50% NH_4^+), which exhibited more ^{13}C enriched values. Glucose and fructose may still mainly reflect day-time photosynthetic storage in the vacuole.

5.3.6 Effect of N-type supply on organic acid contents and $\delta^{13}C$

The organic acids, malate and citrate, were ^{13}C enriched in leaves compared to roots (Fig. 5.11I, J), $\delta^{13}C_{Mal}$ being 2 to 5‰ higher than $\delta^{13}C_{Cit}$. In leaves, the most ^{13}C enriched values (but not significantly) of both malate and citrate were observed at 75% NH_4^+ treatment (–28.36‰ and –33.19‰, respectively). In roots, citrate showed signifcant ^{13}C enrichment at 90% NH_4^+ compared to the low NH_4^+ supply (0%, 25%, 50% and 75%).

In leaves, the malate content was much lower (varying between ca. 0.4 and 3 mg g DW^{-1}) compared with citrate (varying between ca. 2 and 15 mg g DW^{-1}) and about 10-fold lower compared with malate in bean leaves (Fig. 5.11K, L). Citrate content was also lower in spinach than in bean (about 2-fold lower). Contrarily to bean, malate content did not change with N-type gradient in none of the organs in spinach, but citrate content decreased across the N-type gradient and the lowest values were observed at 75% NH_4^+ in both organs (significantly ($p < 0.05$) in leaves, but not significantly in roots), and increased again at higher NH_4^+ (Fig. 5.11K, L). In bean both malate and citrate contents were very high at NO_3^- and decreased progressively and significantly with increasing NH_4^+ (Fig. 4 in Chapter 4).

As discussed in Chapter 4, organic acids play a variety of physiological roles in plants, including their role as respiratory substrates, provision of carbon skeletons for ammonium ion assimilation and a role in the maintenance of charge balance. Malate and citrate were considered to be more ^{13}C enriched compared with soluble sugars (especially in leaves), because they are mainly derived from anaplerotic pathway *via* PEPc for providing carbon skeleton for biosynthesis (e.g. for N assimilation in this case). In spinach, large isotopic difference between malate and soluble sugars (5.5 to 10.3‰) in leaves should mainly be due to a high PEPc activity (Fig. 5.9). Although the PEPc activity in spinach roots was lower than in leaves, the isotopic difference between malate and soluble sugars (ca. 2.5‰) was higher in spinach than in bean roots (ca. 1‰). Citrate was less enriched than malate, but followed the same trend. These verify again the correlation between PEPc activity and $\delta^{13}C_{Mal}$ and $\delta^{13}C_{Cit}$, however, not consistent with its correlation with malate and citrate accumulation.

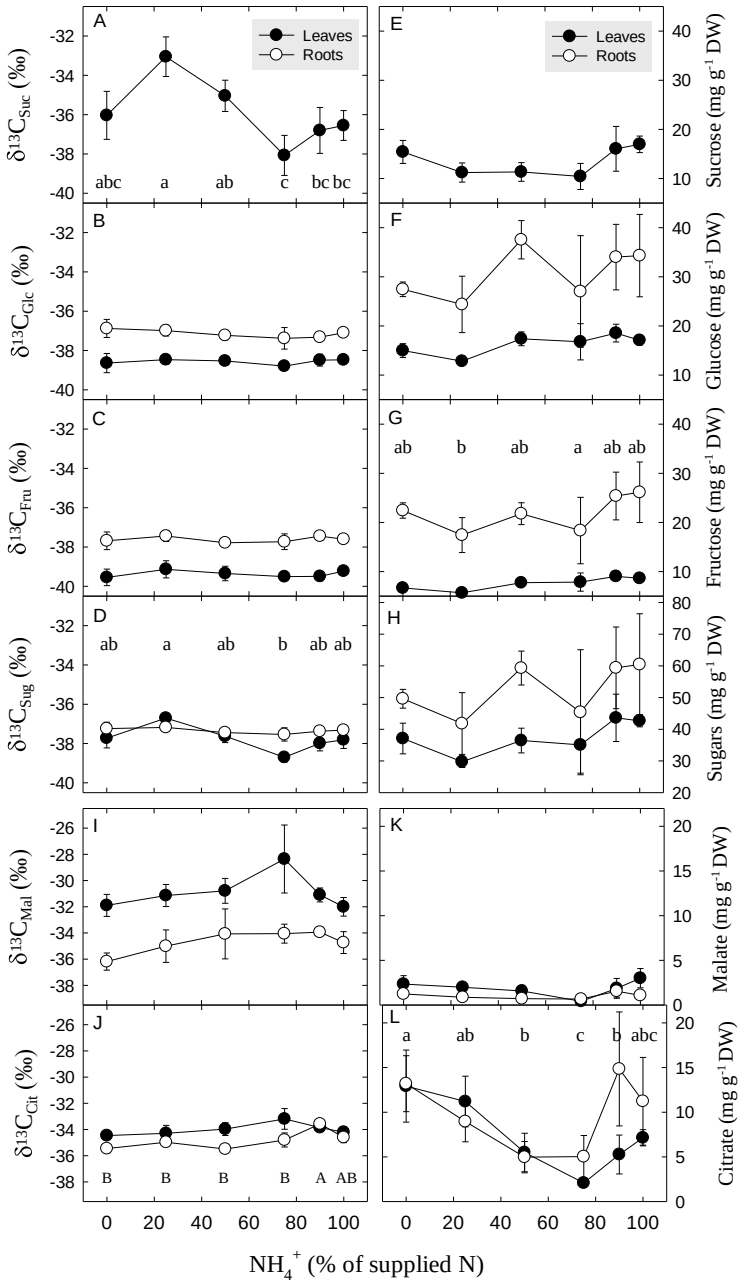

Figure 5.11 $\delta^{13}C$ of sucrose ($\delta^{13}C_{Suc}$; **A**), glucose ($\delta^{13}C_{Glc}$; **B**), fructose ($\delta^{13}C_{Fru}$; **C**), soluble sugars, i.e. sucrose, glucose and fructose ($\delta^{13}C_{Sug}$; **D**), malic acid ($\delta^{13}C_{Mal}$; **I**), citric acid ($\delta^{13}C_{Cit}$; **J**), and their amounts (**E, F, G, H, K, L**), in leaves (black symbols) and roots (white symbols) of spinach plants grown with nutrient solutions containing different % of NH_4^+ and NO_3^- as N source. On the X-axis, 0 and 100 correspond to 0% NH_4^+ (i.e. 100% NO_3^-) and 100% NH_4^+ (i.e. 0% NO_3^-) as % of total N in the nutrient solutions, respectively. Values are shown as means ± SE (n=3). Significant differences ($p < 0.05$) are shown by different letters (lowercase letters for leaves, uppercase letters for roots). Note that the scale for total sugar content is different. In roots, the sucrose amount was too low to be detected.

Malate concentration was quite low in both leaves and roots of spinach plants across N-type gradient (Fig. 5.11K). Generally, organic acids accumulate in cells of many plant species under nitrate nutrition for counterbalancing excess inorganic cations, and organic acid content is positively correlated with excess NO_3^- supply (see reviews by Gerendás *et al.*, 1997; Britto and Kronzucker, 2002; Bittsanszky *et al.*, 2015 and Esteban *et al.*, 2016), which is different from our results. However, we have measured only malate and citrate contents and not all the organic acids. It is known that, spinach accumulates large amount of oxalate in plant tissues (Chang and Beevers, 1968; Elia *et al.*, 1998; Kumar *et al.*, 2019), and the accumulation of oxalate with higher NO_3^- supply were observed in both field and hydroponic culture in laboratory experiments (Elia *et al.*, 1998; Liu *et al.*, 2015), oxalate increasing with higher NO_3^- supply. During our analysis of organic acids, very high signals of oxalate were also observed. However, since its concentration was too high (beyond the detection limit of our analysis standards), which seriously affected the calculation of concentrations and isotope values for other organic acids, we had to skip the peak of oxalate during measurements thus no data concerning oxalate can be shown here. Therefore, we hypothesize that ultra-high content of oxalate had fulfilled the function of ion counterbalance in response to NO_3^- addition in nutrient solution, thus malate and citrate contents were lower than in bean (consistent with data shown by Lasa *et al.* (2002a).

Furthermore, malate is considered to be the main contributor to the highly ^{13}C enriched respired CO_2 under light-enhanced dark-respiration (LEDR), but its contribution to dark respired-CO_2 is still largely unclear. By using multiple linear regression analysis, Lehmann *et al.* (2015) found that $\delta^{13}C_R$ values changed with $\delta^{13}C$ values of malate and concluded that malate was the main respiratory substrate which played a key role in determining $\delta^{13}C_R$ of darkened leaves in potato plants. However, it is not in line with our present results. According to the discussion in Chapter 4, TCA functions in different modes in illuminated leaves (Tcherkez *et al.*, 2009; Sweetlove *et al.*, 2010; Tcherkez *et al.*, 2012; Abadie *et al.*, 2017). This plasticity of TCA gives various possibilities to changes in the $\delta^{13}C$ values of stored organic acids involved in TCA cycle, which are supposed to be substrates for dark respiration. Hanning and Heldt (1993) analysed the products of malate oxidation under steady-state photosynthesis in illuminated spinach leaves, and concluded that the mitochondrial oxidation of malate produced mainly citrate, which was used for nitrogen assimilation *via* GS/GOGAT. In the present work, spinach roots performed similar trend as bean roots: no isotopic-gap was observed between malate and citrate, but in spinach leaves,

different to bean, malate was more ^{13}C enriched than citrate (by about 3‰). That is, in spinach, leaves exhibited larger ^{13}C fractionation between malate and citrate than roots (Fig. 5.12). Fractionation in leaves was positive (between +2.2‰ and +4.8‰), while for roots, the $\delta^{13}C$ difference was low and close to zero (between –0.7‰ and +1.4‰). These results were in agreement with those of Hanning and Heldt (1993). Malate (4-carbon molecule), especially the C-4 originating from OAA *via* PEPc, was converted mainly to citrate (6-carbon molecule). Therefore, $\delta^{13}C_{Cit}$ followed the same trend as $\delta^{13}C_{Mal}$ along the N-type gradient, accompanied with a reasonable and stable isotopic gap between the two organic acids. Furthermore, in recent studies, it was found that fumarate can be accumulated throught malate (Arias *et al.*, 2013), so very low content of malate may also be due to fueling fumarate pool as well (not measured in the present work).

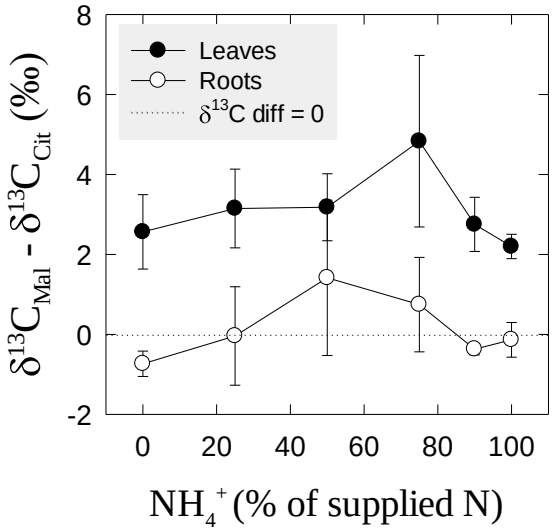

Figure 5.12 ^{13}C-difference between malate ($\delta^{13}C_{Mal}$) and citrate ($\delta^{13}C_{Cit}$) in leaves (black symbols) and roots (white symbols) of spinach plants grown with nutrient solutions containing different % of NH_4^+ and NO_3^- as N source. On the X-axis, 0 and 100 correspond to 0% NH_4^+ (i.e. 100% NO_3^-) and 100% NH_4^+ (i.e. 0% NO_3^-) as % of total N in the nutrient solutions, respectively. Values are shown as means ± SE (n=3).

Additionally, although OAA (precursor for malate) is also considered to be one of the presursors for oxalate, no further related studies were published on this pathway in spinach since the early findings of Chang and Beevers (1968). For the moment, most scientists believe that glyoxylate/glycolate and L-ascorbic acid are the main precursors for oxalate synthesis (Kumar *et al.*, 2019). Hence, we infered that the low content of malate was not caused by the consumption of OAA due to large amounts oxalate synthesis.

5.3.7 Changes in $\delta^{13}C$ of respired CO_2 with changes in $\delta^{13}C$ of respiratory substrates across N-type gradient

The C-isotope differences between individual compounds and bulk OM (as apparent ^{13}C fractionation in metabolites), as well as between respired CO_2 and bulk OM (as apparent respiratory fractionation) along the N-type gradient are compiled in Fig. 5.13 for leaves and roots. Both leaf- and root-respired CO_2 were ^{13}C enriched compared to OM, WSOM and all individual metabolites in corresponding organs. For most of the metabolites this enrichment was much higher in leaves than in roots, but the isotopic differences between respired CO_2 and malate were very close in leaves and roots. In leaves (Fig. 5.13A), glucose and fructose were ^{13}C depleted compared to OM, but sucrose, WSOM and organic acids (malate and citrate) were ^{13}C enriched compared to leaf bulk OM. In roots (Fig. 5.13B), except fructose, all the other metabolites (and WSOM) were ^{13}C enriched compared to root bulk OM (or were very close to OM).

Sucrose was the most ^{13}C enriched sugar in leaves, the mean values of ^{13}C difference between sucrose and leaf OM ranged between +0.7‰ and +4.7‰. Fructose was the most ^{13}C depleted compound analysed, with more negative values in leaves compared to roots, with the ^{13}C difference ranging between –0.75‰ and –1.67‰ in leaves, and between –0.13‰ and +0.32‰ in roots along N-type gradient. The ^{13}C differences between organic acids and bulk OM were always highly positive in both leaves and roots along the N-type gradient.

Similar to bean, no correlation was found between the $\delta^{13}C$ values of respired CO_2 and those of any individual compound analysed in none of the organs (data not shown). The R^2 values were ≤ 0.07, so even smaller than in bean. As listed in Chapter 4, our results are in contrast with those reported by Lehmann et al. (2015) and Ghiasi et al. (unpublished) who observed that malate was the main contributor for determining $\delta^{13}C$ of respired CO_2 in their experiments. In addition**,** The R^2 values between leaf-$\delta^{13}C_R$ and C_i/C_a were near zero (0.07 and 0.06 for PPFD=200 or 400, respectively).

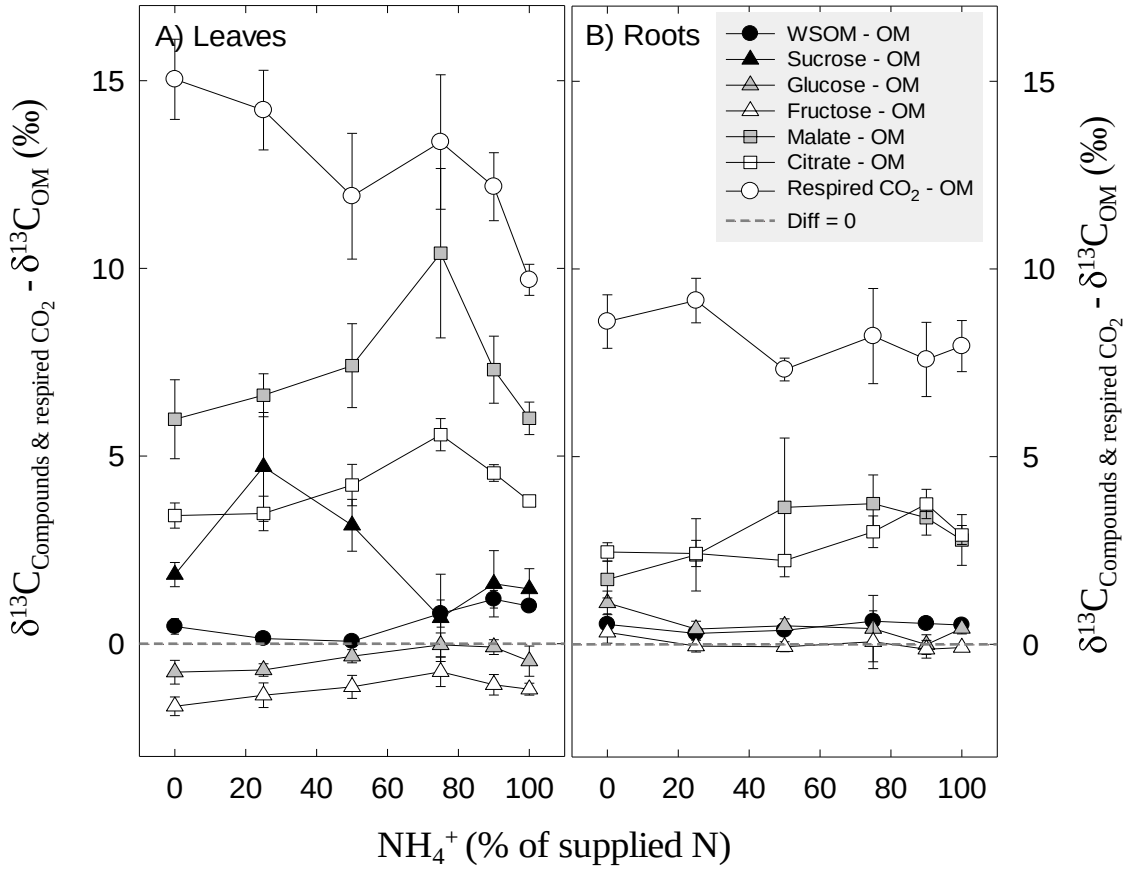

Figure 5.13 Changes in $\delta^{13}C$ of respired CO_2 (white circles), water soluble organic matter (WSOM, black circles), sucrose (black triangles), glucose (grey triangles), fructose (white triangles), malic acid (grey squares) and citric acid (white squares), in leaves (**A**) and roots (**B**) relative to the $\delta^{13}C$ of respective organs (i.e. $\delta^{13}C$ of metabolites – $\delta^{13}C$ of OM) of spinach plants grown with nutrient solutions containing different % of NH_4^+ and NO_3^- as N source. The grey dashed lines correspond to the reference value (i.e. isotopic difference with OM = 0) On the X-axis, 0 and 100 correspond to 0% NH_4^+ (i.e. 100% NO_3^-) and 100% NH_4^+ (i.e. 0% NO_3^-) as % of total N in the nutrient solutions, respectively. Values are means ± SE (n=5 for respired CO_2 and n=3 for metabolites).

Similar to bean, **t**he best correlation was found between changes in leaf-$\delta^{13}C_R$ and in leaf-$\delta^{13}C_{(WSOM-OM)}$ across N-type gradient, but the R^2 value was very low ($R^2 = 0.13$). No correlation was observed between changes in leaf-$\delta^{13}C_R$ and in concentration of organic acids, even less so in carbohydrates. These results did not confirm the hypothesis we postulated in Chapter 4, that the changes in $\delta^{13}C$ of leaf-respired CO_2 across N-type gradient was caused by the changes in the mix of substrates used for respiration. This is probably due to the lack of data for all relevant metabolites, as the lack of correlation with single metabolite $\delta^{13}C$ values also in this case points to a change in the substrate mixture use as cause of the change in $\delta^{13}C$ of respired CO_2.

5.3.8 Changes in $\delta^{13}C$ of respired CO_2 with changes in $\delta^{13}C$ of respiratory substrates across N-type gradient

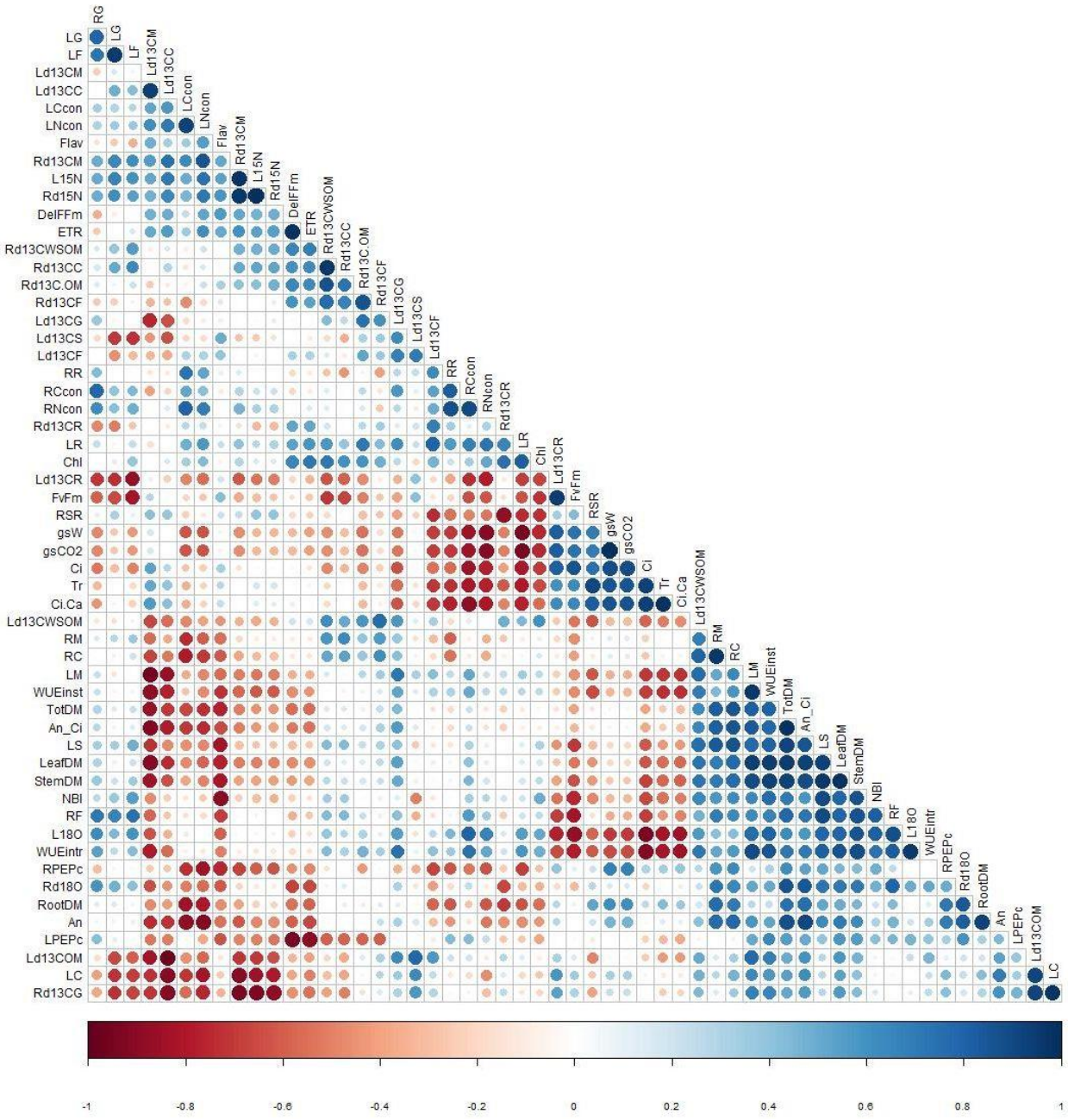

Figure 5.14 Matrix of between-trait correlation coefficients. In general correlations with |r| > 0.8 are significant, i.e. the ones represented by dark coloured big circles. The matrix was ordered with hierarchical clustering.

PCA axis 1 and 2 explained 35.37 and 28.78 of the variation in the full set of measured traits. PCA1 separated treatments with 100% NH_4^+, 90% NH_4^+ and 0% NH_4^+ from the remaining treatments. PCA2 separated treatments with NH_4^+ <= 50% from those with NH_4^+ > 50%. Table S5.1 for every trait reports the PCA axis on which it loaded most. $\delta^{13}C$ of leaf respired CO_2 loaded strongly on PCA2 was significantly negatively correlated with the N-type nutrition gradient (see Table S5.1). In addition, $\delta^{13}C$ of leaf respired CO_2 had negative correlation with leaf fructose content, and positive correlation with the maximum PSII efficiency (Fig. 5.14). No other traits were significantly correlated with N-type gradient.

5.4 Conclusions

C-isotope composition of plant metabolites is a result of a combination of photosynthetic and post-photosynthetic fractionations, and the C-isotope composition of respiratory CO_2 results from the relative contribution of the substrates originating from these pathways. Different N source types (i.e. NO_3^- *versus* NH_4^+) impact both photosynthesis and respiratory processes during their uptake, assimilation and accumulation in plant tissues. In the present work, we examined the effect of N-type gradient on isotopic signature of putative respiratory substrates and that of respired CO_2 in roots *versus* leaves of spinach.

We observed the same results as for bean, with no major changes in gas exchange parameters. Similarly to bean, leaf-respired CO_2 was ^{13}C enriched in spinach under NO_3^- nutrition and became progressively ^{13}C depleted with increasing amount of NH_4^+ in supplied N, while C-isotope composition of glucose, fructose and organic acids (malate and citrate) in both leaves and root, and root-respired CO_2 remained unchanged across N-type gradient. However, the changes in PEPc activity and C-isotope composition of sucrose were very different compared with those found in bean.

PEPc activity in spinach was unexpectedly stable along N-type gradient in both leaves and roots. In roots, the impact of PEPc activity on root-$\delta^{13}C_R$ could be masked by the refixation of more ^{13}C depleted carbon, i.e. root respired CO_2. However, leaf-respired CO_2 was more and more ^{13}C depleted with increasing amount of NH_4^+, suggesting that PEPc activity was probably not the most important factor for determining final $\delta^{13}C_R$ in leaves. Raven and Farquhar (1990) estimated a $\delta^{13}C$ change of only 0.11‰ in OM due to anaplerotic input in plants grown under NO_3^- or NH_4^+ as sole

N sources. They suggested that the isotopic differences in plant organic matter between NO_3^- and NH_4^+ nutrition were mostly affected by the factors impacting organic acid synthesis. Moreover, organic acids are considered as important respiratory substrates, which can strongly affect ^{13}C values of respired CO_2.

However, we have not observed significant isotopic changes in organic acids along N-type gradient in none of the organs. In addition, due to the plasticity of TCA across species, we observed a completely different pattern of ^{13}C-isotopic gap of the malate/citrate and their contents between spinach and bean, suggesting that anaplerotically fixed carbon fluxes through malate- and citrate-valves varied depending on the species. But, those differeces did not affect the trend of leaf-$\delta^{13}C_R$ along N-type gradient.

In general, the ^{13}C enriched carbon fixed *via* PEPc is firstly incorparated into OAA then to malate in cytosol. Subsequently, the ^{13}C enriched malate will undergo one of three fates: it can be remained in the cytosol, transported to the vacuole then accumulated there, or transported to the mitochondria. Only the ^{13}C enriched malate transported to the mitochondria may have an effect on $\delta^{13}C_R$. Plants accumulate more organic ions under NO_3^-, enlarging consistently the pool sizes of malate and/or citrate in mitochondria under NO_3^- compared with NH_4^+ nutrition, leading to a higher ^{13}C enriched carbon flux to leaf-respired CO_2. Therefore, the C-isotope composition of organic acids and correspongding amounts in different cellular compartments need to be investigated.

In summary, cellular compartmental C-isotope composition of organic acids (particularly malate and citrate) may play a key role in determining $\delta^{13}C_R$ in spinach leaves along N-type gradient, but not PEPc activity. Additionally, C-isotope composition of root-respired CO_2 remained unchanged across N-type gradient, probably because PEPc effect on ^{13}C enrichment was blurred by ^{13}C depleted carbon source (root respired CO_2), as observed in bean.

Supplementary material for Chapter 5

Table S5.1 Results of regression of traits on the fraction of NH_4^+ in supplied nitrogen (% of supplied N). Regression type: if linearly correlated with NH_4^+ (% of supplied N), – for negatively and + for positively correlated, log for regression on log transformed NH_4^+ (% of supplied N), log inv for regression on log transformed NO_3^- (i.e. 100 – NH_4^+) % of supplied N. For regressions on abs (NH_4^+ (% of supplied N)-extremum) with extremum at 25 (50, 75) %, min 25 (50, 75) % for minimum and max 25 (50, 75) % for maximum.

Trait	Regression type	R^2	Significance	Loading most on PCA axis
$\delta^{13}C$ of leaf respiration	–	0.89	$p < 0.006$	PCA2
$\delta^{13}C$ of leaf OM	min 75%	0.72	$p < 0.034$	PCA3
$\delta^{13}C$ of leaf WSOM	min 50%	0.65	$p < 0.052$	PCA4
$\delta^{13}C$ of leaf citrate	max 75%	0.75	$p < 0.026$	PCA5
[leaf sucrose]	min 50%	0.66	$p < 0.050$	PCA1
[leaf glucose]	min 25%	0.64	$p < 0.057$	PCA3
[leaf fructose]	min 25%	0.86	$p < 0.008$	PCA3
[leaf citrate]	min 75%	0.95	$p < 0.001$	PCA3
[root citrate]	min 50%	0.655	$p < 0.052$	PCA4
$\delta^{18}O$ of leaf respiration	log inv	0.730	$p < 0.030$	PCA1
$\delta^{13}C$ of root malate	max 75%	0.869	$p < 0.007$	PCA2
	log	0.818	$p < 0.014$	
stomatal conductance	log inv	0.661	$p < 0.050$	PCA2
Ci	log inv	0.793	$p < 0.014$	PCA2
Chl	log inv	0.681	$p < 0.044$	PCA5
Flav	max 50%	0.655	$p < 0.051$	PCA5
NBI	min 50%	0.701	$p < 0.038$	PCA5
leaf N%	log	0.787	$p < 0.019$	PCA2
	max 75%	0.754	$p < 0.025$	
Fv/Fm	log inv	0.916	$p < 0.003$	PCA6
$\delta^{15}N$ of leaf OM	max 75%	0.750	$p < 0.026$	PCA5
	log	0.675	$p < 0.045$	
$\delta^{15}N$ of root OM	max 75%	0.680	$p < 0.044$	PCA5
	log	0.661	$p < 0.050$	
$\delta^{13}C$ of root glucose	min 75%	0.915	$p < 0.003$	PCA3

Not significantly correlated with NH_4^+ (% of supplied N): $\delta^{13}C$ of leaf citrate, Leaf respiration rate, leaf PEPc activity, leaf NR activity, $\delta^{13}C$ of leaf sucrose, $\delta^{13}C$ of leaf glucose, $\delta^{13}C$ of leaf fructose, $\delta^{13}C$ of leaf malate, [leaf malate], leaf C content, root respiration rate, root PEPc activity, root NR activity, $\delta^{13}C$ of root respiration, $\delta^{13}C$ of root OM, $\delta^{13}C$ of root WSOM, $\delta^{13}C$ of root sucrose, $\delta^{13}C$ of root fructose, $\delta^{13}C$ of root citrate, [root glucose], [root fructose], [root malate], $\delta^{18}O$ of root respiration, root C%, root N%, leaf dry mass, root dry mass, stem dry mass, total plant dry mass, root/shoot ratio, Net photosynthesis, photosynthetic NUE, leaf transpiration rate, stomatal conductance, C_i/C_a, WUE_{intr}, WUE_{inst}, Carboxylation efficiency, $\Delta F/Fm$, ETR.

CHAPTER 6 - General Discussion, Conclusions and Perspectives

6.1 General discussion and conclusions

Carbon isotopic fractionations associated with plant respiration have received increasing attention because of their possible influences on efforts to elucidate factors associated with ecosystem carbon balances *via* carbon isotope analyses. Different N-source types (i.e. NO_3^- *versus* NH_4^+) impact both photosynthesis and respiratory processes, which are the most important key carbon isotope fractionation processes for determining the $\delta^{13}C$ of respiratory substrates, thus affecting the C-isotope composition of respiratory CO_2. However, there is a lack of knowledge how inorganic N nutrition type changes affect C and N metabolism interactions and alter respiratory carbon isotopic fractionations. In this thesis, we investigated the changes in the $\delta^{13}C$ of respired CO_2 and of the main metabolic putative pools involved in respiration in both leaves and roots of C_3 plants fed with various NH_4^+:NO_3^- ratios. The main objectives were to examine in which extent the isotopic signature of putative respiratory substrates and respired CO_2 is affected by NH_4^+:NO_3^- ratio gradient in C_3 plants, and in which extent the anaplerotic C-(re)fixation pathway (*via* PEPc) is affected by N-type gradient in roots *versus* leaves.

A preliminary experiment (Chapter 3) was designed on 9 plant species for selecting one NH_4^+-tolerant and one NH_4^+-sensitive. Based on our results on plant growth and carbon isotope composition of organic matter, as well as former studies reported in the literature, bean and spinach were finally selected for the subsequent in-depth research. However, in the experiments on bean and spinach in this thesis (Chapters 4 & 5, respectively), the plants did not show any visual symptoms of NH_4^+ toxicity or growth suppression, probably due to the low light intensity during culture period which alleviated toxic effect of NH_4^+.

We evaluated the effects of varying NH_4^+:NO_3^- ratios on photosynthetic fractionation by measuring the gas exchanges and estimating the $\delta^{13}C$ values of photosynthetic products by using C_i/C_a values in Farquhar's simple model. In both species, only slight changes in gas exchange and fluorescence parameters (see Appendix 3) in response to varying NH_4^+ to NO_3^- ratios were observed, except some decrease (but not always) at 100% NH_4^+. Accordingly, we did not observe any significant change in the estimated values of $\delta^{13}C$ in plant organic material across N-type gradient. Therefore, photosynthetic fractionation was little affected by N-type gradient in the present experiments. However, the estimated $\delta^{13}C$ values of photosynthetic products (from

Farquhar's model) were all higher (i.e. ^{13}C enriched) compared with measured $\delta^{13}C$ values of individual sugars and even those of WSOM in both species, indicating that other factors or processes had affected the $\delta^{13}C$ values. The estimated $\delta^{13}C$ values were rather close to the measured $\delta^{13}C$ values of organic acids in bean and even lower in spinach plants mainly at 75% NH_4^+.

Leaf net photosynthetic activity was lower only at 100% NH_4^+ in both species. In spinach, this was mainly due to a reduction in stomatal conductance, while in bean the assimilation capacity was reduced (conclusion based on measurements of A_n, g_s, C_i/C_a, and carboxylation efficiency). The mechanisms of sensitivity or tolerance to NH_4^+ thus probably vary between species. The respiration rate was much lower in spinach leaves as compared to the roots, but it was more or less equal in bean leaves and roots and did not significantly change across N-type gradient in none of the species (see Appendix 6 for comparison).

Our results highlighted the effect of N-type gradient on post-photosynthetic fractionation, mainly through the anaplerotic pathway, and confirmed our initial hypothesis for C_3 plants: leaf-respired CO_2 was ^{13}C enriched under NO_3^- nutrition and became progressively ^{13}C depleted with increasing amount of NH_4^+ in supplied N. However, the C-isotope composition of root-respired CO_2 remained unchanged across N-type gradient in both species, probably because of the difference in C-source for PEPc (i.e. ^{13}C enriched air CO_2 for leaves and ^{13}C depleted respired CO_2 for roots). Unexpectedly, depending on the species, C-isotope composition of individual metabolites and PEPc activity showed different behaviours in both organs. The PEPc activity was higher in spinach leaves as compared to the roots, but it was more or less equal in bean leaves and roots, demonstrating the different behaviour of N assimilation among species: spinach preferentially assimilates N in the shoots, however bean tends to assimilate it in both leaves and roots (see 5.4 for detailed discussion).

The $\delta^{13}C_R$ value is a comprehensive result of multiple metabolic pathways during post-photosynthetic processes, including glycolysis, PPP, TCA (both cyclic and non-cyclic modes) and anaplerotic pathway, etc. When varying NH_4^+:NO_3^- ratios were supplied in nutrient solutions to C_3 plants, it mainly affected the activity of anaplerotic pathway *via* PEPc activity during N uptake and assimilation. As underlined before (Chapter 5, section 5.4), the ^{13}C enriched carbon fixed via PEPc is firstly incorporated into OAA in the cytosol then to malate, which can be retained there or accumulated in the vacuole or transported to mitochondria, where it can be used in TCA pathway.

In the present work, the role of PEPc is beyond doubt. In leaves, PEPc incorporated more ^{13}C enriched carbon (because fixed C orininated from air CO_2 mainly) into organic acids, consequently raising the differences between $\delta^{13}C$ values of organic acids and sugars, but this was not the case in roots (because fixed C originated from root-respiration mainly) (see Appendix 7). In bean leaves, a higher PEPc activity was expected to explain more ^{13}C enriched leaf-respired CO_2 under NO_3^- nutrition. However, according to the similar changes observed in leaf-$\delta^{13}C_R$ across N-type gradient in both species but different changes in PEPc activity in spinach compared with bean, PEPc activity could not be the sole factor determining the leaf-$\delta^{13}C_R$.

The subsequent fate and allocation of the anaplerotically fixed ^{13}C enriched carbon in leaves is strongly regulated by the plasticity of TCA, which behaves differently among species. According to our results, the great plasticity of the TCA resulted in different C-isotopic gaps within the 2 species, not only between malate and citrate (representing anaplerotically-fixed C pools), but also between WSOM (respresenting mixed substrate for respiration) and bulk OM, and caused different organic acid pool sizes along the N-type gradient. To be more specific, in spinach, leaves exhibited larger isotopic gaps between malate and citrate than roots, while the isotopic gaps were similar between organs in bean. The citrate and mainly malate amount was lower in spinach as compared to bean, and the changes in citrate amount was also different. The synthesis, storage and use of these organic acids and the TCA functioning mode were thus different between the 2 species and organs. The difference between $\delta^{13}C_{WSOM}$ and $\delta^{13}C_{OM}$ in spinach roots was in the range between 0.3‰ and 0.6‰, while it was close to zero in bean roots. The isotopic difference between WSOM and bulk OM was high in bean leaves under pure NO_3^- nutrition and decreased progressively with increasing NH_4^+, while it changed in opposite direction in spinach (see Appendix 8). The bean results showed that it was the change in the concentrations of organic acids and sugars that related to $\delta^{13}C$ of WSOM, not changes in $\delta^{13}C$ of the single substrates. In spinach the substrate concentrations did not markedly change. In addition the concentrations of citrate and mainly malate were low and there are indications that another organic acid (i.e. oxalate) was present in high concentration. As we do not know the fluxes it is not possible to conclude about the substrate used for respiration in spinach. More cautiously it can be stated only that $\delta^{13}C$ of WSOM was correlated with $\delta^{13}C$ of respiration in bean but not so in spinach.

In fact, the ^{13}C differences between cell compartments have to be taken into consideration. If only the ^{13}C enriched malate originated from anaplerotic pathway is transported to the

mitochondria, it can directly affect $\delta^{13}C_R$. We suggested that NO_3^- assimilation in leaves may lead to increased pool sizes and more ^{13}C enriched values of mitochondrial malate and/or citrate, which were the most reasonable possibility to explain more ^{13}C enriched leaf-respired CO_2 under NO_3^- compared with NH_4^+ nutrition. However, samplings at different times during the diurnal cycle are required to capture storage and changes in the pool sizes.

Taken all together, N-type gradient made little effect on photosynthetic fractionation. For post-photosynthetic fractionation, the anaplerotic pathway and the non-cyclic TCA function together could have determined the leaf-$\delta^{13}C_R$ values along N-type gradient. We suggested that changes in the mitochondrial malate and/or citrate pool sizes and their C-isotope composition under different N source types (i.e. NO_3^- *versus* NH_4^+) could be the main reason of leaf-$\delta^{13}C_R$ changes along N-type gradient. However, in roots, the effect of expected PEPc activity under NH_4^+ nutrition was masked by a rather ^{13}C depleted carbon source (i.e. respired CO_2). The results of this thesis just open new insights to be explored on the N-type impact on carbon isotopic respiratory fractionations. In addition, as mentioned in Chapter 4, our results and discussion highlight the potential of the malate/citrate (or other relevant abundant organic acids) C-isotopic gap as a valuable proxy to screen for peculiar metabolic TCA organisations across species.

6.2 Perspectives

Therefore, the diel changes of the measured parameters, as well as double labelling (^{13}C and ^{15}N) experiments together with the use of positionally labelled metabolites followed by NMR analyses should be applied in future works to better track the metabolic pathways involved under each N-type treatment (Plain *et al.*, 2009; Gauthier *et al.*, 2010; Abadie and Tcherkez, 2019). It will make possible to trace the carbon and nitrogen during physiological processes, including carbon uptake and carbon allocation, in order to improve the existing knowledge on the extent of the anaplerotic pathway ^{13}C input in different pools and in respiratory CO_2, and the metabolic plasticity of TCA on respiratory carbon isotopic fractionations among species.

Furthermore, since PEPc is a multipurpose and highly regulated enzyme, it is difficult to conceive how its action could be subordinated to several modulators in the cytosol, and it is difficult to measure its instantaneous activity. Mutants with inhibited PEPc gene expression should be powerful tools for elucidating the contribution of anaplerotic pathway *via* PEPc on isotopic composition of metabolites and respired CO_2.

References

Abadie C, Lothier J, Boex-Fontvieille E, Carroll A, Tcherkez G. 2017. Direct assessment of the metabolic origin of carbon atoms in glutamate from illuminated leaves using ^{13}C-NMR. *New Phytologist* **216**, 1079-1089.

Abadie C, Tcherkez G. 2019**.** In vivo phospho*enol*pyruvate carboxylase activity is controlled by CO_2 and O_2 mole fraction and represents a major flux at high photorespiration rates. *New Phytologist* **221**, 1843-1852.

Abelson PH, Hoering TC. 1961. Carbon Isotope Fractionation in Formation of Amino Acids by Photosynthetic Organisms. *Proceedings of the National Academy of Sciences* **47**, 623-632.

Agren GI, Ingestad T. 1987. Root: shoot ratio as a balance between nitrogen productivity and photosynthesis. *Plant, Cell and Environment* **10**, 579-586.

Allen S, Smith JAC. 1986. Ammonium Nutrition inRicinus communis: Its Effect on Plant Growth and the Chemical Composition of the Whole Plant, Xylem and Phloem Saps. *Journal of Experimental* Botany **37**, 1599-1610.

Andrews JR, Bredenkamp GJ, Baker NR. 1993. Evaluation of the role of State transitions in determining the efficiency of light utilisation for CO_2 assimilation in leaves. *Photosynthesis Research* **38**, 15-26.

Andrews M, Raven JA, Lea PJ. 2013. Do plants need nitrate? The mechanisms by which nitrogen form affects plants. *Annals of Applied Biology* **163**, 174-199.

Aranjuelo I, Cabrera-Bosquet L, Araus JL, Nogues S. 2013. Carbon and nitrogen partitioning during the post-anthesis period is conditioned by N fertilisation and sink strength in three cereals. *Plant Biology* (Stuttg) **15**, 135-143.

Aranjuelo I, Cabrera-Bosquet L, Mottaleb SA, Araus JL, Nogues S. 2009. $^{(13)}$C/$^{(12)}$C isotope labelling to study carbon partitioning and dark respiration in cereals subjected to water stress. *Rapid communications in mass spectrometry* **23**, 2819-2828.

Arias CL, Andreo CS, Drincovich MF, Gerrard Wheeler MC. 2013. Fumarate and cytosolic pH as modulators of the synthesis or consumption of $C_{(4)}$ organic acids through NADP-malic enzyme in Arabidopsis thaliana. *Plant Molecular Biology* **81**, 297-307.

Arnozis PA, Nelemans JA, Findenegg GR. 1988. Phosphoenolpyruvate Carboxylase Activity in Plants Grown with either NO_3^- or NH_4^+ as Inorganic Nitrogen Source. *Journal of Plant Physiology* **132**, 23-27.

Artus NN, Edwards GE. 1985. NAD-malic enzyme from plants. *FEBS Letters* **182**, 225-233.

Atkin OK, Evans JR, Siebke K. 1998. Relationship between the inhibition of leaf respiration by light and enhancement of leaf dark respiration following light treatment. *Functional Plant Biology* **25**, 437-443.

Atkin OK, Millar AH, Gardeström P, Day DA. 2000. Photosynthesis, Carbohydrate Metabolism and Respiration in Leaves of Higher Plants. In: Leegood RC, Sharkey TD, von Caemmerer S, eds. *Photosynthesis: Physiology and Metabolism*. Dordrecht: Springer Netherlands, 153-175.

Azcón-Bieto J, Osmond CB. 1983. Relationship between Photosynthesis and Respiration. *Plant Physiology* **71**, 574.

Badeck FW, Tcherkez G, Nogues S, Piel C, Ghashghaie J. 2005. Post-photosynthetic fractionation of stable carbon isotopes between plant organs--a widespread phenomenon. *Rapid communications in mass spectrometry* **19**, 1381-1391.

Barbour MM, **McDowell NG**, **Tcherkez G**, **Bickford CP**, **Hanson DT.** 2007. A new measurement technique reveals rapid post-illumination changes in the carbon isotope composition of leaf-respired CO_2. *Plant, Cell & Environment* **30,** 469-482.
Bathellier C, Badeck F-W, Ghashghaie J. 2017. Carbon Isotope Fractionation in Plant Respiration. In: Tcherkez G, Ghashghaie J, eds. *Plant Respiration: Metabolic Fluxes and Carbon Balance*. Cham: Springer International Publishing, 43-68.
Bathellier C, Badeck FW, Couzi P, Harscoet S, Mauve C, Ghashghaie J. 2008. Divergence in delta$^{(13)}$C of dark respired CO_2 and bulk organic matter occurs during the transition between heterotrophy and autotrophy in Phaseolus vulgaris plants. *New Phytologist* **177**, 406-418.
Bathellier C, Tcherkez G, Bligny R, Gout E, Cornic G, Ghashghaie J. 2009a. Metabolic origin of the delta13C of respired CO_2 in roots of Phaseolus vulgaris. *New Phytologist* **181**, 387-399.
Bathellier C, Tcherkez G, Mauve C, Bligny R, Gout E, Ghashghaie J. 2009b. On the resilience of nitrogen assimilation by intact roots under starvation, as revealed by isotopic and metabolomic techniques. *Rapid communications in mass spectrometry* **23**, 2847-2856.
Berveiller D, Fresneau C, Damesin C. 2010. Effect of soil nitrogen supply on carbon assimilation by tree stems. *Annals of Forest Science* **67**, 609-609.
Bittsanszky A, Pilinszky K, Gyulai G, Komives T. 2015. Overcoming ammonium toxicity. *Plant Science* **231**, 184-190.
Bligny R, Gout E, Kaiser W, Heber U, Walker D, Douce R. 1997. pH regulation in acid-stressed leaves of pea plants grown in the presence of nitrate or ammonium salts: studies involving 31P-NMR spectroscopy and chlorophyll fluorescence. *Biochimica et Biophysica Acta* (BBA) - *Bioenergetics* **1320**, 142-152.
Bowling DR, Pataki DE, Randerson JT. 2008. Carbon isotopes in terrestrial ecosystem pools and CO_2 fluxes. *New Phytologist* **178**, 24-40.
Britto DT, Kronzucker HJ. 2002. NH_4^+ toxicity in higher plants: a critical review. Journal of *Plant Physiology* **159**, 567-584.
Britto DT, Kronzucker HJ. 2005. Nitrogen acquisition, PEP carboxylase, and cellular pH homeostasis: new views on old paradigms. *Plant, Cell and Environment* **28**, 1396-1409.
Brooks PD, Geilmann H, Werner RA, Brand WA. 2003. Improved precision of coupled delta13C and delta15N measurements from single samples using an elemental analyser/isotope ratio mass spectrometer combination with a post-column six-port valve and selective CO_2 trapping; improved halide robustness of the combustion reactor using CeO_2. *Rapid communications in mass spectrometry* **17**, 1924-1926.
Brugnoli E, Farquhar GD. 2000. Photosynthetic Fractionation of Carbon Isotopes. In: Leegood RC, Sharkey TD, von Caemmerer S, eds. *Photosynthesis: Physiology and Metabolism*. Dordrecht: Springer Netherlands, 399-434.
Brugnoli E, Hubick KT, von Caemmerer S, Wong SC, Farquhar GD. 1988. Correlation between the Carbon Isotope Discrimination in Leaf Starch and Sugars of C_3 Plants and the Ratio of Intercellular and Atmospheric Partial Pressures of Carbon Dioxide. *Plant Physiology* **88**, 1418-1424.
Buchanan BB. 1991. Regulation of CO_2 assimilation in oxygenic photosynthesis: The ferredoxin/thioredoxin system: Perspective on its discovery, present status, and future development. *Archives of Biochemistry and Biophysics* **288**, 1-9.
Buchmann N, Brooks JR, Rapp KD, Ehleringer JR. 1996. Carbon isotope composition of C4 grasses is influenced by light and water supply. *Plant, Cell and Environment* **19**, 392-402.
Cao W, Tibbitts TW. 1993. Study of various NH_4^+/ NO_3^- mixtures for enhancing growth of potatoes. *Journal of Plant Nutrition* **16**, 1691-1704.

Cartelat A, Cerovic ZG, Goulas Y, Meyer S, Lelarge C, Prioul JL, Barbottin A, Jeuffroy MH, Gate P, Agati G, Moya I. 2005. Optically assessed contents of leaf polyphenolics and chlorophyll as indicators of nitrogen deficiency in wheat (Triticum aestivum L.). *Field Crops Research* **91**, 35-49.

Cerovic ZG, Masdoumier G, Ghozlen NB, Latouche G. 2012. A new optical leaf-clip meter for simultaneous non-destructive assessment of leaf chlorophyll and epidermal flavonoids. *Physiologia Plantarum* **146**, 251-260.

Cerezo M, Tillard P, Filleur S, Munos S, Daniel-Vedele F, Gojon A. 2001. Major alterations of the regulation of root NO_3^- uptake are associated with the mutation of Nrt2.1 and Nrt2.2 genes in Arabidopsis. *Plant Physiology* **127**, 262-271.

Cernusak LA, Tcherkez G, Keitel C, Cornwell WK, Santiago LS, Knohl A, Barbour MM, Williams DG, Reich PB, Ellsworth DS, Dawson TE, Griffiths HG, Farquhar GD, Wright IJ. 2009. Why are non-photosynthetic tissues generally ^{13}C enriched compared with leaves in C_3 plants? Review and synthesis of current hypotheses. *Functional Plant Biology* **36**, 199.

Cernusak LA, Ubierna N, Winter K, Holtum JA, Marshall JD, Farquhar GD. 2013. Environmental and physiological determinants of carbon isotope discrimination in terrestrial plants. *New Phytologist* **200**, 950-965.

Chaillou S, Morot-Gaudry JF, Lesaint C, Salsac L, Jolivet E. 1986. Nitrate or ammonium nutrition in french bean. *Plant and Soil* **91**, 363-365.

Chang CC, Beevers H. 1968. Biogenesis of oxalate in plant tissues. *Plant Physiology* **43**, 1821-1828.

Cheung CYM, Poolman MG, Fell DA, Ratcliffe RG, Sweetlove LJ. 2014. A Diel Flux Balance Model Captures Interactions between Light and Dark Metabolism during Day-Night Cycles in C_3 and Crassulacean Acid Metabolism Leaves. *Plant Physiology* **165**, 917.

Chia DW, Yoder TJ, Reiter WD, Gibson SI. 2000. Fumaric acid: an overlooked form of fixed carbon in Arabidopsis and other plant species. *Planta* **211**, 743-751.

Claussen W, Lenz F. 1999. Effect of ammonium or nitrate nutrition on net photosynthesis, growth, and activity of the enzymes nitrate reductase and glutamine synthetase in blueberry, raspberry and strawberry. *Plant and Soil* **208**, 95-102.

Condon AG, Richards RA, Farquhar GD. 1992. The effect of variation in soil water availability, vapour pressure deficit and nitrogen nutrition on carbon isotope discrimination in wheat. *Australian Journal of Agricultural Research* **43**, 935-947.

Cornwell WK, Wright IJ, Turner J, Maire V, Barbour MM, Cernusak LA, Dawson T, Ellsworth D, Farquhar GD, Griffiths H, Keitel C, Knohl A, Reich PB, Williams DG, Bhaskar R, Cornelissen JHC, Richards A, Schmidt S, Valladares F, Körner C, Schulze E-D, Buchmann N, Santiago LS. 2018. Climate and soils together regulate photosynthetic carbon isotope discrimination within C_3 plants worldwide. *Global Ecology and Biogeography* **27**, 1056-1067.

Cramer M, Lewis OAM. 1993a. The Influence of Nitrate and Ammonium Nutrition on the Growth of Wheat (Triticum aestivum) and Maize (Zea mays) Plants. *Annals of Botany* **72**, 359-365.

Cramer M, Lewis OAM. 1993b. The Influence of NO_3^- and NH_4^+ Nutrition on the Gas Exchange Characteristics of the Roots of Wheat (Triticum aestivum) and Maize (Zea mays) Plants. *Annals of Botany* **72**, 37-46.

Cramer MD, Lewis OAM, Lips SH. 1993. Inorganic carbon fixation and metabolism in maize roots as affected by nitrate and ammonium nutrition. *Physiologia Plantarum* **89**, 632-639.

Crawford NM, Forde BG. 2002. Molecular and developmental biology of inorganic nitrogen nutrition. *Arabidopsis Book* **1**, e0011.
Cruz C, Bio AF, Dominguez-Valdivia MD, Aparicio-Tejo PM, Lamsfus C, Martins-Loucao MA. 2006. How does glutamine synthetase activity determine plant tolerance to ammonium? *Planta* **223**, 1068-1080.
Davies DD. 1979. The Central Role of Phosphoenolpyruvate in Plant Metabolism. *Annual Review of Plant Physiology* **30**, 131-158.
DeNiro MJ, Epstein S. 1977. Mechanism of carbon isotope fractionation associated with lipid synthesis. *Science* **197**, 261.
Dennis D, Blakeley S. 2000. Carbohydrate metabolism In: Biochemistry & molecular biology of plants. Ed. By BB Buchanans, W. Gruissem and RL Jones. *American Society of Plant Physiologists*, Rock Ville, Md., USA.
Dieuaide-Noubhani M, Raffard G, Canioni P, Pradet A, Raymond P. 1995. Quantification of Compartmented Metabolic Fluxes in Maize Root Tips Using Isotope Distribution from 13C- or ^{14}C-Labelled Glucose. *Journal of Biological Chemistry* **270**, 13147-13159.
Dominguez-Valdivia MD, Aparicio-Tejo PM, Lamsfus C, Cruz C, Martins-Loucao MA, Moran JF. 2008. Nitrogen nutrition and antioxidant metabolism in ammonium-tolerant and -sensitive plants. *Physiologia Plantarum* **132**, 359-369.
Duranceau M, Ghashghaie J, Badeck F, Deleens E, Cornic G. 1999. δ13C of CO_2 respired in the dark in relation toδ13C of leaf carbohydrates inPhaseolus vulgarisL. under progressive drought. *Plant, Cell and Environment* **22**, 515-523.
Earl HJ, Tollenaar M. 1998. Relationship between thylakoid electron transport and photosynthetic CO_2 uptake in leaves of three maize (Zea mays L.) hybrids. *Photosynthesis Research* **58**, 245-257.
Elia A, Santamaria P, Serio F. 1998. Nitrogen nutrition, yield and quality of spinach. *Journal of the Science of Food and Agriculture* **76**, 341-346.
Esposito S, Guerriero G, Vona V, Di Martino Rigano V, Carfagna S, Rigano C. 2005. Glutamate synthase activities and protein changes in relation to nitrogen nutrition in barley: the dependence on different plastidic glucose-6P dehydrogenase isoforms. *Journal of Experimental Botany* **56**, 55-64.
Esteban R, Ariz I, Cruz C, Moran JF. 2016. Review: Mechanisms of ammonium toxicity and the quest for tolerance. *Plant Science* **248**, 92-101.
Farquhar GD. 1983. On the Nature of Carbon Isotope Discrimination in C4 Species. *Functional Plant Biology* **10**, 205-226.
Farquhar GD, Ehleringer JR, Hubick KT. 1989. Carbon Isotope Discrimination and Photosynthesis. *Annual Review of Plant Physiology and Plant Molecular Biology* **40**, 503-537.
Farquhar GD, O'Leary MH, Berry JA. 1982. On the Relationship Between Carbon Isotope Discrimination and the Intercellular Carbon Dioxide Concentration in Leaves. *Functional Plant Biology* **9**, 121-137.
Farquhar GD, Richards RA. 1984. Isotopic Composition of Plant Carbon Correlates With Water-Use Efficiency of Wheat Genotypes. *Functional Plant Biology* **11**, 539-552.
Farquhar GD, Sharkey TD. 1982. Stomatal Conductance and Photosynthesis. *Annual Review of Plant Physiology* **33**, 317-345.
Feng J, Barker AV. 1992. Ethylene evolution and ammonium accumulation by nutrient-stressed tomato plants. *Journal of Plant Nutrition* **15**, 137-153.

Fernie AR, Carrari F, Sweetlove LJ. 2004. Respiratory metabolism: glycolysis, the TCA cycle and mitochondrial electron transport. *Current Opinion in Plant Biology* **7**, 254-261.
Forde BG, Lea PJ. 2007. Glutamate in plants: metabolism, regulation, and signalling. *Journal of Experimental Botany* **58**, 2339-2358.
Foyer CH, Noctor G, Hodges M. 2011. Respiration and nitrogen assimilation: targeting mitochondria-associated metabolism as a means to enhance nitrogen use efficiency. *Journal of Experimental Botany* **62**, 1467-1482.
Foyer CH, Valadier M-H, Migge A, Becker TW. 1998. Drought-Induced Effects on Nitrate Reductase Activity and mRNA and on the Coordination of Nitrogen and Carbon Metabolism in Maize Leaves. *Plant Physiology* **117**, 283.
Fresneau C, Ghashghaie J, Cornic G. 2007. Drought effect on nitrate reductase and sucrose-phosphate synthase activities in wheat (Triticum durum L.): role of leaf internal CO_2. *Journal of Experimental Botany* **58**, 2983-2992.
Gardeström P, Igamberdiev AU, Raghavendra AS. 2002. Mitochondrial Functions in the Light and Significance to Carbon-Nitrogen Interactions. In: Foyer CH, Noctor G, eds. *Photosynthetic Nitrogen Assimilation and Associated Carbon and Respiratory Metabolism*. Dordrecht: Springer Netherlands, 151-172.
Gauthier PP, Bligny R, Gout E, Mahe A, Nogues S, Hodges M, Tcherkez GG. 2010. In folio isotopic tracing demonstrates that nitrogen assimilation into glutamate is mostly independent from current CO2 assimilation in illuminated leaves of Brassica napus. *New Phytologist* **185**, 988-999.
Genty B, Briantais J-M, Baker NR. 1989. The relationship between the quantum yield of photosynthetic electron transport and quenching of chlorophyll fluorescence. *Biochimica et Biophysica Acta (BBA) - General Subjects* **990**, 87-92.
Gerendás J, Ratcliffe RG. 2000. Intracellular pH regulation in maize root tips exposed to ammonium at high external pH. *Journal of Experimental Botany* **51**, 207-219.
Gerendás J, Zhu Z, Bendixen R, Ratcliffe RG, Sattelmacher B. 1997. Physiological and Biochemical Processes Related to Ammonium Toxicity in Higher Plants. *Zeitschrift für Pflanzenernährung und Bodenkunde* **160**, 239-251.
Gessler A, Tcherkez G, Karyanto O, Keitel C, Ferrio JP, Ghashghaie J, Kreuzwieser J, Farquhar GD. 2009. On the metabolic origin of the carbon isotope composition of CO_2 evolved from darkened light-acclimated leaves in Ricinus communis. *New Phytologist* **181**, 374-386.
Gessler A, Tcherkez G, Peuke AD, Ghashghaie J, Farquhar GD. 2008. Experimental evidence for diel variations of the carbon isotope composition in leaf, stem and phloem sap organic matter in Ricinus communis. *Plant, Cell and Environment* **31**, 941-953.
Ghashghaie J, Badeck F-W, Lanigan G, Nogués S, Tcherkez G, Deléens E, Cornic G, Griffiths H. 2003. Carbon isotope fractionation during dark respiration and photorespiration in C_3 plants. *Phytochemistry Reviews* **2**, 145-161.
Ghashghaie J, Badeck FW. 2014. Opposite carbon isotope discrimination during dark respiration in leaves versus roots - a review. *New Phytologist* **201**, 751-769.
Ghashghaie J, Badeck FW, Girardin C, Huignard C, Aydinlis Z, Fonteny C, Priault P, Fresneau C, Lamothe-Sibold M, Streb P, Terwilliger VJ. 2016. Changes and their possible causes in delta^{13}C of dark-respired CO_2 and its putative bulk and soluble sources during maize ontogeny. *Journal of Experimental Botany* **67**, 2603-2615.
Ghashghaie J, Badeck FW, Girardin C, Sketriene D, Lamothe-Sibold M, Werner RA. 2015. Changes in delta$^{(13)}$C of dark respired CO_2 and organic matter of different organs during early ontogeny in peanut plants. *Isotopes in Environmental and Health Studies* **51**, 93-108.

Ghashghaie J, Duranceau M, Badeck FW, Cornic G, Adeline MT, Deleens E. 2001. $\delta^{13}C$ of CO2 respired in the dark in relation to $\delta^{13}C$ of leaf metabolites: comparison between Nicotiana sylvestris and Helianthus annuus under drought. *Plant, Cell and Environment* **24**, 505-515.
Ghashghaie J, Tcherkez G. 2013. Isotope Ratio Mass Spectrometry Technique to Follow Plant Metabolism: Principles and Applications of $^{12}C/^{13}C$ Isotopes. In: Rolin D, ed. *Advances in Botanical Research*, Vol. 67. Burlington: Academic Press, 377-405.
Gibbs M, Beevers H. 1955. Glucose Dissimilation in the Higher Plant. Effect of Age of Tissue. *Plant Physiology* **30**, 343-347.
Gilbert A, Silvestre V, Robins RJ, Remaud GS, Tcherkez G. 2012. Biochemical and physiological determinants of intramolecular isotope patterns in sucrose from C_3, C_4 and CAM plants accessed by isotopic ^{13}C NMR spectrometry: a viewpoint. *Natual Product Reports***29**, 476-486.
Gilbert A, Silvestre V, Segebarth N, Tcherkez G, Guillou C, Robins RJ, Akoka S, Remaud GS. 2011. The intramolecular ^{13}C-distribution in ethanol reveals the influence of the CO_2-fixation pathway and environmental conditions on the site-specific ^{13}C variation in glucose. *Plant, Cell and Environment* **34**, 1104-1112.
Gleixner G, Schmidt H-L. 1997. Carbon Isotope Effects on the Fructose-1,6-bisphosphate Aldolase Reaction, Origin for Non-statistical ^{13}C Distributions in Carbohydrates. *Journal of Biological Chemistry* **272**, 5382-5387.
Green PT, Juniper PA. 2004. Seed-seedling allometry in tropical rain forest trees: seed mass-related patterns of resource allocation and the 'reserve effect'. *Journal of Ecology* **92**, 397-408.
Guo SW, Zhou Y, Gao YX, Li Y, Shen QR. 2007. New Insights into the Nitrogen Form Effect on Photosynthesis and Photorespiration. *Pedosphere* **17**, 601-610.
Guo S, Brück H, Sattelmacher B. 2002. Effects of supplied nitrogen form on growth and water uptake of French bean (Phaseolus vulgaris L.) plants. *Plant and Soil* **239**, 267-275.
Hachiya T, Sakakibara H. 2016. Interactions between nitrate and ammonium in their uptake, allocation, assimilation, and signaling in plants. *Journal of Experimental Botany* **68**, 2501-2512.
Hanning I, Heldt HW. 1993. On the Function of Mitochondrial Metabolism during Photosynthesis in Spinach (Spinacia oleracea L.) Leaves (Partitioning between Respiration and Export of Redox Equivalents and Precursors for Nitrate Assimilation Products). *Plant Physiology* **103**, 1147-1154.
Hattersley PW. 1982. δ13 Values of C4 Types in Grasses. *Functional Plant Biology* **9**, 139-154.
Hayes JM. 2001. Fractionation of Carbon and Hydrogen Isotopes in Biosynthetic Processes. *Reviews in Mineralogy and Geochemistry* **43**, 225-277.
Hermes JD, Cleland WW. 1984. Evidence from multiple isotope effect determinations for coupled hydrogen motion and tunneling in the reaction catalyzed by glucose-6-phosphate dehydrogenase. *Journal of the American Chemical Society* **106**, 7263-7264.
Hobbie EA, Werner RA. 2004. Intramolecular, compound-specific, and bulk carbon isotope patterns in C_3 and C_4 plants: a review and synthesis. *New Phytologist* **161**, 371-385.
Hoefnagel MHN, Atkin OK, Wiskich JT. 1998. Interdependence between chloroplasts and mitochondria in the light and the dark. *Biochimica et Biophysica Acta (BBA) - Bioenergetics* **1366**, 235-255.
Huppe HC, Turpin DH. 1994. Integration of Carbon and Nitrogen Metabolism in Plant and Algal Cells. *Annual Review of Plant Physiology and Plant Molecular Biology* **45**, 577-607.
Hymus GJ, Maseyk K, Valentini R, Yakir D. 2005. Large daily variation in ^{13}C-enrichment of leaf-respired CO_2 in two Quercus forest canopies. *New Phytologist* **167**, 377-384.

Igamberdiev AU, Bykova NV. 2018. Role of organic acids in the integration of cellular redox metabolism and mediation of redox signalling in photosynthetic tissues of higher plants. *Free Radiccal Biology and Medicine* **122**, 74-85.
Igamberdiev AU, Eprintsev AT. 2016. Organic Acids: The Pools of Fixed Carbon Involved in Redox Regulation and Energy Balance in Higher Plants. *Frontiers in Plant Science* **7**, 1042.
Igamberdiev AU, Zhou G, Malmberg G, Gardeström P. 1997. Respiration of barley protoplasts before and after illumination. Physiologia Plantarum **99**, 15-22.
James WO. 1953. *Plant respiration*: At The Clarendon Press; London.
Klumpp K, SchÄUfele R, LÖTscher M, Lattanzi FA, Feneis W, Schnyder H. 2005. C-isotope composition of CO2 respired by shoots and roots: fractionation during dark respiration? *Plant, Cell and Environment* **28**, 241-250.
Koga N, Ikeda M. 2000. Methionine sulfoximine suppressed the stimulation of dark carbon fixation by ammonium nutrition in wheat roots. *Soil Science and Plant Nutrition* **46**, 393-400.
Kraiser T, Gras DE, Gutierrez AG, Gonzalez B, Gutierrez RA. 2011. A holistic view of nitrogen acquisition in plants. *Journal of Experimental Botany* **62**, 1455-1466.
Kronzucker HJ, Glass AD, Yaeesh Siddiqi M. 1999a. Inhibition of nitrate uptake by ammonium in barley. Analysis Of component fluxes. *Plant Physiology* **120**, 283-292.
Kronzucker HJ, Siddiqi MY, Glass AD, Kirk GJ. 1999b. Nitrate-ammonium synergism in rice. A subcellular flux analysis. *Plant Physiology* **119**, 1041-1046.
Kruger NJ, von Schaewen A. 2003. The oxidative pentose phosphate pathway: structure and organisation. *Current Opinion in Plant Biology* **6**, 236-246.
Kumar V, Irfan M, Datta A. 2019. Manipulation of oxalate metabolism in plants for improving food quality and productivity. *Phytochemistry* **158**, 103-109.
Ladwig F, Stahl M, Ludewig U, Hirner AA, Hammes UZ, Stadler R, Harter K, Koch W. 2012. Siliques are red1 from arabidopsis acts as a bidirectional amino acid transporter that is crucial for the amino acid homeostasis of siliques. *Plant Physiology* **158**, 1643.
Lam HM, Coschigano KT, Oliveira IC, Melo-Oliveira R, Coruzzi GM. 1996. The Molecular-Genetics of Nitrogen Assimilation into Amino Acids in Higher Plants. *Annual Review Plant* Physiology *Plant Molecular Biology* **47**, 569-593.
Lambers H. 1985. Respiration in Intact Plants and Tissues: Its Regulation and Dependence on Environmental Factors, Metabolism and Invaded Organisms. In: Douce R, Day DA, eds. *Higher Plant Cell Respiration*. Berlin, Heidelberg: Springer Berlin Heidelberg, 418-473.
Lanigan GJ, Betson N, Griffiths H, Seibt U. 2008. Carbon isotope fractionation during photorespiration and carboxylation in Senecio. *Plant Physiology* **148**, 2013-2020.
Lanquar V, Loqué D, Hörmann F, Yuan L, Bohner A, Engelsberger WR, Lalonde S, Schulze WX, von Wirén N, Frommer WB. 2009. Feedback inhibition of ammonium uptake by a phospho-dependent allosteric mechanism in Arabidopsis. *The Plant Cell* **21**, 3610-22.
Larsen PO, Cornwell KL, Gee SL, Bassham JA. 1981. Amino acid synthesis in photosynthesizing spinach cells : Effects of ammonia on pool sizes and rates of labelling from 14CO2. *Plant Physiology* **68**, 292-299.
Lasa B, Frechilla S, Aparicio-Tejo PM, Lamsfus C. 2002a. Alternative pathway respiration is associated with ammonium ion sensitivity in spinach and pea plants. *Plant Growth Regulation* **37**, 49-55.
Lasa B, Frechilla S, Aparicio-Tejo PM, Lamsfus C. 2002b. Role of glutamate dehydrogenase and phosphoenolpyruvate carboxylase activity in ammonium nutrition tolerance in roots. *Plant Physiology and Biochemistry* **40**, 969-976.

Latzko E, Kelly GJ. 1983. The many-faceted function of phosphoenolpyruvate carboxylase in C3 plants. *Physiologie Vegetale* **21**, 805-815.
Lawlor DW. 2002. Carbon and nitrogen assimilation in relation to yield: mechanisms are the key to understanding production systems. *Journal of Experimental Botany* **53**, 773-787.
Lehmann MM, Rinne KT, Blessing C, Siegwolf RT, Buchmann N, Werner RA. 2015. Malate as a key carbon source of leaf dark-respired CO2 across different environmental conditions in potato plants. *Journal of Experimental Botany* **66**, 5769-5781.
Lehmann MM, Wegener F, Barthel M, Maurino VG, Siegwolf RT, Buchmann N, Werner C, Werner RA. 2016. Metabolic Fate of the Carboxyl Groups of Malate and Pyruvate and their Influence on delta(13)C of Leaf-Respired CO2 during Light Enhanced Dark Respiration. *Frontiers in Plant Science* **7**, 739.
Lehninger A, Nelson D, Cox MM. 1993. Biosynthesis of amino acids, nucleotides and related molecules. *Principles of biochemistry:* Worth New York, 688-734.
Lepiniec L, Thomas M, Vidal J. 2003. From enzyme activity to plant biotechnology: 30 years of research on phosphoenolpyruvate carboxylase. *Plant Physiology and Biochemistry* **41**, 533-539.
Linka N, Weber APM. 2010. Intracellular Metabolite Transporters in Plants. *Molecular Plant* **3**, 21-53.
Liu X, Lu L, Chen Q, Ding W, Dai P, Hu Y, Yu Y, Jin C, Lin X. 2015. Ammonium reduces oxalate accumulation in different spinach (*Spinacia oleracea* L.) genotypes by inhibiting root uptake of nitrate. *Food Chemistry* **186**, 312-318.
Livingston NJ, Guy RD, Sun ZJ, Ethier GJ. 1999. The effects of nitrogen stress on the stable carbon isotope composition, productivity and water use efficiency of white spruce (Picea glauca (Moench) Voss) seedlings. *Plant, Cell and Environment* **22**, 281-289.
Lopes MS, Araus JL. 2006. Nitrogen source and water regime effects on durum wheat photosynthesis and stable carbon and nitrogen isotope composition. *Physiologia Plantarum* **126**, 435-445.
Ludewig U, Neuhauser B, Dynowski M. 2007. Molecular mechanisms of ammonium transport and accumulation in plants. *FEBS Letters* **581**, 2301-2308.
Magalhaes JR, Huber DM. 1989. Maize growth and ammonium assimilation enzyme activity in response to nitrogen forms and pH control. *Journal of Plant Nutrition* **12**, 985-996.
Magalhaes JR, Huber DM. 1991. Response of ammonium assimilation enzymes to nitrogen form treatments in different plant species. *Journal of Plant Nutrition* **14**, 175-185.
Marques IA, Oberholzer MJ, Erismann KH. 1983. Effects of Different Inorganic Nitrogen Sources on Photosynthetic Carbon Metabolism in Primary Leaves of Non-nodulated *Phaseolus vulgaris* L. *Plant Physiology* **71**, 555-561.
Marschner H, Kirkby EA, Cakmak I. 1996. Effect of mineral nutritional status on shoot—root partitioning of photoassimilates and cycling of mineral nutrients. *Journal of Experimental Botany* **47**, 1255-1263.
Masclaux-Daubresse C, Daniel-Vedele F, Dechorgnat J, Chardon F, Gaufichon L, Suzuki A. 2010. Nitrogen uptake, assimilation and remobilization in plants: challenges for sustainable and productive agriculture. *Annals of Botany* **105**, 1141-1157.
Masumoto C, Miyazawa S, Ohkawa H, Fukuda T, Taniguchi Y, Murayama S, Kusano M, Saito K, Fukayama H, Miyao M. 2010. Phosphoenolpyruvate carboxylase intrinsically located in the chloroplast of rice plays a crucial role in ammonium assimilation. *Proceedings of the National Academy of Sciences of U.S.A. (PNAS)* **107**, 5226-5231.

McKinney CR, McCrea JM, Epstein S, Allen HA, Urey HC. 1950. Improvements in Mass Spectrometers for the Measurement of Small Differences in Isotope Abundance Ratios. *Review of Scientific Instruments* **21**, 724-730.
Meharg AA, Blatt MR. 1995. NO_3^- transport across the plasma membrane of Arabidopsis thaliana root hairs: Kinetic control by pH and membrane voltage. *The Journal of Membrane Biology* **145**, 49-66.
Melzer E, O'Leary MH. 1987. Anapleurotic CO_2 Fixation by Phosphoenolpyruvate Carboxylase in C3 Plants. *Plant Physiology* **84**, 58-60.
Melzer E, Schmidt HL. 1987. Carbon isotope effects on the pyruvate dehydrogenase reaction and their importance for relative carbon-13 depletion in lipids. *Journal of Biological Chemistry* **262**, 8159-8164.
Mengel K, Robin P, Salsac L. 1983. Nitrate Reductase Activity in Shoots and Roots of Maize Seedlings as Affected by the Form of Nitrogen Nutrition and the pH of the Nutrient Solution. *Plant Physiology* **71**, 618-622.
Miller AJ, Fan X, Orsel M, Smith SJ, Wells DM. 2007. Nitrate transport and signalling. *Journal of Experimental Botany* **58**, 2297-2306.
Monson KD, Hayes JM. 1982. Carbon isotopic fractionation in the biosynthesis of bacterial fatty acids. Ozonolysis of unsaturated fatty acids as a means of determining the intramolecular distribution of carbon isotopes. *Geochimica et Cosmochimica Acta* **46**, 139-149.
Nalborczyk E. 1978. Dark carboxylation and its possible effect on the value of $\delta^{13}C$ in C_3 plants. *Acta Physiologia Plantarum* **1**, 53-58.
Nobel PS. 1983. *Biophysical plant physiology and ecology*. San Francisco, California: W.H. Freeman and Company.
Noggle GR, Fritz GJ. 1983. *Introductory plant physiology*. Englewood Cliffs, New Jersey: Prentice-Hall Inc.
Nogués S, Damesin C, Tcherkez G, Maunoury F, Cornic G, Ghashghaie J. 2006. $^{(13)}C/^{(12)}C$ isotope labelling to study leaf carbon respiration and allocation in twigs of field-grown beech trees. *Rapid Communications in Mass Spectrometry* **20**, 219-226.
Nogués S, Tcherkez G, Cornic G, Ghashghaie J. 2004. Respiratory carbon metabolism following illumination in intact French bean leaves using $^{(13)}C/^{(12)}C$ isotope labelling. *Plant Physiology* **136**, 3245-3254.
O'Leary MH. 1981. Carbon isotope fractionation in plants. Phytochemistry **20**, 553-567.
O'Leary MH. 1988. Carbon isotopes in photosynthesis. *Bioscience* **38**, 328-336.
Oaks A. 1994. Primary nitrogen assimilation in higher plants and its regulation. *Canadian Journal of Botany* **72**, 739-750.
Ocheltree TW, Marshall JD. 2004. Apparent respiratory discrimination is correlated with growth rate in the shoot apex of sunflower (*Helianthus annuus*). *Journal of Experimental Botany* **55**, 2599-2605.
Ohlrogge J, Browse J. 1995. Lipid biosynthesis. The Plant Cell **7**, 957-970.
Ohsugi RYU, Samejima M, Chonan N, Murata T. 1988. δ13C Values and the Occurrence of Suberized Lamellae in Some Panicum Species. *Annals of Botany* **62**, 53-59.
Oliver DJ. 1995. The biochemistry of the mitochondrial matrix. In: McIntosh CA, ed. *The Molecular Biology of Plant Mitochondria*. Dordrecht ; Boston: Kluwer Academic Publishers, 237-280.
Ortiz-Ramirez C, Mora SI, Trejo J, Pantoja O. 2011. PvAMT1;1, a highly selective ammonium transporter that functions as an H^+/ NH_4^+symporter. *Journal of Biological Chemistry* **286**,31113-31122.

Oxborough K, Baker NR. 1997. Resolving chlorophyll a fluorescence images of photosynthetic efficiency into photochemical and non-photochemical components – calculation of qP and F_v-/F_m-; without measuring F_o-;. *Photosynthesis Research* **54**, 135-142.
Park R, Epstein S. 1961. Metabolic fractionation of 13C & 12C in plants. *Plant Physiology* **36**, 133-138.
Pate JS, Layzell DB. 1990. Energetics and biological costs of nitrogen assimilation. *The biochemistry of plants* **16**, 1-42.
Paz H, MartÍnez-Ramos M. 2003. Seed Mass and Seedling Performance within Eight Species of Psychotria (Rubiaceae). *Ecology* **84**, 439-450.
Plain C, Gerant D, Maillard P, Dannoura M, Dong Y, Zeller B, Priault P, Parent F, Epron D. 2009. Tracing of recently assimilated carbon in respiration at high temporal resolution in the field with a tuneable diode laser absorption spectrometer after in situ $^{13}CO_2$ pulse labelling of 20-year-old beech trees. *Tree Physiology* **29**, 1433-1445.
Plaxton WC. 1996. The Organization and Regulation of Plant Glycolysis. Annu Rev Plant Physiol *Plant Molecular Biology* **47**, 185-214.
Poxleitner M, Rogers SW, Lacey Samuels A, Browse J, Rogers JC. 2006. A role for caleosin in degradation of oil-body storage lipid during seed germination. *The Plant Journal* **47**, 917-933.
Pracharoenwattana I, Zhou W, Keech O, Francisco PB, Udomchalothorn T, Tschoep H, Stitt M, Gibon Y, Smith SM. 2010. Arabidopsis has a cytosolic fumarase required for the massive allocation of photosynthate into fumaric acid and for rapid plant growth on high nitrogen. *Plant Journal* **62**, 785-795.
Prater JL, Mortazavi B, Chanton JP. 2006. Diurnal variation of the $\delta^{13}C$ of pine needle respired CO_2 evolved in darkness. *Plant, Cell and Environment* **29**, 202-211.
Priault P, Wegener F, Werner C. 2009. Pronounced differences in diurnal variation of carbon isotope composition of leaf respired CO2 among functional groups. *New Phytologist* **181**, 400-412.
Quero JL, Villar R, Maranon T, Zamora R, Poorter L. 2007. Seed-mass effects in four Mediterranean Quercus species (Fagaceae) growing in contrasting light environments. American Journal of Botany **94** (11), 1795-1803.
Raab TK, Terry N. 1994. Nitrogen-Source Regulation of Growth and Photosynthesis in Beta-Vulgaris L. *Plant Physiology* **105**, 1159-1166.
Raab TK, Terry N. 1995. Carbon, Nitrogen, and Nutrient Interactions in Beta-Vulgaris L as Influenced by Nitrogen-Source, NO_3^- Versus NH_4^+. *Plant Physiology* **107**, 575-584.
Raven JA. 1985. Tansley review no. 2. Regulation of pH and generation of osmolarity in vascular plants: a cost-benefit analysis in relation to efficiency of use of energy, nitrogen and water. *New Phytologist*, **101**, 25-77.
Raven JA, Farquhar GD. 1990. The influence of N metabolism and organic acid synthesis on the natural abundance of isotopes of carbon in plants. *New Phytologist* **116**, 505-529.
Raven JA, Smith FA. 1976. Nitrogen Assimilation and Transport in Vascular Land Plants in Relation to Intracellular pH Regulation. *New Phytologist* **76**, 415-431.
Rees TA. 1980. Assessment of the Contributions of Metabolic Pathways to Plant Respiration. In: Davies DD, ed. *Metabolism and Respiration*: Academic Press, 1-29.
Rendina AR, Hermes JD, Cleland WW. 1984. Use of multiple isotope effects to study the mechanism of 6-phosphogluconate dehydrogenase. *Biochemistry* **23**, 6257-6262.
Rodrıguez-Concepción M, Boronat A. 2002. Elucidation of the methylerythritol phosphate pathway for isoprenoid biosynthesis in bacteria and plastids. A metabolic milestone achieved through genomics. *Plant Physiology* **130**, 1079-1089.

Roeske CA, O'Leary MH. 1984. Carbon isotope effects on enzyme-catalyzed carboxylation of ribulose bisphosphate. *Biochemistry* **23**, 6275-6284.
Romek KM, Nun P, Remaud GS, Silvestre V, Taïwe GS, Lecerf-Schmidt F, Boumendjel A, De Waard M, Robins RJ. 2015. A retro-biosynthetic approach to the prediction of biosynthetic pathways from position-specific isotope analysis as shown for tramadol. *Proceedings of the National Academy of Sciences*, **112**, 82-96.
Romek KM, Remaud GS, Silvestre V, Paneth P, Robins RJ. 2016. Non-statistical 13C fractionation distinguishes co-incident and divergent steps in the biosynthesis of the alkaloids nicotine and tropine. *Journal of Biological Chemistry*, **291**, 16620-16629.
Roosta HR, Sajjadinia A, Rahimi A, Schjoerring JK. 2009. Responses of cucumber plant to NH_4^+ and NO_3^- nutrition: The relative addition rate technique vs. cultivation at constant nitrogen concentration. *Scientia Horticulturae* **121**, 397-403.
Rossmann A, Butzenlechner M, Schmidt HL. 1991. Evidence for a Nonstatistical Carbon Isotope Distribution in Natural Glucose. *Plant Physiology* **96**, 609-614.
Sagi M, Dovrat A, Kipnis T, Lips H. 1998. Nitrate reductase, phosphoenolpyruvate carboxylase, and glutamine synthetase in annual ryegrass as affected by salinity and nitrogen. *Journal of Plant Nutrition* **21**, 707-723.
Salsac L. 1987. Nitrate and ammonium nutrition in plants. *Plant Physiology and Biochemistry* **25**, 805-812.
Sarasketa A, González-Moro MB, González-Murua C, Marino D. 2016. Nitrogen Source and External Medium pH Interaction Differentially Affects Root and Shoot Metabolism in Arabidopsis. *Frontiers in Plant Science* **7**, 29.
Sasaki Y, Konishi T, Nagano Y. 1995. The Compartmentation of Acetyl-Coenzyme A Carboxylase in Plants. *Plant Physiology* **108**, 445-449.
Scheibe R. 2004. Malate valves to balance cellular energy supply. *Physiologia Plantarum* **120**, 21-26.
Scheible WR, Gonzalez-Fontes A, Lauerer M, Muller-Rober B, Caboche M, Stitt M. 1997. Nitrate Acts as a Signal to Induce Organic Acid Metabolism and Repress Starch Metabolism in Tobacco. *Plant Cell* **9**, 783-798.
Scheible WR, Krapp A, Stitt M. 2000. Reciprocal diurnal changes of phosphoenolpyruvate carboxylase expression and cytosolic pyruvate kinase, citrate synthase and NADP-isocitrate dehydrogenase expression regulate organic acid metabolism during nitrate assimilation in tobacco leaves. *Plant, Cell and Environment* **23**, 1155-1167.
Scheurwater I. 2002. The contribution of roots and shoots to whole plant nitrate reduction in fast- and slow-growing grass species. *Journal of Experimental Botany* **53**, 1635-1642.
Schjoerring JK, Husted S, Mäck G, Mattsson M. 2002. The regulation of ammonium translocation in plants. *Journal of Experimental Botany* **53**, 883-890.
Schmidt HL, Gleixner G. 1998. Carbon isotope effects on key reactions in plant metabolism and 13C-patterns in natural compounds. *Stable isotopes*: BIOS Scientific Publisher, 13-25.
Schmidt SN, Olden JD, Solomon CT, Zanden MJV. 2007. Quantitative Approaches to the Analysis of Stable Isotope Food Web Data. *Ecology* **88**, 2793-2802.
Schnyder H, Lattanzi FA. 2005. Partitioning respiration of C3-C4 mixed communities using the natural abundance 13C approach--testing assumptions in a controlled environment. *Plant Biology* (Stuttg) **7**, 592-600.
Schweizer P, Erismann KH. 1985. Effect of Nitrate and Ammonium Nutrition of Nonnodulated Phaseolus vulgaris L. on Phosphoenolpyruvate Carboxylase and Pyruvate Kinase Activity. *Plant Physiology* **78**, 455-458.

Seel WE, Parsons AN, Press MC. 1993. Do inorganic solutes limit growth of the facultative hemiparasite Rhinanthus minor L in the absence of a host? *New Phytologist* **124**, 283-289.
Setien I, Vega-Mas I, Celestino N, Calleja-Cervantes ME, Gonzalez-Murua C, Estavillo JM, Gonzalez-Moro MB. 2014. Root phosphoenolpyruvate carboxylase and NAD-malic enzymes activity increase the ammonium-assimilating capacity in tomato. *Journal of Plant Physiology* **171**, 49-63.
Shetty K. 2004. Role of proline-linked pentose phosphate pathway in biosynthesis of plant phenolics for functional food and environmental applications: a review. *Process Biochemistry* **39**, 789-804.
Siddiqi MY, Malhotra B, Min X, Glass ADM. 2002. Effects of ammonium and inorganic carbon enrichment on growth and yield of a hydroponic tomato crop. *Journal of Plant Nutrition and Soil Science* **165**, 191.
Siedow JN, Umbach AL. 1995. Plant Mitochondrial Electron Transfer and Molecular Biology. *The Plant Cell* **7**, 821-831.
Sindelar JJ, Milkowski AL. 2012. Human safety controversies surrounding nitrate and nitrite in the diet. *Nitric Oxide* **26**, 259-266.
Skopelitis DS, Paranychianakis NV, Paschalidis KA, Pliakonis ED, Delis ID, Yakoumakis DI, Kouvarakis A, Papadakis AK, Stephanou EG, Roubelakis-Angelakis KA. 2006. Abiotic Stress Generates ROS That Signal Expression of Anionic Glutamate Dehydrogenases to Form Glutamate for Proline Synthesis in Tobacco and Grapevine. *The Plant Cell* **18**, 2767.
Smith BN, Epstein S. 1971. Two Categories of 13C/12C Ratios for Higher Plants. *Plant Physiology* **47**, 380-384.
Sugiharto B, Sugiyama T. 1992. Effects of Nitrate and Ammonium on Gene Expression of Phosphoenolpyruvate Carboxylase and Nitrogen Metabolism in Maize Leaf Tissue during Recovery from Nitrogen Stress. *Plant Physiology* **98**, 1403-1408.
Suzuki A, Knaff DB. 2005. Glutamate synthase: structural, mechanistic and regulatory properties, and role in the amino acid metabolism. *Photosynthesis Research* **83**, 191-217.
Sweetlove LJ, Beard KF, Nunes-Nesi A, Fernie AR, Ratcliffe RG. 2010. Not just a circle: flux modes in the plant TCA cycle. *Trends in Plant Science* **15**, 462-470.
Taiz L, Zeiger E. 2006. *Plant physiology., 4th edn*. Sunderland, Mass., EUA: Sinauer Associate.
Tcherkez G. 2013. Modelling the reaction mechanism of ribulose-1,5-bisphosphate carboxylase/oxygenase and consequences for kinetic parameters. *Plant, Cell and Environment* **36**, 1586-1596.
Tcherkez G, Boex-Fontvieille E, Mahe A, Hodges M. 2012. Respiratory carbon fluxes in leaves. *Current Opinion in Plant Biology* **15**, 308-314.
Tcherkez G, Cornic G, Bligny R, Gout E, Ghashghaie J. 2005. In vivo respiratory metabolism of illuminated leaves. *Plant Physiology* **138**, 1596-1606.
Tcherkez G, Farquhar G, Badeck F, Ghashghaie J. 2004. Theoretical considerations about carbon isotope distribution in glucose of C_3 plants. *Functional Plant Biology* **31**, 857.
Tcherkez G, Mahe A, Gauthier P, Mauve C, Gout E, Bligny R, Cornic G, Hodges M. 2009. In folio respiratory fluxomics revealed by 13C isotopic labelling and H/D isotope effects highlight the noncyclic nature of the tricarboxylic acid "cycle" in illuminated leaves. *Plant Physiology* **151**, 620-630.
Tcherkez G, Mauve C, Lamothe M, Le Bras C, Grapin A. 2011. The $^{13}C/^{12}C$ isotopic signal of day-respired CO2 in variegated leaves of Pelargonium×hortorum. *Plant, Cell and Environment* **34**, 270-283.

Tcherkez G, Nogues S, Bleton J, Cornic G, Badeck F, Ghashghaie J. 2003. Metabolic origin of carbon isotope composition of leaf dark-respired CO2 in French bean. Plant Physiol **131**, 237-244.
Tegeder M. 2014. Transporters involved in source to sink partitioning of amino acids and ureides: opportunities for crop improvement. *Journal of Experimental Botany* **65**, 1865-1878.
Vanlerberghe GC, Schuller KA, Smith RG, Feil R, Plaxton WC, Turpin DH. 1990. Relationship between NH+4 Assimilation Rate and in Vivo Phosphoenolpyruvate Carboxylase Activity : Regulation of Anaplerotic Carbon Flow in the Green Alga Selenastrum minutum. *Plant Physiology* **94**, 284-290.
Vanoni MA. 2015. Glutamate synthase: A case-study for in silico drug screening on a complex iron–sulfur flavoenzyme? *Gene* **564**, 233-235.
Wamelink MMC, Struys EA, Jakobs C. 2008. The biochemistry, metabolism and inherited defects of the pentose phosphate pathway: A review. *Journal of Inherited Metabolic Disease* **31**, 703-717.
Warner RL, Kleinhofs A. 1992. Genetics and molecular biology of nitrate metabolism in higher plants. *Physiologia Plantarum* **85**, 245-252.
Werner C, Gessler A. 2011. Diel variations in the carbon isotope composition of respired CO $_{(2)}$ and associated carbon sources: a review of dynamics and mechanisms. *Biogeosciences* **8**, 2437-2459.
Werner RA, Brand WA. 2001. Referencing strategies and techniques in stable isotope ratio analysis. *Rapid communications in mass spectrometry* **15**, 501-519.
Werner RA, Bruch BA, Brand WA. 1999. ConFlo III - an interface for high precision $\delta^{13}C$ and δ15N analysis with an extended dynamic range. *Rapid Communications in Mass Spectrometry* **13**, 1237-1241.
Werth M, Kuzyakov Y. 2005. Below-ground partitioning (^{14}C) and isotopic fractionation (δ13C) of carbon recently assimilated by maize. *Isotopes in Environmental and Health Studies* **41**, 237-248.
Wingate L, Seibt U, Moncrieff JB, Jarvis PG, Lloyd JON. 2007. Variations in 13C discrimination during CO_2 exchange by Picea sitchensis branches in the field. *Plant Cell and Environment* **30**, 600-616.
Xing S, Wang J, Zhou YI, Bloszies SA, Tu C, Hu S. 2015. Effects of NH_4^+–N/NO_3^-–N Ratios on Photosynthetic Characteristics, Dry Matter Yield and Nitrate Concentration of Spinach. *Experimental Agriculture* **51**, 151-160.
Xu DQ, Gifford RM, Chow WS. 1994. Photosynthetic Acclimation in Pea and Soybean to High Atmospheric CO_2 Partial Pressure. *Plant Physiology* **106**, 661-671.
Yakir D, Sternberg LD. 2000. The use of stable isotopes to study ecosystem gas exchange. *Oecologia* **123**, 297-311.
Yin Z-H, Raven JA. 1998. Influences of different nitrogen sources on nitrogen- and water-use efficiency, and carbon isotope discrimination, in C_3 Triticum aestivum L. and C_4 Zea mays L. plants. *Planta* **205**, 574-580.
Zhu Z, Gerendás J, Bendixen R, Schinner K, Tabrizi H, Sattelmacher B, Hansen UP. 2000. Different Tolerance to Light Stress in NO_3^-- and NH_4^+-Grown *Phaseolus vulgaris* L. *Plant Biology* **2**, 558-570.
Zoglowek C, Kromer S, Heldt HW. 1988. Oxaloacetate and Malate Transport by Plant Mitochondria. *Plant Physiology* **87**, 109-115.

Appendix

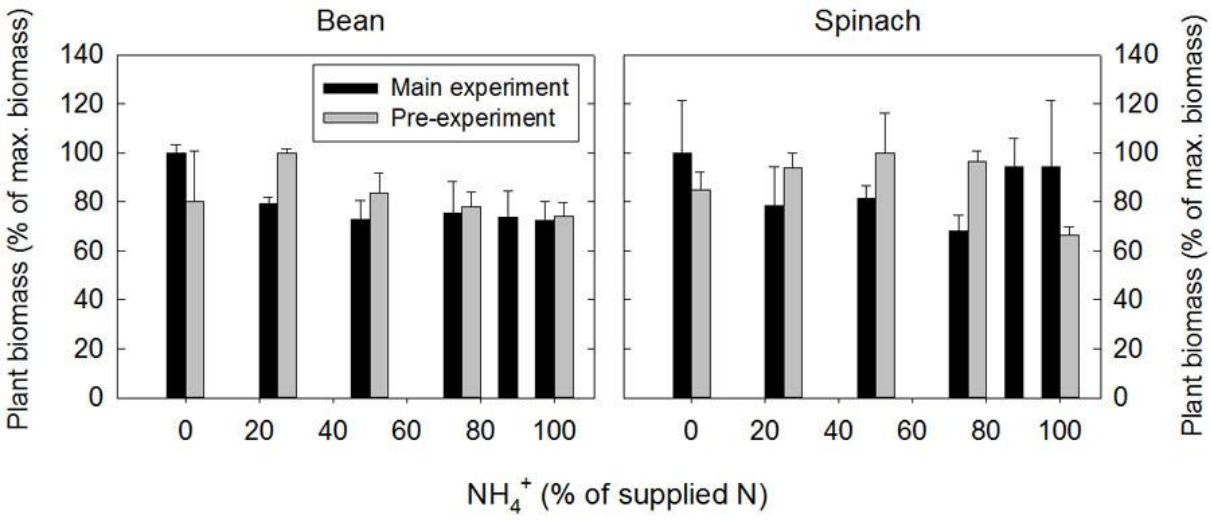

Appendix 1. Relative biomass (as % of maximum biomass within the N-type treatment) for bean (left side) and spinach (right side) plants of the main experiment (black) and pre-experiment (grey) cultured under different % of NH_4^+ and NO_3^- as N source in nutrient solutions used for watering the pots. On the X-axis, 0 and 100 correspond to 0% NH_4^+ (i.e. 100% NO_3^-) and 100% NH_4^+ (i.e. 0% NO_3^-) as % of supplied N in the nutrient solutions, respectively. Values are means ± SE (n=3 for bean and n=5 for spinach in the main experiment, and n=5 in pre-experiment for both species). Different letters on the top of the bar charts indicate significant differences (p =0.05).

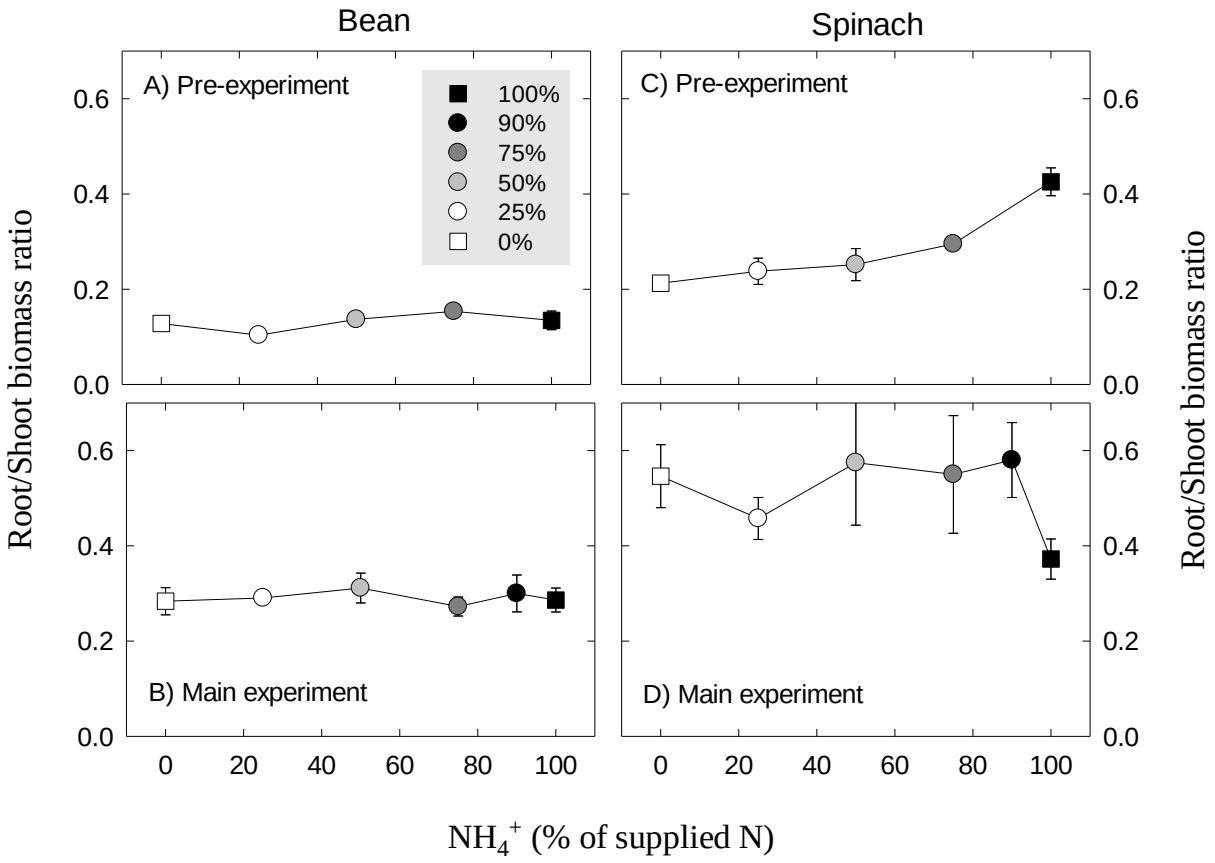

Appendix 2. Root to shoot biomass ratio of bean (A, B) and spinach , (C, D) plants from pre-experiment (upper panels) and the main experiment (bottom panels) cultured under different % of NH_4^+ and NO_3^- as N source in nutrient solutions used for watering the pots. On the X-axis (and in the legend box), 0% and 100% correspond to 0% $NH4^+$ (i.e. 100% NO_3^-, white squares) and 100% $NH4^+$ (i.e. 0% NO_3^-, black squares) as % of total N in the nutrient solutions, respectively. The other N-treatments are shown by circles, as a gradient of increasing NH_4^+ in the solutions, from low NH_4^+ (white) to medium NH_4^+) (grey) and high NH_4^+ (black). Values are means ± SE (n=3 for bean and n=5 for spinach in the main experiment and n=5 for both species in the pre-experiment).

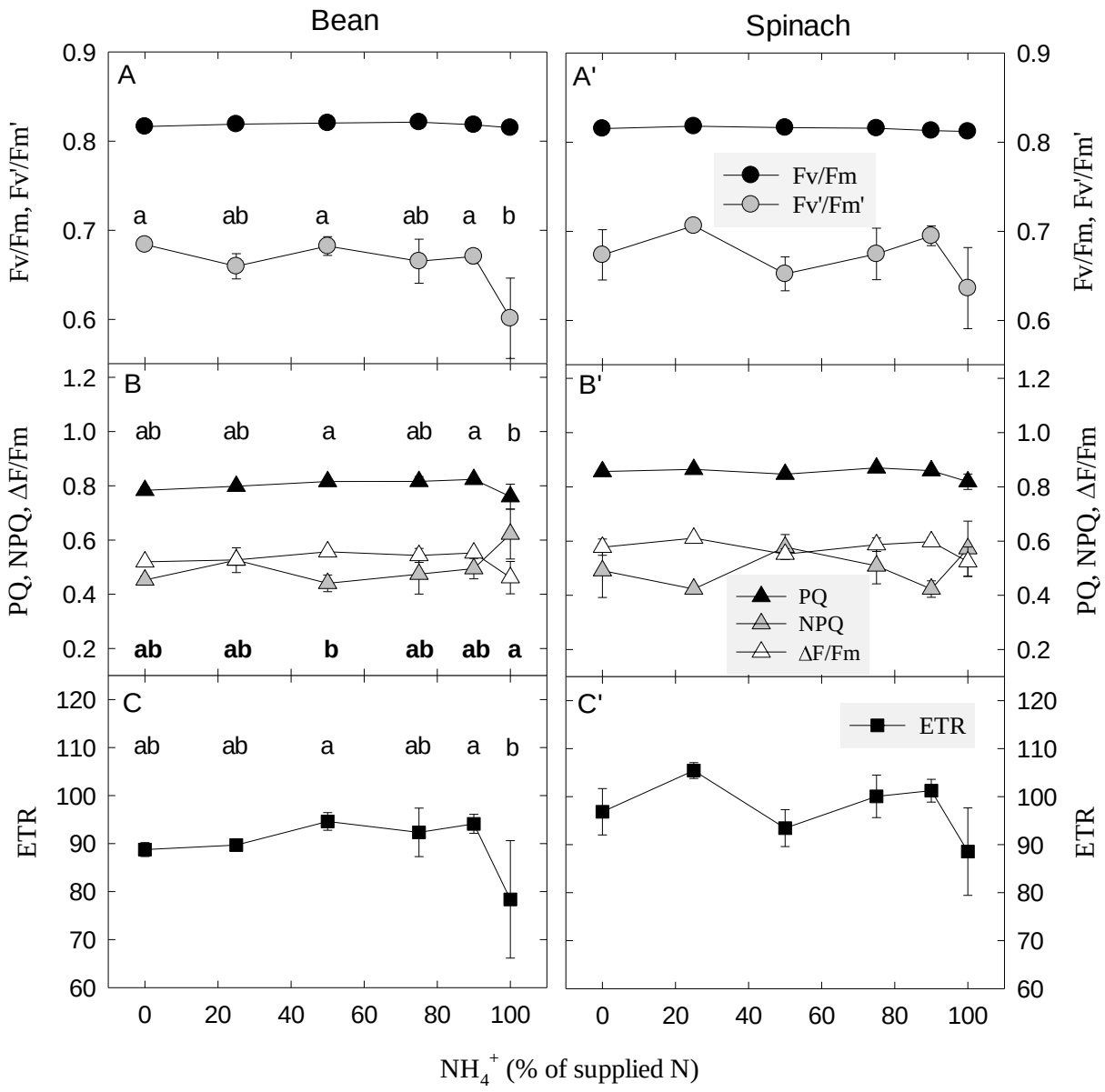

Appendix 3. Fluorescence parameters measured at PPFD = 400 µmol photons m^{-2} s^{-1}, on dark adapted (30 min) leaves of bean (left side panel) and spinach (right side panel) plants grown with nutrient solutions containing different ratios of NH_4^+ and NO_3^- as N source. In A, the maximum PSII efficiency after dark adaptation and in the light (F_v/F_m and F_v'/F_m', respectively), in B, the photochemical (PQ) and non-photochemical (NPQ) quenching, and the relative quantum efficiency of photosystem II (ΔF/Fm), and in C, the electron transport rate (ETR) are presented. On the X-axis, 0 and 100 correspond to 0% NH_4^+ (i.e. 100% NO_3^-) and 100% NH_4^+ (i.e. 0% NO_3^-) as % of total N in the nutrient solutions, respectively. Data points are means values (±SE) of 3 measurements on independent plants. Significant differences (p = 0.05) are shown by different letters for each parameter. Note that the scales are different for bean and spinach in B and C.

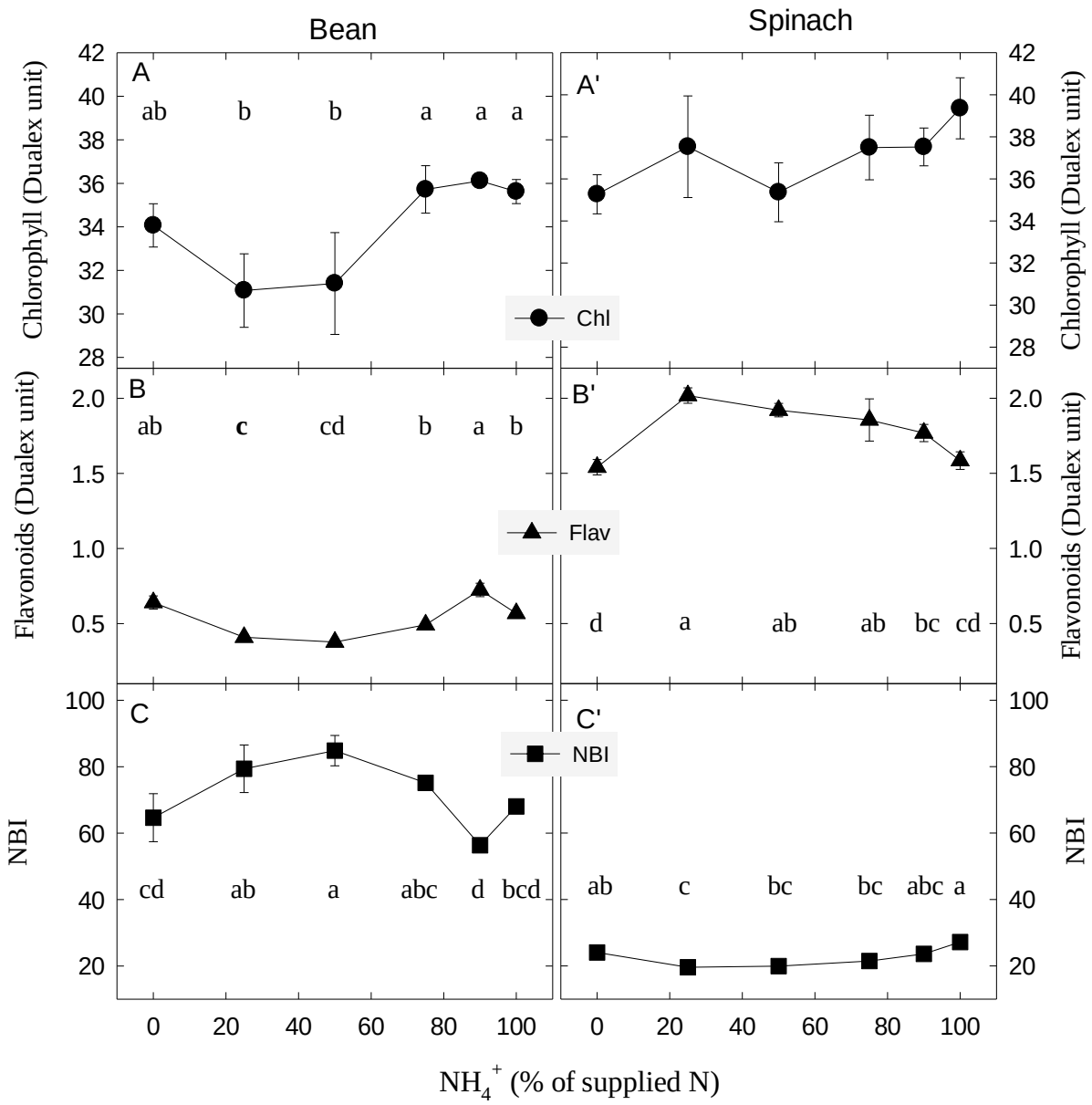

Appendix 4. Chlorophyll (A) and flavonoid (B) contents and nitrogen balance index (NBI) calculated as the ratio of the 2 parameters (C) measured with Dualex on leaves of bean (left side panel) and spinach (right side panel) plants grown with nutrient solutions containing different ratios of NH_4^+ and NO_3^- as N source. On the X-axis, 0 and 100 correspond to 0% NH_4^+ (i.e. 100% NO_3^-) and 100% NH_4^+ (i.e. 0% NO_3^-) as % of total N in the nutrient solutions, respectively. Data points are means values (±SE) of 3 measurements for bean and 5 for spinach on independent plants. Significant differences (p = 0.05) are shown by different letters for each parameter. Note that the scales are different for bean and spinach in B and C.

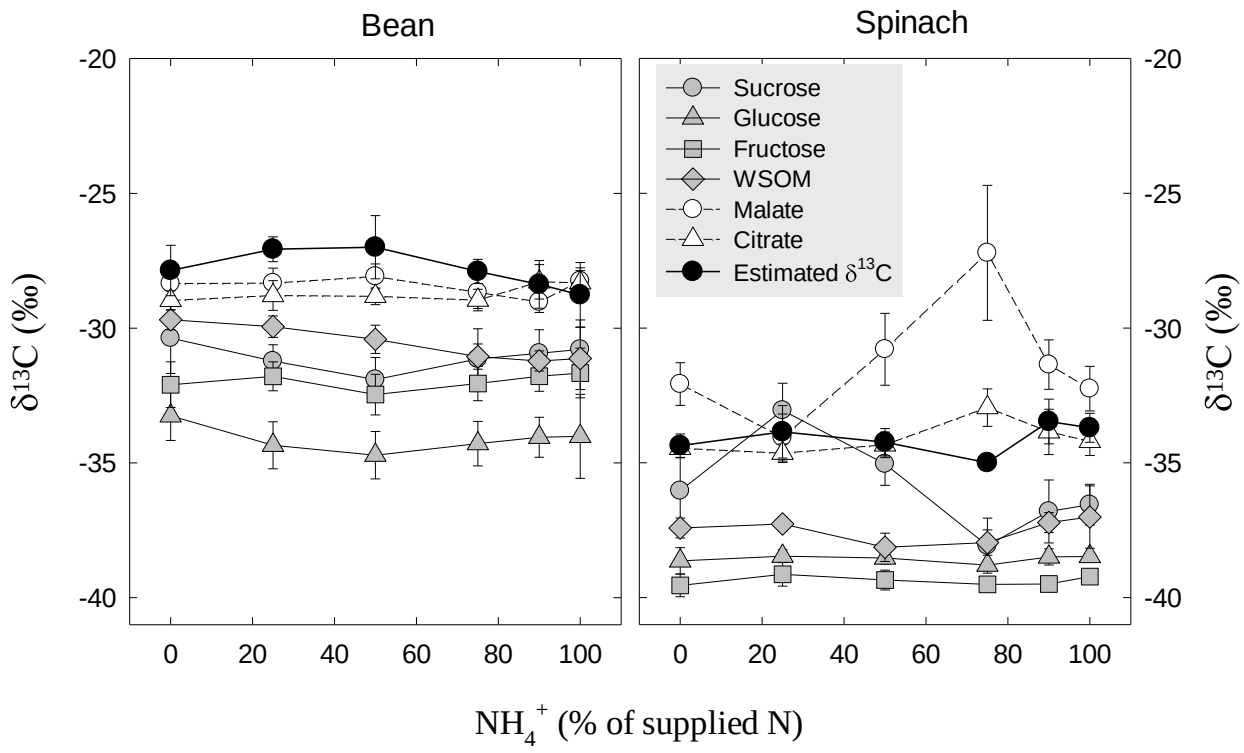

Appendix 5. Measured (grey symbols) and estimated (black symbols) values of leaf-$\delta^{13}C_{WSOM}$ (A), leaf-$\delta^{13}C_{sug}$ (B), leaf-$\delta^{13}C_{Suc}$ (C), leaf-$\delta^{13}C_{Glc}$ (D), and leaf-$\delta^{13}C_{Fru}$ (E), as a function of N-treatment in bean plants. On the X-axis, 0 and 100 correspond to 0% NH_4^+ (i.e. 100% NO_3^-) and 100% NH_4^+ (i.e. 0% NO_3^-) in nutrient solutions, respectively. Estimated $\delta^{13}C$ values are calculated using simple model of Farquhar et al. (1982) using the C_i/C_a values at PPFD=400 µmol m^{-2} s^{-1}, and taking a = 4.4‰ and b=27‰. Means ±SE are presented (n=3). $\delta^{13}C$ of ambient CO_2 in the culture room was estimated to be around –8‰ for bean and around –12 for spinach. Data are from Fig. S9 (Chapter 4) for bean and from Fig. 5.6 for spinach.

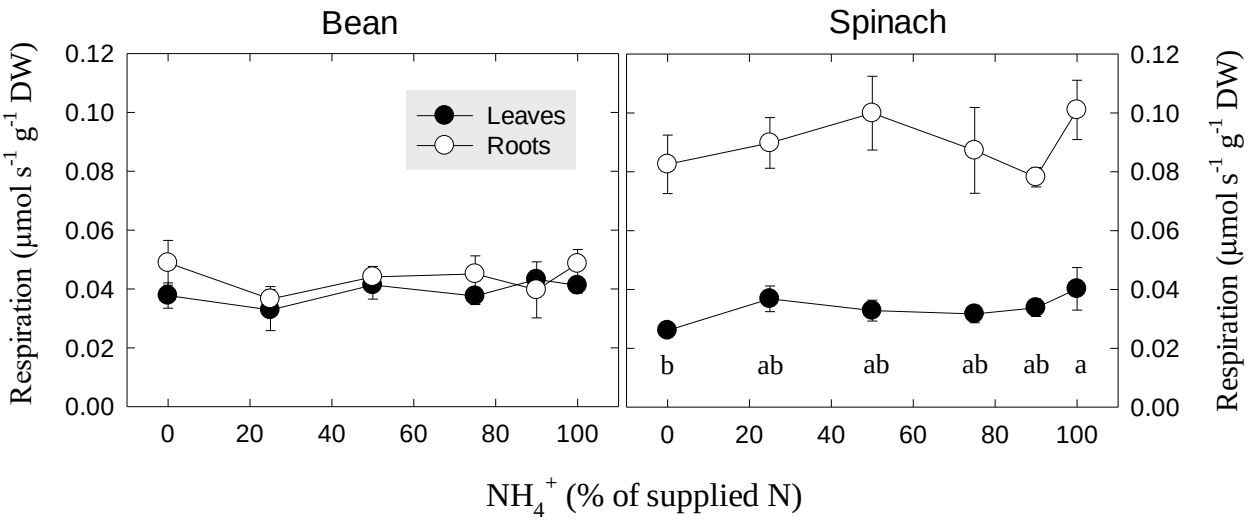

Appendix 6. Respiration rates of leaves (black circles) and roots (white circles) of bean (left side panel) and spinach (right side panel) plants grown with nutrient solutions containing different ratios of NH_4^+ and NO_3^- as N source. On the X-axis, 0 and 100 correspond to 0% NH_4^+ (i.e. 100% NO_3^-) and 100% NH_4^+ (i.e. 0% NO_3^-) as % of total N in the nutrient solutions, respectively. The respiration rates were measured during CO_2 collection on samples in the darkened flasks before respired CO_2 isotopic analyses. Values are shown as means ± SE (n=3 and n=5, for bean and spinach, respectively). Significant differences ($p < 0.05$) are shown by different lowercase letters for spinach leaves. There is no significant difference for bean and for spinach roots.

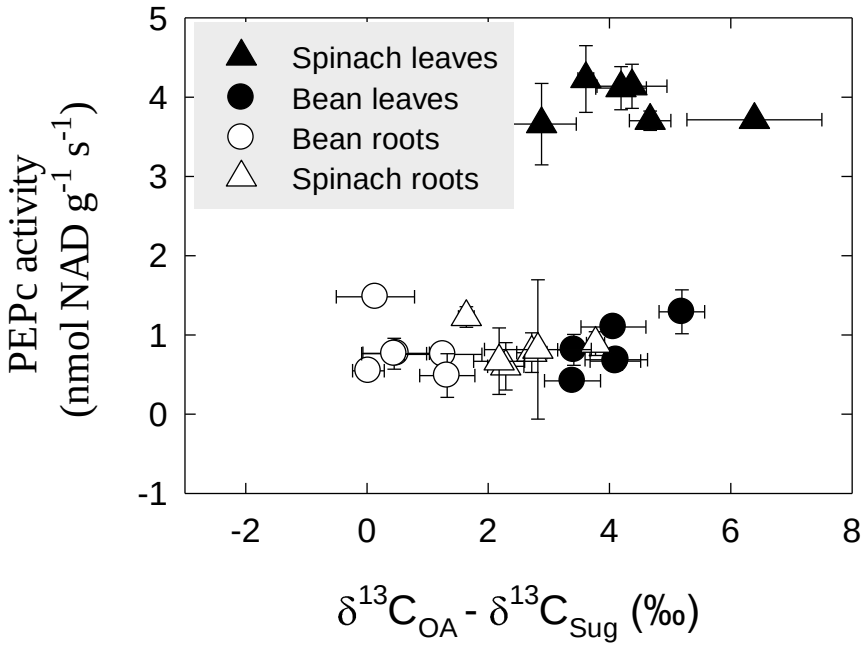

Appendix 7. PEPc activity *versus* the differences between $\delta^{13}C$ of organic acids ($\delta^{13}C_{OA}$ and that of total sugars ($\delta^{13}C_{Sug}$) in leaves (black symbols) and roots (white symbols) of bean (circles) and spinach (triangles) plants cultured under different % of NH_4^+ and NO_3^- as N source in nutrient solutions used for watering the pots. Mean values ± SE are presented (n=3 for both species).

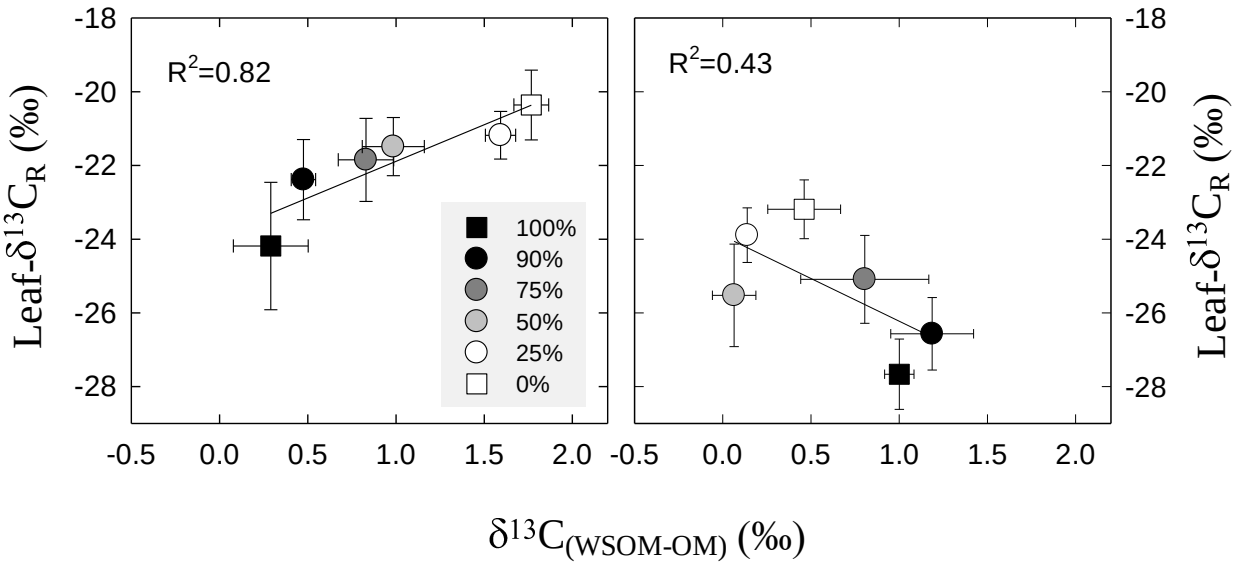

Appendix 8. Variation in $\delta^{13}C$ of respired CO_2 as a function of ^{13}C-difference between WSOM and OM ($\delta^{13}C_{WSOM-OM}$) in leaves of bean (left side panel) and spinach (right side panel) plants cultured under different % of NH_4^+ and NO_3^- as N source in nutrient solution used for watering the pots. In the legend box, 0% and 100% correspond to 0% $NH4^+$ (i.e. 100% NO_3^-, white squares) and 100% $NH4^+$ (i.e. 0% NO_3^-, black squares) as % of total N in the nutrient solutions, respectively. The other N-treatments are shown by circles, as a gradient of increasing NH_4^+ fraction in supplied N, from low NH_4^+ (white) to medium NH_4^+ (grey) and high NH_4^+ (black). Values are means ± SE (n=3 for both species, except n=5 for spinach respired CO_2). When individual data (instead of means) were used for regression, the R^2 values were much lower (0.42 and 0.13, for bean and spinach, respectively).

Appendix 9.

Namelist of abbreviations for Figure 8 (in Chapter 4) and Figure 5.13 (in Chapter 5).

Abbreviation	Variable
An	net assimilation rate
An_C_i	carboxylation efficiency
Chl_1901	chlorophyll index, January 19th
Chl_2201	chlorophyll index, January 22nd
Chl_2701	chlorophyll index, January 27th
C_iC_a	C_i/C_a
DeltaFFm	DF/F_m
ETR	electron transport rate
Flav_1901	flavonoid index, January 19th
Flav_2201	flavonoid index, January 22nd
Flav_2701	flavonoid index, January 27th
FvFm	F_v/F_m
$gsCO_2$	stomatal conductance for CO_2
gsW	stomatal conductance for water vapour
L15N	leaf δ^{15} N
L18O	δ^{18}O of leaf respired CO_2
LC	leaf citrate content
LCcon	leaf carbon content, C%
Ld13CC	leaf citrate δ^{13}C
Ld13CF	leaf fructose δ^{13}C
Ld13CG	leaf glucose δ^{13}C
Ld13CM	leaf malate δ^{13}C
Ld13COM	leaf organic mass δ^{13}C
Ld13CR	leaf respiratory δ^{13}C
Ld13CS	leaf sucrose δ^{13}C
Ld13CWSOM	leaf water soluble organic matter δ^{13}C
LeafDM	leaf dry mass
LF	leaf fructose content
LG	leaf glucose content
LM	leaf malate content
LNcon	leaf nitrogen content, N%
LNR	leaf nitrate reductase activity
LPEPc	leaf PEPc activity
LR	leaf dark respiration rate
LS	leaf sucrose content
NBI_1901	nitrogen balance index, January 19th
NBI_2201	nitrogen balance index, January 22nd
NBI_2701	nitrogen balance index, January 27th
NUEPS	photosynthetic nitrogen use efficiency
R15N	root δ^{15} N
R18O	δ^{18}O of root respired CO_2

RC	root citrate content
RCcon	root carbon content, C%
Rd13CC	root citrate $\delta^{13}C$
Rd13CF	root fructose $\delta^{13}C$
Rd13CG	root glucose $\delta^{13}C$
Rd13CM	root malate $\delta^{13}C$
Rd13COM	root organic mass $\delta^{13}C$
Rd13CR	root respiratory $\delta^{13}C$
Rd13CS	root sucrose $\delta^{13}C$
Rd13CWSOM	root water soluble organic matter $\delta^{13}C$
RF	root fructose content
RG	root glucose content
RM	root malate content
RNcon	root nitrogen content, N%
RNR	root nitrate reductase activity
RootDM	root dry mass
RPEPc	root PEPc activity
RR	root dark respiration rate
RS	root sucrose content
StemDM	stem dry mass
Tr	leaf transpiration rate
WUEinst	instantaneous water use efficiency
WUEintr	intrinsic water use efficiency

université PARIS-SACLAY | ÉCOLE DOCTORALE Sciences du végétal : du gène à l'écosystème

Titre : Impact de divers rapports NH_4^+: NO_3^- dans une solution nutritive sur la composition en isotopique ($^{13}C/^{12}C$) du CO_2 respiré par les feuilles et les racines et les substrats respiratoires putatifs chez les plantes C_3

Mots clés : Différent NH_4^+: NO_3^- ; métabolisme respiratoire; isotopes stables du C; voie anaplérotique

Résumé : L'origine métabolique de la composition isotopique ($^{13}C/^{12}C$) du CO_2 respiré par les feuilles et les racines des plantes ont fait l'objet d'une attention croissante. Cependant, l'impact de la fixation anaplérotique du C *via* la PEPc, étroitement liée à la nutrition azotée, sur le fractionnement isotopique respiratoire n'a pas encore été élucidé. Afin de mieux comprendre (i) dans quelle mesure la composition isotopique des substrats respiratoires présumés et du CO_2 respiré est affectée par la forme d'azote fourni et (ii) dans quelle mesure la voie anaplerotique pourrait expliquer les modifications isotopiques entre organes hétérotrophes et autotrophes liées au type d'azote fourni, les plants du haricot (*Phaseolus vulgaris* L.) et de l'épinard (*Spinacia oleracea* L.) ont été cultivés dans du sable avec différents rapports NH_4^+: NO_3^- dans N fourni. Les résultats ont montré que le CO_2 respiré par les feuilles était enrichi en ^{13}C sous NO_3^- s'appauvrissant avec l'augmentation du % NH_4^+ fourni, tandis que la co-mposition isotopique du CO_2 issu de la respiration des racines restait inchangée quel que soit le rapport NH_4^+:NO_3^-. Nous avons suggéré qu'une plus grande quantité de pools enrichis en ^{13}C fixés par la PEPc *via* la voie anaplérotique contribuait à la respiration foliaire sous NO_3^-. Cependant, un effet similaire dans les racines attendu sous NH_4^+ a été masqué en raison d'une refixation (par la PEPc) du CO_2 respiré (appauvrie en ^{13}C). De manière inattendue, les modifications de la composition isotopique du C des métabolites individuels, leurs quantités, ainsi que l'activité de l'enzyme PEPc, présentaient des profils différents entre les deux espèces étudiées. Des expériences de double marquage (^{13}C et ^{15}N) sont nécessaires pour mieux comprendre l'impact de la plasticité métabolique du TCA sur l'écart isotopique entre le malate et le citrate et sur la composition isotopique du CO_2 respiré chez différentes espèces sous différentes formes d'azote.

Title: Impact of varying NH_4^+: NO_3^- ratios in nutrient solution on C-isotope composition of leaf- and root-respired CO_2 and putative respiratory substrates in C_3 plants

Keywords : Various NH_4^+: NO_3^-; respiratory metabolism; carbon stable isotopes; anaplerotic pathway

Abstract: Metabolic origin of the C-isotope composition of plant respired CO_2 has received increasing interest in the past years. However, the impact of anaplerotic C-fixation *via* PEPc (strongly linked with N assimilation) on respiratory fractionation is not elucidated yet. In order to better understand in which extent (i) the isotopic composition of putative respiratory substrates and respired CO_2 is affected by N-type nutrition in plants, and (ii) the anaplerotic pathway could explain isotope changes in leaves and roots under different N-type nutrition, bean (*Phaseolus vulgaris* L.) and spinach (*Spinacia oleracea* L.) plants were grown with varying NH_4^+:NO_3^- ratios in supplied N. The results showed that leaf-respired CO_2 was ^{13}C enriched under NO_3^- and became ^{13}C depleted with increasing amount of NH_4^+ in supplied N, while C-isotope composition of root-respired CO_2 remained unchanged across N-type gradient. We suggested that a higher amount of ^{13}C enriched C-pools fixed by PEPc through anaplerotic pathway contributed to respired CO_2 in leaves under NO_3^- nutrition. However, a similar effect in roots expected under NH_4^+ nutrition was masked because of a rather ^{13}C depleted C source (i.e. respired CO_2) refixation by PEPc. Unexpectedly, the changes in C-isotope composition of individual metabolites and their amounts as well as PEPc activity exhibited different patterns between the two species. Double labelling experiments (^{13}C and ^{15}N) are needed for better understanding the impact of metabolic plasticity of TCA on isotopic gap between malate and citrate and on C-isotope composition of respired CO_2 in different species under varying N-type nutrition.

Université Paris-Saclay
Espace Technologique / Immeuble Discovery
Route de l'Orme aux Merisiers RD 128 / 91190 Saint-Aubin, France